

# ***CROSS-ROADS IN ASTROPHYSICS***

***A Dissident's Story about Quasars, Stars, and Planets***

*by Dr Kiril P. Panov*

*Former Director, Institute of Astronomy and National  
Astronomical Observatory  
Bulgarian Academy of Sciences  
Sofia, Bulgaria*

***Copyright 2017, BWW Publishers and Kiril P. Panov***

***DEDICATION***

***To my daughters and grand-daughters***

*Contents*

*Dedication*

*Preface*

*Chapter 1. The advent of disintegration processes in astrophysics*

*Chapter 2. The story of local quasars - a ~ 50 year long controversy*

*Chapter 3. Physical characteristics of possible local quasars*

*Chapter 4. Relations for quasars. Effects of discretization*

*Chapter 5. Evidence of evolution of quasars. The linear density relation*

*Chapter 6. Stellar evolution in the concept of disintegration*

*Chapter 7. Quasar-stellar-planetary connection? A lead to the atomic structure*

*Chapter 8. From quasars to planets: a cascade of “jumps” in evolution?*

*Chapter 9. Looking for a planetary orbital distances law*

*Chapter 10. The inevitable rotation*

*Chapter 11. Earth’s expansion and the extinction of dinosaurs*

*Chapter 12. Black holes and the limits of science*

*Chapter 13. Pride and prejudice in astrophysics*

*Closing words*

*Acknowledgements*

*Bibliography*



## ***Preface***

There it is. You are “holding” a heretic book. I have long hesitated, is it not premature? Every astronomer knows from his student days the standard and orthodox theory of the gravitational collapse that has built supposedly all structures in the Universe – galaxies, stars, and planets. During the past ~60 years, it was the only theory applied to the origin of galaxies, stars, and planets - and still is. All textbooks, all research papers in high-ranking journals, all reports on astrophysical symposia – in short, all professionals in the field seem to have absolutely no doubt about the gravitational collapse theory. Or, may be, with one exception? Many years ago I encountered papers of Victor Ambartsumian – the famous Armenian astronomer. He suggested a different approach to the origin of stars - disintegration of some primordial dense matter of unknown origin and unknown properties. It was for me like a lightning stroke. At that time and all the way to the present days the evidence of possible disintegration processes in the Universe was not compelling, and this concept went “unnoticed” for the last ~ 60 y. There is, I believe so, also a psychological reason for that. People don’t like to introduce concepts where something “strange” and “unknown” plays such an important role. It has always been preferred to invoke laws that are well known when researchers encounter new facts. This is a reasonable attitude, I agree. For the origin of planets, stars, and galaxies there was already the famous law of gravitational attraction and this law made such an impressive success in the 18<sup>th</sup> and the 19<sup>th</sup> centuries. Besides, young stars are often found in “clouds” of interstellar dust and gas. Is this compelling evidence that stars originate from gas and dust? It looks plausible, but not compelling. There could be an alternative. One could imagine that some dense body disintegrated (like Ambartsumian says), leaving behind stars, and dust, and gas. In fundamental matters like this it is of utmost importance to consider alternatives. The psychological advantage of the theory of gravitational collapse was that astronomers could develop models and compare them with observations. On the other hand, developing of models on the basis of presumed processes of disintegration is not yet possible - these processes are still completely obscure. Yet, the lack of specific knowledge only makes this concept difficult, but not at all impossible. From the point of view of the expanding Universe (generally accepted now) disintegration processes look much more “natural” than some local gravitational collapses. Indeed, disintegration means expansion. On the other hand, collapse should start with some previously built kernels and how was it possible to build these kernels in an expanding (even “inflationary” expanding - at the beginning) Universe? Not an easy problem. There is also conceptual contradiction between these two concepts: expansion works against gravitation. In such a situation the question most important, “*la question fatidique*”, should be: is there any direct evidence for a gravitational collapse in the Universe? My answer to this question is: “NO”. There is no direct evidence. All the evidence we have is indirect. But the evidence in favor of the concept of disintegration is also scares may be because it has been totally neglected. Well, this book is going to deal with processes that may well be understood within the concept of disintegration. There are no ultimate proofs for any concept in this book. There are some tantalizing findings presented here and which show that the world around us is much more complex and mysterious than the

presentations in all textbooks suggest. Speaking of mysterious concepts we already have several concepts in wide use which are most controversial, e.g. *black holes, dark matter and dark energy*. Is it not possible that a connection may exist between the black holes, the dark matter, and the concept of disintegration?

Some of the results presented in this book have already been published in research papers, mainly in *The Open Astronomy Journal*. I had some difficulties in publishing my “heretic” results and ideas - one of my papers has been rejected several times by several international journals. Rejection of new ideas on pure ideological grounds is unacceptable, but it should be no wonder. For the better, or the worse scientists are very conservative people and radically new ideas are seldom welcome. On the other hand, there is no doubt that the purpose of science is to look for the truth. The important matter in astrophysics, I believe so, is to keep open alternatives in the solution of fundamental problems. Competition of alternatives always provides a better solution.

There is now disturbing evidence that the most basic theory of the origin of galaxies, stars, and planets – the theory of gravitational collapse is in trouble. There are a number of other problems that are connected with that issue and might be put in doubt if this theory fails. Stellar structure, stellar energy production, and stellar evolution are closely related to the theory of origin. These problems are far too important and possible alternative views should not be neglected. Is there enough evidence to introduce such profound changes in astrophysics? This is for you - the reader, to decide. It would be good to be prepared for approaching changes and it is my intention to show what options and prospective we could face if the theory of gravitational collapse would have to be abandoned.

Vera Rubin said once, quote: “*In a very real sense, astronomy begins anew*”. No better words could describe the present day situation in astronomy.

## ***Chapter 1.***

### ***The advent of disintegration processes in astrophysics.***

This review intends to show a build up of facts, problems and controversies in contemporary astrophysics. It is by no means complete and only such problems are included that made a significant impact in recent years and which will possibly be involved in the following discussion. Since my early years as an astronomer something made a big impression on me: the stability of solar irradiation. The solar irradiation on Earth seems to have been stable over hundreds of millions of years. Otherwise the thriving of life and its diversity on our planet would have been impossible. This is how it looks on first glance. Strictly speaking, stable temperature on the Earth's surface could be the result of the combined effect of solar irradiance and the Earth's own internal heat. It is quite possible that the stable and favorable climate conditions on Earth are the result of a decreasing Earth's internal heat and a compensating increase of the solar luminosity during the last hundreds of millions of years. Without changes in other factors, such as the distance from the Sun, or the internal Earth's activity, only a few percent changes in the solar luminosity would have had disastrous consequences for life on Earth and even possible extinction. The fact that life survived for such a long time means that we can make two bold assumptions: the orbit of our planet remained stable and the solar luminosity did not change dramatically, at least during the last hundreds of millions of years. Therefore, looking for a process that could produce the solar energy one condition that has to be fulfilled is relative stability over the last hundreds of millions of years. This does not exclude possible evolutionary trend of increasing solar luminosity if longer periods like billions of years are considered. It is now established that only nuclear processes could provide for the necessary energy output and its stability. The question is what kind of nuclear processes? Generally accepted now is that hydrogen fusion should be the solar engine, converting hydrogen into helium. However, the stability of hydrogen fusion over long periods of time is a problem that remains to be solved. There are other nuclear processes that could be considered as possible solar engines: e.g. spontaneous fission of heavy radioactive elements and the radioactive decay. These processes are very stable in time with their respective half-life times of decay. But there is a time problem. Even the longest of half-life times of radioactive decay are not long enough to cover billions of years of solar luminosity ( $U^{238}$  has a half-life  $T_{1/2} = 4.47 \cdot 10^9$  y,  $Th^{232}$  has a  $T_{1/2} = 1.41 \cdot 10^{10}$  y). Spontaneous fission half-life times could be longer, but these same atoms would be destroyed faster by alpha decay, according to their respective half-life times. So, it seems that this possibility should be rejected for two reasons: the "engine" work-time is too short and the standard theory of stellar origin does not suppose that newly born stars could have large amounts of heavy radioactive elements in their cores. Stars are supposed to contain mainly hydrogen and helium with only traces of heavier elements. It should be noted that the second argument is model-dependent. If the origin of stars would be different the second argument might fall out. But the time- controversy remains. Unless there is a replenishment of the fissile material, in solar core the time-problem could not be solved. I will get back to this problem in the following chapters. In the late 1960s the solar neutrino problem became famous. In the Homestake experiment carried out by R. Davis and J. Bahcall the solar neutrinos have been measured

for the first time and their deficiency with respect to the predicted theoretical value became obvious. The experimental value of solar neutrinos is only about one third of the predicted value. This result was later confirmed and the missing solar neutrinos became a considerable problem for the standard theory of hydrogen fusion. Is the standard theory wrong? Or, may be, the fusion reaction in the solar core temporarily decayed? If we witness decay of fusion now in the solar core this should be visible on the solar surface much later. But then, if fusion would be unstable, this could have happened also in the past and it did not since life on Earth survived? Neutrino oscillations [1-3] were invoked to “save” the problem of missing solar neutrinos and it seems now that this solution is accepted. Or, at least, there is a majority agreement that it is solved. Is this problem really closed? Could it be that different nuclear processes could lead to the same result? And another unsettling question: are we sure we have considered properly all sources in our neutrino-environment? What are these neutrinos that have been registered by the neutrino experiments? These questions may seem here unfounded but I will turn to them in the last chapter.

Already in the 1970s the nuclear chemistry professor O. Manuel (University of MR, USA) reported his surprising results and suggested that the Sun has to be an iron rich star ([www.omatumr.com](http://www.omatumr.com)). He maintained his claim ever since. O. Manuel suggested a scenario where the Sun harbors a neutron star in its interior. According to the standard theory a neutron star (pulsar) forms after super-novae explosion (SN) of a massive star after all nuclear “fuel” for maintaining energy production has been exhausted. As the solar appearance doesn’t look like a neutron star O. Manuel suggests that the neutron core should be hidden inside the Sun. Needless to say, if an iron core is hidden inside the Sun this would change the astrophysics. No doubt Manuel’s results are extremely important although an iron core in the Sun could develop in a different way – not in the orthodox scenario of evolution. All general stellar characteristics of the Sun are consistent with a normal, main sequence star of spectral class G2. So, if normal stars like Sun do indeed have an iron core then our theory of stellar origin, stellar structure, and stellar energy production should be terribly wrong. Solar seismology provided information about solar interior, but is this method able to penetrate to the solar core? Interestingly, studies revealed that the solar core could be in rigid rotation and rigid rotation could be a hint for a core of heavy elements. No doubt, it is of utmost importance to prove or to revoke the existence of an iron-rich core in the Sun. This should be done by observations and not by model-dependant arguments. If the Sun has an iron core it is probably not the result of a standard evolution as Manuel assumes, but it could have existed there from the beginning - since the solar origin. This, however, means a different scenario of origin. If confirmed it would change astrophysics completely. No wonder that orthodox theory supporters denied Manuel’s results.

There is an old problem about orbital distances law in planetary systems. The story of the orbital distances law in the Solar system is most remarkable. It started in the late 18<sup>th</sup> century with the Titius – Bode law (TBL) which predicts the mean planetary distances from the Sun as:

$$a_n = 0.4 + 0.3 \cdot 2^n$$

Here “n” is the orbital number. The TBL had initial success in predicting the distances of Uranus and Ceres. Later a whole belt of asteroids was found at about the distance of Ceres. However, by the discovery of Neptune in 1846 the TBL failed to predict the correct distance. Neptune was found much closer to the Sun than predicted. By the discovery of Pluto in 1930 it became clear that the TBL failed completely. The TBL represents now only historical interest. Many researchers, fascinated by the TBL and the possibility that a better formula might exist continued to look for an orbital distances law. A great number of TBL –like formulas have been suggested and all these could be regarded (including the TBL itself) like more or less successful approximations to yet unknown orbital distances law. Recent reviews could be found in [4-5]. But why is it so important to look for an orbital distances law during more than two centuries? It is because there is too much at stake, no doubt. If an orbital distances law exists in the Solar system it would be natural to expect similar laws in the extra-solar planetary systems. This will help researchers to predict the locations of yet missing planets in some exoplanetary system using the respective distances formula for that system. But there is much more than that. The existence of orbital distances law in planetary systems contradicts to the most popular theory of planetary origin - the theory of gravitational collapse. Indeed, the gravitational collapse should be a random process in space and time and a planetary system should be regarded as a series of randomly occurred collapses. But then, how is it possible to create regularity in the distances of the planets from the respective central star – an orbital distances law? Moreover, there is the famous problem in the extra-solar planetary systems that could also concern the origin of planets. In many systems planets were found very close to the respective central star. In fact, these “close-by” planets are so close to their respective central star that a gravitational collapse at that distance that supposedly built those planets would be impossible to occur. The strong attraction of the nearby central star should have prevented the build-up of a planet. An outcome was found in the assumption that the “close-by” planets were built far away from the star and that they “spiraled down” to the star due to friction (or drag) with the environment. This “spiraling – down” scenario would be severely compromised if an orbital distances law exists, whatever the formula may be. Indeed, friction (or drag) is also a random process and it would be too much of coincidence to assume that a random friction action could possibly bring the spiraling down planet to the exact distance from central star, in order to fulfill the orbital distances law for this planetary system. The alternative would be that the “close-by” planets originated “*in situ*” - in these same places we find them now. Only that in this case the theory of gravitational collapse should be abandoned and a different scenario for the origin of planets should be invoked.

My next point is the mystery of the “dark matter”. In 1933 Fritz Zwicky studied the velocities of galaxies in clusters and found that these velocities are too large. The total of the observed masses of clusters of galaxies could not keep the clusters stable because of the large velocities of galaxies. Therefore, galaxies should be flying apart, but they did not. The stability of clusters of galaxies could not be achieved unless there is a “*hidden, dark mass*” in these clusters. It is this additional dark mass that prevents the cluster of galaxies from flying apart. So began the story of the “*dark matter*” which remains unresolved to the present day. The next development of this story concerns the flat rotational curves of galaxies. The revival of the dark matter hypotheses came from the

studies of Vera Rubin and collaborators in the 1970s. They found (“Rubin – Ford” effect) that in many spiral galaxies the rotational curves remain flat at large distances from the respective galactic center [6]. This is inconceivable and contradicts to the Newtonian dynamics. If stars revolve on Keplerian orbits at large distances from galactic center their orbital velocity should decrease. How is it possible that flat rotational curves exist? In order to deal with this problem some very exotic hypotheses were invoked, including possible departure from the Newtonian dynamics (MOND – Modified Newtonian Dynamics) or a “dark matter” in the galactic halos. On the other hand, since the velocities of stars in a galaxy are far from being relativistic the Newtonian dynamics should determine these rotational curves. So far researchers took it for granted that spiral arms in galaxies are dynamically stable. This could be the reason why such exotic hypotheses had to be invoked like MOND and the dark matter in the halos of galaxies. But are we sure that spirals are dynamically stable? The presently popular theory of the origin of spirals is the “*gravitational waves theory*”. However, there might also be alternative origin of the spirals. It could not be ruled out that spirals were ejected from the galactic nuclei by activity processes we don’t yet understand. This idea has already been suggested by Halton Arp. If we don’t know for sure how spiral arms originated we could also not be sure that they are dynamically stable. It is the instability of the spiral arms that could be the key to solve the mystery of the flat rotational curves in galaxies.

*Black holes* are now believed to exist in the nuclei of most (may be all?) galaxies. Black hole is supposed to exist also in the central region of our galaxy with a mass of about  $4.2 \cdot 10^6$  solar masses [7-8]. The concept of “*black holes*” is controversial and clearly shows that researchers are prone to accept and to use concepts that still remain a mystery. Indeed, black holes are believed to “swallow” in-falling matter that is never to appear again. According to the theory nothing could escape from a black hole, not even the light, but this point could be questioned. There are other inconsistencies that will be discussed below (chapter 12). As it now looks, a black hole should have an infinite density. Is this not a clear sign of the limits of science? We have to admit that we don’t know what a black hole really is. But we still use this concept to study orbital movement of stars in the gravitational field of a black hole. It may be that we would need deeper insight into the sub-atomic structure of matter in order to understand a “*black hole*”. What we could say now is that a black hole could be a body of “enormous”, but finite density and “very small” dimensions with yet unknown physics and structure. Having in mind the unknown structure and physics of a black hole, I could ask a heretic question: is it possible that a black hole could eject matter and energy through its “*event horizon*”? Is it possible that a black hole ejects the matter that later builds stars and, may be, a whole galaxy around this black hole? If so, a black hole may also be called a “*white hole*” in the active phases of ejections. This could put the whole theory of the galactic origin into an entirely new prospective. Clearly, in this case the definition of “*event horizon*” would no longer be valid in its original sense. From the structures we can observe quasars may be most close to a black hole in their structure. In the scenario of galaxy origin quasars could also be involved.

But does it make sense to introduce such a concept like a “*white hole*”? Is it possible that the concept of Ambartsumian [9] and the supposed dense matter disintegration could be

related to the concept of “*white holes*”? In the 1950s, Ambartsumian [9] introduced this radically new astrophysical concept – the disintegration of some primordial dense matter, based on his studies of expansion and dissipation of stellar associations. It may be that some evidence of disintegration processes could be obtained from the study of quasars. Looking for answers, I am going to the next chapters.

## Chapter 2.

### *The story of local quasars - a ~ 50 year long controversy..*

Quasars (QSOs, quasi-stellar objects) have been discovered in 1963 following the optical identification of some radio-sources as quasi-stellar objects. Their optical spectra remained puzzling until M. Schmidt was able to identify the spectra of two objects, 3C273 and 3C48, as red-shifted by 16% for 3C273 and by 37% for 3C48. These large redshifts were unprecedented in astrophysics and their discovery started a new chapter of discoveries. Other quasars followed soon and in all cases QSOs exhibit large redshifts in their spectra. However, later studies also revealed that the majority of quasars do not radiate in the radio-band, some 90% of all known quasars are actually radio-quiet. The total number of quasars now exceeds 150 000.

In the classical book of G. Burbidge and E.M. Burbidge, *Quasi Stellar Objects (1967)*, following characteristics of quasars are given:

- star-like object
- radio-source identification
- variable light
- large ultraviolet flux
- large redshifts
- broad emission in their spectra, with some absorption lines in some QSOs.

Typically, quasars show also strong and variable X-ray emission. From the time of variability in several spectral bands – optical, radio, and X-ray- it was possible to derive that the emitting region in quasars is very small (quasi-stellar objects). It is, however, the large redshifts that triggered a long and controversial discussion that goes on to the present day. Different hypothesis were suggested to explain the large redshifts, but the most likely candidates that need attention are:

- Doppler shifts, due to relative motions, could only be a small component in the quasars' redshifts, but not the main cause. Quasars exhibit always redshifts, therefore, there is a different cause that determine their redshifts.
- Gravitational reddening. It follows from the theory of *general relativity*. Gravitational redshifts are intrinsic in origin.
- There could be other causes for intrinsic redshifts than the gravitational reddening. That is why some researchers prefer not to specify the origin of the intrinsic redshifts.
- Cosmological redshifts following from the expansion of the Universe.

Presently, most popular with astronomers is the hypothesis of cosmological redshifts. In the Standard Quasar Model (SQM) quasar redshifts are entirely attributed to the expansion of the Universe and therefore quasars should be at cosmological distances. Their luminosities therefore have to be huge - up to  $\sim 10^{45}$  erg/s. The only known process that could provide for these luminosities is accretion on a huge (up to  $10^{10}$  solar masses) black hole [10-12].

Already during the first years after their discovery attempts have been made to explain the quasars' redshifts in a different, non-cosmological way. Among the most debated are ideas based on the intrinsic origin of the redshifts: gravitational reddening [13-15], and the "variable mass" hypothesis [16-17]. If the redshifts of quasars are intrinsic in origin, the quasars are probably of local origin – local quasars. The debate between supporters of the SQM and the "intrinsic-origin" supporters continues for more than 50 years. Both the SQM and the "local quasar concept" have their observational support but also their weak points. Strong observational support for the SQM comes from observations of quasars "hosted" by galaxies. In a few cases [18-19] the redshift of the "hosted" quasar was found to be identical with the redshift of the "hosting" galaxy. However, there is a major observational difficulty, due to the overwhelming brightness of the quasar. If the observations of the galaxy would be "contaminated" by the quasar's light this could explain the identical redshifts. Furthermore, there is one reported case [20] where quasar of  $z = 2.114$  was found very close to the nucleus of the galaxy NGC 7319 with  $z = 0.022$ . Clearly, observations are controversial and only future studies of "hosted" quasars could resolve that controversy.

There is also disturbing fact about quasars from the beginning. Quasars simply do not follow the Hubble relation found for galaxies. How then can we be sure that we could apply the Hubble relation to determine the distances to quasars? An outcome was suggested in the (supposed) large spread of quasars' luminosities. Whether or not this could be the true explanation, the simple fact remains that QSOs do not obey the Hubble relation and a different cause could not be ruled out.

There are other peculiar findings, e.g. not only are the quasar luminosities huge but they also seem to increase with cosmological distance. Peculiar remains also the deficiency of high luminosity quasars at low redshifts. There is also the question, why is the number of QSOs with  $z > 3$  sharply decreasing? In the SQM we should have an increasing number of quasars with increasing distance i.e. with increasing cosmological redshift. Increasing reddening with distance could account for some reduction of QSO visibility, but would the "reddening factor" be sufficient to explain the missing quasars at large redshifts? It seems that the number of QSOs decreases very sharply for  $z > 3$ . The SQM does not provide for satisfactory answers to all these questions. But there are more questions. An interesting problem concerning all hypotheses for quasars is the Karlsson sequence of quasar redshifts. This is a sequence of specific and preferred redshifts: 0.06, 0.30, 0.60, 0.96, 1.41, 1.96, and so on [21-24]. The Karlsson sequence could be obtained by:  $\Delta \log(1+z) = 0.089$ . Interestingly, the Karlsson sequence was found with the early surveys of quasars but later not confirmed with modern redshift catalogues. The easy answer to this problem would be that the preliminary findings were discarded by later, larger data samples. Easy answers are, however, not always correct. For a SQM - supporter this view would be a relief. If confirmed the Karlsson sequence would require in the SQM that the Universe should expand in shells of different and specific velocities and that is inconceivable. The Karlsson sequence is a major obstacle also for the local quasar concept. The gravitational reddening scenario for redshifts could provide for an outcome, but only at a major sacrifice – the departure from a basic physical concept and introduction of new ideas [25]. Do we have to take such a bold

step? How then is to be explained the lack of confirmation of the Karlsson sequence with modern large data bases?

The local quasar concept also relies on observational support. It has been known for many years that large redshift QSOs are associated with low redshift galaxies [26-37]. A nice sample of such “discordant redshift associations” (as Halton Arp calls them) is presented in [26]. Prominent examples are NGC 4319 and Mk 205 [38] where a filament is possibly seen, connecting the quasar with the galaxy, although they have different redshifts. Another example is NGC 3067 and 3C232 [39-40]. In other cases quasars have been found very close to a low redshift galaxy [20, 41]. Chance projection in these cases is considered very unlikely with probability being of the order of  $\sim 10^{-8}$  and lower [42-43]. There are reports of large groups of quasars clustering around low redshift galaxies [44-48]. All these findings could lead to the conclusion that quasars around low redshift active galaxies have been ejected by the respective parent galaxy [49-55]. Taking the same distance for a group of quasars as the distance of their parent galaxy, it was possible to derive some physical characteristics of these quasars [25, 54, 55].

Quasars release huge amounts of energy. In the SQM these energies are released by accretion onto a black hole (up to  $\sim 10^{45}$  erg/s, in a life time of  $10^7 - 10^8$  y). In the framework of the gravitational reddening hypothesis the energies released by local quasars are:  $10^{39} - 10^{42}$  erg/s, i.e. they should be about three orders of magnitude less luminous [25, 54, 55]. The local quasar model has as yet no specific physical engine. All that could be said is that the known physical processes are probably insufficient to explain the quasars’ huge energy output, though some kind of disintegration processes could not be ruled out.

There is another quasar riddle concerning the quasar metal abundances. In the SQM quasars should be most young as they are considered to be the most distant objects. Then they should also be expected to be metal deficient. Surprisingly, high metal abundances were found in high redshift QSOs [56-58]. How is this possible? The only way known to produce heavy elements are nuclear processes in stars at late stages of their evolution. Are these metal abundances produced by rapidly evolved stellar population around the respective quasar? Or, may be, we are confronted with yet another quasar riddle? Although the high metal abundances are an obvious difficulty for the SQM it is a major stumbling block also for the local quasar concept. If these metal abundances are produced by the quasar itself and not by nearby stars then, may be, we should have to consider a different way by which these heavy elements were produced. This is another fundamental problem with QSOs.

Some quasars exhibit jets of yet unknown nature. In some cases, e.g. 3C345, moving structures along the jet were found by radio-observations [59-60]. If quasars are supposed to be at cosmological distances the velocity of the moving structures should be super-luminous. If, on the other hand, quasars are of local origin (e.g. 3C345 would be at about the distance of the neighboring galaxy NGC 6212) the velocity of the moving structures would be reduced below the velocity of light [61].

Where should we start to resolve all these controversies? The basic problem is, no doubt, the origin of quasars - cosmological origin or a local origin. Everything depends on its solution. It should also be stressed that the "local quasar concept" applied to some QSOs does not exclude the existence of other QSOs at large cosmological distances. Decisive observations could be observations of "host" galaxies. During the last years there is increasing number of studies of "host" galaxies [62-67]. It looks promising that we could have this problem resolved. In the next chapter evidence will be presented that at least some QSOs of local origin could exist and with this assumption some physical characteristics for local quasars could be obtained.

### ***Chapter 3.***

#### ***Physical characteristics of possible local quasars.***

Assuming that the clustering of quasars around active low-redshift galaxies is real as claimed in many research studies, physical characteristics of local quasars could be obtained [25, 54, 55]. The basic assumption in these cases is that for a group of QSOs, clustering around a galaxy the same distance is taken for all the quasars of this group as for their “parent” galaxy. In other words, the redshift of the parent galaxy determines the distances of all QSOs of this respective group. The observed quasar redshift  $z_o$  could be taken as composed by three components of different origin, according to Burbidge [68]:

$$(1 + z_o) = (1 + z_c) \cdot (1 + z_{gr}) \cdot (1 + z_d) \quad (1)$$

Here  $z_c$  is the cosmological redshift of the quasar which is equal to the redshift of the respective parent galaxy (i.e.  $z_c = z_{gal}$ ),  $z_{gr}$  is the intrinsic redshift, specified here as gravitational redshift, and  $z_d$  is the Doppler shift. From eq (1) it is obvious that a model of expanding Universe is required, i.e. the Big Bang model. With the eq (1) we could turn to the previously asked question and possibly find an answer: why modern redshift surveys do not confirm the Karlsson sequence of redshifts? Modern surveys probably contain more distant, faint QSOs than the early surveys. This is due to the natural extension to fainter QSOs with improving observational facilities. If distant quasars are predominant in a sample their cosmological redshifts will contribute substantially (see eq 1) to the observed quasar redshifts. Therefore, if a specific pattern (e.g. the Karlsson sequence) exists with the gravitational redshifts it would be impossible to detect it. The absence of positive detection in this case does not necessarily mean that the Karlsson sequence does not exist – it could be undetectable. In the old quasar surveys the inferior observing techniques at that time seems to have “sorted” in a natural way the nearby quasars by their brighter magnitudes which made the detection of the Karlsson sequence possible. Ironically, it could be that the improvement of observing facilities allowing for fainter and more distant quasars to be observed made the confirmation of the Karlsson sequence a hopeless task.

The following procedure has been adopted to decompose redshifts of quasars [25, 54, 55]. First, for all quasars of a group around a low redshift galaxy the redshift of this galaxy (assumed cosmological) is taken out from each quasar’s observed redshift by:

$$z_i = (z_o - z_{gal}) / (1 + z_{gal}) \quad (2)$$

Here  $z_i$  is the “intrinsic” redshift, composed by the gravitational redshift  $z_{gr}$  and the Doppler shift. This procedure uses the above assumption that all QSOs of a group clustering around an active galaxy have about the same distance as their parent galaxy. In [55] it was found that the distribution of the projected Doppler shifts is approximately symmetrical and the Doppler components are mostly less than 0.1 c. This could make determination of gravitational redshifts possible by simply comparing each quasar’s  $z_i$  – value with the Karlsson sequence. Generally, each  $z_i$  value falls between two redshifts

of this sequence and in most cases it is the nearest of the Karlsson redshifts that has to be taken for  $z_{gr}$ . After the  $z_{gr}$  is decomposed the remaining Doppler shift  $z_d$  could be determined by:

$$z_d = (z_i - z_{gr}) / (1 + z_{gr}) \quad (3)$$

The distribution of the Doppler shifts is nearly symmetrical [55]. In a few cases, however, the  $z_i$  –values are near the middle between the two redshifts in the Karlsson sequence. Then both “limiting” redshifts should be checked by calculating the respective Doppler shifts and by comparing each  $z_d$  with the Doppler-shifts distribution. In a few such cases I have taken for  $z_{gr}$  the more distant Karlsson redshift value because it leads to a  $z_d$  value that better matches the Doppler-shifts distribution (see Fig 2 below). This procedure was applied to the sample of local quasars listed in Table 1.

**Table 1. Sample of 341 local quasars (data from Veron-Cetty and Veron , 2010, 13 th ed. [69]).**

| Galaxy redshift  | Quasar              | Redshift $Z_0$ | Visual mag | B-V  | References |
|------------------|---------------------|----------------|------------|------|------------|
| NGC0007<br>0.005 | Q1= 2QZJ000827-2954 | 2.062          | 19.53      | -    | [70]       |
|                  | Q2= 2QZJ000826-2957 | 2.041          | 20.74      | -    |            |
|                  | Q3 2QZJ000802-2956  | 1.591          | 20.23      | -    |            |
| NGC450<br>0.006  | Q1= Q0107+0022      | 1.968          | 18.89      | 0.21 | [44]       |
|                  | Q2= Q0107-0235      | 0.958          | 17.80      | -    |            |
|                  | Q3 Q0107-0232       | 0.728          | 18.85      | -    |            |
|                  | Q4 PB6291           | 0.956          | 17.60      | -    |            |
|                  | Q5 Q0107-025c       | 1.893          | 19.45      | -    |            |
|                  | Q6 NGC450 No24      | 0.070          | 18.90      | -    |            |
|                  | Q7 Q0107-001        | 0.468          | 19.38      | 0.09 |            |
|                  | Q8 Q0108-007        | 1.424          | 19.23      | 0.50 |            |
|                  | Q9 Q0108+0028       | 2.005          | 18.25      | -    |            |
|                  | Q10 Q0108-025       | 1.240          | 18.10      | -    |            |
|                  | Q11 Q0108-020       | 1.302          | 19.60      | -    |            |
|                  | Q12 Q0108+001       | 1.003          | 18.67      | 0.26 |            |
|                  | Q13 Q0109-0128      | 1.758          | 18.37      | 0.26 |            |
|                  | Q14 Q0110-0107      | 1.896          | 19.29      | 0.22 |            |
|                  | Q15 Q0110-0157      | 1.102          | 17.30      | -    |            |
|                  | Q16 PB6317          | 0.238          | 17.85      | 0.28 |            |
|                  | Q17 Q0110+004       | 0.910          | 20.08      | 0.21 |            |
|                  | Q18 Q0110-0015      | 0.976          | 18.55      | -    |            |
|                  | Q19 Q0110-030       | 1.235          | 17.70      | -    |            |
|                  | Q20 Q0110-0047      | 0.412          | 19.06      | 0.29 |            |
|                  | Q21 Q0110-006       | 0.935          | 19.70      | -    |            |
|                  | Q22 Q0111-007       | 0.995          | 18.63      | 0.28 |            |

|                 |                  |       |       |      |      |
|-----------------|------------------|-------|-------|------|------|
|                 | Q23 Q0111-008    | 0.181 | 18.93 | 0.58 |      |
|                 | Q24 Q0111-010    | 0.350 | 19.02 | 0.33 |      |
|                 | Q25 Q0111-005    | 1.908 | 19.45 | -    |      |
|                 | Q26 PKS0112-017  | 1.365 | 17.50 | -    |      |
|                 | Q27 Q0112-012    | 1.585 | 19.89 | 0.20 |      |
|                 | Q28 Q0113+000    | 1.279 | 19.19 | 0.37 |      |
|                 | Q29 Q0113-010    | 1.968 | 19.58 | 0.20 |      |
|                 | Q30 Q0113-013    | 2.055 | 19.60 | -    |      |
|                 | Q31 Q0113-009    | 1.263 | 18.96 | 0.36 |      |
|                 | Q32 Q0114-001    | 1.316 | 18.94 | 0.35 |      |
|                 | Q33 UM314        | 2.190 | 18.32 | 0.22 |      |
|                 | Q34 UM315        | 2.050 | 18.70 | -    |      |
|                 | Q35 Q0116-010    | 1.052 | 18.60 | 0.32 |      |
|                 | Q36 NGC450 No86  | 0.090 | 17.35 | 0.44 |      |
|                 | Q37 Q0117-023    | 2.019 | 19.80 | -    |      |
|                 | Q38 Q0117+001    | 0.649 | 19.30 | 0.17 |      |
|                 | Q39 UM316        | 0.960 | 17.90 | -    |      |
|                 | Q40 Q0117-012    | 0.202 | 19.13 | 0.65 |      |
|                 | Q41 NGC450 No87  | 0.078 | 19.45 | -    |      |
|                 | Q42 Q0118-031A   | 1.445 | 18.35 | -    |      |
|                 | Q43 Q0118-018    | 1.911 | 19.45 | -    |      |
|                 | Q44 PB8737       | 1.165 | 18.45 | -    |      |
|                 | Q45 PB8736       | 2.112 | 19.00 | -    |      |
|                 | Q46 Q0118+003    | 0.328 | 19.11 | 0.28 |      |
|                 | Q47 NGC450 No217 | 0.135 | 18.75 | -    |      |
|                 | Q48 Q0119-009    | 1.943 | 19.30 | 0.20 |      |
|                 | Q49 Q0120-001    | 0.909 | 19.21 | 0.37 |      |
|                 | Q50 Q0120-029A   | 1.073 | 18.55 | -    |      |
|                 | Q51 Q0120-002    | 1.355 | 19.01 | 0.45 |      |
|                 | Q52 Q0120-029B   | 0.438 | 18.10 | -    |      |
|                 | Q53 Q0120+002    | 0.772 | 19.25 | -    |      |
|                 | Q54 Q0121+007    | 1.310 | 19.60 | -    |      |
|                 | Q55 Q0121+009    | 1.555 | 19.04 | 0.33 |      |
|                 | Q56 Q0121-008    | 2.252 | 19.30 | -    |      |
|                 | Q57 Q0121+008    | 2.043 | 19.50 | -    |      |
|                 | Q58 Q0121-022    | 0.988 | 19.05 | -    |      |
|                 | Q59 Q0122-028    | 2.022 | 19.50 | -    |      |
|                 | Q60 Q0123-005A   | 1.889 | 19.00 | -    |      |
|                 | Q61 Q0123-005B   | 1.763 | 18.90 | 0.26 |      |
|                 | Q62 UM322        | 1.930 | 18.40 | -    |      |
|                 | Q63 UM324        | 0.355 | 17.35 | -    |      |
| NGC470<br>0.008 | Q1=NGC470.68D    | 1.533 | 18.50 | -    | [71] |
|                 | Q2 =NGC470.68    | 1.875 | 19.80 | -    |      |
| NGC520          |                  |       |       |      |      |

|                  |                      |       |       |      |           |
|------------------|----------------------|-------|-------|------|-----------|
| 0.008            | Q1=NGC520.D9         | 1.670 | 18.60 | -    | [72]      |
|                  | Q2 =NGC520.D2        | 0.311 | 18.90 | -    |           |
|                  | Q3 NGC520.192        | 2.000 | 20.20 | -    |           |
|                  | Q4 NGC520.D5         | 1.609 | 19.80 | -    |           |
|                  | Q5 NGC520.D8         | 2.090 | 19.30 | -    |           |
|                  | Q6 NGC520.57         | 1.902 | 19.20 | -    |           |
| NGC613<br>0.005  | Q1 = 2QZJ013356-2922 | 2.222 | 20.09 | -    | [73]      |
|                  | Q2 = 2QZJ013445-2928 | 2.059 | 20.32 | -    |           |
|                  | Q3 2QZJ013454-2925   | 2.062 | 20.01 | -    |           |
|                  | Q4 2QZJ013348-2920   | 1.855 | 20.30 | -    |           |
|                  | Q5 2QZJ013345-2917   | 1.413 | 20.50 | -    |           |
|                  | Q6 2QZJ013508-2930   | 1.482 | 20.31 | -    |           |
| NGC622<br>0.017  | Q1 = NGC622 UB1      | 0.910 | 18.36 | 0.32 | [73]      |
|                  | Q2 = NGC622 BS01     | 1.460 | 19.13 | 0.20 |           |
| NGC936<br>0.005  | Q1 = PKS0225-014     | 2.042 | 18.60 | -    | [73] [74] |
|                  | Q2 = SDSSJ02274-0106 | 2.176 | 18.84 | 0.37 |           |
|                  | Q3 NGC936UB1         | 1.130 | 19.13 | 0.30 |           |
| NGC1068<br>0.003 | Q1 = RXSJ02393-0001  | 0.261 | 15.48 | 0.30 | [75]      |
|                  | Q2 = Q0238-0001      | 0.468 | 19.07 | 0.24 |           |
|                  | Q3 Q0238-0058        | 0.726 | 18.52 | 0.19 |           |
|                  | Q4 Q0239-0008        | 0.649 | 18.72 | 0.12 |           |
|                  | Q5 Q0239+0021        | 1.054 | 18.92 | 0.30 |           |
|                  | Q6 Q0239-0005        | 1.552 | 18.47 | 0.25 |           |
|                  | Q7 Q0239-0012        | 1.112 | 18.70 | 0.00 |           |
|                  | Q8 1WGAJ0242.1+0000  | 0.385 | 19.67 | 0.31 |           |
|                  | Q9 Q0240-0012        | 2.018 | 18.45 | 0.28 |           |
|                  | Q10 Q0241+0005       | 0.684 | 18.92 | 0.17 |           |
|                  | Q11 1WGAJ0245.5-0007 | 0.655 | 18.91 | 0.09 |           |
|                  | Q12 1WGA 0242.6+0022 | 0.630 | 20.33 | 0.03 |           |
|                  | Q13 US3137           | 1.139 | 18.44 | 0.34 |           |
|                  | Q14 US3139           | 1.292 | 18.75 | 0.41 |           |
|                  | Q15 US3146           | 1.815 | 18.63 | 0.19 |           |
|                  | Q16 Q0244-0015       | 2.315 | 20.16 | 0.20 |           |
| NGC1073<br>0.004 | Q1 = NGC1073U2       | 0.601 | 19.00 | -    | [76] [77] |
|                  | Q2 = PKS0241+011     | 1.400 | 20.30 | -    |           |
|                  | Q3 NGC1073U1         | 1.941 | 19.60 | -    |           |
|                  | Q4 US3115            | 0.546 | 19.18 | 0.13 |           |
| NGC1097<br>0.004 | Q2 = Q0238-315       | 2.143 | 19.60 | -    | [45]      |
|                  | Q3 = Q0238-301       | 2.265 | 18.30 | -    |           |

|                   |                  |       |       |      |           |
|-------------------|------------------|-------|-------|------|-----------|
|                   | Q6 Q0238-310     | 2.034 | 19.50 | -    |           |
|                   | Q7 Q0240-309     | 0.374 | 18.50 | -    |           |
|                   | Q9 Q0241-316     | 1.588 | 19.90 | -    |           |
|                   | Q10 Q0241-302    | 0.359 | 19.50 | -    |           |
|                   | Q12 Q0242.0-3104 | 0.874 | 19.10 | -    |           |
|                   | Q13 Q0242.1-3104 | 1.985 | 19.60 | -    |           |
|                   | Q14 Q0242-305    | 1.045 | 18.80 | -    |           |
|                   | Q15 Q0242.9-3010 | 2.269 | 19.90 | -    |           |
|                   | Q16 Q0242.9-3009 | 0.783 | 19.60 | -    |           |
|                   | Q18 Q0243.5-2946 | 1.577 | 20.20 | -    |           |
|                   | Q19 Q0243.6-2947 | 2.063 | 20.10 | -    |           |
|                   | Q20 Q0243-308    | 0.088 | 20.00 | -    |           |
|                   | Q21 Q0243-318    | 1.875 | 18.50 | -    |           |
|                   | Q23 QN1097.3     | 1.000 | 17.50 | -    |           |
|                   | Q24 QN1097.4     | 0.340 | 18.20 | -    |           |
|                   | Q25 QN1097.6     | 1.100 | 20.50 | -    |           |
|                   | Q26 QN1097.5     | 0.887 | 20.00 | -    |           |
| NGC2639<br>0.011  | Q1 = NGC2639U1   | 1.177 | 18.06 | 0.29 | [50] [78] |
|                   | Q2 = NGC2639U2   | 1.105 | 19.16 | 0.36 |           |
|                   | Q3 NGC2639U3     | 1.522 | 19.43 | 0.33 |           |
|                   | Q4 NGC2639U4     | 0.780 | 18.87 | 0.49 |           |
|                   | Q5 NGC2639U5     | 1.494 | 17.92 | 0.55 |           |
|                   | Q7 NGC2639U7     | 2.000 | 19.37 | 0.37 |           |
|                   | Q8 NGC2639U8     | 2.800 | 19.00 | 0.32 |           |
|                   | Q10 NGC2639U10   | 0.305 | 17.80 | 0.22 |           |
|                   | Q14 NGC2639U14   | 2.124 | 18.74 | 0.31 |           |
|                   | Q15 NGC2639U15   | 1.525 | 18.78 | 0.22 |           |
|                   | Q16 NGC2639 No3  | 0.323 | 18.40 | 0.17 |           |
| NGC2683<br>0.0014 | Q1= NGC2683U3    | 1.252 | 19.04 | 0.31 | [79]      |
|                   | Q2 =NGC2683U2    | 1.262 | 19.65 | 0.55 |           |
|                   | Q3 NGC2683U8     | 0.065 | 18.60 | -    |           |
|                   | Q4 NGC2683U1     | 0.621 | 17.79 | 0.15 |           |
| NGC2841<br>0.0021 | Q1= NGC2841UB2   | 0.120 | 18.70 | -    | [80]      |
|                   | Q2 =NGC2841UB1   | 2.028 | 19.28 | 0.21 |           |
| NGC2859<br>0.0056 | Q1= NGC2859U1    | 0.230 | 18.74 | 0.41 | [81]      |
|                   | Q2 =NGC2859U2    | 2.250 | 19.70 | -    |           |
|                   | Q3 NGC2859U3     | 1.460 | 20.30 | -    |           |
|                   | Q6 NGC2859U6     | 0.027 | 18.50 | -    |           |
| NGC2916<br>0.0124 | Q1= NGC2916UB5   | 1.546 | 19.23 | 0.35 | [80]      |
|                   | Q2 =NGC2916UB1   | 0.238 | 19.20 | -    |           |

|                   |                      |       |       |      |      |
|-------------------|----------------------|-------|-------|------|------|
|                   | Q3 NGC2916UB2        | 0.793 | 19.00 | -    |      |
|                   | Q4 NGC2916UB4        | 1.868 | 19.35 | 0.13 |      |
|                   | Q5 NGC2916UB3        | 1.279 | 19.09 | 0.43 |      |
| NGC3034<br>0.001  | = M82                |       |       |      |      |
|                   | Q1 = M82 No95        | 1.010 | 19.44 | 0.36 | [82] |
|                   | Q2 = Hoag 1          | 2.048 | 19.50 | 0.30 |      |
|                   | Q3 Hoag 2            | 2.054 | 20.33 | 0.22 |      |
|                   | Q4 NGC3031U4         | 0.85  | 20.12 | 0.70 |      |
|                   | Q5 Hoag 3            | 2.040 | 20.31 | 0.16 |      |
|                   | Q6 Bol 105           | 2.240 | 21.40 | -    |      |
|                   | Q7 M82 No69          | 0.930 | 19.38 | 0.70 |      |
|                   | Q8 M82 No22          | 0.960 | 19.04 | 1.31 |      |
|                   | Q9 Bol 75            | 0.740 | 22.00 | -    |      |
|                   | Q10 Dahlem 7         | 0.675 | 19.80 | -    |      |
|                   | Q11 Dahlem 12        | 0.626 | 18.90 | -    |      |
|                   | Q12 Dahlem 17        | 1.086 | 17.99 | 0.33 |      |
| NGC3079<br>0.004  | Q1 = SBS0953+556     | 1.410 | 18.45 | 0.17 | [83] |
|                   | Q2 = 4C55.17         | 0.898 | 17.89 | 0.35 |      |
|                   | Q3 SBS0955+560       | 1.021 | 17.68 | 0.47 |      |
|                   | Q4 RXJ10005+5536     | 0.215 | 19.37 | 0.62 |      |
|                   | Q5 1WGAJ1000.9+5541  | 1.037 | 19.99 | 0.57 |      |
|                   | Q6 NGC3073UB1        | 1.530 | 19.04 | 0.32 |      |
|                   | Q7 ASV1              | 0.072 | 17.28 | -    |      |
|                   | Q8 SBS0957+557       | 2.102 | 17.60 | -    |      |
|                   | Q9 Q0957+561A        | 1.413 | 16.95 | 0.21 |      |
|                   | Q10 Q0957+561B       | 1.415 | 16.95 | 0.21 |      |
|                   | Q11 ASV24            | 1.154 | 23.03 | -    |      |
|                   | Q12 ASV31            | 0.352 | 21.14 | -    |      |
|                   | Q13 MARK132          | 1.760 | 16.05 | 0.28 |      |
|                   | Q14 NGC3073UB4       | 1.154 | 18.38 | 0.38 |      |
|                   | Q15 1WGAJ1002.7+5558 | 0.219 | 21.20 | -    |      |
|                   | Q16 Q0958+5625       | 3.216 | 20.08 | -    |      |
| NGC3184<br>0.002  | Q1 = NGC3184UB4      | 0.675 | 18.23 | 0.13 | [80] |
|                   | Q2 = NGC3184UB3      | 0.920 | 19.21 | 0.35 |      |
|                   | Q3 NGC3184UB1        | 0.152 | 17.70 | -    |      |
| NGC3384<br>0.0023 | Q1= NGC3384U1        | 0.442 | 19.31 | 0.19 | [84] |
|                   | Q2 = NGC3384U2       | 1.280 | 19.27 | 0.34 |      |
|                   | Q4 NGC3384U4         | 1.107 | 19.06 | 0.25 |      |
|                   | Q5 NGC3384U5         | 1.192 | 20.00 | -    |      |
|                   | Q8 NGC3384U8         | 1.134 | 18.56 | 0.45 |      |
|                   | Q13 NGC3384U13       | 0.497 | 19.57 | 0.43 |      |
|                   | Q14 NGC3384U14       | 0.520 | 19.94 | 0.21 |      |

|                   |                       |       |       |      |           |
|-------------------|-----------------------|-------|-------|------|-----------|
|                   | Q15 NGC3384U15        | 1.131 | 19.76 | 0.44 |           |
| NGC3516<br>0.009  | Q1= 1WGAJ1107.7+7232  | 2.100 | 18.50 | -    | [85]      |
|                   | Q2 =1WGAJ1105.4+7238  | 1.399 | 20.00 | -    |           |
|                   | Q3 1WGAJ1105.1+7242   | 0.930 | 20.00 | -    |           |
|                   | Q4 1WGAJ1106.2+7244   | 0.690 | 19.10 | -    |           |
|                   | Q5 1WGAJ1108.5+7226   | 0.328 | 20.20 | -    |           |
|                   | Q6 NGC3516U2          | 1.710 | 18.60 | -    |           |
| NGC3628<br>0.003  | Q1 = Wee 47           | 1.413 | 19.06 | 0.26 | [46]      |
|                   | Q2 = Wee 48           | 2.060 | 18.91 | 0.26 |           |
|                   | Q3 Wee 50             | 1.750 | 19.58 | 0.18 |           |
|                   | Q4 Wee 51             | 2.150 | 19.44 | 0.29 |           |
|                   | Q8 Wee 52             | 2.430 | 20.97 | 0.24 |           |
|                   | Q9 Wee 55             | 1.940 | 19.06 | 0.26 |           |
|                   | Q10 Wee 36            | 2.490 | 20.70 | -    |           |
|                   | Q11 Wee 38            | 2.370 | 20.05 | 0.48 |           |
|                   | Q12 Wee 45            | 2.100 | 20.12 | 0.08 |           |
|                   | Q13 Wee 37            | 2.140 | 20.02 | 0.55 |           |
|                   | Q14 Wee 40            | 1.740 | 20.09 | 0.13 |           |
|                   | Q15 Wee 34            | 2.320 | 17.85 | 0.65 |           |
|                   | Q16 Wee 46            | 0.060 | 20.20 | -    |           |
|                   | Q17 Wee 41            | 2.540 | 20.02 | 0.25 |           |
|                   | Q18 Wee 44            | 2.380 | 19.57 | 0.25 |           |
|                   | Q19 Wee 42            | 2.110 | 20.97 | 0.16 |           |
|                   | Q20 Wee 43            | 3.009 | 19.83 | 0.33 |           |
| NGC3842<br>0.0211 | Q1= Q1141+2013        | 0.335 | 18.50 | -    | [86] [87] |
|                   | Q2 = Q1141+2014       | 0.946 | 19.08 | 0.24 |           |
|                   | Q3 Q1141+2012         | 2.200 | 20.18 | 0.25 |           |
| NGC4235<br>0.007  | Q1 = PG1216+069       | 0.334 | 15.65 | -    | [78]      |
|                   | Q2 = 1ES1212+078 (BL) | 0.137 | 16.00 | -    |           |
| NGC4258<br>0.002  | Q1 = QJ1218+472       | 0.398 | 19.88 | 0.21 | [49]      |
|                   | Q2 = QJ1219+473       | 0.654 | 19.43 | 0.17 |           |
| NGC4410<br>0.025  | Q1 = SDSSJ12260+0853  | 2.237 | 19.57 | 0.27 | [47]      |
|                   | Q2 = SDSSJ12260+0912  | 0.662 | 19.24 | 0.09 |           |
|                   | Q3 SDSSJ12255+0859    | 1.903 | 19.57 | 0.21 |           |
|                   | Q5 Q1222+0901         | 0.535 | 17.29 | 0.10 |           |
|                   | Q6 SDSSJ12273+0923    | 1.776 | 19.39 | 0.13 |           |
|                   | Q8 2E1225+0858        | 0.085 | 16.64 | 0.38 |           |
|                   | Q9 SDSSJ12281+0915    | 1.590 | 20.03 | 0.45 |           |
|                   | Q10 SDSSJ12279+0922   | 1.502 | 18.82 | 0.26 |           |

|                  |                     |       |       |      |      |
|------------------|---------------------|-------|-------|------|------|
|                  | Q11 SDSSJ12261+0935 | 0.628 | 19.33 | 0.12 |      |
|                  | Q12 SDSSJ12238+0856 | 1.043 | 18.74 | 0.30 |      |
|                  | Q13 SDSSJ12235+0902 | 1.363 | 19.24 | 0.34 |      |
|                  | Q15 Q1225+0836      | 1.471 | 17.59 | 0.30 |      |
|                  | Q16 SDSSJ12178+0913 | 1.076 | 19.48 | 0.21 |      |
|                  | Q17 SDSSJ12240+0935 | 1.345 | 19.32 | 0.24 |      |
|                  | Q18 SDSSJ12230+0856 | 1.090 | 19.12 | 0.34 |      |
|                  | Q19 SDSSJ12231+0914 | 1.715 | 19.49 | 0.09 |      |
|                  | Q20 Q1220+0939      | 0.681 | 17.74 | 0.09 |      |
|                  | Q21 SDSSJ12291+0938 | 2.649 | 20.08 | 0.33 |      |
|                  | Q22 SDSSJ12227+0853 | 0.773 | 18.78 | 0.15 |      |
|                  | Q23 SDSSJ12281+0951 | 0.064 | 17.72 | 0.65 |      |
|                  | Q24 Q1222+1010      | 0.398 | 18.58 | 0.12 |      |
|                  | Q25 SDSSJ12250+0955 | 1.429 | 19.04 | 0.26 |      |
| NGC4579<br>0.005 | Q2 = Q1234+1217     | 0.662 | 18.61 | 0.11 | [88] |
| NGC5548<br>0.017 | Q1 = QJ14172+2534   | 0.852 | 18.40 | -    | [48] |
|                  | Q2 = EXO1415.2+2607 | 0.184 | 18.03 | 0.32 |      |
|                  | Q3 QJ14182+2500     | 0.727 | 18.90 | -    |      |
|                  | Q4 Q1408.0+2696     | 2.425 | 19.08 | 0.20 |      |
|                  | Q5 Q1408.3+2626     | 2.100 | 20.22 | 0.52 |      |
|                  | Q6 Q1408.7+2665     | 1.928 | 18.74 | 0.22 |      |
|                  | Q7 FIRSTJ14162+2649 | 2.297 | 19.00 | 0.43 |      |
|                  | Q8 Q14144+256       | 1.800 | 20.50 | 0.18 |      |
|                  | Q9 Q14148+252       | 1.830 | 20.71 | 0.15 |      |
|                  | Q10 Q14149+251      | 1.917 | 18.86 | 0.22 |      |
|                  | Q11 2E1414+2513     | 1.057 | 19.50 | 0.46 |      |
|                  | Q12 1E14151+254     | 0.560 | 19.50 | 0.24 |      |
|                  | Q13 Q14151+254      | 2.310 | 19.57 | 0.35 |      |
|                  | Q14 HS1415+2701     | 2.500 | 17.70 | 0.46 |      |
|                  | Q15 2E1415+2557     | 0.237 | 17.20 | 0.80 |      |
|                  | Q16 2E1416+2523     | 0.674 | 18.70 | -    |      |
|                  | Q17 HS1417+2547     | 2.200 | 18.10 | 0.52 |      |
|                  | Q18 KUV14189+2552   | 1.053 | 16.06 | 0.33 |      |
|                  | Q19 RXSJ14215+2408  | 0.084 | 17.27 | 0.30 |      |
|                  | Q20 PKS1423+24      | 0.649 | 17.26 | 0.36 |      |
| NGC5985<br>0.008 | Q1 = SBS1537+595    | 2.125 | 19.00 | 0.14 | [41] |
|                  | Q2 = SBS1535+596    | 1.968 | 18.66 | 0.29 |      |
|                  | Q3 HS1543+5921      | 0.807 | 17.63 | 0.28 |      |
|                  | Q4 SBS1532+598      | 0.690 | 17.57 | 0.19 |      |
|                  | Q5 SBS1549+590      | 0.348 | 17.42 | 0.21 |      |
|                  | Q6 SBS1533+588      | 1.895 | 18.39 | 0.19 |      |
| NGC6212          |                     |       |       |      |      |

|          |                        |       |       |      |      |
|----------|------------------------|-------|-------|------|------|
| 0.030    | Q1=Q1636.8+3956        | 1.864 | 19.82 | 0.24 | [61] |
|          | Q2 = Q1636.9+4004      | 2.010 | 21.30 | 0.16 |      |
|          | Q3 Q1637.1+4008        | 1.898 | 19.63 | 0.43 |      |
|          | Q4 Q1637.6+3910        | 0.461 | 17.43 | 0.29 |      |
|          | Q5 FIRSTJ16395+3908    | 0.143 | 18.38 | 0.43 |      |
|          | Q6 Q1638.0+3938        | 0.030 | 17.80 | -    |      |
|          | Q7 Q1638.2+4019        | 1.965 | 19.20 | -    |      |
|          | Q8 Q1638.8+4012        | 1.183 | 20.40 | 0.21 |      |
|          | Q9 NRAO 512            | 1.666 | 19.37 | -    |      |
|          | Q10 Q1639.4+4006       | 2.253 | 19.08 | 0.19 |      |
|          | Q11 Q1638.9+4002       | 1.625 | 18.60 | 0.19 |      |
|          | Q12 Q1639.8+3940       | 2.614 | 19.09 | 0.16 |      |
|          | Q13 MS16400+3940       | 0.540 | 19.83 | 0.18 |      |
|          | Q14 2E1640+4007        | 1.005 | 18.05 | 0.24 |      |
|          | Q15 Q1640.5+397        | 0.625 | 20.51 | 0.08 |      |
|          | Q16 Q1640.8+401        | 2.529 | 20.32 | 0.34 |      |
|          | Q17 Q1640.8+398        | 1.860 | 18.85 | 0.36 |      |
|          | Q18 Q1640.9+4048       | 1.580 | 20.85 | 0.33 |      |
|          | Q19 Q1640.9+401        | 1.595 | 19.62 | 0.26 |      |
|          | Q20 Q1640.9+395        | 1.466 | 19.47 | 0.34 |      |
|          | Q21 Q1640.0+397        | 1.414 | 20.00 | 0.33 |      |
|          | Q22 SDSSJ16428+3924    | 2.384 | 19.27 | 0.22 |      |
|          | Q23 3C345.0            | 0.595 | 16.59 | 0.22 |      |
|          | Q24 Q1641.4+4049       | 1.360 | 18.24 | 0.26 |      |
|          | Q25 Q1641.5+399        | 2.000 | 20.01 | 0.19 |      |
|          | Q26 Q1641.6+4060       | 2.260 | 20.02 | 0.35 |      |
|          | Q27 Q1641.6+398        | 2.000 | 20.82 | 0.27 |      |
|          | Q28 Q1641.7+396        | 0.443 | 19.30 | 0.00 |      |
|          | Q29 E1641.7+3998       | 0.704 | 18.32 | 0.12 |      |
|          | Q30 Q1641.8+399        | 1.083 | 19.06 | 0.26 |      |
|          | Q31 Q1641.9+401        | 2.113 | 19.31 | 0.24 |      |
|          | Q32 E1641+399          | 0.594 | 19.50 | 0.06 |      |
|          | Q33 Q1642.0+4015       | 1.358 | 18.55 | 0.36 |      |
|          | Q34 Q1642.0+395        | 0.434 | 19.39 | 0.17 |      |
|          | Q35 Q1642.6+400        | 1.377 | 19.45 | 0.30 |      |
|          | Q36 Q1642.7+4016       | 0.608 | 19.13 | 0.02 |      |
|          | Q37 Q1643.0+4006       | 1.268 | 19.31 | 0.51 |      |
|          | Q39 Q1643.1+4062       | 1.451 | 19.04 | 0.17 |      |
|          | Q40 Q1643.5+401        | 1.877 | 19.49 | 0.11 |      |
|          | Q41 Q1643.3+395        | 2.145 | 19.61 | 0.33 |      |
|          | Q42 RXSJ16464+3929     | 0.100 | 17.60 | 0.24 |      |
| NGC6217  |                        |       |       |      |      |
| 0.005    | Q1 = 1WG AJ1630.9+7810 | 0.358 | 20.60 | -    | [89] |
|          | Q2 = 1WG AJ1634.4+7809 | 0.376 | 20.80 | -    |      |
| IC4553 = | Arp 220                |       |       |      |      |

|                         |                        |       |       |      |           |
|-------------------------|------------------------|-------|-------|------|-----------|
| 0.018                   | Q1 = 1WGAJ1533.8+2356  | 0.232 | 18.37 | 0.42 | [90]      |
|                         | Q2 = Q1532+2332 (Arp9) | 1.249 | 19.82 | -    |           |
|                         | Q3 1WGAJ1535.0+2336    | 1.258 | 20.52 | 0.70 |           |
|                         | Q4 1WGAJ1537.2+2300    | 0.463 | 19.20 | 0.12 |           |
| Mark231<br>0.042        | Q1= 3C277.1            | 0.320 | 18.11 | 0.31 | [91] [92] |
|                         | Q2= RXJ12548+5644      | 0.124 | 17.20 | -    |           |
|                         | Q3 RXJ12549+5649       | 1.272 | 20.87 | 0.46 |           |
|                         | Q4 J12550+5649         | 1.232 | 19.76 | 0.33 |           |
|                         | Q5 J12554+5656         | 1.190 | 19.51 | 0.26 |           |
|                         | Q6 J13005+5728         | 0.330 | 18.83 | 0.18 |           |
|                         | Q7 SBS1258+569         | 0.072 | 17.35 | 0.28 |           |
| Mark273<br>0.037        | Q1 = J13416+5514       | 0.207 | 18.46 | 0.85 | [91] [92] |
|                         | Q2 = SBS1342+560       | 0.941 | 17.67 | 0.26 |           |
|                         | Q3 Mark273X            | 0.458 | 20.80 | -    |           |
|                         | Q4 J1345.1+5547        | 1.166 | 18.78 | 0.36 |           |
|                         | Q5 J1346.0+5604        | 0.486 | 19.48 | 0.09 |           |
|                         | Q6 J13469+5607         | 0.377 | 19.45 | 0.36 |           |
| AM2230<br>-284<br>0.064 | Q1 = 2QZJ223105-2926   | 2.141 | 19.93 | -    | [93]      |
|                         | Q2 = 2QZJ223119-2816   | 2.152 | 20.67 | -    |           |
|                         | Q3 2QZJ223155-2859     | 2.165 | 19.51 | -    |           |
|                         | Q4 2QZJ223231-2818     | 2.161 | 20.15 | -    |           |
|                         | Q5 2QZJ223233-2841     | 2.155 | 19.93 | -    |           |
|                         | Q6 2QZJ223341-2807     | 2.134 | 20.49 | -    |           |
|                         | Q7 2QZJ223337-2822     | 2.133 | 20.48 | -    |           |
|                         | Q8 2QZJ223349-2909     | 2.154 | 20.33 | -    |           |
|                         | Q10 2QZJ223426-2907    | 2.155 | 20.76 | -    |           |
|                         | Q11 2QZJ223552-2811    | 2.136 | 20.39 | -    |           |
|                         | Q12 2QZJ223716-2832    | 2.168 | 20.83 | -    |           |
|                         | Q13 2QZJ223755-2822    | 2.139 | 20.00 | -    |           |
|                         | Q14 2QZJ223755-2901    | 2.137 | 20.36 | -    |           |

In the following, assumptions will be made in order to determine physical characteristics of local quasars. Here is the summary:

- The sample of QSOs (Table 1) consists of groups of quasars spatially associated with respective low redshift (parent) galaxy, according to published studies;
- The observed redshift of each quasar is considered to be composed by three components, according to eq (1);
- The component of cosmological redshift of each quasar is taken to be the redshift of the respective parent galaxy;
- Quasars are single bodies and they have thermal outer layer;

- The intrinsic redshift of each quasar is due to gravitational reddening. For local quasars it is the largest component in each observed redshift;
- Gravitational redshifts are quantized, according to the Karlsson sequence.

The reality of these assumptions will be tested with the results and the relations obtained. A single failure of the above assumptions will lead to inconsistent results. The radii of local quasars could be obtained from:

$$\log (r_q/r_o) = 1/2 \log (L_q/L_o) + 2 \cdot \log (T_o/T_q) \quad (4)$$

In eq (4),  $r$ ,  $L$ , and  $T$  are the radius, luminosity, and the temperature, respectively. Subscripts “q” and “o” denote quasar and Sun, respectively.

Implementation of eq (4) supposes the existence of a thermal outer layer. It could also be expected that large redshifts in the quasars’ spectra could lead to errors in determination of the radii. The effects of the redshifts on radii determination are difficult to assess and their influence on the results will be judged by the consistency of the results. We could further determine the ratio  $r_{gr}/r_q$ , where  $r_{gr}$  is the gravitational radius of each quasar from:

$$1 + z_{gr} = (1 - r_{gr}/r_q)^{-1/2} \quad (5)$$

Substituting respective  $z_{gr}$  and the  $r_q$  for each quasar we can get the quasar gravitational radius  $r_{gr}$ . The quasar mass  $m_q$  can further be obtained from:

$$r_{gr} = 2Gm_q/c^2 \quad (6)$$

Here  $G$  and  $c$  are the gravitational constant and the velocity of light. It is now possible to obtain also the quasar density  $\rho_q$ . Redshifts, magnitudes, and colours for quasars are taken from Veron-Cetty and Veron, 13<sup>th</sup> ed. [69]. For all quasars with unknown colour B-V quasar radii are determined from the relation “absolute mag – radius” [25], obtained with a sample of QSOs with known B-V:

$$M_q = 48.099 - 4.318 \cdot \log r_q \quad (7)$$

Clearly, if we assume that gravitational reddening is the main contribution to the local quasars’ redshifts, relation between quasar density and gravitational redshifts has to be expected. Using simple physical relations in [25] was established the relation between quasar density and its gravitational redshift as:

$$\rho_q = 3/(8\pi) \cdot c^2/G \cdot 1/r_q^2 \cdot \{1 - 1/(1 + z_{gr})^2\} \quad (8)$$

In the eq (8) quasar density depends also on the inverse square of quasar radius. In order to avoid the dependence on radius, it is possible to introduce another density function, the “reduced density” [25]. Reduced density is the density reduced to some radius of choice (reference), e.g.  $r_q = 8 \cdot 10^{13}$  cm. It should be noted that the choice of this radius is

not essential for the conclusions that follow. Therefore, the reduced density function  $\rho\tilde{}$  could be defined by:

$$\rho\tilde{=} (r_q/8.10^{13})^2 \cdot \rho_q \quad (9)$$

With that definition of reduced density by substituting eq (9) in eq (8) we get:

$$\rho\tilde{=} 3/(8\pi) \cdot c^2/G \cdot 1/(8.10^{13})^2 \cdot \{1 - 1/(1 + z_{gr})^2\} \quad (10)$$

Eq (10) is the same as eq (8) but with fixed radius  $r_q = 8.10^{13}$  cm. In Table 2 physical characteristics data are listed for the sample quasars of Table 1.

**Table 2. Physical characteristics of 341 sample quasars. Columns are: 1 – ID of quasar, according to Table 1; 2 – observed redshift; 3 – gravitational redshift; 4 - Doppler shift; 5 – absolute magnitude; 6 – radius, log  $r_q$  [cm]; 7 – luminosity, log  $L_q$  [erg/s]; 8 – mass, log  $m_q$  [g]; 9 – density  $\rho_q$  [g/cm<sup>3</sup>]; 10 – reduced density [g/cm<sup>3</sup>] to a radius of  $8.10^{13}$  cm; 11 – ratio  $r_{gr}/r_q$ ; 12 – quasar mass in units of  $10^6$  solar masses.**

| <i>1</i> | <i>2</i> | <i>3</i> | <i>4</i> | <i>5</i> | <i>6</i> | <i>7</i> | <i>8</i> | <i>9</i> | <i>10</i> | <i>11</i> | <i>12</i> |
|----------|----------|----------|----------|----------|----------|----------|----------|----------|-----------|-----------|-----------|
|          | NGC 007  |          |          |          |          |          |          |          |           |           |           |
| Q1       | 2.062    | 1.96     | 0.029    | -12.17   | 13.958   | 40.344   | 41.734   | 0.173    | 0.223     | 0.89      | 270.9     |
| Q2       | 2.041    | 1.96     | 0.022    | -10.96   | 13.677   | 39.860   | 41.454   | 0.630    | 0.223     | 0.89      | 142.1     |
| Q3       | 1.591    | 1.41     | 0.070    | -11.47   | 13.796   | 40.064   | 41.542   | 0.342    | 0.208     | 0.83      | 174.3     |
|          | NGC 450  |          |          |          |          |          |          |          |           |           |           |
| Q1       | 1.968    | 1.96     | -0.003   | -12.62   | 13.947   | 40.524   | 41.723   | 0.182    | 0.223     | 0.89      | 264.5     |
| Q2       | 0.958    | 0.96     | -0.007   | -13.71   | 14.314   | 40.960   | 42.012   | 0.028    | 0.186     | 0.74      | 515       |
| Q3       | 0.728    | 0.60     | 0.074    | -12.66   | 14.071   | 40.540   | 41.685   | 0.071    | 0.154     | 0.61      | 242       |
| Q4       | 0.956    | 0.96     | -0.008   | -13.91   | 14.361   | 41.040   | 42.059   | 0.023    | 0.188     | 0.74      | 570       |
| Q5       | 1.893    | 1.96     | -0.028   | -12.06   | 13.932   | 40.300   | 41.708   | 0.195    | 0.223     | 0.89      | 255.5     |
| Q6       | 0.070    | 0.06     | 0.004    | -12.61   | 14.060   | 40.520   | 40.930   | 0.013    | 0.027     | 0.11      | 42.6      |
| Q7       | 0.468    | 0.60     | -0.088   | -12.13   | 13.694   | 40.328   | 41.308   | 0.402    | 0.153     | 0.61      | 101.5     |
| Q8       | 1.424    | 1.41     | 0.0      | -12.28   | 14.174   | 40.388   | 41.921   | 0.060    | 0.208     | 0.83      | 416.5     |
| Q9       | 2.005    | 1.96     | 0.009    | -13.26   | 14.210   | 40.780   | 41.986   | 0.054    | 0.222     | 0.89      | 484.5     |
| Q10      | 1.240    | 1.41     | -0.076   | -13.41   | 14.245   | 40.840   | 41.992   | 0.043    | 0.208     | 0.83      | 490.5     |
| Q11      | 1.302    | 1.41     | -0.051   | -11.91   | 13.897   | 40.240   | 41.644   | 0.214    | 0.209     | 0.83      | 220.5     |
| Q12      | 1.003    | 0.96     | 0.016    | -12.84   | 14.053   | 40.612   | 41.751   | 0.093    | 0.186     | 0.74      | 281.5     |
| Q13      | 1.758    | 1.96     | -0.074   | -13.14   | 14.113   | 40.732   | 41.889   | 0.085    | 0.224     | 0.89      | 387.5     |
| Q14      | 1.896    | 1.96     | -0.027   | -12.22   | 13.879   | 40.364   | 41.655   | 0.249    | 0.223     | 0.89      | 226       |
| Q15      | 1.102    | 0.96     | 0.066    | -14.21   | 14.430   | 41.160   | 42.128   | 0.016    | 0.181     | 0.74      | 670       |
| Q16      | 0.238    | 0.30     | -0.053   | -13.66   | 14.243   | 40.940   | 41.682   | 0.022    | 0.105     | 0.41      | 240.5     |
| Q17      | 0.910    | 0.96     | -0.031   | -11.43   | 13.709   | 40.048   | 41.407   | 0.455    | 0.186     | 0.74      | 130       |
| Q18      | 0.976    | 0.96     | 0.002    | -12.96   | 14.141   | 40.660   | 41.839   | 0.062    | 0.184     | 0.74      | 345       |



|     |       |      |        |        |        |        |        |       |       |      |       |
|-----|-------|------|--------|--------|--------|--------|--------|-------|-------|------|-------|
|     | 470   |      |        |        |        |        |        |       |       |      |       |
| Q1  | 1.533 | 1.41 | 0.043  | -14.50 | 14.497 | 41.276 | 42.244 | 0.014 | 0.208 | 0.83 | 877   |
| Q2  | 1.875 | 1.96 | -0.036 | -13.20 | 14.196 | 40.756 | 41.972 | 0.058 | 0.223 | 0.89 | 469.2 |
|     | NGC   |      |        |        |        |        |        |       |       |      |       |
|     | 520   |      |        |        |        |        |        |       |       |      |       |
| Q1  | 1.670 | 1.41 | 0.099  | -13.62 | 14.293 | 40.924 | 42.040 | 0.035 | 0.208 | 0.83 | 548.5 |
| Q2  | 0.311 | 0.30 | 0.001  | -13.32 | 14.224 | 40.804 | 41.664 | 0.023 | 0.103 | 0.41 | 230.6 |
| Q3  | 2.000 | 1.96 | 0.005  | -12.02 | 13.923 | 40.284 | 41.699 | 0.203 | 0.223 | 0.89 | 250.1 |
| Q4  | 1.609 | 1.41 | 0.074  | -12.42 | 14.016 | 40.444 | 41.762 | 0.124 | 0.208 | 0.83 | 289.3 |
| Q5  | 2.090 | 1.96 | 0.035  | -12.92 | 14.131 | 40.644 | 41.908 | 0.078 | 0.223 | 0.89 | 404.2 |
| Q6  | 1.902 | 1.96 | -0.027 | -13.02 | 14.154 | 40.684 | 41.931 | 0.070 | 0.223 | 0.89 | 426.3 |
|     | NGC   |      |        |        |        |        |        |       |       |      |       |
|     | 613   |      |        |        |        |        |        |       |       |      |       |
| Q1  | 2.222 | 1.96 | 0.083  | -10.32 | 13.529 | 39.604 | 41.305 | 1.247 | 0.223 | 0.89 | 101   |
| Q2  | 2.059 | 1.96 | 0.028  | -10.09 | 13.476 | 39.512 | 41.252 | 1.593 | 0.223 | 0.89 | 89.5  |
| Q3  | 2.062 | 1.96 | 0.029  | -10.40 | 13.548 | 39.636 | 41.324 | 1.145 | 0.223 | 0.89 | 105.5 |
| Q4  | 1.855 | 1.96 | -0.041 | -10.11 | 13.481 | 39.520 | 41.257 | 1.560 | 0.223 | 0.89 | 90.5  |
| Q5  | 1.413 | 1.41 | -0.004 | -9.91  | 13.434 | 39.440 | 41.181 | 1.804 | 0.208 | 0.83 | 76    |
| Q6  | 1.482 | 1.41 | 0.025  | -10.10 | 13.478 | 39.516 | 41.225 | 1.473 | 0.208 | 0.83 | 84    |
|     | NGC   |      |        |        |        |        |        |       |       |      |       |
|     | 622   |      |        |        |        |        |        |       |       |      |       |
| Q1  | 0.910 | 0.96 | -0.042 | -15.79 | 14.714 | 41.792 | 42.412 | 0.004 | 0.167 | 0.74 | 1290  |
| Q2  | 1.460 | 1.41 | 0.004  | -15.02 | 14.415 | 41.484 | 42.162 | 0.020 | 0.212 | 0.83 | 726.5 |
|     | NGC   |      |        |        |        |        |        |       |       |      |       |
|     | 936   |      |        |        |        |        |        |       |       |      |       |
| Q1  | 2.042 | 1.96 | 0.023  | -12.96 | 14.141 | 40.660 | 41.917 | 0.075 | 0.223 | 0.89 | 412.9 |
| Q2  | 2.176 | 1.96 | 0.068  | -12.72 | 14.147 | 40.564 | 41.923 | 0.072 | 0.223 | 0.89 | 419.1 |
| Q3  | 1.130 | 0.96 | 0.081  | -12.43 | 14.023 | 40.448 | 41.721 | 0.107 | 0.186 | 0.74 | 263.2 |
|     | NGC   |      |        |        |        |        |        |       |       |      |       |
|     | 1068  |      |        |        |        |        |        |       |       |      |       |
| Q1  | 0.261 | 0.30 | -0.033 | -14.15 | 14.367 | 41.136 | 41.807 | 0.012 | 0.102 | 0.41 | 320.8 |
| Q2  | 0.468 | 0.60 | -0.085 | -10.56 | 13.572 | 39.700 | 41.186 | 0.705 | 0.153 | 0.61 | 76.7  |
| Q3  | 0.726 | 0.60 | 0.076  | -11.11 | 13.621 | 39.920 | 41.235 | 0.561 | 0.153 | 0.61 | 86    |
| Q4  | 0.649 | 0.60 | 0.028  | -10.91 | 13.495 | 39.840 | 41.109 | 1.005 | 0.153 | 0.61 | 64.2  |
| Q5  | 1.054 | 0.96 | 0.045  | -10.71 | 13.680 | 39.760 | 41.378 | 0.521 | 0.186 | 0.74 | 119.3 |
| Q6  | 1.552 | 1.41 | 0.056  | -11.16 | 13.704 | 39.940 | 41.451 | 0.521 | 0.208 | 0.83 | 141.3 |
| Q7  | 1.112 | 0.96 | 0.074  | -10.93 | 13.308 | 39.848 | 41.006 | 2.883 | 0.186 | 0.74 | 50.7  |
| Q8  | 0.385 | 0.30 | 0.062  | -9.96  | 13.538 | 39.460 | 40.978 | 0.552 | 0.103 | 0.41 | 47.5  |
| Q9  | 2.018 | 1.96 | 0.017  | -11.18 | 13.747 | 39.948 | 41.523 | 0.458 | 0.223 | 0.89 | 166.8 |
| Q10 | 0.684 | 0.60 | 0.049  | -10.71 | 13.518 | 39.760 | 41.132 | 0.901 | 0.153 | 0.61 | 67.8  |
| Q11 | 0.655 | 0.60 | 0.031  | -10.72 | 13.412 | 39.764 | 41.026 | 1.471 | 0.153 | 0.61 | 53.1  |
| Q12 | 0.630 | 0.60 | 0.016  | -9.30  | 13.045 | 39.196 | 40.659 | 7.961 | 0.153 | 0.61 | 22.8  |
| Q13 | 1.139 | 0.96 | 0.088  | -11.19 | 13.812 | 39.952 | 41.510 | 0.282 | 0.186 | 0.74 | 162   |
| Q14 | 1.292 | 1.41 | -0.052 | -10.88 | 13.819 | 39.828 | 41.566 | 0.306 | 0.208 | 0.83 | 184.1 |
| Q15 | 1.815 | 1.96 | -0.052 | -11.00 | 13.600 | 39.876 | 41.376 | 0.900 | 0.223 | 0.89 | 118.9 |
| Q16 | 2.315 | 2.64 | -0.092 | -9.47  | 13.305 | 39.264 | 41.100 | 3.653 | 0.233 | 0.92 | 62.9  |

|     |          |      |        |        |        |        |        |       |       |      |       |
|-----|----------|------|--------|--------|--------|--------|--------|-------|-------|------|-------|
|     | NGC 1073 |      |        |        |        |        |        |       |       |      |       |
| Q1  | 0.601    | 0.60 | -0.003 | -11.91 | 13.897 | 40.240 | 41.511 | 0.157 | 0.153 | 0.61 | 162.3 |
| Q2  | 1.400    | 1.41 | -0.008 | -10.61 | 13.596 | 39.720 | 41.343 | 0.855 | 0.208 | 0.83 | 110   |
| Q3  | 1.941    | 1.96 | -0.010 | -11.31 | 13.758 | 40.000 | 41.535 | 0.434 | 0.223 | 0.89 | 171   |
| Q4  | 0.546    | 0.60 | -0.038 | -11.73 | 13.674 | 40.168 | 41.288 | 0.441 | 0.153 | 0.61 | 97    |
|     | NGC 1097 |      |        |        |        |        |        |       |       |      |       |
| Q2  | 2.143    | 1.96 | 0.057  | -10.58 | 13.589 | 39.708 | 41.366 | 0.945 | 0.223 | 0.89 | 116.1 |
| Q3  | 2.265    | 1.96 | 0.099  | -11.88 | 13.890 | 40.228 | 41.667 | 0.236 | 0.223 | 0.89 | 232.1 |
| Q6  | 2.034    | 1.96 | 0.021  | -10.68 | 13.613 | 39.748 | 41.389 | 0.849 | 0.223 | 0.89 | 122.4 |
| Q7  | 0.374    | 0.30 | 0.053  | -11.68 | 13.844 | 40.148 | 41.284 | 0.135 | 0.103 | 0.41 | 96.2  |
| Q9  | 1.588    | 1.41 | 0.070  | -10.28 | 13.520 | 39.588 | 41.267 | 1.216 | 0.208 | 0.83 | 92.4  |
| Q10 | 0.359    | 0.30 | 0.042  | -10.68 | 13.613 | 39.748 | 41.052 | 0.391 | 0.103 | 0.41 | 56.4  |
| Q12 | 0.874    | 0.96 | -0.047 | -11.08 | 13.705 | 39.908 | 41.403 | 0.463 | 0.186 | 0.74 | 126.5 |
| Q13 | 1.985    | 1.96 | 0.004  | -10.58 | 13.589 | 39.708 | 41.366 | 0.945 | 0.223 | 0.89 | 116.1 |
| Q14 | 1.045    | 0.96 | 0.039  | -11.38 | 13.775 | 40.028 | 41.473 | 0.336 | 0.186 | 0.74 | 148.5 |
| Q15 | 2.269    | 1.96 | 0.100  | -10.28 | 13.520 | 39.588 | 41.296 | 1.301 | 0.223 | 0.89 | 98.9  |
| Q16 | 0.783    | 0.60 | 0.110  | -10.58 | 13.589 | 39.708 | 41.203 | 0.650 | 0.153 | 0.61 | 79.9  |
| Q18 | 1.577    | 1.41 | 0.065  | -9.98  | 13.450 | 39.468 | 41.197 | 1.674 | 0.208 | 0.83 | 78.8  |
| Q19 | 2.063    | 1.96 | 0.031  | -10.08 | 13.474 | 39.508 | 41.250 | 1.611 | 0.223 | 0.89 | 88.9  |
| Q20 | 0.088    | 0.06 | 0.023  | -10.18 | 13.497 | 39.548 | 40.367 | 0.180 | 0.028 | 0.11 | 11.6  |
| Q21 | 1.875    | 1.96 | -0.032 | -11.68 | 13.844 | 40.148 | 41.620 | 0.292 | 0.223 | 0.89 | 208.7 |
| Q23 | 1.000    | 0.96 | 0.016  | -12.68 | 14.076 | 40.548 | 41.774 | 0.084 | 0.186 | 0.74 | 296.9 |
| Q24 | 0.340    | 0.30 | 0.027  | -11.98 | 13.914 | 40.268 | 41.353 | 0.098 | 0.103 | 0.41 | 112.9 |
| Q25 | 1.100    | 0.96 | 0.067  | -9.68  | 13.381 | 39.348 | 41.079 | 2.060 | 0.186 | 0.74 | 60    |
| Q26 | 0.887    | 0.96 | -0.041 | -10.18 | 13.497 | 39.548 | 41.195 | 1.209 | 0.186 | 0.74 | 78.3  |
|     | NGC 2639 |      |        |        |        |        |        |       |       |      |       |
| Q1  | 1.177    | 0.96 | 0.098  | -14.12 | 14.348 | 41.124 | 42.046 | 0.024 | 0.186 | 0.74 | 556   |
| Q2  | 1.105    | 0.96 | 0.062  | -13.02 | 14.197 | 40.684 | 41.895 | 0.048 | 0.186 | 0.74 | 393   |
| Q3  | 1.522    | 1.41 | 0.035  | -12.75 | 14.115 | 40.576 | 41.862 | 0.079 | 0.210 | 0.83 | 363.7 |
| Q4  | 0.780    | 0.60 | 0.101  | -13.31 | 14.372 | 40.800 | 41.986 | 0.018 | 0.156 | 0.61 | 483.7 |
| Q5  | 1.494    | 1.41 | 0.024  | -14.26 | 14.612 | 41.180 | 42.359 | 0.008 | 0.210 | 0.83 | 1143  |
| Q7  | 2.000    | 1.96 | 0.002  | -12.81 | 14.165 | 40.600 | 41.941 | 0.067 | 0.224 | 0.89 | 436.6 |
| Q8  | 2.800    | 2.64 | 0.033  | -13.18 | 14.192 | 40.748 | 41.987 | 0.062 | 0.234 | 0.92 | 484.7 |
| Q10 | 0.305    | 0.30 | -0.007 | -14.38 | 14.311 | 41.228 | 41.751 | 0.016 | 0.105 | 0.41 | 281.8 |
| Q14 | 2.124    | 1.96 | 0.044  | -13.44 | 14.234 | 40.852 | 42.011 | 0.048 | 0.221 | 0.89 | 512.5 |
| Q15 | 1.525    | 1.41 | 0.037  | -13.40 | 14.115 | 40.836 | 41.862 | 0.078 | 0.207 | 0.83 | 363.9 |
| Q16 | 0.323    | 0.30 | 0.007  | -13.78 | 14.133 | 40.988 | 41.573 | 0.036 | 0.104 | 0.41 | 187   |
|     | NGC 2683 |      |        |        |        |        |        |       |       |      |       |
| Q1  | 1.252    | 1.41 | -0.067 | -10.94 | 13.735 | 39.852 | 41.482 | 0.452 | 0.208 | 0.83 | 151.5 |
| Q2  | 1.262    | 1.41 | -0.063 | -10.33 | 13.827 | 39.608 | 41.574 | 0.296 | 0.208 | 0.83 | 187.3 |
| Q3  | 0.065    | 0.06 | 0.004  | -11.38 | 13.775 | 40.028 | 40.645 | 0.050 | 0.028 | 0.11 | 22.1  |
| Q4  | 0.621    | 0.60 | 0.012  | -12.19 | 13.792 | 40.352 | 41.406 | 0.255 | 0.153 | 0.61 | 127.4 |

|     |       |      |        |        |        |        |        |        |       |      |       |
|-----|-------|------|--------|--------|--------|--------|--------|--------|-------|------|-------|
|     | NGC   |      |        |        |        |        |        |        |       |      |       |
|     | 2841  |      |        |        |        |        |        |        |       |      |       |
| Q1  | 0.120 | 0.06 | 0.055  | -12.32 | 13.992 | 40.404 | 40.863 | 0.018  | 0.028 | 0.11 | 36.4  |
| Q2  | 2.028 | 1.96 | 0.021  | -11.74 | 13.771 | 40.172 | 41.547 | 0.409  | 0.223 | 0.89 | 176.3 |
|     | NGC   |      |        |        |        |        |        |        |       |      |       |
|     | 2859  |      |        |        |        |        |        |        |       |      |       |
| Q1  | 0.230 | 0.30 | -0.059 | -13.29 | 14.301 | 40.792 | 41.741 | 0.016  | 0.103 | 0.41 | 275.5 |
| Q2  | 2.250 | 1.96 | 0.092  | -12.33 | 13.995 | 40.408 | 41.771 | 0.146  | 0.223 | 0.89 | 295.1 |
| Q3  | 1.460 | 1.41 | 0.015  | -11.73 | 13.856 | 40.168 | 41.603 | 0.259  | 0.208 | 0.83 | 200.2 |
| Q6  | 0.027 | 0.06 | -0.037 | -13.53 | 14.273 | 40.888 | 41.143 | 0.005  | 0.028 | 0.11 | 69.5  |
|     | NGC   |      |        |        |        |        |        |        |       |      |       |
|     | 2916  |      |        |        |        |        |        |        |       |      |       |
| Q1  | 1.546 | 1.41 | 0.044  | -13.81 | 14.346 | 41.000 | 42.093 | 0.027  | 0.208 | 0.83 | 619.0 |
| Q2  | 0.238 | 0.30 | -0.059 | -13.84 | 14.344 | 41.012 | 41.784 | 0.013  | 0.103 | 0.41 | 304.3 |
| Q3  | 0.793 | 0.60 | 0.107  | -14.04 | 14.391 | 41.092 | 42.004 | 0.016  | 0.153 | 0.61 | 505.0 |
| Q4  | 1.868 | 1.96 | -0.043 | -13.69 | 14.066 | 40.952 | 41.842 | 0.105  | 0.223 | 0.89 | 347.6 |
| Q5  | 1.279 | 1.41 | -0.066 | -13.95 | 14.451 | 41.056 | 42.198 | 0.017  | 0.208 | 0.83 | 788.8 |
|     | NGC   | =    | M82    |        |        |        |        |        |       |      |       |
|     | 3034  |      |        |        |        |        |        |        |       |      |       |
| Q1  | 1.010 | 0.96 | 0.024  | -8.39  | 13.271 | 38.832 | 40.969 | 3.423  | 0.186 | 0.74 | 46.5  |
| Q2  | 2.048 | 1.96 | 0.029  | -8.33  | 13.203 | 38.808 | 40.980 | 5.590  | 0.223 | 0.89 | 47.7  |
| Q3  | 2.054 | 1.96 | 0.031  | -7.50  | 12.936 | 38.476 | 40.712 | 19.147 | 0.223 | 0.89 | 25.8  |
| Q4  | 0.85  | 0.96 | -0.057 | -7.71  | 13.411 | 38.560 | 41.109 | 1.796  | 0.186 | 0.74 | 64.3  |
| Q5  | 2.040 | 1.96 | 0.026  | -7.52  | 12.868 | 38.484 | 40.644 | 26.202 | 0.223 | 0.89 | 22    |
| Q6  | 2.240 | 1.96 | 0.094  | -6.43  | 12.628 | 38.048 | 40.457 | 89.168 | 0.252 | 0.89 | 14.3  |
| Q7  | 0.930 | 0.96 | -0.016 | -8.45  | 13.561 | 38.856 | 41.259 | 0.899  | 0.186 | 0.74 | 90.8  |
| Q8  | 0.960 | 0.96 | -0.001 | -8.79  | 13.982 | 38.992 | 41.680 | 0.129  | 0.185 | 0.74 | 239.2 |
| Q9  | 0.740 | 0.60 | 0.086  | -5.83  | 12.489 | 37.808 | 40.103 | 103.04 | 0.153 | 0.61 | 6.3   |
| Q10 | 0.675 | 0.60 | 0.046  | -8.03  | 12.999 | 38.688 | 40.613 | 9.863  | 0.153 | 0.61 | 20.5  |
| Q11 | 0.626 | 0.60 | 0.015  | -8.93  | 13.207 | 39.048 | 40.821 | 3.777  | 0.153 | 0.61 | 33.1  |
| Q12 | 1.086 | 0.96 | 0.063  | -9.84  | 13.533 | 39.412 | 41.231 | 1.024  | 0.186 | 0.74 | 85.1  |
|     | NGC   |      |        |        |        |        |        |        |       |      |       |
|     | 3079  |      |        |        |        |        |        |        |       |      |       |
| Q1  | 1.410 | 1.41 | -0.004 | -11.83 | 13.743 | 40.208 | 41.490 | 0.435  | 0.208 | 0.83 | 154.5 |
| Q2  | 0.898 | 0.96 | -0.036 | -12.39 | 14.062 | 40.432 | 41.760 | 0.090  | 0.187 | 0.74 | 287.7 |
| Q3  | 1.021 | 0.96 | 0.027  | -12.60 | 14.213 | 40.516 | 41.911 | 0.045  | 0.187 | 0.74 | 407.3 |
| Q4  | 0.215 | 0.30 | -0.069 | -10.91 | 13.996 | 39.840 | 41.436 | 0.067  | 0.103 | 0.41 | 136.5 |
| Q5  | 1.037 | 0.96 | 0.035  | -10.29 | 13.836 | 39.592 | 41.534 | 0.253  | 0.186 | 0.74 | 171   |
| Q6  | 1.530 | 1.41 | 0.046  | -11.24 | 13.804 | 39.972 | 41.550 | 0.329  | 0.208 | 0.83 | 177.6 |
| Q7  | 0.072 | 0.06 | 0.008  | -13.00 | 14.150 | 40.676 | 41.020 | 0.009  | 0.028 | 0.11 | 52.4  |
| Q8  | 2.102 | 1.96 | 0.044  | -12.68 | 14.076 | 40.548 | 41.852 | 0.101  | 0.224 | 0.89 | 355.6 |
| Q9  | 1.413 | 1.41 | -0.003 | -13.33 | 14.089 | 40.808 | 41.836 | 0.088  | 0.207 | 0.83 | 342.7 |
| Q10 | 1.415 | 1.41 | -0.002 | -13.33 | 14.089 | 40.808 | 41.836 | 0.088  | 0.207 | 0.83 | 342.7 |
| Q11 | 1.154 | 0.96 | 0.094  | -7.25  | 12.818 | 38.376 | 40.516 | 27.507 | 0.186 | 0.74 | 16.4  |
| Q12 | 0.352 | 0.30 | 0.036  | -9.14  | 13.256 | 39.132 | 40.696 | 2.023  | 0.103 | 0.41 | 24.8  |
| Q13 | 1.760 | 1.96 | -0.071 | -14.23 | 14.357 | 41.168 | 42.133 | 0.028  | 0.226 | 0.89 | 679   |

|          |       |      |        |        |        |        |        |       |       |      |       |
|----------|-------|------|--------|--------|--------|--------|--------|-------|-------|------|-------|
| Q14      | 1.154 | 0.96 | 0.094  | -11.90 | 13.993 | 40.236 | 41.691 | 0.123 | 0.186 | 0.74 | 245.5 |
| Q15      | 0.219 | 0.30 | -0.066 | -9.08  | 13.242 | 39.108 | 40.682 | 2.156 | 0.103 | 0.41 | 24    |
| Q16      | 3.216 | 3.47 | -0.061 | -10.20 | 13.501 | 39.556 | 41.308 | 1.520 | 0.239 | 0.95 | 101.6 |
| NGC 3184 |       |      |        |        |        |        |        |       |       |      |       |
| Q1       | 0.675 | 0.60 | 0.045  | -12.11 | 13.750 | 40.320 | 41.364 | 0.310 | 0.153 | 0.61 | 115.6 |
| Q2       | 0.920 | 0.96 | -0.022 | -11.13 | 13.810 | 39.928 | 41.508 | 0.286 | 0.186 | 0.74 | 161.1 |
| Q3       | 0.152 | 0.06 | 0.085  | -12.64 | 14.066 | 40.532 | 40.937 | 0.013 | 0.028 | 0.11 | 43.2  |
| NGC 3384 |       |      |        |        |        |        |        |       |       |      |       |
| Q1       | 0.442 | 0.30 | 0.077  | -10.94 | 13.588 | 39.852 | 41.028 | 0.439 | 0.103 | 0.41 | 53.3  |
| Q2       | 1.280 | 1.41 | -0.081 | -10.98 | 13.770 | 39.868 | 41.517 | 0.384 | 0.208 | 0.83 | 164.6 |
| Q4       | 1.107 | 0.96 | 0.044  | -11.19 | 13.710 | 39.952 | 41.408 | 0.453 | 0.186 | 0.74 | 127.9 |
| Q5       | 1.192 | 0.96 | 0.086  | -10.25 | 13.513 | 39.576 | 41.211 | 1.122 | 0.186 | 0.74 | 81.3  |
| Q8       | 1.134 | 0.96 | 0.057  | -11.69 | 14.015 | 40.152 | 41.713 | 0.111 | 0.186 | 0.74 | 258.1 |
| Q13      | 0.497 | 0.60 | -0.092 | -10.68 | 13.797 | 39.748 | 41.411 | 0.250 | 0.153 | 0.61 | 128.9 |
| Q14      | 0.520 | 0.60 | -0.078 | -10.31 | 13.485 | 39.600 | 41.099 | 1.051 | 0.153 | 0.61 | 62.8  |
| Q15      | 1.131 | 0.96 | 0.056  | -10.49 | 13.767 | 39.672 | 41.465 | 0.348 | 0.186 | 0.74 | 145.8 |
| NGC 3516 |       |      |        |        |        |        |        |       |       |      |       |
| Q1       | 2.100 | 1.96 | 0.038  | -14.45 | 14.486 | 41.256 | 42.262 | 0.015 | 0.222 | 0.89 | 914.0 |
| Q2       | 1.399 | 1.41 | -0.013 | -12.95 | 14.138 | 40.656 | 41.885 | 0.071 | 0.208 | 0.83 | 383.8 |
| Q3       | 0.930 | 0.96 | -0.024 | -12.95 | 14.138 | 40.656 | 41.836 | 0.063 | 0.186 | 0.74 | 342.9 |
| Q4       | 0.690 | 0.60 | 0.047  | -13.85 | 14.347 | 41.016 | 41.960 | 0.020 | 0.153 | 0.61 | 456.5 |
| Q5       | 0.328 | 0.30 | 0.012  | -12.75 | 14.092 | 40.576 | 41.532 | 0.043 | 0.103 | 0.41 | 170.1 |
| Q6       | 1.710 | 1.96 | -0.093 | -14.35 | 14.462 | 41.216 | 42.239 | 0.017 | 0.223 | 0.89 | 866.5 |
| NGC 3628 |       |      |        |        |        |        |        |       |       |      |       |
| Q1       | 1.413 | 1.41 | -0.002 | -11.24 | 13.733 | 39.972 | 41.480 | 0.456 | 0.208 | 0.83 | 151   |
| Q2       | 2.060 | 1.96 | 0.031  | -11.39 | 13.763 | 40.032 | 41.539 | 0.425 | 0.223 | 0.89 | 173   |
| Q3       | 1.750 | 1.96 | -0.074 | -10.72 | 13.532 | 39.764 | 41.308 | 1.231 | 0.223 | 0.89 | 101.7 |
| Q4       | 2.150 | 1.96 | 0.061  | -10.86 | 13.696 | 39.820 | 41.472 | 0.579 | 0.223 | 0.89 | 148.3 |
| Q8       | 2.430 | 2.64 | -0.060 | -9.33  | 13.325 | 39.208 | 41.120 | 3.325 | 0.233 | 0.92 | 66    |
| Q9       | 1.940 | 1.96 | -0.010 | -11.24 | 13.733 | 39.972 | 41.509 | 0.488 | 0.223 | 0.89 | 161.6 |
| Q10      | 2.490 | 2.64 | -0.044 | -9.60  | 13.362 | 39.316 | 41.157 | 2.804 | 0.233 | 0.92 | 72    |
| Q11      | 2.370 | 2.64 | -0.077 | -10.25 | 13.751 | 39.576 | 41.546 | 0.468 | 0.232 | 0.92 | 175.8 |
| Q12      | 2.100 | 1.96 | 0.044  | -10.18 | 13.290 | 39.548 | 41.066 | 3.755 | 0.223 | 0.89 | 58.2  |
| Q13      | 2.140 | 1.96 | 0.058  | -10.28 | 13.816 | 39.588 | 41.592 | 0.332 | 0.223 | 0.89 | 195.7 |
| Q14      | 1.740 | 1.96 | -0.077 | -10.21 | 13.370 | 39.560 | 41.146 | 2.594 | 0.223 | 0.89 | 70.1  |
| Q15      | 2.320 | 2.64 | -0.091 | -12.45 | 14.325 | 40.456 | 42.120 | 0.033 | 0.230 | 0.92 | 658.7 |
| Q16      | 0.060 | 0.06 | -0.003 | -10.10 | 13.478 | 39.516 | 40.349 | 0.196 | 0.028 | 0.11 | 11.2  |
| Q17      | 2.540 | 2.64 | -0.030 | -10.28 | 13.528 | 39.588 | 41.323 | 1.308 | 0.233 | 0.92 | 105.2 |
| Q18      | 2.380 | 2.64 | -0.074 | -10.73 | 13.618 | 39.768 | 41.413 | 0.864 | 0.233 | 0.92 | 129.4 |
| Q19      | 2.110 | 1.96 | 0.048  | -9.33  | 13.232 | 39.208 | 41.008 | 4.909 | 0.223 | 0.89 | 50.9  |
| Q20      | 3.009 | 2.64 | 0.098  | -10.47 | 13.659 | 39.664 | 41.454 | 0.716 | 0.233 | 0.92 | 142.2 |
| NGC      |       |      |        |        |        |        |        |       |       |      |       |

|     |       |      |        |        |        |        |        |        |       |      |        |
|-----|-------|------|--------|--------|--------|--------|--------|--------|-------|------|--------|
|     | 3842  |      |        |        |        |        |        |        |       |      |        |
| Q1  | 0.335 | 0.30 | 0.005  | -16.21 | 14.893 | 41.960 | 42.333 | 0.001  | 0.102 | 0.41 | 1076.5 |
| Q2  | 0.946 | 0.96 | -0.028 | -15.63 | 14.586 | 41.728 | 42.284 | 0.008  | 0.186 | 0.74 | 960.5  |
| Q3  | 2.200 | 1.96 | 0.059  | -14.53 | 14.378 | 41.288 | 42.154 | 0.025  | 0.223 | 0.89 | 713.5  |
|     | NGC   |      |        |        |        |        |        |        |       |      |        |
|     | 4235  |      |        |        |        |        |        |        |       |      |        |
| Q1  | 0.334 | 0.30 | 0.019  | -15.65 | 14.764 | 41.736 | 42.203 | 0.002  | 0.105 | 0.41 | 798.5  |
| Q2  | 0.137 | 0.06 | 0.065  | -15.30 | 14.682 | 41.596 | 41.553 | 0.0008 | 0.029 | 0.11 | 178.6  |
|     | NGC   |      |        |        |        |        |        |        |       |      |        |
|     | 4258  |      |        |        |        |        |        |        |       |      |        |
| Q1  | 0.398 | 0.30 | 0.073  | -8.97  | 13.217 | 39.064 | 40.657 | 2.416  | 0.103 | 0.41 | 22.7   |
| Q2  | 0.654 | 0.60 | 0.032  | -9.42  | 13.261 | 39.244 | 40.875 | 2.950  | 0.153 | 0.61 | 37.5   |
|     | NGC   |      |        |        |        |        |        |        |       |      |        |
|     | 4410  |      |        |        |        |        |        |        |       |      |        |
| Q1  | 2.237 | 1.96 | 0.067  | -15.61 | 14.619 | 41.720 | 42.395 | 0.008  | 0.216 | 0.89 | 1243   |
| Q2  | 0.662 | 0.60 | 0.013  | -15.94 | 14.456 | 41.852 | 42.070 | 0.012  | 0.153 | 0.61 | 587    |
| Q3  | 1.903 | 1.96 | -0.043 | -15.61 | 14.546 | 41.720 | 42.322 | 0.012  | 0.231 | 0.89 | 1049   |
| Q5  | 0.535 | 0.60 | -0.064 | -17.89 | 14.361 | 41.632 | 41.974 | 0.019  | 0.156 | 0.61 | 471.4  |
| Q6  | 1.776 | 1.96 | -0.085 | -15.79 | 14.486 | 41.792 | 42.262 | 0.015  | 0.220 | 0.89 | 914.5  |
| Q8  | 0.085 | 0.06 | -0.001 | -18.54 | 14.821 | 41.892 | 41.691 | 0.0004 | 0.027 | 0.11 | 245.7  |
| Q9  | 1.590 | 1.41 | 0.049  | -15.15 | 14.707 | 41.536 | 42.454 | 0.005  | 0.203 | 0.83 | 1421.5 |
| Q10 | 1.502 | 1.41 | 0.013  | -16.36 | 14.757 | 42.020 | 42.504 | 0.004  | 0.204 | 0.83 | 1594.5 |
| Q11 | 0.628 | 0.60 | -0.008 | -15.85 | 14.483 | 41.816 | 42.096 | 0.011  | 0.159 | 0.61 | 624    |
| Q12 | 1.043 | 0.96 | 0.017  | -16.44 | 14.825 | 42.052 | 42.523 | 0.003  | 0.210 | 0.74 | 1668.5 |
| Q13 | 1.363 | 1.41 | -0.044 | -15.94 | 14.762 | 41.852 | 42.509 | 0.004  | 0.209 | 0.83 | 1615   |
| Q15 | 1.471 | 1.41 | 0.0    | -17.59 | 14.555 | 41.512 | 42.302 | 0.010  | 0.202 | 0.83 | 1003   |
| Q16 | 1.076 | 0.96 | 0.033  | -15.70 | 14.563 | 41.756 | 42.261 | 0.009  | 0.188 | 0.74 | 912    |
| Q17 | 1.345 | 1.41 | -0.051 | -15.86 | 14.632 | 41.820 | 42.378 | 0.007  | 0.201 | 0.83 | 1195   |
| Q18 | 1.090 | 0.96 | 0.040  | -16.06 | 14.786 | 41.900 | 42.484 | 0.003  | 0.175 | 0.74 | 1525   |
| Q19 | 1.715 | 1.41 | 0.099  | -15.69 | 14.406 | 41.752 | 42.153 | 0.021  | 0.213 | 0.83 | 711    |
| Q20 | 0.681 | 0.60 | 0.025  | -17.44 | 14.756 | 42.452 | 42.370 | 0.003  | 0.152 | 0.61 | 1171.5 |
| Q21 | 2.649 | 2.64 | -0.022 | -15.10 | 14.585 | 41.516 | 42.380 | 0.010  | 0.231 | 0.92 | 1199   |
| Q22 | 0.773 | 0.60 | 0.081  | -16.40 | 14.635 | 42.036 | 42.248 | 0.005  | 0.145 | 0.61 | 885.5  |
| Q23 | 0.064 | 0.06 | -0.021 | -17.46 | 15.327 | 42.460 | 42.197 | .00004 | 0.028 | 0.11 | 787    |
| Q24 | 0.398 | 0.30 | 0.049  | -16.60 | 14.633 | 42.116 | 42.072 | 0.004  | 0.115 | 0.41 | 590.5  |
| Q25 | 1.429 | 1.41 | -0.017 | -16.14 | 14.713 | 41.932 | 42.460 | 0.005  | 0.208 | 0.83 | 1440.5 |
|     | NGC   |      |        |        |        |        |        |        |       |      |        |
|     | 4579  |      |        |        |        |        |        |        |       |      |        |
| Q2  | 0.662 | 0.60 | 0.034  | -11.61 | 13.619 | 40.120 | 41.233 | 0.566  | 0.153 | 0.61 | 85.5   |
|     | NGC   |      |        |        |        |        |        |        |       |      |        |
|     | 5548  |      |        |        |        |        |        |        |       |      |        |
| Q1  | 0.852 | 0.96 | -0.071 | -15.23 | 14.666 | 41.568 | 42.364 | 0.006  | 0.202 | 0.74 | 1156.5 |
| Q2  | 0.184 | 0.06 | 0.098  | -15.60 | 14.676 | 41.716 | 41.546 | 0.0008 | 0.028 | 0.11 | 175.8  |
| Q3  | 0.727 | 0.60 | 0.061  | -14.73 | 14.550 | 41.368 | 42.164 | 0.008  | 0.158 | 0.61 | 730    |
| Q4  | 2.425 | 2.64 | -0.075 | -14.55 | 14.321 | 41.296 | 42.116 | 0.034  | 0.233 | 0.92 | 653.5  |
| Q5  | 2.100 | 1.96 | 0.030  | -13.41 | 14.416 | 40.840 | 42.192 | 0.021  | 0.223 | 0.89 | 778.5  |

|      |       |      |        |        |        |        |        |        |       |      |        |
|------|-------|------|--------|--------|--------|--------|--------|--------|-------|------|--------|
| Q6   | 1.928 | 1.96 | -0.027 | -14.89 | 14.413 | 41.432 | 42.189 | 0.021  | 0.220 | 0.89 | 773.5  |
| Q7   | 2.297 | 1.96 | 0.095  | -14.63 | 14.587 | 41.328 | 42.363 | 0.0095 | 0.222 | 0.89 | 1154.5 |
| Q8   | 1.800 | 1.96 | -0.070 | -13.13 | 14.014 | 40.728 | 41.790 | 0.134  | 0.223 | 0.89 | 308.5  |
| Q9   | 1.830 | 1.96 | -0.060 | -12.92 | 13.938 | 40.644 | 41.715 | 0.189  | 0.222 | 0.89 | 259.3  |
| Q10  | 1.917 | 1.96 | -0.031 | -14.77 | 14.389 | 41.384 | 42.165 | 0.024  | 0.225 | 0.89 | 732    |
| Q11  | 1.057 | 0.96 | 0.032  | -14.13 | 14.511 | 41.128 | 42.209 | 0.011  | 0.181 | 0.74 | 809    |
| Q12  | 0.560 | 0.60 | -0.041 | -14.13 | 14.286 | 41.128 | 41.899 | 0.026  | 0.151 | 0.61 | 396.6  |
| Q13  | 2.310 | 1.96 | 0.100  | -14.06 | 14.396 | 41.100 | 42.173 | 0.023  | 0.223 | 0.89 | 744    |
| Q14  | 2.500 | 2.64 | -0.055 | -15.93 | 14.871 | 41.848 | 42.666 | 0.003  | 0.259 | 0.92 | 2316.5 |
| Q15  | 0.237 | 0.30 | -0.065 | -16.43 | 15.232 | 42.048 | 42.672 | 0.0002 | 0.091 | 0.41 | 2347   |
| Q16  | 0.674 | 0.60 | 0.029  | -14.93 | 14.597 | 41.448 | 42.211 | 0.006  | 0.146 | 0.61 | 812    |
| Q17  | 2.200 | 1.96 | 0.063  | -15.53 | 14.841 | 41.688 | 42.617 | 0.003  | 0.225 | 0.89 | 2069.5 |
| Q18  | 1.053 | 0.96 | 0.030  | -17.57 | 15.079 | 42.504 | 42.777 | 0.0008 | 0.180 | 0.74 | 2992   |
| Q19  | 0.084 | 0.06 | 0.006  | -16.36 | 14.809 | 42.020 | 41.680 | 0.0004 | 0.026 | 0.11 | 239.2  |
| Q20  | 0.649 | 0.60 | 0.013  | -16.37 | 14.868 | 42.024 | 42.481 | 0.002  | 0.170 | 0.61 | 1514.5 |
| NGC  |       |      |        |        |        |        |        |        |       |      |        |
| 5985 |       |      |        |        |        |        |        |        |       |      |        |
| Q1   | 2.125 | 1.96 | 0.047  | -12.62 | 13.868 | 40.524 | 41.644 | 0.263  | 0.223 | 0.89 | 220.2  |
| Q2   | 1.968 | 1.96 | -0.005 | -12.96 | 14.116 | 40.660 | 41.892 | 0.084  | 0.224 | 0.89 | 390.2  |
| Q3   | 0.807 | 0.96 | -0.085 | -13.99 | 14.309 | 41.072 | 42.007 | 0.029  | 0.188 | 0.74 | 507.8  |
| Q4   | 0.690 | 0.60 | 0.048  | -14.05 | 14.210 | 41.096 | 41.823 | 0.037  | 0.152 | 0.61 | 332.9  |
| Q5   | 0.348 | 0.30 | 0.028  | -14.20 | 14.263 | 41.156 | 41.703 | 0.020  | 0.105 | 0.41 | 252.4  |
| Q6   | 1.895 | 1.96 | -0.030 | -13.23 | 14.046 | 40.768 | 41.822 | 0.116  | 0.224 | 0.89 | 331.8  |
| NGC  |       |      |        |        |        |        |        |        |       |      |        |
| 6212 |       |      |        |        |        |        |        |        |       |      |        |
| Q1   | 1.864 | 1.96 | -0.060 | -15.68 | 14.596 | 41.748 | 42.372 | 0.0092 | 0.223 | 0.89 | 1177.0 |
| Q2   | 2.010 | 1.96 | -0.013 | -14.20 | 14.206 | 41.156 | 41.982 | 0.0553 | 0.223 | 0.89 | 479.6  |
| Q3   | 1.898 | 1.96 | -0.049 | -15.87 | 14.835 | 41.824 | 42.611 | 0.003  | 0.219 | 0.89 | 2043.5 |
| Q4   | 0.461 | 0.30 | 0.091  | -18.07 | 15.138 | 42.704 | 42.578 | 0.0004 | 0.103 | 0.41 | 1891.5 |
| Q5   | 0.143 | 0.06 | 0.047  | -17.12 | 15.085 | 42.324 | 41.955 | 0.0001 | 0.028 | 0.11 | 451.3  |
| Q6   | 0.030 | 0.06 | -0.057 | -17.70 | 15.238 | 42.556 | 42.109 | 0.0001 | 0.028 | 0.11 | 642.0  |
| Q7   | 1.965 | 1.96 | -0.027 | -16.30 | 14.914 | 41.996 | 42.690 | 0.0021 | 0.221 | 0.89 | 2451.0 |
| Q8   | 1.183 | 0.96 | 0.081  | -15.10 | 14.443 | 41.516 | 42.141 | 0.016  | 0.186 | 0.74 | 692.0  |
| Q9   | 1.666 | 1.41 | 0.074  | -16.13 | 14.875 | 41.928 | 42.622 | 0.0024 | 0.211 | 0.83 | 2092.0 |
| Q10  | 2.253 | 1.96 | 0.067  | -16.42 | 14.684 | 42.044 | 42.460 | 0.0061 | 0.222 | 0.89 | 1441.5 |
| Q11  | 1.625 | 1.41 | 0.058  | -16.90 | 14.780 | 42.236 | 42.527 | 0.0037 | 0.210 | 0.83 | 1680.7 |
| Q12  | 2.614 | 2.64 | -0.036 | -16.41 | 14.648 | 42.040 | 42.442 | 0.0075 | 0.231 | 0.92 | 1384.9 |
| Q13  | 0.540 | 0.60 | -0.066 | -15.67 | 14.522 | 41.744 | 42.136 | 0.009  | 0.154 | 0.61 | 683.5  |
| Q14  | 1.005 | 0.96 | -0.007 | -17.45 | 14.950 | 42.456 | 42.648 | 0.002  | 0.186 | 0.74 | 2221.0 |
| Q15  | 0.625 | 0.60 | -0.014 | -14.99 | 14.252 | 41.472 | 41.865 | 0.031  | 0.153 | 0.61 | 366.8  |
| Q16  | 2.529 | 2.64 | -0.059 | -15.18 | 14.610 | 41.548 | 42.405 | 0.009  | 0.232 | 0.92 | 1271.0 |
| Q17  | 1.860 | 1.96 | -0.062 | -16.65 | 14.923 | 42.136 | 42.700 | 0.002  | 0.220 | 0.89 | 2504.5 |
| Q18  | 1.580 | 1.41 | 0.039  | -14.65 | 14.495 | 41.336 | 42.242 | 0.0136 | 0.207 | 0.83 | 872.5  |
| Q19  | 1.595 | 1.41 | 0.045  | -15.88 | 14.661 | 41.828 | 42.408 | 0.0064 | 0.210 | 0.83 | 1278.0 |
| Q20  | 1.466 | 1.41 | -0.007 | -16.03 | 14.780 | 41.888 | 42.527 | 0.0037 | 0.210 | 0.83 | 1683.5 |
| Q21  | 1.414 | 1.41 | -0.027 | -15.50 | 14.665 | 41.676 | 42.412 | 0.0062 | 0.207 | 0.83 | 1291.0 |

|      |       |      |        |        |        |        |        |                     |       |      |        |
|------|-------|------|--------|--------|--------|--------|--------|---------------------|-------|------|--------|
| Q22  | 2.384 | 2.64 | -0.098 | -16.23 | 14.681 | 41.968 | 42.476 | 0.0065              | 0.234 | 0.92 | 1496.0 |
| Q23  | 0.595 | 0.60 | -0.032 | -18.91 | 15.217 | 43.040 | 42.831 | 0.0004              | 0.153 | 0.61 | 3387.5 |
| Q24  | 1.360 | 1.41 | -0.049 | -17.26 | 14.937 | 42.380 | 42.684 | 0.0018              | 0.210 | 0.83 | 2413.0 |
| Q25  | 2.000 | 1.96 | -0.016 | -15.49 | 14.498 | 41.672 | 42.274 | 0.0144              | 0.223 | 0.89 | 939.5  |
| Q26  | 2.260 | 1.96 | 0.069  | -15.48 | 14.680 | 41.668 | 42.456 | 0.0062              | 0.222 | 0.89 | 1428.5 |
| Q27  | 2.000 | 1.96 | -0.016 | -14.68 | 14.434 | 41.348 | 42.210 | 0.0194              | 0.223 | 0.89 | 811.0  |
| Q28  | 0.443 | 0.30 | 0.078  | -16.20 | 14.362 | 41.956 | 41.802 | 0.0124              | 0.103 | 0.41 | 317.2  |
| Q29  | 0.704 | 0.60 | 0.034  | -17.18 | 14.749 | 42.348 | 42.362 | 0.0031              | 0.152 | 0.61 | 1151.5 |
| Q30  | 1.083 | 0.96 | 0.032  | -16.44 | 14.773 | 42.052 | 42.471 | 0.0034              | 0.187 | 0.74 | 1478.0 |
| Q31  | 2.113 | 1.96 | 0.021  | -16.19 | 14.698 | 41.952 | 42.474 | 0.0057              | 0.221 | 0.89 | 1488.5 |
| Q32  | 0.594 | 0.60 | -0.033 | -16.00 | 14.426 | 41.876 | 42.040 | 0.014               | 0.153 | 0.61 | 547.5  |
| Q33  | 1.358 | 1.41 | -0.050 | -16.95 | 14.983 | 42.256 | 42.730 | 0.0014              | 0.203 | 0.83 | 2687.0 |
| Q34  | 0.434 | 0.30 | 0.071  | -16.11 | 14.599 | 41.920 | 42.039 | 0.004               | 0.103 | 0.41 | 546.5  |
| Q35  | 1.377 | 1.41 | -0.042 | -16.05 | 14.747 | 41.896 | 42.494 | 0.0043              | 0.210 | 0.83 | 1560.5 |
| Q36  | 0.608 | 0.60 | -0.024 | -16.37 | 14.438 | 42.024 | 42.052 | 0.013               | 0.154 | 0.61 | 563.0  |
| Q37  | 1.268 | 1.41 | -0.086 | -16.19 | 14.964 | 41.952 | 42.711 | 0.0016              | 0.212 | 0.83 | 2570.0 |
| Q39  | 1.451 | 1.41 | -0.012 | -16.46 | 14.669 | 42.060 | 42.416 | 0.006               | 0.207 | 0.83 | 1302.0 |
| Q40  | 1.877 | 1.96 | -0.056 | -16.01 | 14.500 | 41.880 | 42.276 | 0.0143              | 0.223 | 0.89 | 943.5  |
| Q41  | 2.145 | 1.96 | 0.031  | -15.89 | 14.743 | 41.832 | 42.519 | 0.0047              | 0.225 | 0.89 | 1653.0 |
| Q42  | 0.100 | 0.06 | 0.008  | -17.90 | 15.040 | 42.636 | 41.910 | 0.0002              | 0.028 | 0.11 | 406.4  |
| NGC  |       |      |        |        |        |        |        |                     |       |      |        |
| 6217 |       |      |        |        |        |        |        |                     |       |      |        |
| Q1   | 0.358 | 0.30 | 0.039  | -10.08 | 13.474 | 39.508 | 40.913 | 0.742               | 0.103 | 0.41 | 41     |
| Q2   | 0.376 | 0.30 | 0.053  | -9.88  | 13.427 | 39.428 | 40.867 | 0.919               | 0.103 | 0.41 | 36.8   |
| IC   |       |      |        |        |        |        |        |                     |       |      |        |
| 4553 |       |      |        |        |        |        |        |                     |       |      |        |
| Q1   | 0.232 | 0.30 | -0.069 | -15.01 | 14.655 | 41.480 | 42.095 | 0.003               | 0.102 | 0.41 | 622.5  |
| Q2   | 1.249 | 1.41 | -0.083 | -13.56 | 14.280 | 40.900 | 42.026 | 0.037               | 0.209 | 0.83 | 531.5  |
| Q3   | 1.258 | 1.41 | -0.080 | -12.86 | 14.442 | 40.620 | 42.189 | 0.017               | 0.203 | 0.83 | 772.5  |
| Q4   | 0.463 | 0.30 | 0.105  | -14.18 | 14.149 | 41.148 | 41.588 | 0.033               | 0.102 | 0.41 | 193.9  |
| Mark |       |      |        |        |        |        |        |                     |       |      |        |
| 231  |       |      |        |        |        |        |        |                     |       |      |        |
| Q1   | 0.320 | 0.30 | -0.025 | -18.15 | 15.176 | 42.736 | 42.616 | 0.0003              | 0.103 | 0.41 | 2067.0 |
| Q2   | 0.124 | 0.06 | 0.018  | -19.06 | 15.553 | 43.100 | 42.424 | 1. 10 <sup>-5</sup> | 0.028 | 0.11 | 1326.0 |
| Q3   | 1.272 | 1.41 | -0.095 | -15.39 | 14.763 | 41.632 | 42.510 | 0.0040              | 0.208 | 0.83 | 1617.5 |
| Q4   | 1.232 | 0.96 | 0.093  | -16.50 | 14.865 | 42.076 | 42.563 | 0.0022              | 0.186 | 0.74 | 1827.5 |
| Q5   | 1.190 | 0.96 | 0.072  | -16.75 | 14.835 | 42.176 | 42.533 | 0.0026              | 0.186 | 0.74 | 1705.0 |
| Q6   | 0.330 | 0.30 | -0.018 | -17.43 | 14.874 | 42.448 | 42.314 | 0.0012              | 0.102 | 0.41 | 1030.5 |
| Q7   | 0.072 | 0.06 | -0.029 | -18.91 | 15.293 | 43.040 | 42.163 | 5. 10 <sup>-5</sup> | 0.028 | 0.11 | 727.5  |
| Mark |       |      |        |        |        |        |        |                     |       |      |        |
| 273  |       |      |        |        |        |        |        |                     |       |      |        |
| Q1   | 0.207 | 0.06 | 0.098  | -17.65 | 15.505 | 42.536 | 42.375 | 2. 10 <sup>-5</sup> | 0.027 | 0.11 | 1187.0 |
| Q2   | 0.941 | 0.96 | -0.045 | -18.44 | 15.173 | 42.852 | 42.871 | 0.0005              | 0.187 | 0.74 | 3712.5 |
| Q3   | 0.458 | 0.30 | 0.082  | -15.31 | 14.685 | 41.600 | 42.125 | 0.0028              | 0.103 | 0.41 | 666.0  |
| Q4   | 1.166 | 0.96 | 0.066  | -17.33 | 15.059 | 42.408 | 42.757 | 0.0009              | 0.186 | 0.74 | 2860.0 |
| Q5   | 0.486 | 0.30 | 0.102  | -16.63 | 14.594 | 42.128 | 42.034 | 0.0043              | 0.103 | 0.41 | 540.5  |

|     |       |      |        |        |        |        |        |        |       |      |        |
|-----|-------|------|--------|--------|--------|--------|--------|--------|-------|------|--------|
| Q6  | 0.377 | 0.30 | 0.022  | -16.66 | 14.926 | 42.140 | 42.365 | 0.0009 | 0.103 | 0.41 | 1159.5 |
|     | AM    |      |        |        |        |        |        |        |       |      |        |
|     | 2230  |      |        |        |        |        |        |        |       |      |        |
|     | -284  |      |        |        |        |        |        |        |       |      |        |
| Q1  | 2.141 | 1.96 | -0.003 | -17.14 | 15.109 | 42.332 | 42.885 | 0.0009 | 0.223 | 0.89 | 3835.5 |
| Q2  | 2.152 | 1.96 | 0.001  | -16.40 | 14.937 | 42.036 | 42.713 | 0.0019 | 0.222 | 0.89 | 2585.0 |
| Q3  | 2.165 | 1.96 | 0.005  | -17.56 | 15.206 | 42.500 | 42.982 | 0.0006 | 0.222 | 0.89 | 4798.5 |
| Q4  | 2.161 | 1.96 | 0.004  | -16.92 | 15.058 | 42.244 | 42.834 | 0.0011 | 0.224 | 0.89 | 3411.0 |
| Q5  | 2.155 | 1.96 | 0.002  | -17.14 | 15.109 | 42.332 | 42.885 | 0.0009 | 0.222 | 0.89 | 3835.5 |
| Q6  | 2.134 | 1.96 | -0.005 | -16.58 | 14.979 | 42.108 | 42.755 | 0.0016 | 0.227 | 0.89 | 2845.5 |
| Q7  | 2.133 | 1.96 | -0.005 | -16.59 | 14.981 | 42.112 | 42.758 | 0.0016 | 0.229 | 0.89 | 2860.5 |
| Q8  | 2.154 | 1.96 | 0.001  | -16.74 | 15.016 | 42.172 | 42.792 | 0.0013 | 0.219 | 0.89 | 3099.0 |
| Q10 | 2.155 | 1.96 | 0.002  | -16.31 | 14.916 | 42.000 | 42.693 | 0.0021 | 0.223 | 0.89 | 2464.0 |
| Q11 | 2.136 | 1.96 | -0.004 | -16.68 | 15.002 | 42.148 | 42.778 | 0.0014 | 0.222 | 0.89 | 3001.5 |
| Q12 | 2.168 | 1.96 | 0.006  | -16.24 | 14.900 | 41.972 | 42.676 | 0.0023 | 0.223 | 0.89 | 2373.5 |
| Q13 | 2.139 | 1.96 | -0.003 | -17.07 | 15.092 | 42.304 | 42.869 | 0.0009 | 0.223 | 0.89 | 3695.0 |
| Q14 | 2.137 | 1.96 | -0.004 | -16.71 | 15.009 | 42.160 | 42.785 | 0.0014 | 0.223 | 0.89 | 3049.8 |

From eq (10) corresponding values of reduced density for the Karlsson sequence of redshifts (assumed gravitational) can be reckoned. These are listed in Table 3, together with the respective values of  $r_{gr}/r_q$ , reckoned from eq (5). Note that the Karlsson sequence is truncated at  $z_{gr} = 2.64$ .

**Table 3. Reduced densities for the Karlsson sequence of redshifts**

|                                    |       |       |       |       |       |       |       |
|------------------------------------|-------|-------|-------|-------|-------|-------|-------|
| $z_{gr}$                           | 0.06  | 0.30  | 0.60  | 0.96  | 1.41  | 1.96  | 2.64  |
| $\rho \sim [\text{g}/\text{cm}^3]$ | 0.028 | 0.103 | 0.153 | 0.186 | 0.208 | 0.223 | 0.233 |
| $r_{gr}/r_q$                       | 0.11  | 0.41  | 0.61  | 0.74  | 0.83  | 0.89  | 0.92  |

Data for the reduced densities of 341 sample quasars are also listed in Table 2 and they are plotted versus the observed redshifts  $z_o$  in Fig (1). For this plot the observed redshifts are used although eq (10) should actually be plotted with the gravitational redshifts. This causes the spread of data in the  $z$ -direction for each value of reduced density. The  $z$ -spread of data is tolerable for small cosmological redshifts (nearby parent galaxies). Comparison of the observational data on Fig (1) with the respective theoretical values (Table 3) reveals satisfactory agreement, but this is to be expected by the definition of reduced densities. It is, however, important to note the distribution of QSOs over this diagram. Is it possible that on Fig (1) some physical reasons determine the observed distribution of data? Obviously, we should look for reasons in the local quasar concept. We could assume that quasars evolve with decreasing density and corresponding drop in the redshifts. It should be noted that only the gravitational components depend on density, but as they are the main components of redshifts in local QSOs a drop in gravitational redshifts also means a drop in the observed redshifts of

quasars. It looks, however, not to be a smooth, continuous transition, but a series of jumps to lower densities and corresponding jumps in redshifts to the next lower value of the Karlsson sequence. This scenario has already been suggested by Arp [52, 94]. Decreasing density could mean disintegration of matter. This would be the only logical explanation. This could be the first evidence from QSOs study pointing to a disintegration scenario. There are, however, other ramifications. The general trend of decreasing gravitational redshifts is consistent with the concept of quasar expansion and the change of gravitational potential at the quasar surface because of the expansion. However, the evolution should follow the Karlsson sequence of redshifts, i.e. an evolution with discrete steps. Correspondingly, the expansion should follow in discrete steps, following a sequence of gravitational potentials. It looks like a “discretization”, but on scale of the “macro-world”. From Fig (1) it looks like evolution proceeds with more rapid transitions between the values of the Karlsson sequence and slows down at each of these values. How this should be possible remains obscure and unexplained. The density curve on Fig (1) goes apparently to an asymptotic limit with increasing gravitational redshift. The general expression for this limit is obtained from eq (8), if  $z_{gr} = \infty$  :

$$\rho_{limit} = 3/(8\pi) \cdot c^2/G \cdot 1/r_q^2 \quad (11)$$

For a quasar with  $r = 8 \cdot 10^{13}$  [cm] this limit is  $\sim 0.252$  g/cm<sup>3</sup>. This is also the limiting density in Fig (1). It could easily be shown that:

$$r_{gr}/r_q = 1 - 1/(1 + z_{gr})^2 \quad (12)$$

For  $z_{gr} = \infty$ ,  $r_{gr}/r_q = 1$ . The limiting density in the disintegration scenario is therefore the density at the “event horizon” with which a quasar enters the world that we “know”. For me the “other” world - beyond the event horizon is still a “mystery unexplored”.

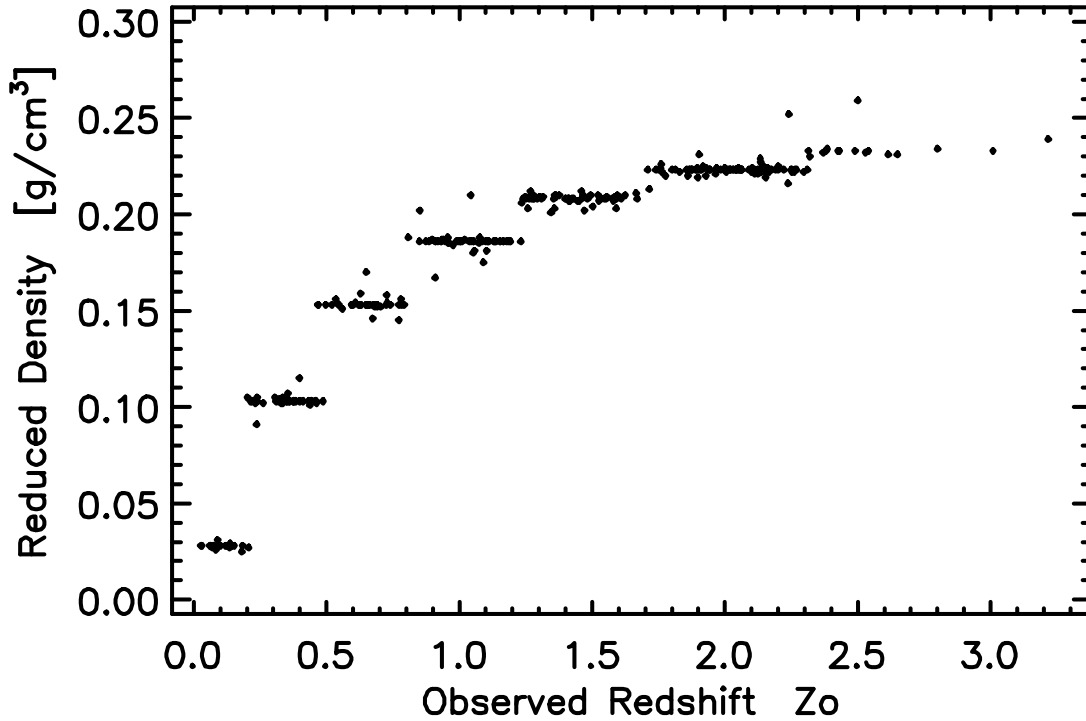


**Fig (1). "Reduced density- observed redshift" diagram for the sample of 341 quasars. All densities are reduced to a radius of  $8.10^{13}$  cm. Courtesy of Bentham Open, OAJ [55].**

There is an important consequence from the asymptotic relation on Fig (1). At large redshifts a small drop in density causes large shift in the gravitational redshift. This means that the evolution of quasars on the diagram (Fig 1) is very fast at large redshifts, down to about redshift of  $z_{gr} = 1.96$ . This could explain in a natural way the deficiency of quasars with large redshifts and the sharply decreasing number of QSOs for  $z > 3$ . It could simply be due to rapid quasar evolution to lower redshifts. It should also be noted that at  $z_{gr} = 1.96$  starts the turn of the curve, therefore, slow down in evolution if the above scenario holds.

After the decomposition of gravitational redshifts, the Doppler shifts are also decomposed and listed in Table 2. The distribution of the Doppler shifts is also an important indicator for consistency of this procedure. For the Doppler shifts several assumptions seem realistic and are expected to be fulfilled:

- Doppler shifts reflect only the projection of ejection velocity of quasars along the line of sight. The real ejection velocity could be larger.
- Lower ejection velocities are more likely because of energy considerations. Whatever the physics behind this ejection, events of lower energy should be expected to be more likely than big ones. If the sample of quasars is large enough a peak in the distribution should therefore be expected around the zero Doppler shift.
- The distribution should be symmetric with respect to the zero velocity if all directions of ejection have the same probability. There are reports [26] where the ejection has been revealed to proceed along the minor (rotational) axis of the parent

galaxy. This effect, if real, could introduce some distortion of the Doppler shifts distribution with small samples of galaxies and quasars. However, with large samples of parent galaxies and their ejected quasars the above effects should cancel out and the distribution of Doppler shifts of quasars should be symmetric.

- Ejection velocities should be limited.

In Fig (2) the distribution of the Doppler shifts of the 341 sample QSOs is plotted and it seems to be consistent with the above assumptions. The highest projected ejection velocity seems to be slightly over 30 000 km.s<sup>-1</sup>.

The distributions of Doppler velocities could also be useful to determine the gravitational redshift if the value of  $z_i$  happens to be near the middle of the neighboring values of the Karlsson sequence of redshifts. In this case it is the corresponding value of the Doppler shift which better fits the distribution of the Doppler shifts on Fig (2) that could help to solve this ambiguity.

The ejection of quasars from active galactic nuclei certainly involves huge energies but this problem remains unsolved. As a working hypothesis it could be possible to assume again some disintegration processes in the active galactic nuclei. These events should present a clear indication of the limits of our present knowledge.

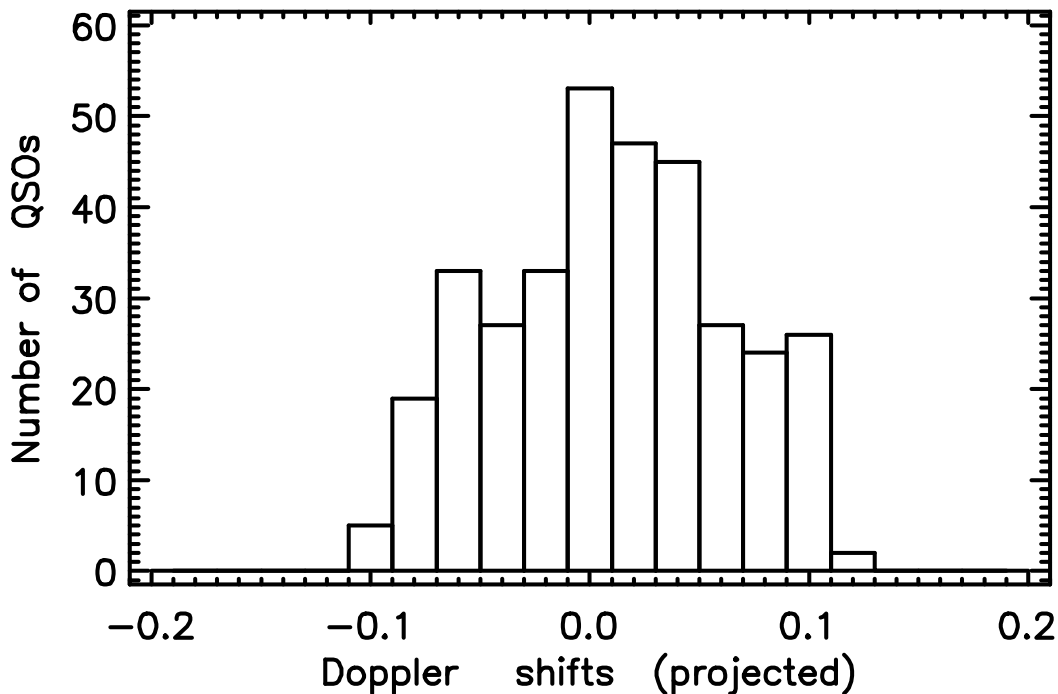


**Fig (2). Distribution of the Doppler shifts of the 341 sample quasars. Courtesy of Bentham Open OAJ [55].**

## Chapter 4.

### *Relations for quasars. Effects of discretization.*

Several relations could be established for quasars, using their physical characteristics. The eq (7) “absolute magnitude – radius” for a sample of 74 QSOs was established in [25], using only quasars with known B-V:

$$M_q = 48.099 - 4.318 \cdot \log r_q$$

It has been later confirmed (with slightly different coefficients) in [54-55]. Fig (3) shows this relation with a sample of 341 QSOs. This relation could be useful to determine radii of QSOs with unknown color B – V, i.e. in cases where the standard procedure is impossible. All quasars in Table 2 are associated with galaxies with known distances. Therefore, it is possible to get quasars’ absolute magnitudes  $M_q$  knowing their visual magnitudes and the distance to the respective associated galaxy. Relation (7) would give then the quasar radius.

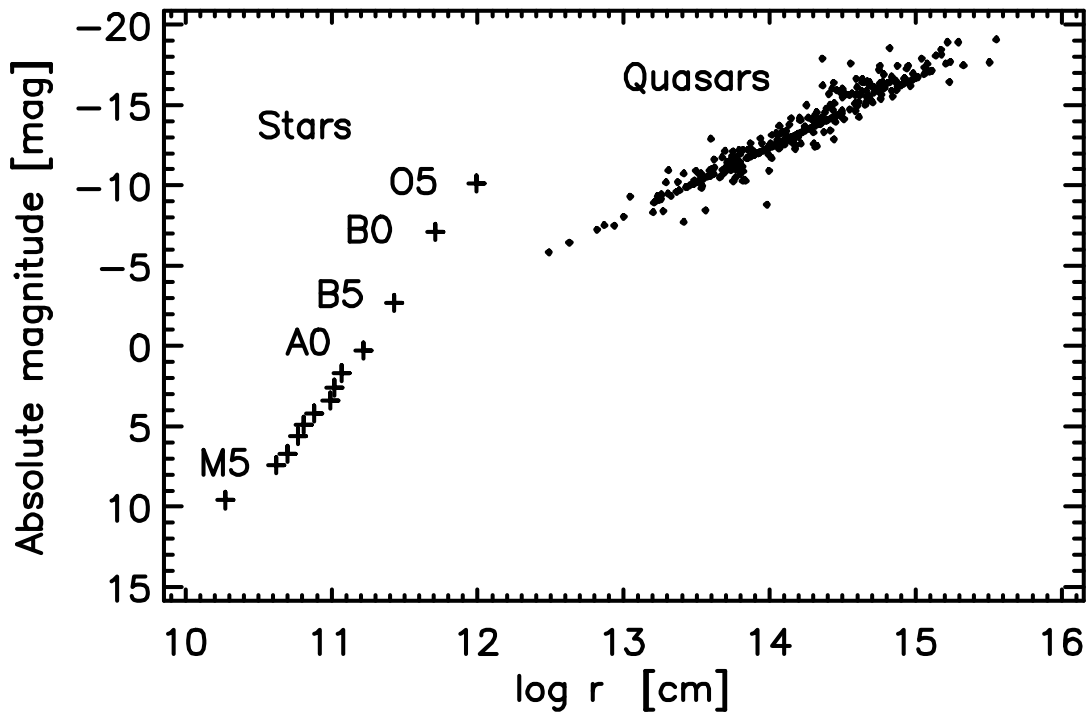


**Fig (3).** The relation “absolute magnitude – radius” for 341 sample quasars (dots). The same relation is shown also for stars (crosses) as mean values for O5, B0,...,M5. Note that the faintest quasars are less luminous than O stars. Courtesy of Bentham Open OAJ [55].

The relation “absolute magnitude – mass” for a sample of 74 QSOs was established in [25]:

$$M_q = 158.808 - 4.107 \cdot \log m_q \quad (13)$$

It has been later confirmed (with slightly different coefficients) in [54-55]. Fig (4) shows this relation with a sample of 341 QSOs, Table 2.

The physical meaning of relation (7) is that QSOs with larger radii have also brighter absolute magnitudes, which is to be expected. However, it also means that if the radius of a quasar increases (e.g. during the process of evolution), so does also its absolute brightness. From eq (13) the absolute magnitude depends also on the quasar mass. This is indicative that also relation “luminosity – mass” could exist. Indeed, in [25] this “luminosity – mass” relation was established:

$$\log L_q = -28.060 + 1.643 \cdot \log m_q \quad (14)$$

It was later confirmed (again, with slightly different coefficients) in [54-55]. The “luminosity – mass” relation is shown in Fig (5) with a sample of 341 QSOs, Table 2.

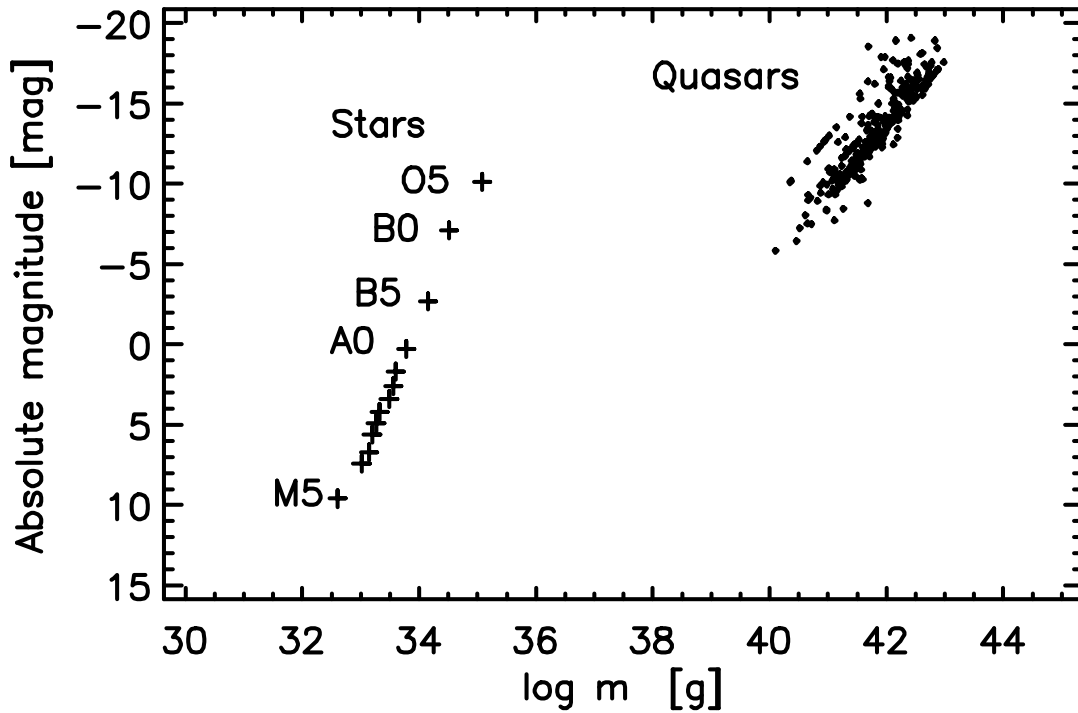


**Fig (4).** The relation “absolute magnitude – mass” for 341 sample quasars (dots). The same relation is shown also for stars (crosses), as mean values for O5, B0,..,M5. Courtesy of Bentham Open OAJ [55].

The “mass – radius” relation is shown in Fig (6) for the sample of 341 QSOs. It was first established in [25], and later confirmed in [54-55]. This relation [55] is:

$$\log m_q = 28.67 + 0.93 \log r_q \quad (15)$$

It has been already pointed out in [25, 54, 55] that the “mass – radius” relation for quasars implies that fainter local quasars should have larger gravitational redshifts and therefore also larger observed redshifts, which has been discussed already by Greenstein and Schmidt [13]. In the next chapter this is also shown on Figs (9, 10, 11). In the QSOs sample (Table 2) from quasars associated with the same galaxy, the faintest quasars seem to be with largest redshifts. Possible effects of evolution will be discussed below.

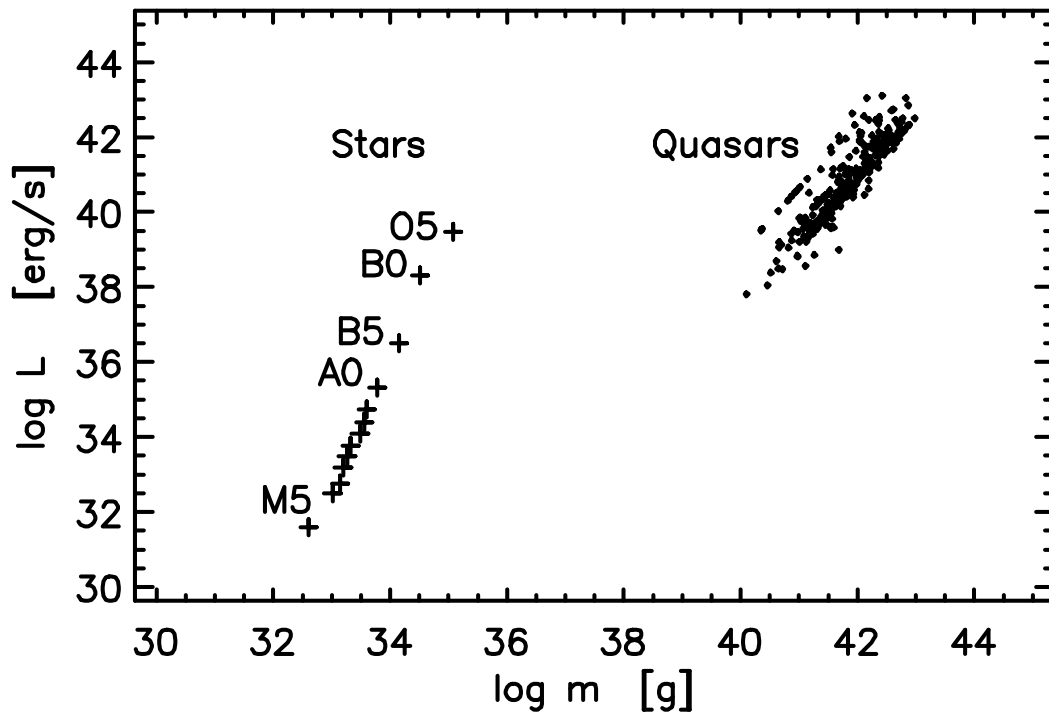


**Fig (5).** The “mass-luminosity” relation for 341 sample quasars (dots). The same relation is shown also for stars (crosses) as mean values for O5, B0, B5,..., M5. Courtesy of Bentham Open OAJ [55].

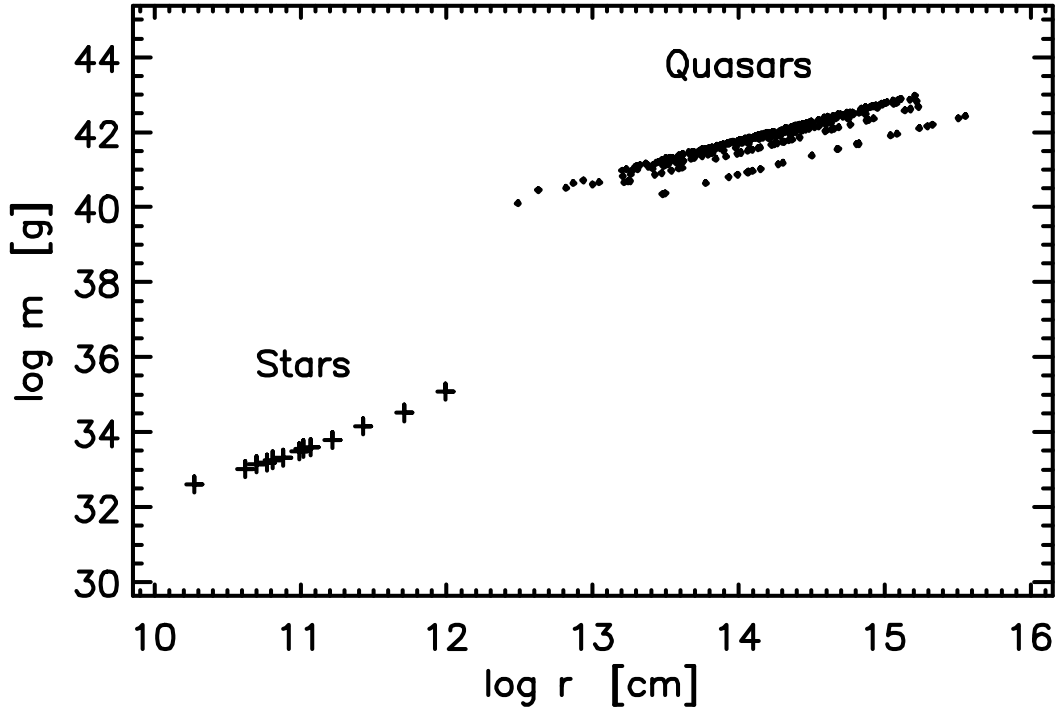


**Fig (6). The relation “mass – radius” for 341 sample quasars (dots). The same is shown also for stars (crosses) as mean values for O5, B0, B5,..,M5. Courtesy of Bentham Open OAJ [55].**

Fig (6) shows an unusual appearance, it is unusually fragmented in parallel sequences of observations, apparently having the same slope. Some of these parallel sequences seem to be more densely “populated” with observations than others. This strange appearance does not look as being caused by random errors and it may even cast doubt on the procedure used. What could be the reason for this strange appearance? To answer this question some theoretical treatment is necessary [95]. From eq (8) and eq (12) we get:

$$\rho_q = 3/(8\pi) \cdot c^2/G \cdot 1/r_q^2 \cdot (r_{gr}/r_q) \quad (16)$$

and further:

$$m_q/r_q = c^2/(2G) \cdot (r_{gr}/r_q) \quad (17)$$

Substituting the constants c and G (in the cm, g, s – system) we get:

$$\log m_q = 27.83 + \log r_q + \log (r_{gr}/r_q) \quad (18)$$

Eq (18) is the “mass – radius” relation (see also eq 15), but there is an additional term, depending on  $r_{gr}/r_q$ . This term should be regarded as an independent term determined from eq (5). There is also slight difference of the coefficients between eq (15) and eq (18) and which could be explained with eq (15) being an average relation with all the “parallel” lines included. As shown in [25, 54, 55] (see also Table 3), for each  $z_{gr}$  value of the Karlsson sequence there is a corresponding value of the  $r_{gr}/r_q$ , building a sequence

of discrete values: 0.11, 0.41, 0.61, 0.74, 0.83, 0.89, 0.92 and so on. These correspond respectively to the sequence of  $z_{gr}$  - redshifts: 0.06, 0.30, 0.60, 0.96, 1.41, 1.96, 2.64, and so on. Therefore, with substitution of the respective  $r_{gr}/r_q$  in eq (18) we get a whole “family” of relations:

$$\begin{array}{l}
 \text{for } r_{gr}/r_q = 0.11, \quad \log m_q = 26.87 + \log r_q \\
 \text{for } r_{gr}/r_q = 0.41, \quad \log m_q = 27.44 + \log r_q \\
 \dots\dots\dots \\
 \text{for } r_{gr}/r_q = 0.92, \quad \log m_q = 27.79 + \log r_q \\
 \dots\dots\dots \\
 \text{for } r_{gr}/r_q = 1.0, \quad \log m_q = 27.83 + \log r_q
 \end{array} \quad \} \quad (19)$$

The family of equations (19) defines a family of parallel lines with a slope of 1 each, and which are indeed seen in Fig (6). The lowest line in this figure corresponds to  $r_{gr}/r_q = 0.11$  and in the direction of increasing values of  $r_{gr}/r_q$  the parallel lines get closer and “converge” to a line-limit corresponding to  $r_{gr}/r_q = 1.0$ . With decreasing distance between successive parallel lines they become undistinguishable for high values of  $r_{gr}/r_q$ , due to observational uncertainties. The limit of convergence of eqs (19) could easily be obtained from eq (12), if  $z_{gr}$  gets to  $\infty$ . In order to test eqs (19) with observations the sample of QSOs in Table 2 was divided in groups, with QSOs in each group having the same value of  $r_{gr}/r_q$ . In each group  $r_{gr}/r_q$  and therefore also  $z_{gr}$  are the same for all quasars of this group. The linear equations were solved (note that the number of quasars in each group is different!) and results are shown in Table 4.

**Table 4. Fitting coeff for eqs (19) for the sample of 341 QSOs of Table 2, divided in groups according to respective  $r_{gr}/r_q$ .**

| Number QSOs | $r_{gr}/r_q$ | $z_{gr}$ | Coefficients from eqs (19) |     | Coefficients from observations |       | Corr. coeff |
|-------------|--------------|----------|----------------------------|-----|--------------------------------|-------|-------------|
|             |              |          | a                          | b   | a                              | b     |             |
| 23          | 0.11         | 0.06     | 26.87                      | 1.0 | 26.87                          | 0.999 | 0.999       |
| 40          | 0.41         | 0.30     | 27.44                      | 1.0 | 27.44                          | 1.0   | 1.0         |
| 41          | 0.61         | 0.60     | 27.62                      | 1.0 | 27.62                          | 0.999 | 1.0         |
| 57          | 0.74         | 0.96     | 27.70                      | 1.0 | 27.70                          | 1.0   | 1.0         |
| 61          | 0.83         | 1.41     | 27.75                      | 1.0 | 27.75                          | 1.0   | 1.0         |
| 103         | 0.89         | 1.96     | 27.78                      | 1.0 | 27.81                          | 0.997 | 1.0         |
| 15          | 0.92         | 2.64     | 27.79                      | 1.0 | 27.80                          | 1.0   | 1.0         |

Comparison of the coefficients of eqs (19) in column 4 with coefficients of the fit of observations in column 5 shows satisfactory agreement. This is confirmation that fragmentation of the “mass – radius” diagram is described by the family of relations (19) with each individual relation having respective  $r_{gr}/r_q$ . We should now ask the more difficult question, what is the cause for this family of equations? The answer to this could take us to the problem of evolution of quasars. This problem will be addressed in the next chapter but we could say here that quasars probably evolve and the evolution could proceed with stepwise decreasing gravitational redshifts. This decreasing sequence

is shown in column 3, from bottom to top. In a decreasing sequence evolve also the corresponding values of  $r_{gr}/r_q$ , (column 2), starting (theoretically) with  $r_{gr}/r_q = 1$  (“event horizon”). Therefore, the “mass – radius” relation also evolves, starting by the limit of convergence at  $r_{gr}/r_q = 1$ , and proceeding downward on Fig 6 with parallel shifts to the last line corresponding to  $r_{gr}/r_q = 0.11$ . Note that there is also gradual shift (evolution) of the parallel lines toward larger quasar radii and smaller quasar masses. Therefore, the presumed evolution of the “mass- radius” relation may also reveal possible increase of radius and possible decrease of mass (Fig 6).

The “density – mass” relation is shown in Fig (7) for the sample of 341 QSOs. The average relation has been established in [25] and confirmed in [54, 55, 95]. This diagram is also fragmented and parallel sequences of observations are seen, each sequence with slope of -2. We could apply the same strategy and look for an equation that should include a term depending on  $r_{gr}/r_q$ .

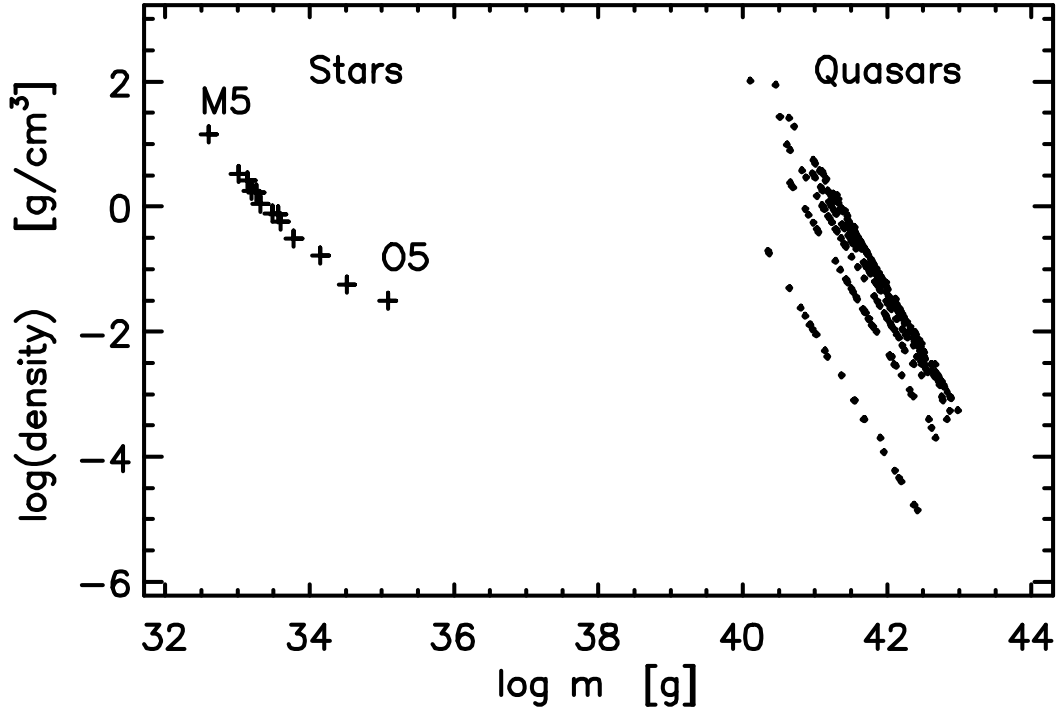


**Fig (7). Relation “density - mass” for the sample of 341 quasars (dots). The same is shown for stars (crosses) as mean values for O5, B0, B5,....., M5. Courtesy of Bentham Open OAJ [55].**

One could start again with eq (17) and with the obvious relation:

$$\rho_q = 3.m_q/(4\pi.r_q^3) \quad (20)$$

With some simple transformations we get:

$$\rho_q = 3/(32\pi) \cdot (c^6/G^3) \cdot (1/m_q^2) \cdot (r_{gr}/r_q)^3 \quad (21)$$

and further:

$$\log \rho_q = 82.86 - 2 \cdot \log m_q + 3 \cdot \log (r_{gr}/r_q) \quad (22)$$

This is the “density – mass” relation which also defines a family of relations, corresponding to the sequence of the  $r_{gr}/r_q$  values:

$$\left. \begin{array}{l} \text{for } r_{gr}/r_q = 0.11, \quad \log \rho_q = 79.98 - 2 \cdot \log m_q \\ \text{for } r_{gr}/r_q = 0.41, \quad \log \rho_q = 81.70 - 2 \cdot \log m_q \\ \dots\dots\dots \\ \text{for } r_{gr}/r_q = 0.92, \quad \log \rho_q = 82.75 - 2 \cdot \log m_q \\ \dots\dots\dots \\ \text{for } r_{gr}/r_q = 1.0, \quad \log \rho_q = 82.86 - 2 \cdot \log m_q \end{array} \right\} (23)$$

The family of eqs (23) represents a family of parallel lines with slopes of -2 each, and which are seen on Fig (7). With increasing values of  $r_{gr}/r_q$ , these lines converge to a limit-line for  $r_{gr}/r_q = 1$  (“event horizon”). The last lower relation on Fig (7) corresponds to  $r_{gr}/r_q = 0.11$ . In order to test eqs (23) with observations the sample of 341 QSOs of Table 2 was divided again in groups, each group having respective  $r_{gr}/r_q$ , which are the same groups as in Table 4. The results are shown in Table 5.

**Table 5. Fitting coeff for eqs (23) for the sample of 341 QSOs of Table 2, divided in groups according to respective  $r_{gr}/r_q$ .**

| Number QSOs | $r_{gr}/r_q$ | $z_{gr}$ | Coefficients from eqs (23) |      | Coefficients from observations |       | Corr. coeff |
|-------------|--------------|----------|----------------------------|------|--------------------------------|-------|-------------|
|             |              |          | a                          | b    | a                              | b     |             |
| 23          | 0.11         | 0.06     | 79.98                      | -2.0 | 79.21                          | -1.98 | -0.999      |
| 40          | 0.41         | 0.30     | 81.70                      | -2.0 | 81.71                          | -2.0  | -1.0        |
| 41          | 0.61         | 0.60     | 82.22                      | -2.0 | 81.98                          | -2.0  | -1.0        |
| 57          | 0.74         | 0.96     | 82.47                      | -2.0 | 82.28                          | -2.0  | -1.0        |
| 61          | 0.83         | 1.41     | 82.62                      | -2.0 | 82.63                          | -2.0  | -1.0        |
| 103         | 0.89         | 1.96     | 82.71                      | -2.0 | 82.94                          | -2.0  | -1.0        |
| 15          | 0.92         | 2.64     | 82.75                      | -2.0 | 82.42                          | -1.99 | -1.0        |

Comparison of the coefficients of eqs (23) with the fit of observations (columns 4 and 5, respectively) shows satisfactory agreement. Therefore, fragmentation of the “density-mass” diagram seems to be consistent with the family of relations (23) which describe this diagram. Also in this case it is the presumed evolution of quasars that causes the shift (evolution) of the “density – mass” relation from the locus of convergence ( $r_{gr}/r_q = 1$ ) to the lowest line of the diagram corresponding to  $r_{gr}/r_q = 0.11$ . Note also that the evolution of this diagram (the parallel lines) seems to proceed with possible decrease of mass and with clearly decreasing density (the lowest line on Fig 7 is shifted to lower densities!). Stars and QSOs on Fig (7) show the same trend - most massive stars and also most massive QSOs have the lowest density. If evolution proceeds with decreasing density

(disintegration scenario) the more massive stars and quasars should evolve faster. This conclusion is well known for stars in the standard (orthodox) theory. Obviously, the same conclusion is true also in the disintegration scenario and it is true for stars and for quasars. More massive quasars also evolve faster. Note however, the large spread of quasar densities on Fig (7).

The “radius – density” relation for quasars was established in [55, 95] and is shown on Fig (8) for the sample of 341 QSOs of Table 2. The fragmentation of this diagram due to parallel sequences of observations is also clearly seen. Searching for a suitable formula, we could start again with the eq (16). With simple transformations we get:

$$\log r_q = 13.60 - \frac{1}{2} \log \rho_q + \frac{1}{2} \log (r_{gr}/r_q) \quad (24)$$

Eq (24) is the “radius – density” relation found in [55, 95]. For the sequence of  $r_{gr}/r_q$  values, this equation becomes a family of relations:

$$\left. \begin{array}{l} \text{for } r_{gr}/r_q = 0.11, \quad \log r_q = 13.12 - \frac{1}{2} \log \rho_q \\ \text{for } r_{gr}/r_q = 0.41, \quad \log r_q = 13.41 - \frac{1}{2} \log \rho_q \\ \dots\dots\dots \\ \text{for } r_{gr}/r_q = 0.92, \quad \log r_q = 13.58 - \frac{1}{2} \log \rho_q \\ \dots\dots\dots \\ \text{for } r_{gr}/r_q = 1.0, \quad \log r_q = 13.60 - \frac{1}{2} \log \rho_q \end{array} \right\} (25)$$

Equations (25) represent a family of parallel lines with slopes of -0.5 each, seen also on Fig (8). The line of convergence is again for  $r_{gr}/r_q = 1$  (“event horizon”). The sample of 341 QSOs was divided again in the same groups as above in Tables 4 and 5, according to respective  $r_{gr}/r_q$ . The eqs (25) were solved for each respective group of observations and results are shown in Table 6.

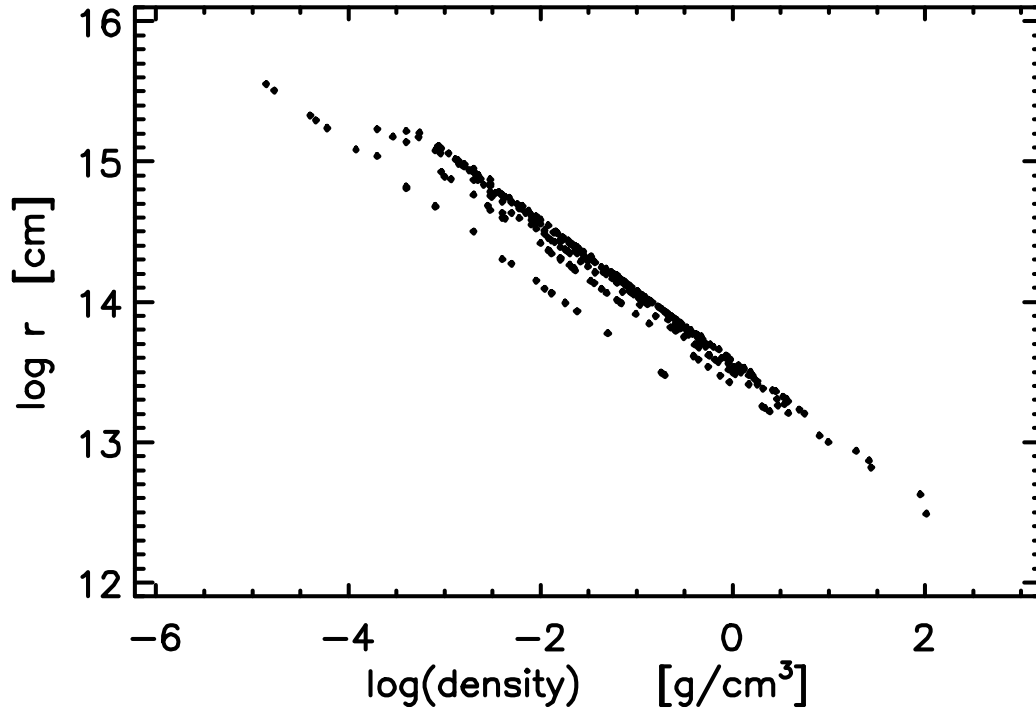


Fig (8). Relation “radius – density” for 341 sample quasars. The lowest sequence corresponds to  $r_{gr}/r_q = 0.11$  . Courtesy of Bentham Open OAJ [55].

Table 6. Fitting coeff for eqs (25) for the sample of 341 QSOs of Table 2, divided in groups according to respective  $r_{gr}/r_q$  .

| Number QSOs | $r_{gr}/r_q$ | $z_{gr}$ | Coefficients from eqs (25) |       | Coefficients from observations |       | Corr. coeff |
|-------------|--------------|----------|----------------------------|-------|--------------------------------|-------|-------------|
|             |              |          | a                          | b     | a                              | b     |             |
| 23          | 0.11         | 0.06     | 13.12                      | -0.50 | 13.12                          | -0.50 | -1.0        |
| 40          | 0.41         | 0.30     | 13.41                      | -0.50 | 13.41                          | -0.50 | -1.0        |
| 41          | 0.61         | 0.60     | 13.49                      | -0.50 | 13.495                         | -0.50 | -1.0        |
| 57          | 0.74         | 0.96     | 13.53                      | -0.50 | 13.54                          | -0.50 | -1.0        |
| 61          | 0.83         | 1.41     | 13.56                      | -0.50 | 13.56                          | -0.50 | -1.0        |
| 103         | 0.89         | 1.96     | 13.57                      | -0.50 | 13.578                         | -0.50 | -1.0        |
| 15          | 0.92         | 2.64     | 13.58                      | -0.50 | 13.586                         | -0.50 | -1.0        |

The agreement between eqs (25) and the observations in all groups of Table 6 is satisfactory, which confirms eqs (25). Presumably, as quasars evolve following the sequence of decreasing values of  $r_{gr}/r_q$  also the “radius – density” relation evolves, starting at  $r_{gr}/r_q = 1$  and proceeding to the lowest relation on Fig (8), for  $r_{gr}/r_q = 0.11$ . Note that the evolution of the “radius – density” diagram also indicates a shift (evolution) of parallel lines to larger radii and to decreasing densities. The same conclusion (evolution to larger radii) was reached also from Fig (6) and evolution to lower densities is indicated also on Fig (7). There is one more remark about Fig (8). At the right lower end are

quasars with the lowest masses and there seems to be a trend of (generally) increasing mass to the left upper end. Therefore, if disintegration processes are responsible for the relation on Fig (8) and the evolution proceeds with decreasing densities and increasing radii then the quasars with larger masses are “leading” in this evolution. It is the same conclusion that is implied by Fig (7): quasars with larger masses evolve faster. However, at the upper end of this diagram are also quasars with the largest cosmological redshifts. Does Fig (8) reflect effects of cosmological distances, or effects of evolution by disintegration, or both? I will come back to this question in the next chapter. One important remark should be mentioned at this point. On all diagrams of this chapter QSOs are presented from different cosmological distances. Since on all diagrams the relations shown seem to hold for quasars of different cosmological redshifts, I am tempted to conclude that the same physical processes are operating at all cosmological distances and which determine quasar properties and evolution. This should be an important conclusion.

The fragmentation of the relations shown on Figs (6- 8) has been discussed in [95]. These effects could have some impact also in other relations (e.g. on Figs (3- 5) where they could increase the scatter on respective diagram. The apparent exact fitting of data with relations [19], [23], and [25] confirms the consistence of theory and observations and the proposed procedure in Chapter 3.

## ***Chapter 5.***

### ***Evidence of evolution of quasars. The linear density relation.***

In the previous chapters we already discussed possible effects of evolution of QSOs. On Fig (1) the diagram “reduced density – redshift” could be explained in a natural way by decreasing density of quasars and respective drop in the gravitational redshift component, which leads also to decrease of the observed redshift. Assuming disintegration scenario it should be noted that the evolution of quasars on this diagram should be very fast at large redshifts. As apparent from Fig (1) only a small decrease of density (and reduced density) at large redshifts leads to a large drop of the redshift. This effect could explain the deficiency of quasars with  $z_o > 3$ , which possibly evolved rapidly to lower redshifts. Assuming this evolutionary picture there is another important consequence: evolution from high to lower values of redshift on this diagram could be due to increasing quasar dimensions all the way from high to low redshifts. This is in agreement with Fig (8) of the previous chapter and with the disintegration hypothesis for QSOs. If the masses of quasars are preserved (we could assume this as first approximation), the disintegration of the “primordial” matter in quasars would lead to decreasing density and increasing radii. A rough estimate of the radius increase factor could be obtained by increasing stepwise the radius of some large redshift quasar. The “test-quasar” will “travel” along the diagram, from  $z_{gr}$  of  $\sim 3.2$  to  $z_{gr} \sim$  of  $0.07$  if the initial radius is increased  $\sim 8$  times. This is only a rough estimate because there are indications of mass loss from quasars which would require additional considerations.

Discussing the effects of discretization in the last chapter the fragmentation of the “mass – radius”, “density – mass”, and “radius – density” relations was explained in a natural way by assuming evolution of each respective relation due to the evolution of quasars, and the evolution of  $r_{gr}/r_q$  from 1.0 stepwise down to 0.11. The “mass – radius” relation evolves also in the sense of decreasing masses and increasing radii (Fig 6). The evolution of the “density – mass” relation indicates a shift to decreasing density and also possible decrease of mass (Fig 7). The evolution of the “radius – density” relation is also in the sense of decreasing density and increasing radii (Fig 8). All these findings are consistent with the assumption of disintegration of matter and (possible) mass loss in the late stages of evolution of quasars. An interesting question is where did the lost mass go?

Presumably, the lost mass from a quasar could have gone to build stellar population around the quasar. Such a scenario has been proposed by Arp [52, 94]. We could have more evidence of it by the end of this chapter.

Considering effects of quasar evolution we should look for effects at different cosmological distances, as well as in QSOs at about the same distance. In Table 2 there are large enough groups of quasars clustering around the same galaxy. These groups provide for a possibility to study effects of evolution of quasars at the distance of the respective parent galaxy (e.g. 63 QSOs of NGC 450 and 41 QSOs of NGC 6212). Using these groups the next question could be asked, what happens with the quasar luminosity by the evolution of quasars? Already evidence was found above of increasing radii by

decreasing density, i.e. by the evolution of quasars (Fig 8). This is not enough to conclude about the quasar luminosity evolution since we don't know what the physical processes are and what the temperature behavior is in the process of evolution. In order to look for answers observational evidence could be used from Table 2. Let us consider first the two groups of quasars mentioned above clustering around NGC 450 and NGC 6212, respectively, each one at specific cosmological distance. On Fig (9) the 63 QSOs of NGC 450 are shown. In the upper panel the quasars' absolute magnitudes (Table 2) are plotted versus observed redshift. A trend of increasing brightness could be noticed but there is considerable scatter. This scatter could be reduced if all magnitudes are reduced to a single mass arbitrarily chosen as:  $5.3 \cdot 10^{41}$  [g]. Why we should do that? In the previous chapter the relation "absolute mag – mass" was shown on Fig (4). As quasars have different masses this could contribute to the scatter in the upper panel of Fig (9). Therefore, in this panel we could have a diagram due to the contribution of two factors: dependence of luminosity on evolution and dependence of luminosity on mass. Since we are looking here to the effects of evolution we should eliminate the dependence on mass. Indeed, we could reduce all absolute magnitudes to a single (arbitrary) mass, e.g.  $5.3 \cdot 10^{41}$  [g], using the eq (13):

$$M_q = 158.808 - 4.107 \cdot \log m_q$$

The dependence of luminosity on mass is therefore eliminated and the evolutionary increase of luminosity could be seen more clearly in the second panel of Fig (9). The 3<sup>rd</sup> panel of the same figure shows the trend of increasing QSOs radii with decreasing redshift, using the original data from Table 2. Also in this diagram there could be a contribution to the scatter due to the "mass – radius" relation, superposed to an evolutionary trend. In the last (lowest) panel the same data for the radii are reduced to the same mass,  $5.3 \cdot 10^{41}$  [g] with eq (15). In this way the scatter is reduced and the evolutionary increase of quasar radius is seen more clearly (last panel). The quasars of NGC 450 seem to indicate that both quasar radius and quasar luminosity increase with decreasing redshift, i.e. by the assumed process of evolution. Thus Fig (9) shows the evolution of brightness and radius at the distance of the galaxy NGC 450 ( $z_{gal} = 0.006$ ). However, we need more evidence. On Fig (10) the same panels are presented for the 41 QSOs of NGC 6212. The same procedure as for Fig (9) was applied and the same trends as on Fig (9) are clearly seen. Reduced quasars magnitudes and radii in this case are done to a mass of  $2.5 \cdot 10^{42}$  [g] which eliminates the dependence on mass. The evolution of brightness and radius on Fig (10) are clearly seen on panels two and four with the reduced magnitudes and the reduced radii, respectively. The evidence from Fig (10) is in agreement with the evidence from Fig (9). Both figures point out to a possible evolution with quasar expansion and increasing quasar brightness (luminosity).

On Fig (11) several more groups of quasars are shown and in all cases the trend of increasing luminosity with decreasing quasar redshift is clearly seen. On this diagram for each group of quasars reduction of absolute magnitudes was applied to an arbitrary mass (different mass for each group), in order to eliminate the dependence of brightness on mass. Again, the evidence from Fig (11) seems to corroborate the evidence from the two previous figures. It now seems that there is substantial evidence consistent with the

assumption that quasars are evolving with increasing radii and increasing luminosity by decreasing redshift. This conclusion is corroborated by 10 different groups (for the luminosity) of quasars on Figs (9-11). The sampling of quasars on Fig (11) will be explained below.

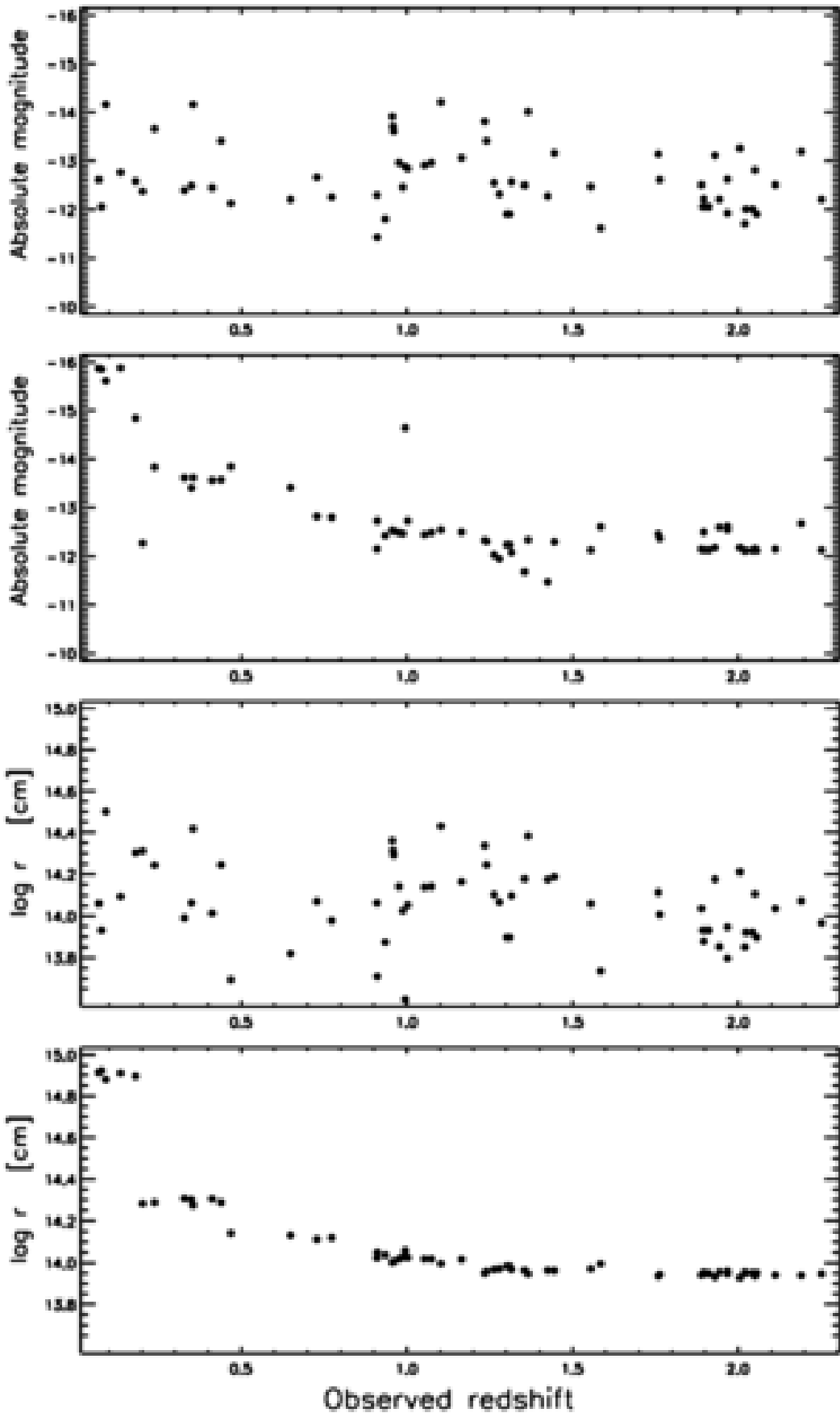


**Fig (9).** (upper panel) Relation of absolute magnitude with observed redshift for 63 quasars of NGC450 (data from Table 2). Note the trend of increasing brightness with decreasing redshift; (second panel) The same relation for the same 63 quasars of NGC450 with all magnitudes reduced to a mass of  $5.3 \times 10^{41}$  [g] (see text); (third panel) Relation of quasar radii versus observed redshift for the same 63 quasars of NGC 450 (data from Table 2); (last lower panel) The same relation for quasar radii versus observed redshift for the same 63 quasars of NGC 450 with all radii reduced to the mass of  $5.3 \times 10^{41}$  [g] (see text). Courtesy of ZITI Publishing, Thessaloniki, [54].

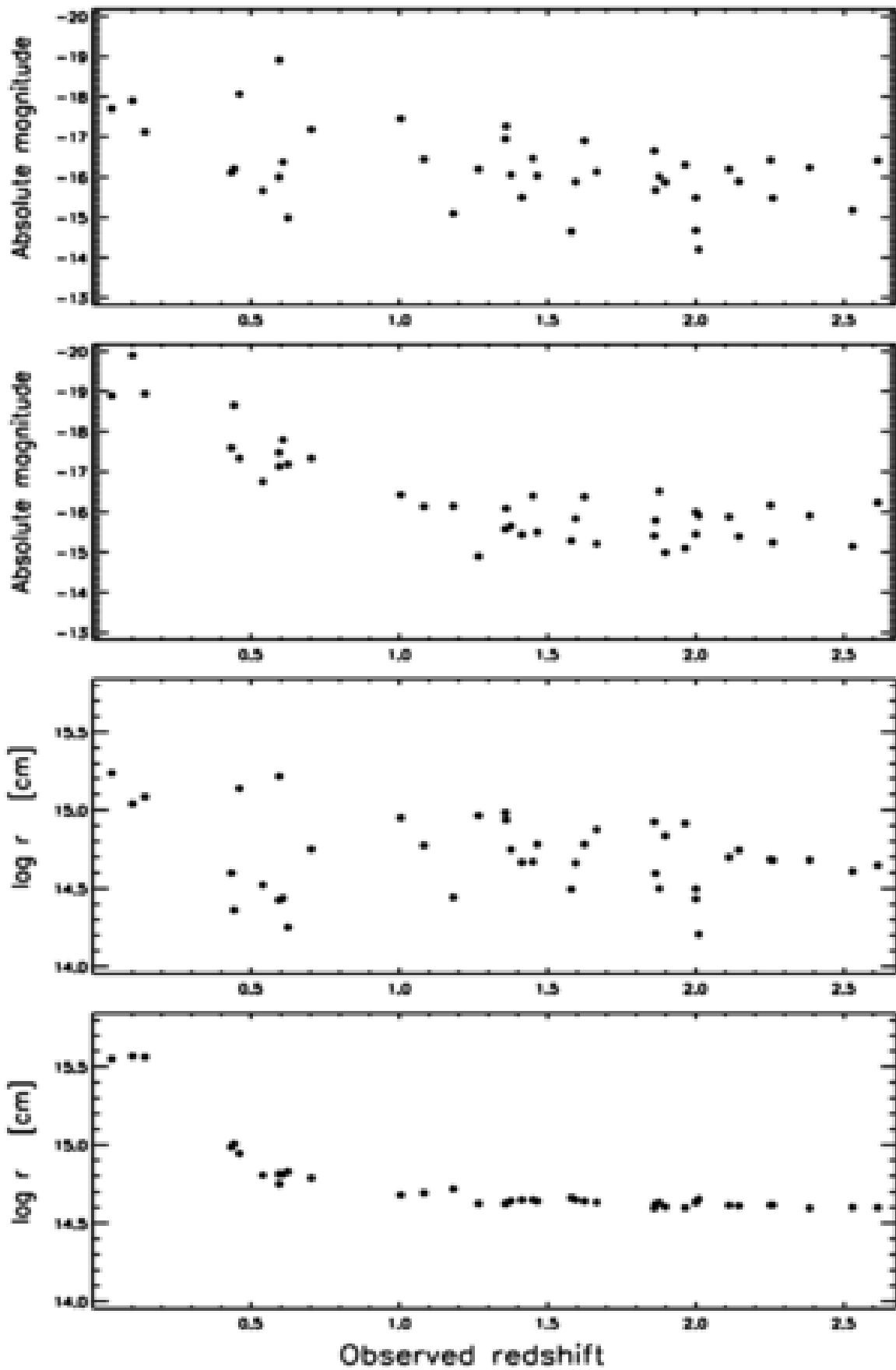


**Fig (10).** (upper panel) Relation of absolute magnitude with observed redshift for 41 quasars of NGC 6212 (data from Table 2). Note the trend of increasing brightness with decreasing redshift; (second panel) The same relation for the same 41 quasars of NGC 6212 with all magnitudes reduced to a mass of  $2.5 \cdot 10^{42}$  [g] (see text); (third panel) Relation of quasar radii versus observed redshift for the same 41 quasars of NGC 6212 (data from Table 2); (lowest panel) The same relation for quasar radii versus observed redshift for the same 41 quasars with all radii reduced to a mass of  $2.5 \cdot 10^{42}$  [g].

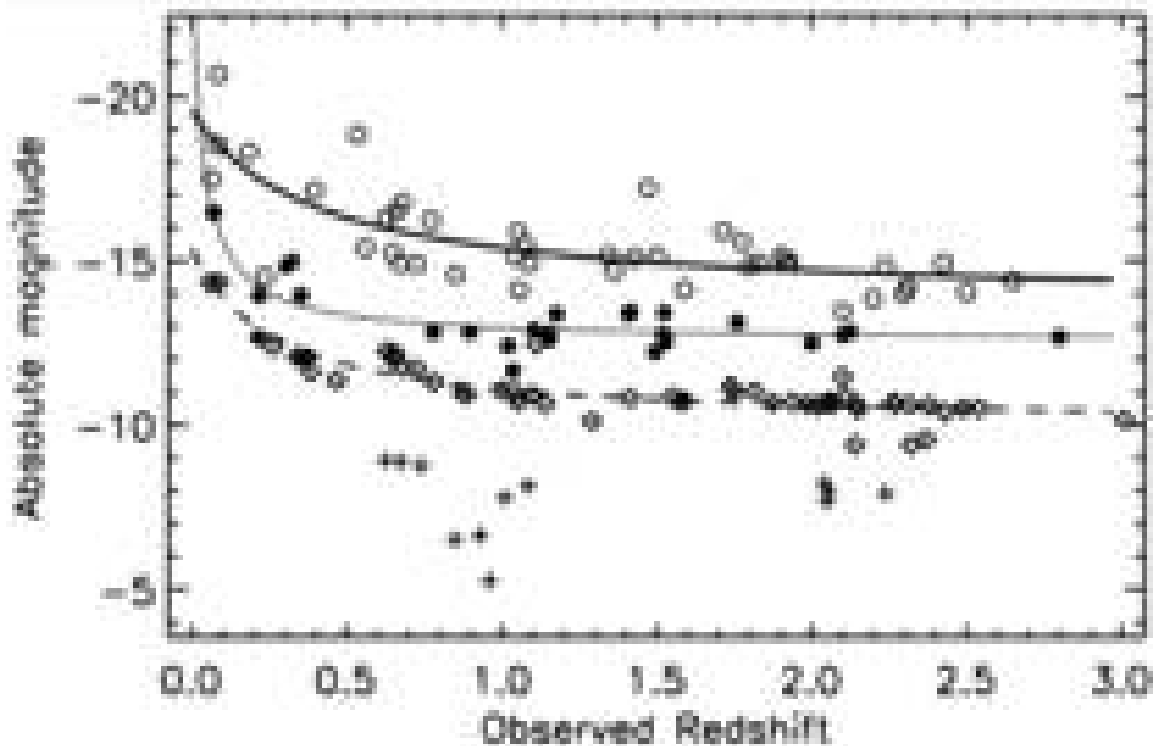


**Fig (11).** Relation of absolute magnitude with observed redshift for quasars of: M82 (crosses), all magnitudes are reduced to a mass of  $6.6 \times 10^{40}$  [g]; NGC1068, NGC1097, and NGC3628 (rhombs), all magnitudes are reduced to a mass of  $2.4 \times 10^{41}$  [g]; NGC2639 and NGC3079 (dots), all magnitudes are reduced to a mass of  $7.3 \times 10^{41}$  [g]; NGC4410 and NGC5548 (circles), all magnitudes are reduced to a mass of  $1.6 \times 10^{42}$  [g]. Courtesy of ZITI Publishing, Greece [54].

One more piece of evidence is shown in Fig (12) with the relation “absolute magnitude – density“. Clearly seen is the trend of increasing brightness (luminosity) with decreasing density, i.e. in the presumed direction of evolution. It should be noted that in the same direction quasar masses increase, being largest at the left upper end of this diagram. This result is consistent with the previous conclusions supporting the conclusion that evolution depends on mass. Summarizing, the more massive quasars are also more luminous and

with larger radii, but with lower density. In the presumed direction of evolution by decreasing redshift quasars radii and luminosities increase, while quasars densities decrease. This is consistent with the disintegration scenario. As on Fig (8), also on Fig (12) the most massive and luminous quasars are also quasars with larger cosmological redshifts. Thus it seems possible that Figs (8) and (12) could also present effects of quasar cosmological redshifts (effects of evolution due to the expansion of the Universe!) in addition to the effects of evolution at specific cosmological distances. On both Figs (8) and (12) QSOs at different cosmological distances behave in the same way on the respective diagram. Therefore, it seems possible that the physical processes which determine the respective relation: “radius-density” on Fig (8) and “absolute magnitude-density” on Fig (12) should be the same at all cosmological distances. The common “absolute magnitude – density” relation with quasars at different stages of evolution and at different cosmological distances could only be understood if the physical processes causing the evolution are the same at each cosmological distance. This seems to be an important conclusion.

Fig (12) could also provide for evidence in a rather different aspect. With increasing density quasars are fainter. Could this have a bearing on the much discussed problem of the “dark matter” in the Universe? Is it possible that large masses in the Universe could be “dark” (invisible) because of being very dense? This is a tantalizing possibility that deserves further study.

We could try to obtain more evidence of the “cosmological effects” on the quasars physical characteristics. Let me turn back to the sampling of groups of quasars on Fig (11). It could be noticed that the lowest sample includes the QSOs of M82 which are the most faint and generally less massive, but also this galaxy has the lowest redshift ( $z_{\text{gal}} = 0.001$ ). The most upper sequence of observations on the same plot includes QSOs from NGC 4410 and NGC 5548 which quasars are brighter and more massive, but these galaxies have larger cosmological redshifts ( $z_{\text{gal}} = 0.025$  and  $0.017$ , respectively). Could there be a dependence of quasar luminosities on cosmological distance? Looking for answers, plots are presented of the absolute magnitudes of quasars versus cosmological redshifts (Fig 13) and the quasar masses versus cosmological redshifts (Fig 14).

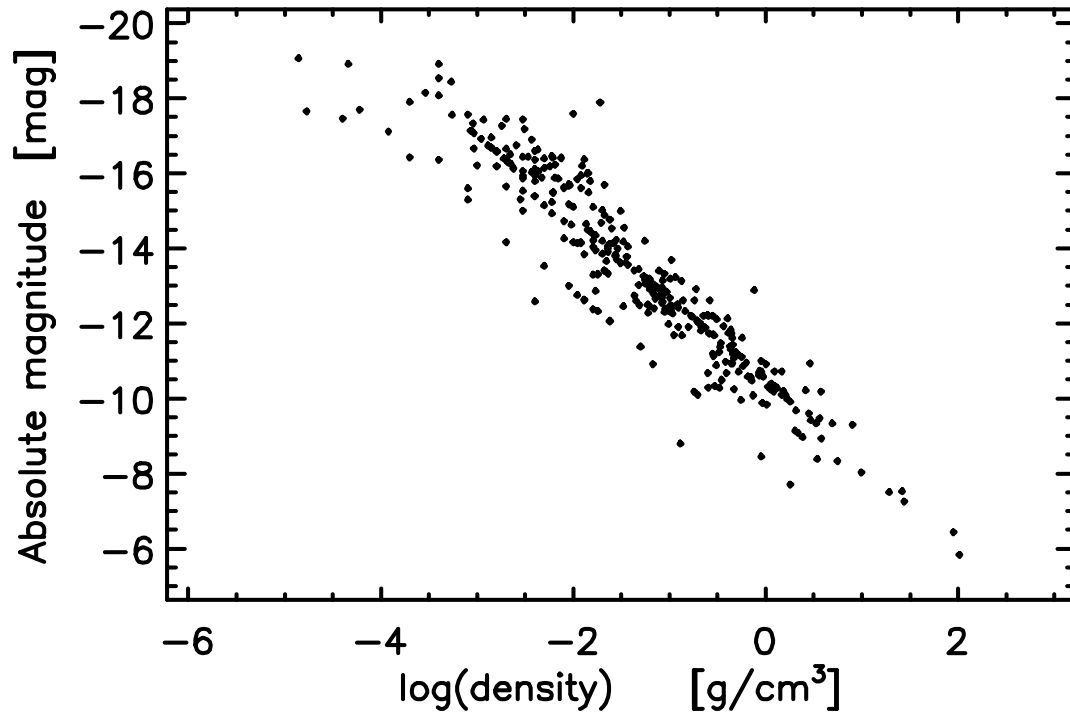


Fig (12). Relation “absolute magnitude – density” for 341 sample quasars. Courtesy of Bentham Open OAJ [55].

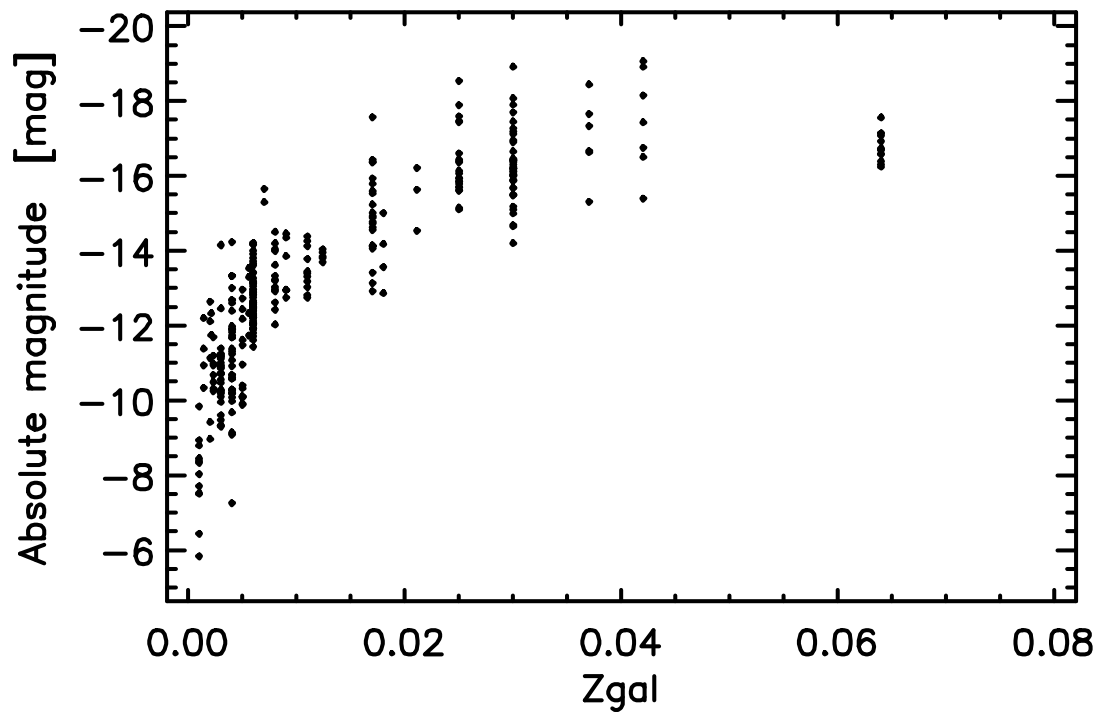
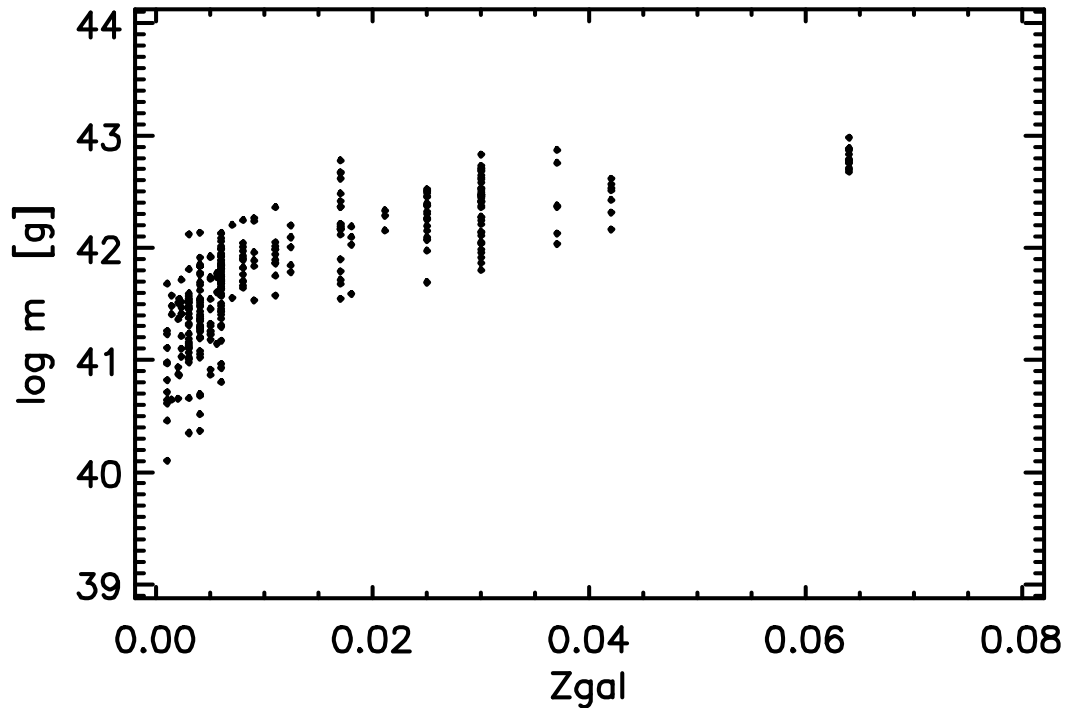


Fig (13). Dependence of quasar absolute magnitude on distance for 341 sample QSOs. Note the increasing “mean” luminosity to about  $z_{gal} = 0.025$ . Courtesy of Bentham Open OAJ [55].



**Fig (14). Dependence of quasar masses on distance for 341 sample QSOs. Note the increasing “mean” mass to about  $z_{gal} = 0.025$ . Courtesy of Bentham Open OAJ [55].**

Indeed, it seems that both the masses and the luminosities of quasars depend on distance, being on “average” more massive and more luminous at earlier epochs. Is this consistent with the concept of disintegration? It might be. If this concept is true, Figs (13) and (14) could indicate that at earlier epochs QSOs were more massive and more luminous and in the course of evolution (expansion of the Universe) quasar masses and luminosities become smaller. Thus the effect of evolution on luminosity due to cosmological expansion is opposite to the effect of evolution on a “local” scale. In late cosmological epochs quasar luminosities get fainter, but on a local scale these luminosities should increase as evolution proceeds. A plot of luminosities versus redshifts should understandably show large scatter due to both opposite tendencies. We could still try to reduce the dependence on distance (Figs 13 and 14) by eliminating from the sample all QSOs from the very late epochs. The dependence on distance could be partly avoided if from the sample of 341 QSOs only the quasars are taken with cosmological redshifts which are not less than 0.003. In this way a part of the scatter will be removed but the remaining scatter is still quite large. On Figs (15) and (16) plots of absolute quasar magnitudes versus observed redshift and quasar radii versus observed redshift are shown, respectively. Despite of the large scatter trends of increasing luminosities and radii with decreasing observed redshift could be noticed, meaning that effects of the presumed quasar expansion in direction of decreasing redshifts show up again. Let me stress the

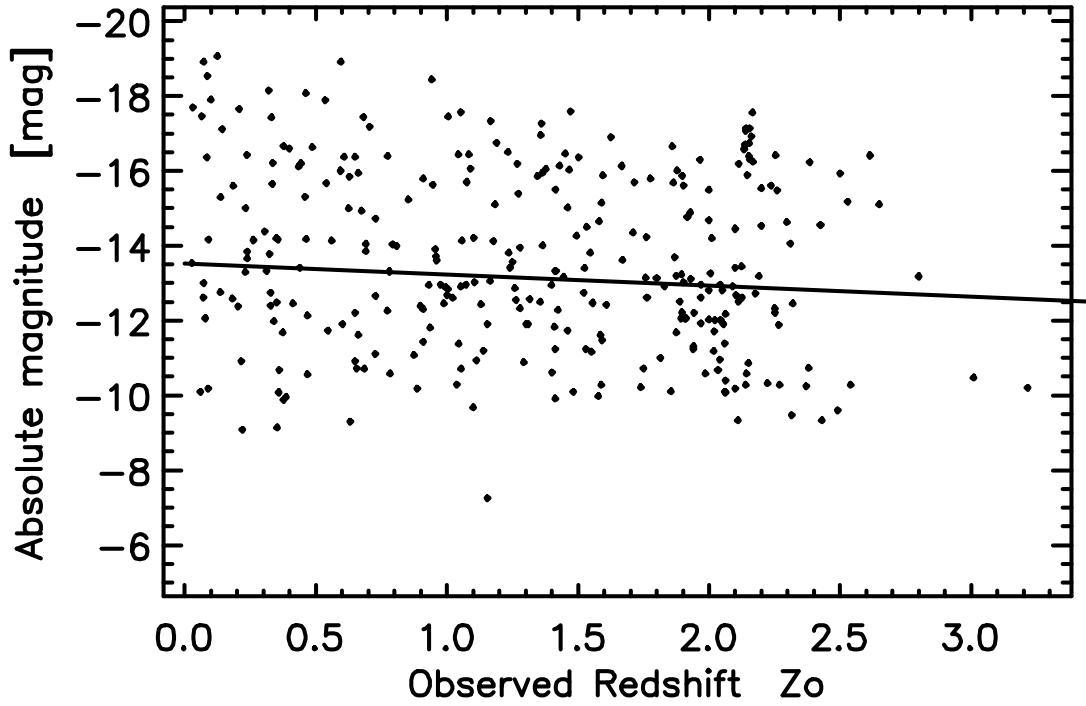


Fig (15). Plot of quasar absolute magnitudes versus observed redshift for the sample quasars with  $z_{\text{gal}} > 0.003$  ( $z_{\text{gal}} = z_c$ ). Courtesy of Bentham Open [55].

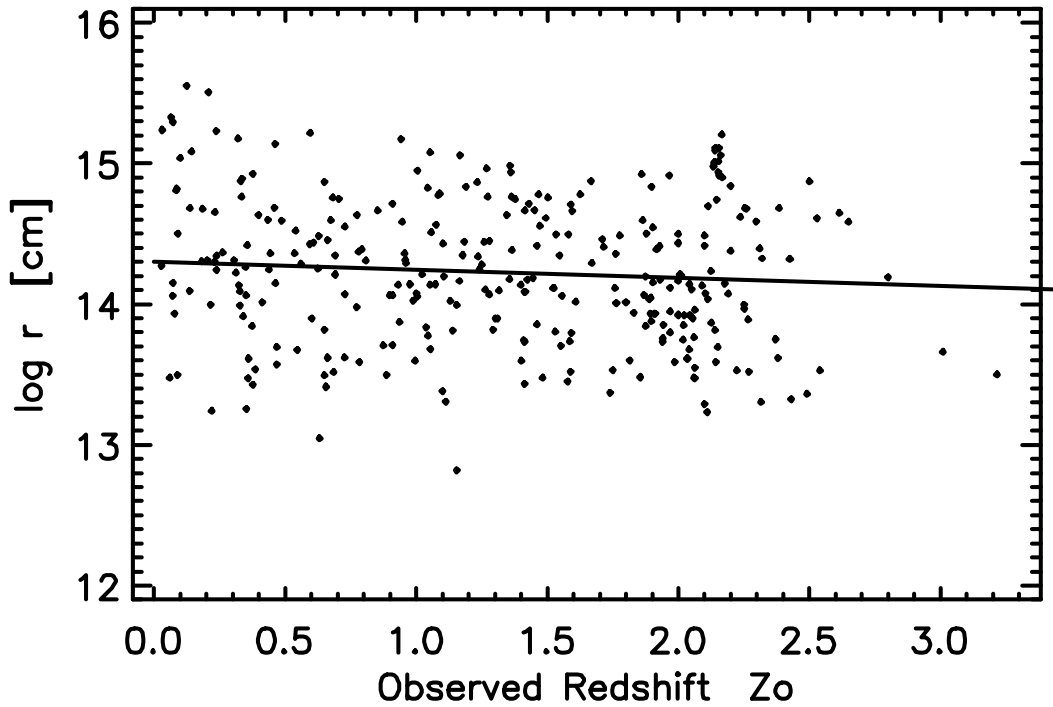
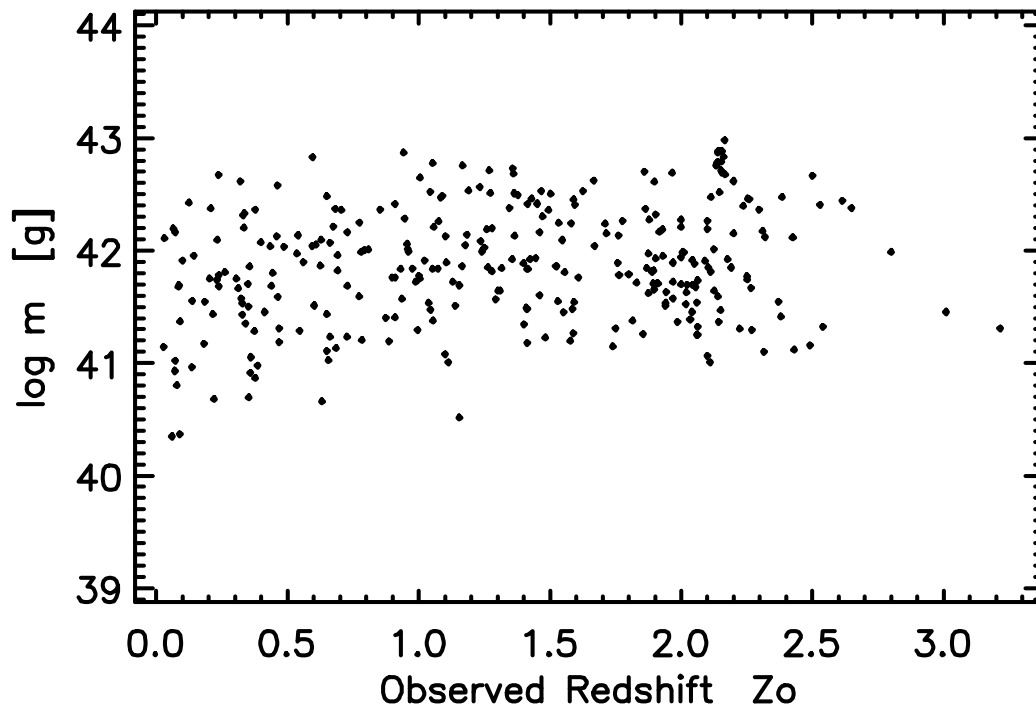


Fig (16). Plot of quasar radius versus observed redshift for the sample quasars with  $z_{\text{gal}} > 0.003$  ( $z_{\text{gal}} = z_c$ ). Courtesy of Bentham Open OAJ [55].

point that seems important. Different aspects of quasar evolution were shown on Figs (6, 7, 8, 12) with the whole sample of 341 QSOs, i.e. all quasars at different cosmological distances. This could only be possible if the physical processes which determine quasar properties and evolution are the same at all considered cosmological distances. Evolution of quasars should not be different at different cosmological redshifts. From the point of view of consistency the physics should be the same at all cosmological distances.

In the previous chapter we found evidence in (Figs 6 and 7) of quasar evolution with decreasing mass. In order to approach this problem from a different point of view quasar masses are plotted on Fig (17) versus observed redshifts. Again, QSOs from the late cosmological epochs are eliminated and the presumed evolution (local scale) is in the direction of decreasing quasar redshifts. (From the sample of 341 QSOs only these QSOs are plotted with cosmological redshifts not less than  $z_{gal} = 0.003$ ).

From Fig (17) there could be some drop in the masses of quasars in the late stages of evolution, for  $z_o < 0.60$ , but the evidence is slim. What could be the cause – if the effect is real, for mass loss from quasars? May be, this could be an indication of building stellar population around the respective quasar. The evidence from Fig (17) is however not compelling because some rest of the cosmological trend (see Fig 14) could still be present. Mass loss from quasars, if confirmed, could put the theory of origin of galaxies in an entirely new prospective.



**Fig (17).** Plot of quasar mass versus observed redshift for quasars with  $z_{gal} > 0.003$ . Courtesy of Bentham Open OAJ [55].

On Fig (17) yet another tendency could be considered. Since larger masses evolve faster, we should expect to see first a trend of increasing masses with decreasing redshift. This tendency should be inverted eventually if there is a mass loss from the quasars in the later stages. The evidence of both tendencies here is inconclusive and the main reason should be the interference of the opposite cosmological trend.

These findings (if confirmed) seem to be in agreement with the Arp's scenario [52, 94] – local quasars could have been ejected by active galactic nuclei and they may evolve as they recede from their respective parent galaxy into small mass, companion galaxies. Generally, the results presented here support such a scenario but the physical processes responsible for this ejection and evolution remain unknown. The highest projected velocity of ejection could be about  $30\,000\text{ km}\cdot\text{s}^{-1}$  (see Fig 2). The procedure presented here means that quasars have to be single objects with dimensions close to their respective gravitational radius. They are possibly the structures most close to their respective “event horizon”. A theory of such massive bodies does not yet exist. The present knowledge seems insufficient to answer this and many other questions. At the beginning the evolution of quasar redshifts due to decreasing density could be very fast - a small drop of density (see Fig 1) leads to a large drop of redshift to lower gravitational redshifts. Evidence was presented of possible increase of quasar radius and brightness as a result of the evolution. This seems to be consistent with the disintegration scenario since quasar expansion should result in a weaker gravitational attraction at the quasar surface and to a corresponding trend of the gravitational potential. Therefore, expansion should result in a trend of decreasing gravitational redshift. However, the evolution seems not to be continuous, but rather a sequence of “jumps” - prolonged “stops” at specific values of the redshift of the Karlsson sequence, and faster transition to the next lower value of this sequence. If we turn to the disintegration scenario this would require that expansion of the quasar (which generally explains the decreasing gravitational redshifts) should proceed stepwise with prolonged “stops” at specific quasar dimensions (i.e. at specific gravitational potentials), corresponding to the redshifts of the Karlsson sequence, and more rapid transition to a larger radius, corresponding to the next lower value of redshift in this sequence. This is how the Karlsson sequence could be explained. The faster transition to the next larger radius (the next lower gravitational potential) explains why gravitational redshifts of quasars are clustering around the values of the Karlsson sequence. What is the physics behind this process remains a mystery. Turning back to Chapter 3 it seems to be well possible that some gravitational redshifts of quasars are not exactly coincident with the respective Karlsson's value, simply because the quasar is observed “in transition” to this respective redshift. The treatment applied in Chapter 3 assumes all deviations of quasar redshift from the values of the Karlsson's sequence (after reduction for cosmological redshift) as due to Doppler shifts. The overall consistency of the results makes this treatment realistic. We should keep in mind, however, that gravitational redshifts need not to be exactly equal to the respective value of the Karlsson's sequence, if the transition to this value is not complete. Presently, it is not possible to distinguish such “deviations due to transit” from the Doppler shift components. Therefore, the data in Table 2 may still need some “fine tuning” in future. We may need a deeper insight into the subatomic physics to understand processes of quasar evolution.

There is one gravitational redshift - 1.96, that deserves special attention. On Fig (18) the distribution of quasars over  $r_{gr}/r_q$  is shown. Clearly, there is a maximum in this distribution at  $r_{gr}/r_q = 0.89$  ( $z_{gr} = 1.96$ ). Why are there so many quasars with  $z_{gr} = 1.96$ ? In the scenario described above it would appear that at this particular redshift there is a more prolonged slow-down in evolution. In the context of quasar evolution Fig (18) could point to a very fast evolution from  $r_{gr}/r_q = 1$  to  $r_{gr}/r_q = 0.89$ , and a prolonged “stop” at  $r_{gr}/r_q = 0.89$ . Again, the cause of these “stops” remains unknown.

Summarizing the evidence, the concept of decreasing quasar density which results in decreasing gravitational redshifts, and increasing quasar radii and luminosities is consistent with the observational data at present. There is also substantial evidence that evolution depends on the quasar mass - more massive quasars evolve faster.

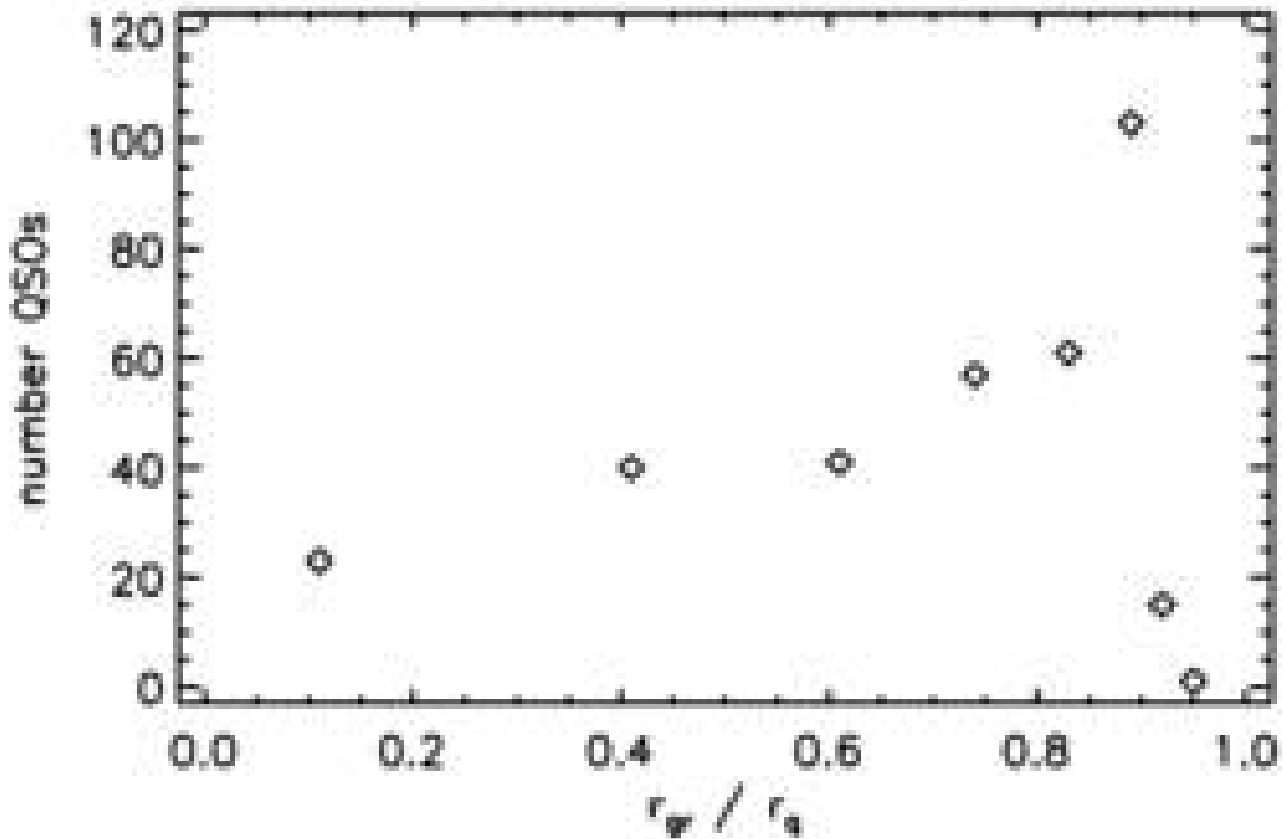


**Fig (18). Distribution of number of QSOs over  $r_{gr}/r_q$  for the sample of 341 QSOs. Courtesy of Bentham Open OAJ [95].**

On the “reduced density – redshift” diagram (Fig 1) there are no quasars below reduced density of  $\sim 0.02 \text{ g/cm}^3$ . Could that mean that QSOs already evolved into galaxies? Could it be that there are some galaxies, e.g. the compact galaxies that could present the first stages of the galaxy evolution? If yes, is it possible that some small gravitational components may exist in the redshifts of distant compact galaxies?

The relation of reduced density with gravitational redshift in eq (10) could be replaced by a similar relation with the ratio  $r_{gr}/r_q$ . From eq (12) we have:

$$r_{gr}/r_q = 1 - 1/(1 + z_{gr})^2$$

Substituting this expression in eq (10) we get:

$$\rho \sim 3/(8\pi) \cdot c^2/G \cdot 1/(8 \cdot 10^{13})^2 \cdot (r_{gr}/r_q) \quad (26)$$

With the system [g, cm, s] it will be:

$$\rho \sim 0.251549 \cdot r_{gr}/r_q \quad (27)$$

This is a simple linear density equation with respect to  $r_{gr}/r_q$  and a slope coefficient  $b = 0.251549$  [g/cm<sup>3</sup>]. On Fig (19) the sample of 341 QSOs (Table 2) is plotted on a “reduced density versus  $r_{gr}/r_q$ ” plot.

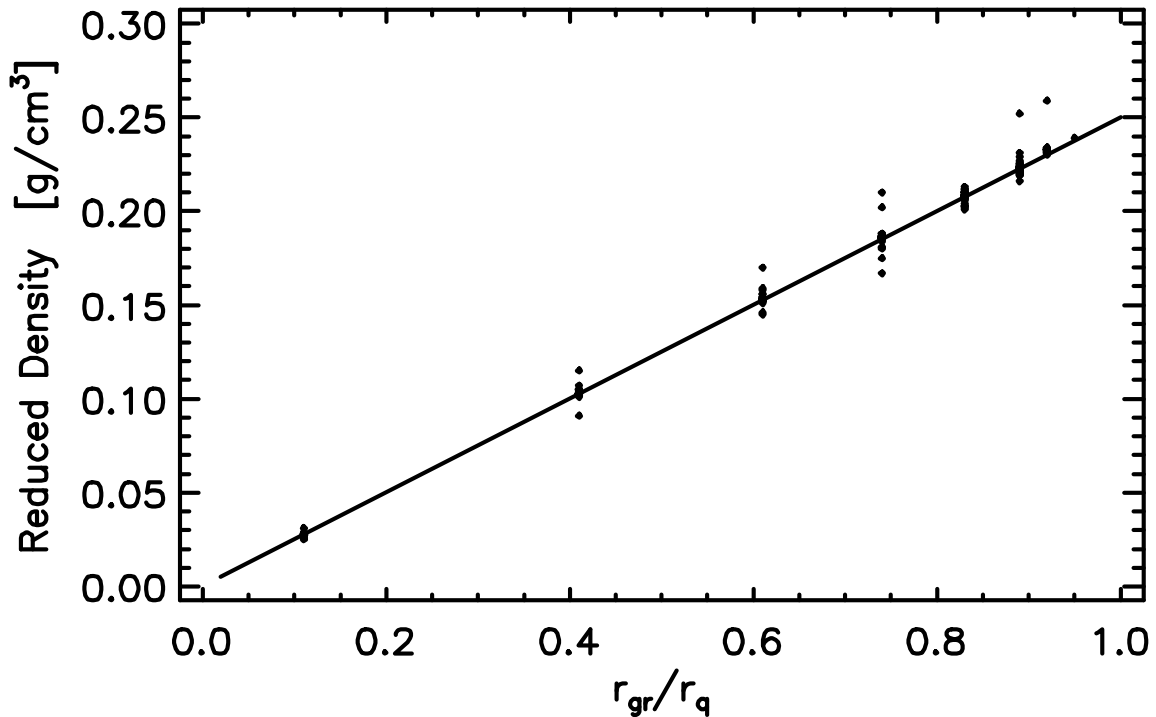


**Fig (19).** The linear relation of quasar reduced density with  $r_{gr}/r_q$  for the sample of 341 QSOs [55]. The mean line equation is:  $\rho \sim 0.0002 + 0.251 \cdot r_{gr}/r_q$  (see text). Courtesy of Bentham Open OAJ [55].

In the linear density relation (27) the slope coefficient  $\sim 0.252$  [g/cm<sup>3</sup>] is the density of a quasar ( $\rho = \rho \sim$ ) of  $r_q = 8 \cdot 10^{13}$  cm and with  $r_{gr}/r_q = 1$ , i.e. at the “event horizon”. It is the same limiting density as obtained from eq (8) above for  $z_{gr} = \infty$ . It should be noted that the linear solution of quasar data on Fig (19) is to be expected (as long as  $r_{gr}/r_q < 1$ ) by the definition of reduced densities. What is important is the position of quasars on this linear

density diagram (LDD) and quasars obviously occupy a distinct part of this diagram. They are not randomly distributed on the LDD. In the following it will be shown that also other structures – stars, planets, and satellites have their distinct positions on the same diagram.

The LDD on Fig (19) is consistent with the eq (27) as it should be by definition of the reduced density. If we accept the concept of evolution with decreasing density (and also reduced density) quasars should be evolving along the linear density diagram from the upper right end to the lower left end by increasing radius and preserved mass. As already pointed out preservation of mass is only a first approximation and considering quasar expansion together with mass loss could also result in “sliding down” on the LDD if the  $r_{gr}/r_q$  decreases. It should also be noted that most massive quasars are predominantly placed at the upper (right) part of the linear diagram. The next remark concerns both Figs (1) and (19). Assuming that evolution due to expansion follows with decreasing densities on both diagrams there are positions where the evolution slows down – these are the positions where the reduced densities correspond to the Karlsson sequence of redshifts (the same positions on both diagrams!). Only the gravitational components of redshifts depend on density, but as they are supposed to be the main components of redshifts in local QSOs, a drop of gravitational redshifts also means a drop in the observed redshifts of quasars. Summarizing, an evolutionary scenario could be invoked to describe the diagrams on Figs (1) and (19) which is consistent with the concept of disintegration. It has been discussed in the past that if quasars are of local origin this would contradict the concept of the expanding Universe. This is not necessarily so.

We started this presentation with the eq (1) which contains the term of the expanding Universe. The effects of cosmological redshifts were considered also with the quasar evolution (Figs 13 and 14). It seems that the expansion of the Universe and the gravitational reddening are two different sources attributing to the redshifts of extragalactic objects. The problem is, how these two components (and the third one, the Doppler shift) could be disentangled. With the local quasars this seems possible. On the other hand there is no doubt that QSOs should also exist at large cosmological distances. Decomposition of the redshift components in distant quasars is not at all obvious and could prove to be much more difficult.

Here is a summary of possible findings in this chapter, assuming disintegration scenario:

- Quasars seem to evolve with decreasing density, decreasing gravitational redshift, increasing radii, and increasing luminosities;
- On the LDD evolution of QSOs with increasing radii results in “sliding down” on the same diagram. The applicability of the linear density diagram to studies of evolution will be discussed further in the next chapter.
- Quasars may lose mass during the process of evolution;
- The evolution of quasars depends on their mass and more massive quasars should be evolving faster. This is true also for stars as is well known from the orthodox theory of stellar evolution. The same conclusion is confirmed also in the disintegration scenario - massive stars evolve faster.

- Quasar masses and luminosities depend on distance, being larger and brighter, respectively, at earlier epochs (i.e. at larger cosmological distances);
- Luminosity depends on density, therefore, it could be possible that very dense masses could also be very faint, being actually “dark matter”;
- Evolution of quasars seems not to be continuous, but proceeds in steps corresponding to the gravitational redshifts of the Karlsson sequence. These steps should correspond to the “steps” in the gravitational potential of the quasar by the quasar expansion. It looks like there is a slow down at each “step” and faster transition to the next lower value of the Karlsson sequence. In this respect the gravitational redshift of 1.96 is especially conspicuous.
- There are discretization effects in some physical quasar characteristics, corresponding to the same “steps” of evolution, and which are most pronounced in the relations: “mass – radius”, the “density – mass”, and the “radius – density”.

## ***Chapter 6.***

### ***Stellar evolution in the concept of disintegration.***

The orthodox theory assumes that stars originate in gas and dust clouds by gravitational collapse. The first stage of stellar evolution is therefore the contraction phase towards the main sequence (MS). On the “zero age main sequence” (ZAMS) follows the ignition of nuclear hydrogen burning which is the source of energy during the stellar life on the MS. After the hydrogen is depleted ignition of nuclear burning with heavier elements could follow and the star gradually expands and evolves off the MS to the stage of the red giant stars. I am not going into details of this evolutionary scenario. For the purpose of this study it is important to stress that stellar evolution proceeds from the main sequence to the red giant stars. This transition is clearly seen on the Hertzsprung – Russell diagram (HR – diagram) of stellar clusters and it represents important fact in stellar astrophysics. The evolution after the red giant stage in the orthodox theory depends on the stellar mass. Less massive stars, after losing substantial part of their mass evolve into white dwarfs [96]. Stars more massive than  $\sim 10$  solar masses should explode as SN [96], thereby ejecting a lot of “processed” material enriched with heavy elements into the interstellar medium. Presently, the nuclear fusion in stellar cores is the only known way to produce heavy elements. These are the basic ideas in contemporary astrophysics. In the following an attempt will be presented to describe possible scenario of stellar evolution assuming the concept of disintegration. Starting with the MS stars I will try to proceed to the red giants, following the well established direction of stellar evolution. For this study the already used linear density equation eq (27) will be applied again. The same radius of reference,  $r = 8 \cdot 10^{13}$  cm will be used to reduce the stellar densities. Mean values are used for the stellar data of spectral classes B0, B5, A0, A5, F0, F5, G0, G5, K0, K5, M0, M5 from published sources. The stellar data used is presented bellow in Table 7 and the linear density diagram with reduced stellar densities is shown on Fig (20). The straight line on Fig (20) closely corresponds to the eq (27) and the coefficients are:  $a = -2 \cdot 10^{-9}$ ,  $b = 0.2505$ . Since mean values were used for each spectral class the result on Fig (20) should be significant. The sequence of spectral classes on Fig (20) is not in the same order as written above (i. e. the normal spectral main sequence) but follows as: B0, B5, A0, F0, A5, F5, G5, G0, K0, M0, M5. (The position of K5 on this diagram coincides with the position of G0). These are details that will be left for future studies. From Fig (20) it is apparent that eq (27) describes the LDD, as should be expected by the definition of reduced densities.

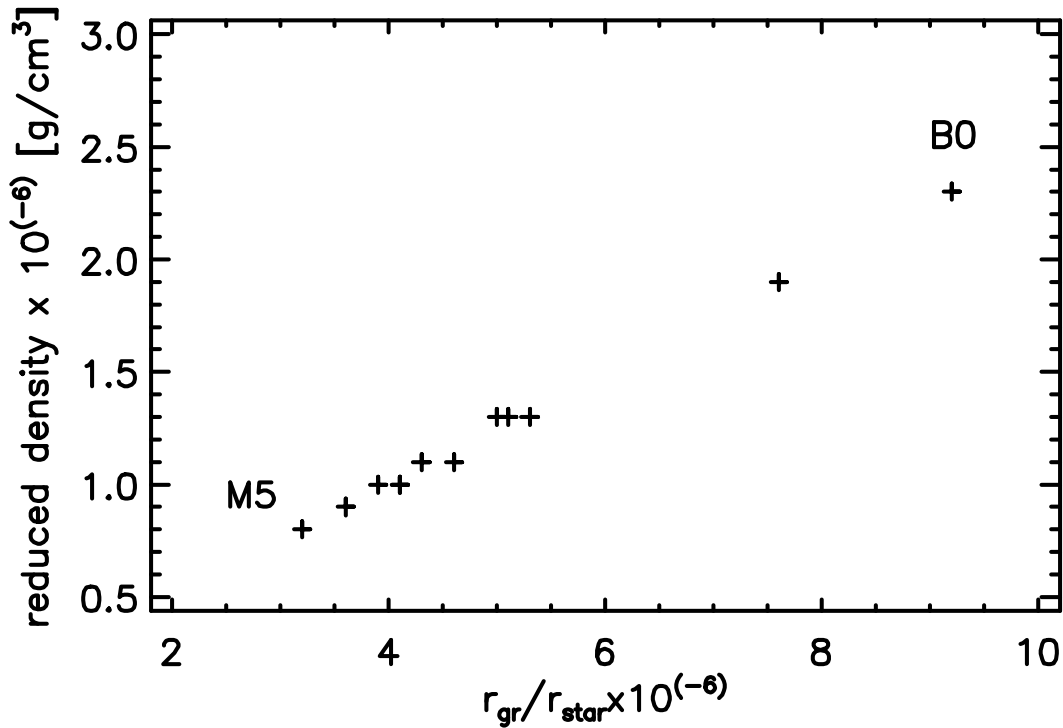


Fig (20). The linear relation of stellar reduced density (to a radius of  $8. \cdot 10^{13}$  cm) with the stellar  $r_{gr}/r_{star}$ . The sequence is: B0, B5, A0, F0, A5, F5, G5, G0, K0, M0, M5. The linear equation is:  $\rho \sim -2. \cdot 10^{-9} + 0.2505 \cdot r_{gr}/r_{star}$ . Courtesy of Bentham Open OAJ [55].

It is the position of the MS stars on the LDD which is the important characteristic of this group of stars and this position is obviously very different from the position of the QSOs on the same diagram. In the following other groups of stars will be considered on the same linear density diagram in an attempt to establish an evolutionary scenario. As will be shown below the different groups of structures – QSOs, stars and planets occupy different parts of the LDD. It could be that these positions on the diagram, occupied by different groups of structures reflect the evolutionary status of each respective group of structures. This statement seems obvious if we consider the position of the MS stars and the position of the evolved giants on the same LDD. The next question to be addressed is, therefore, where is the position of the evolved giants on the LDD? In Table 8 sample of well known evolved giant stars are presented from published data. Reduced densities are calculated as always to a radius of reference  $r = 8. \cdot 10^{13}$  cm. Therefore, these stars should also be placed on the same LDD discussed above and which is shown on Fig (21).

**Table 7. Data for main sequence stars as mean values for spectral classes B0, B5, A0,....., M5 (columns 2- 6). In column 7, all radii from column 2 are increased 50 times. Columns 8 – 9 show the  $r_{gr}/r$  and the reduced densities for the expanded stars. (Reduced densities as always are calculated to radius of reference  $r = 8. \cdot 10^{13}$  cm).**

| Spectral Class | r [cm]                 | m [g]                 | density [g/cm <sup>3</sup> ] | r <sub>gr</sub> /r .10 <sup>-6</sup> | reduced density .10 <sup>-6</sup> [g/cm <sup>3</sup> ] | r x 50 [cm]            | r <sub>gr</sub> /r .10 <sup>-9</sup> | reduced density .10 <sup>-9</sup> [g/cm <sup>3</sup> ] |
|----------------|------------------------|-----------------------|------------------------------|--------------------------------------|--|------------------------|--------------------------------------|--|
| B0             | 5.150.10 <sup>11</sup> | 3.2.10 <sup>34</sup>  | 0.056                        | 9.2                                  | 2.3  | 2.575.10 <sup>13</sup> | 184                                  | 46   |
| B5             | 2.714.10 <sup>11</sup> | 1.4.10 <sup>34</sup>  | 0.167                        | 7.6                                  | 1.9  | 1.357.10 <sup>13</sup> | 152                                  | 38   |
| A0             | 1.670.10 <sup>11</sup> | 6. 10 <sup>33</sup>   | 0.307                        | 5.3                                  | 1.3  | 8.35 .10 <sup>12</sup> | 106                                  | 27   |
| A5             | 1.183.10 <sup>11</sup> | 4. 10 <sup>33</sup>   | 0.576                        | 5.0                                  | 1.3  | 5.915.10 <sup>12</sup> | 100                                  | 25   |
| F0             | 1.044.10 <sup>11</sup> | 3.6.10 <sup>33</sup>  | 0.755                        | 5.1                                  | 1.3  | 5.22.10 <sup>12</sup>  | 102                                  | 26   |
| F5             | 9.744.10 <sup>10</sup> | 3. 10 <sup>33</sup>   | 0.774                        | 4.6                                  | 1.1  | 4.872.10 <sup>12</sup> | 92                                   | 23   |
| G0             | 7.656.10 <sup>10</sup> | 2.1.10 <sup>33</sup>  | 1.117                        | 4.1                                  | 1.0  | 3.828.10 <sup>12</sup> | 82                                   | 20   |
| G5             | 6.403.10 <sup>10</sup> | 1.84.10 <sup>33</sup> | 1.673                        | 4.3                                  | 1.1  | 3.202.10 <sup>12</sup> | 86                                   | 21   |
| K0             | 5.916.10 <sup>10</sup> | 1.56.10 <sup>33</sup> | 1.799                        | 3.9                                  | 1.0  | 2.958.10 <sup>12</sup> | 78                                   | 20   |
| K5             | 5.011.10 <sup>10</sup> | 1.38.10 <sup>33</sup> | 2.618                        | 4.1                                  | 1.0  | 2.506.10 <sup>12</sup> | 82                                   | 21   |
| M0             | 4.176.10 <sup>10</sup> | 1.02.10 <sup>33</sup> | 3.344                        | 3.6                                  | 0.9  | 2.088.10 <sup>12</sup> | 72                                   | 18   |
| M5             | 1.879.10 <sup>10</sup> | 4. 10 <sup>32</sup>   | 14.390                       | 3.2                                  | 0.8  | 9.395.10 <sup>11</sup> | 64                                   | 16   |

**Table 8. Data for evolved giant stars (from published sources)**

| Star ID                 | Sp class  | r <sub>gr</sub> /r x 10 <sup>-7</sup> | red density x 10 <sup>-7</sup> [g/cm <sup>3</sup> ] | log (density) [g/cm <sup>3</sup> ] | log(reduced density) [g/cm <sup>3</sup> ] |
|-------------------------|-----------|---------------------------------------|---|------------------------------------|---|
| Pollux                  | K0 III    | 9.9                                   | 2.5   | -2.373                             | -6.602                                    |
| Capella A               | G8 III    | 9.4                                   | 2.4   | -2.678                             | -6.620                                    |
| Capella B               | K0 III    | 11.9                                  | 3.0   | -2.332                             | -6.523                                    |
| Epsilon Cyg             | K0 III    | 7.9                                   | 2.0   | -2.651                             | -6.699                                    |
| Iota Draconis           | K2 III    | 6.5                                   | 1.6   | -2.825                             | -6.796                                    |
| Cygnus X-1 = HDE 226868 | O9.7 Iab  | 30.4                                  | 7.7   | -2.639                             | -6.114                                    |
| Arcturus                | K1.5 III  | 1.8                                   | 0.46  | -4.037                             | -7.337                                    |
| Aldebaran               | K5 III    | 1.6                                   | 0.41  | -4.555                             | -7.387                                    |
| Polaris A               | F7 Ib     | 4.2                                   | 1.05  | -4.184                             | -6.979                                    |
| Alphard                 | K3 II-III | 2.6                                   | 0.6   | -4.477                             | -7.222                                    |
| HD 208527               | M1 III    | 1.3                                   | 0.3   | -4.770                             | -7.523                                    |
| HD 220074               | M2 III    | 1.0                                   | 0.3   | -4.859                             | -7.523                                    |
| Eta CMa                 | B5 Ia     | 14.5                                  | 3.65  | -3.817                             | -6.438                                    |
| Rigel                   | B8 Ia     | 10.4                                  | 2.6   | -4.201                             | -6.585                                    |
| Canopus                 | F0 II-Ib  | 5.9                                   | 1.5   | -4.419                             | -6.824                                    |
| Gamma Crucis            | M3.5 III  | 0.66                                  | 0.2   | -5.508                             | -7.699                                    |
| Deneb                   | A2 Ia     | 4.0                                   | 1.0   | -5.492                             | -7.000                                    |
| R Doradus               | M8 III    | 0.14                                  | 0.04  | -7.469                             | -8.398                                    |
| Alpha Herculis          | M5 Ivar   | 0.2                                   | 0.1   | -7.276                             | -8.000                                    |
| Mira Ceti               | M7 IIIe   | 0.14                                  | 0.03  | -7.469                             | -8.523                                    |

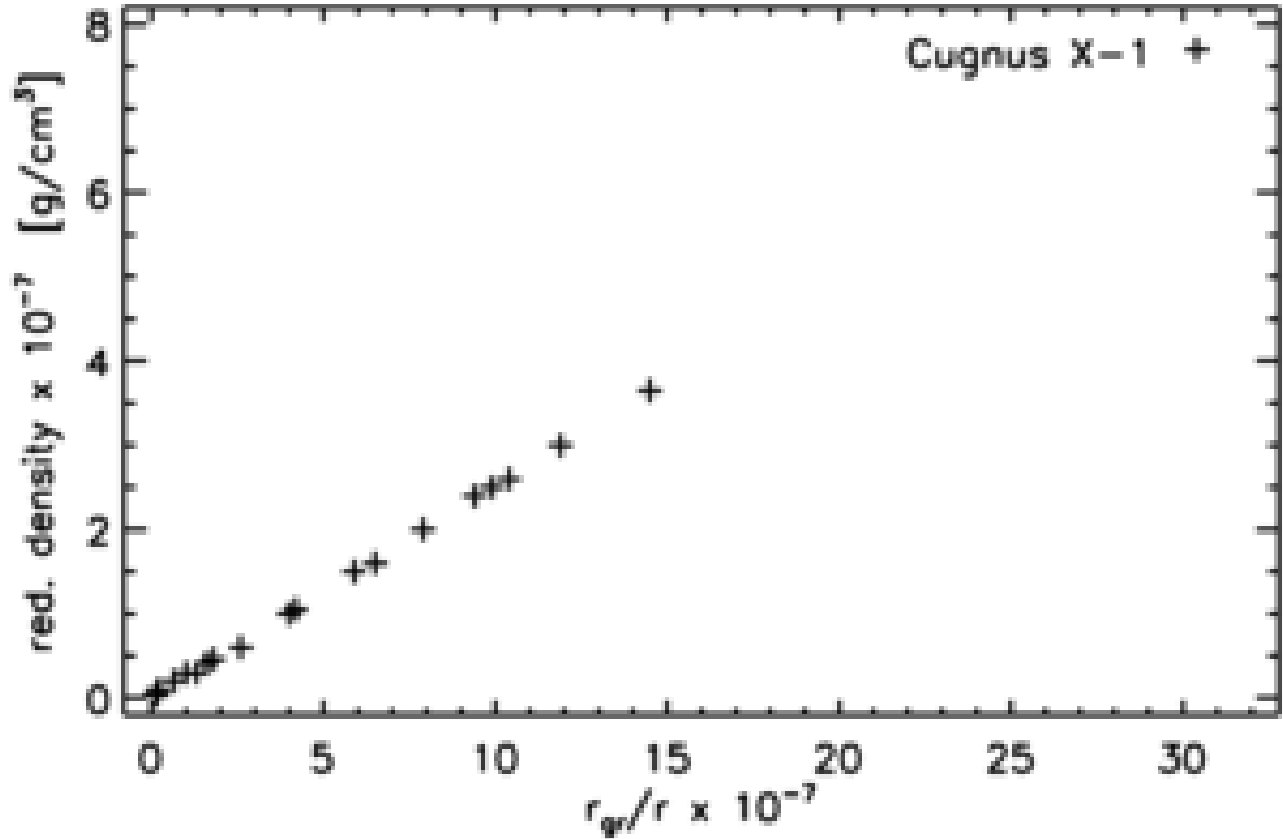


**Fig (21). Linear density diagram for evolved (yellow and red) giants of Table 8. All reduced densities are calculated to a radius of  $8 \cdot 10^{13}$  cm. In the upper right corner is Cygnus X-1 (HDE 226868). The linear equation is:  $\rho_{\sim} = 7 \cdot 10^{-11} + 0.2525 \cdot r_{gr}/r$**

The parameters of the straight line on Fig (21) are:  $a = 7 \cdot 10^{-11}$  and  $b = 0.2525$ . No doubt, the fit is significant and the linear density diagram for evolved giant stars closely corresponds to eq (27), which is to be expected as explained above. Comparison of this diagram with the respective linear density diagram for main sequence stars on Fig (20) shows that the evolved giant stars are simply shifted along the same diagram to lower reduced densities. This transition could be explained by increasing the radii of the main sequence stars due to evolution. This is illustrated in the last columns of Table 7, where the radii of the main sequence stars are increased by the same factor of 50. The “expanded” stars follow the same linear density relation eq (27) and “expansion” results in a shift of all spectral classes to lower reduced densities. There is one important conclusion following from Fig (21). We already know that main sequence stars evolve to the red giant stars. Therefore, on the linear density diagram the evolution of main sequence stars should proceed along the same LDD to lower reduced densities. In the previous chapter the same scenario was considered for QSOs when discussing the linear density diagram on Fig (19). The slope of trend in eq (27) does not depend on radius, neither on the masses of the stars, and therefore we could increase the radii of the main sequence stars by different and arbitrary factors for the different spectral classes – the relation (27) will still be preserved. The change of the stellar masses alone does not have

an impact on the linear density relation, either, and mass loss alone will result in proportional decrease of  $r_{gr}$ . Therefore, mass loss alone results in a “sliding down” on the LDD. In reality stellar evolution with mass loss should be more complicated with respect to the LDD, because substantial loss of mass will result also in decrease of stellar radius. Decreasing stellar radius will shift the star in the opposite direction – upward on the LDD. Therefore, the combined effect of stellar expansion with mass loss is more complicated to consider and the position of the star on the LDD will depend on the  $r_{gr}/r$  in the course of evolution. How much is the stellar radius decreasing by loss of mass depends on the density gradient in the stellar interior, which is uncertain. Thus the combined effect of expanding star with a mass loss depends on the impact of both processes on the ratio  $r_{gr}/r$ . Since we do know that stellar evolution off the main sequence proceeds with both expansion and mass loss, and Fig (21) shows that evolved stars slide down on the linear density diagram, we could conclude that the “combined effect” by this evolution is a net decrease of  $r_{gr}/r$ , at least for the stars considered here. This is essential to understand the diagram on Fig (21). The picture of “expanded” stars by a factor of 50 for each spectral class presented in Table 7 is just a simplified example – to see how expansion works on the LDD. The real case is obviously much more complex. Stars of different spectral classes have probably expanded by different factors and mass loss during the expansion (evolution) is probably also to be expected. Effectively, it means that main sequence stars evolve “down the linear density diagram” by expanding and possibly losing mass to reach the position of the evolved giants on the same diagram, Fig (21).

It appears that the *linear density diagram* could be used as an additional tool in studies of evolution and could be applied to stars, as well as to quasars. By introducing this new tool for evolutionary studies the importance of the HR - diagram for stellar evolution is by no means neglected. The linear density diagram shows just a different approach to stellar evolution and could be an additional (supplementary) tool.

At this point it is necessary to address a question that has been so far left out of the discussion. To get a linear density diagram we need to fix the radius of reference, in this presentation it is  $8 \cdot 10^{13}$  cm. There are countless other possibilities to fix this radius and each of them will lead to a different slope of the linear density relation. The choice of reference radius also goes into the determination of the reduced densities. Could we trust then the evolutionary picture presented here for just one specific radius of reference? The answer should be positive. The position of each star (or a QSO) on the linear density diagram is determined by its ratio  $r_{gr}/r$  and this ratio is independent of the choice of reference radius. Therefore, with a different radius of reference the slope of the linear density diagram will be different, but the relative positions of all stars (and QSOs) on that new diagram will remain the same. The evolved giants will be “sliding down” on the linear density diagram with respect to the main sequence stars, no matter what the choice of the reference radius may be. All conclusions about evolution on the linear density diagram will remain the same.

The reader may be disturbed by yet another question. By definition of the reduced densities and the LDD it can be noticed that also arbitrary chosen pair of radius and mass will produce a “data-point” on the same LDD. Does this mean that the LDD is ill-defined and “meaningless”? The answer seems simple to me. If arbitrary and “meaningless” data

are put on the LDD, then this diagram will indeed be meaningless. If, however, real stars, or quasars, or other structures are put on the LDD this is different matter and quite meaningful diagram. The different groups of stars have each their distinct position on the LDD and the evolution from MS-stars to the evolved giant stars on the LDD is clearly and undoubtedly seen. In the following also other structures will be put on the same LDD and they also have their specific places (parts) on this LDD. It is important to note, however, that the LDD is only a special kind of presentation of masses and radii of structures and from the LDD diagram alone no conclusions can be reached about internal physics of the structures considered.

The next question to address will be more difficult – what are the pre-main sequence stars, the evolutionary stage prior to the main sequence? Looking for answers, I am going to apply the same principle: evolution should proceed with decreasing densities and therefore also decreasing reduced densities, due to expansion of the pre-main sequence stars. I will look for candidates that follow the same linear density diagram but with higher than for MS stars reduced densities. My guess would be to put on trial the white dwarfs (WDs). This idea is obviously very controversial from the point of view of the orthodox theory of stellar evolution. White dwarfs are presently believed to be the last stage of evolution of low mass stars following the stage of the red giant stars.

On Fig (22) the linear density diagram is presented with 129 WDs from the sample of Shipman [97], listed also in Table 9. The fitting line on Fig (22) is almost an exact match of eq (27) (again, this should be expected by definition), and WDs are obviously on the part of this diagram with higher reduced densities than the MS stars. We therefore have on the same LDD three groups of stars, WDs, main sequence stars, and red giant stars, and their locations on this diagram follow with decreasing reduced densities (and simultaneously decreasing  $r_{gr}/r$ ) in the same order: WDs – MS stars – red giant stars. In the concept of disintegration this could be strong indication of evolution along the LDD from the WDs to the MS stars, and from the MS to the red giant stars. Clearly, the white dwarf stars satisfy the condition to be on the same linear density diagram with higher reduced densities, i.e. they satisfy the evolutionary scenario according to the disintegration concept. But assuming that WDs are the previous stage to the main sequence stars in stellar evolution opens a vast discussion and I could only mention here a few of the most pressing questions that need to be addressed. First, why do we see only white dwarfs with low masses, usually less than one solar mass? The answer could be found in the fact that WDs are very low luminous stars and we can observe them only in the solar neighborhood - no WDs could be observed in distant parts of the galaxy. The other important consideration is that evolution depends on the stellar mass and, therefore, all of the high mass WDs in the solar neighborhood could have already evolved into MS stars, and some of them may even have evolved to the red giants. Such a possibility could not be ruled out. Additional evidence may also come from the distribution of masses of the WDs. On Fig (23) the mass-distribution of the same 129 WDs from the Shipman's sample [97] is shown.

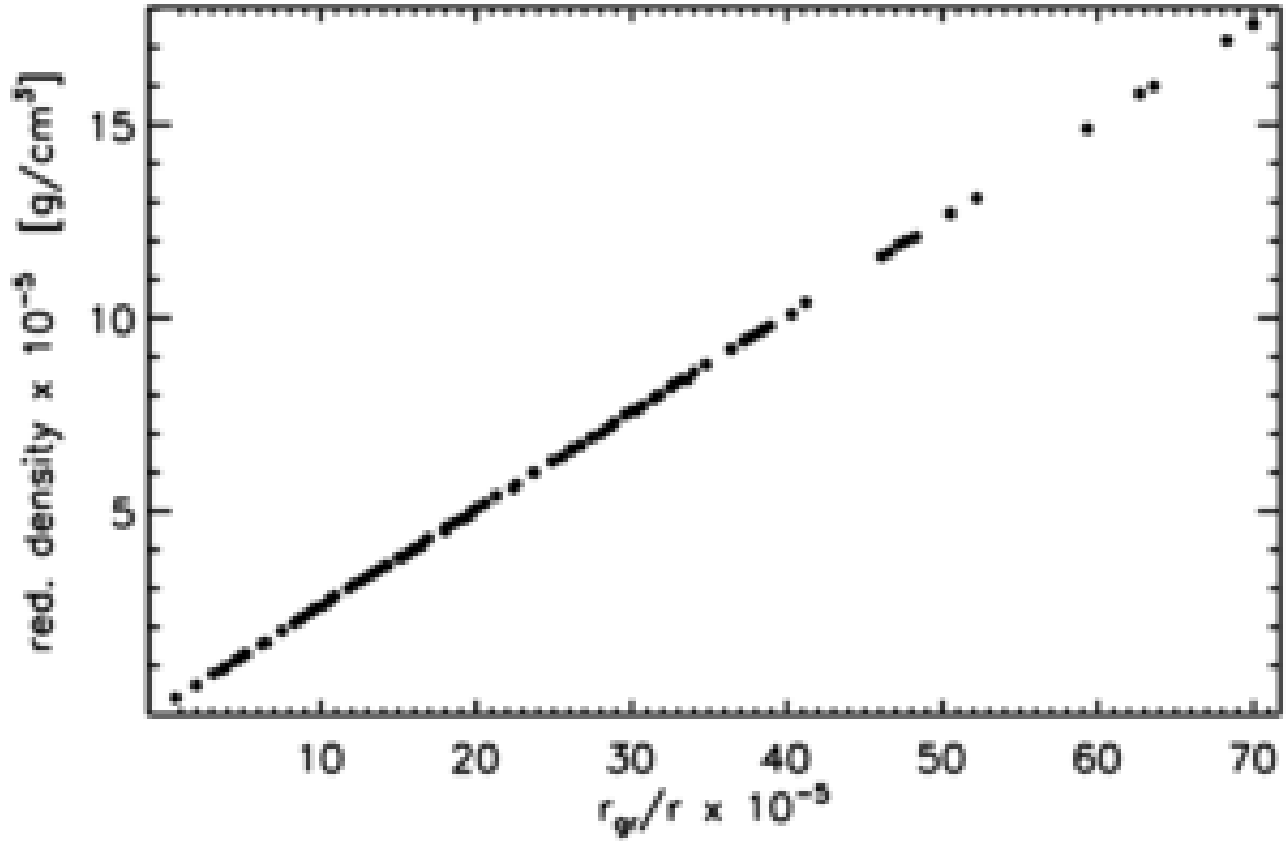


**Fig (22). Linear density diagram for 129 white dwarfs (data from Shipman [97], Table 9). All densities are reduced to a radius of  $8 \cdot 10^{13}$  [cm]. The linear equation is:  $\rho \sim 8 \cdot 10^{-8} + 0.25145 \cdot r_{gr}/r$ .**

**Table 9. White dwarfs data from Shipman [97]**

| Star ID | log r<br>[cm] | log m<br>[g] | log (density)<br>[g/cm <sup>3</sup> ] | $r_{gr}/r$<br>$\times 10^{-5}$ | Red. density<br>$\times 10^{-5}$<br>[g/cm <sup>3</sup> ] |
|---------|---------------|--------------|---------------------------------------|--------------------------------|--|
| 0011+00 | 8.860         | 33.176       | 5.975                                 | 30.7                           | 7.73   |
| 0030+44 | 9.078         | 32.699       | 4.842                                 | 6.2                            | 1.56   |
| 0033+01 | 8.751         | 33.283       | 6.408                                 | 50.5                           | 12.70  |
| 0101+04 | 9.022         | 32.857       | 5.170                                 | 10.2                           | 2.56   |
| 0126+10 | 9.119         | 32.602       | 4.623                                 | 4.5                            | 1.13   |
| 0133-11 | 9.345         | 32.000       | 3.343                                 | 0.67                           | 0.17   |
| 0135-05 | 9.137         | 32.556       | 4.523                                 | 3.9                            | 0.98   |
| 0205+25 | 8.966         | 33.000       | 5.479                                 | 16.0                           | 4.03   |
| 0208+39 | 8.950         | 33.033       | 5.562                                 | 18.0                           | 4.52   |
| 0220+22 | 8.675         | 33.338       | 6.691                                 | 68.3                           | 17.18  |
| 0232+03 | 9.221         | 32.342       | 4.057                                 | 1.96                           | 0.49   |
| 0257+08 | 8.888         | 33.134       | 5.848                                 | 26.1                           | 6.57   |

|         |       |        |       |       |      |
|---------|-------|--------|-------|-------|------|
| 0349+24 | 8.751 | 33.283 | 6.408 | 50.5  | 12.7 |
| 0352+09 | 8.922 | 33.079 | 5.692 | 21.3  | 5.4  |
| 0401+25 | 8.880 | 33.146 | 5.884 | 27.4  | 6.9  |
| 0406+16 | 8.772 | 33.265 | 6.327 | 46.1  | 11.6 |
| 0413-07 | 8.936 | 33.049 | 5.619 | 19.2  | 4.8  |
| 0421+16 | 8.896 | 33.121 | 5.811 | 24.9  | 6.3  |
| 0425+16 | 8.884 | 33.140 | 5.866 | 26.7  | 6.7  |
| 0431+12 | 8.876 | 33.152 | 5.902 | 28.0  | 7.0  |
| 0438+10 | 8.834 | 33.204 | 6.081 | 34.8  | 8.75 |
| 0501+52 | 9.057 | 32.763 | 4.969 | 7.5   | 1.9  |
| 0518+33 | 8.970 | 32.991 | 5.460 | 15.6  | 3.9  |
| 0612+17 | 8.880 | 33.146 | 5.884 | 27.4  | 6.9  |
| 0642-16 | 8.712 | 33.314 | 6.556 | 59.3  | 14.9 |
| 0644+37 | 8.816 | 33.220 | 6.151 | 37.6  | 9.5  |
| 0752+36 | 8.855 | 33.182 | 5.993 | 31.4  | 7.9  |
| 0816+38 | 8.843 | 33.193 | 6.043 | 33.2  | 8.4  |
| 0827+32 | 8.767 | 33.274 | 6.351 | 47.7  | 12.0 |
| 0836+20 | 8.992 | 32.934 | 5.337 | 13.0  | 3.3  |
| 0836+19 | 8.811 | 33.230 | 6.175 | 38.9  | 9.8  |
| 0837+19 | 8.914 | 33.093 | 5.728 | 22.4  | 5.6  |
| 0839-32 | 9.036 | 32.820 | 5.090 | 9.0   | 2.3  |
| 0913+44 | 9.103 | 32.643 | 4.713 | 5.2   | 1.3  |
| 0921+35 | 8.995 | 32.924 | 5.317 | 12.6  | 3.2  |
| 0930+29 | 8.847 | 33.188 | 6.025 | 32.5  | 8.2  |
| 0943+44 | 9.073 | 32.716 | 4.875 | 6.5   | 1.6  |
| 0955+24 | 8.864 | 33.170 | 5.957 | 30.0  | 7.55 |
| 1055-07 | 8.767 | 33.270 | 6.347 | 47.2  | 11.9 |
| 1104+60 | 8.979 | 32.964 | 5.404 | 14.3  | 3.6  |
| 1105-04 | 8.943 | 33.041 | 5.950 | 18.6  | 4.7  |
| 1314+29 | 8.973 | 32.982 | 5.441 | 15.15 | 3.8  |
| 1327-08 | 9.001 | 32.914 | 5.289 | 12.1  | 3.05 |
| 1334-16 | 8.762 | 33.274 | 6.367 | 48.3  | 12.1 |
| 1344+10 | 8.888 | 33.134 | 5.848 | 26.1  | 6.6  |
| 1354+34 | 8.843 | 33.188 | 6.038 | 32.8  | 8.25 |
| 1408+32 | 8.933 | 33.064 | 5.645 | 20.1  | 5.05 |
| 1455+29 | 8.914 | 33.093 | 5.728 | 22.4  | 5.6  |
| 1510+56 | 9.105 | 32.643 | 4.706 | 5.1   | 1.3  |
| 1544+00 | 8.816 | 33.220 | 6.151 | 37.6  | 9.5  |
| 1544-37 | 9.139 | 32.531 | 4.492 | 3.7   | 0.9  |
| 1555-08 | 9.030 | 32.833 | 5.120 | 9.4   | 2.4  |
| 1559+36 | 8.888 | 33.134 | 5.848 | 26.1  | 6.6  |
| 1609+13 | 8.669 | 33.342 | 6.714 | 69.96 | 17.6 |
| 1637+33 | 8.960 | 33.017 | 5.515 | 16.9  | 4.3  |
| 1647+59 | 8.936 | 33.057 | 5.627 | 19.6  | 4.9  |
| 1655+21 | 8.976 | 32.982 | 5.432 | 15.0  | 3.8  |

|         |       |        |       |      |      |
|---------|-------|--------|-------|------|------|
| 1659-53 | 9.039 | 32.806 | 5.069 | 8.7  | 2.2  |
| 1706+33 | 8.851 | 33.182 | 6.006 | 31.7 | 8.0  |
| 1716+02 | 9.013 | 32.881 | 5.220 | 10.9 | 2.75 |
| 1736+05 | 8.963 | 33.009 | 5.497 | 16.5 | 4.1  |
| 1743-13 | 9.112 | 32.623 | 4.665 | 4.8  | 1.2  |
| 1756+82 | 8.973 | 32.982 | 5.441 | 15.2 | 3.8  |
| 1826-04 | 8.986 | 32.954 | 5.375 | 13.8 | 3.5  |
| 1855+33 | 8.943 | 33.041 | 5.590 | 18.6 | 4.7  |
| 1911+13 | 9.013 | 32.881 | 5.220 | 10.9 | 2.8  |
| 1917-07 | 8.872 | 33.152 | 5.914 | 28.3 | 7.1  |
| 1932-13 | 8.940 | 33.049 | 5.609 | 19.1 | 4.8  |
| 1935+27 | 9.016 | 32.869 | 5.200 | 10.6 | 2.7  |
| 1943+16 | 8.896 | 33.121 | 5.811 | 24.9 | 6.3  |
| 1953-01 | 8.888 | 33.134 | 5.848 | 26.1 | 6.6  |
| 2032+24 | 8.929 | 33.072 | 5.663 | 20.6 | 5.2  |
| 2059+19 | 8.989 | 32.944 | 5.356 | 13.4 | 3.4  |
| 2111+26 | 9.004 | 32.903 | 5.269 | 11.8 | 2.96 |
| 2124+55 | 8.811 | 33.225 | 6.170 | 38.5 | 9.7  |
| 2126+73 | 9.027 | 32.845 | 5.141 | 9.7  | 2.45 |
| 2136+22 | 8.884 | 33.140 | 5.866 | 26.7 | 6.7  |
| 2136+82 | 9.041 | 32.806 | 5.060 | 8.6  | 2.2  |
| 2149+02 | 8.960 | 33.017 | 5.515 | 16.9 | 4.25 |
| 2246+22 | 8.772 | 33.270 | 6.331 | 46.6 | 11.7 |
| 2248+29 | 9.047 | 32.792 | 5.030 | 8.3  | 2.1  |
| 2253-08 | 8.986 | 32.954 | 5.375 | 13.8 | 3.5  |
| 0213+42 | 8.880 | 33.146 | 5.884 | 27.4 | 6.9  |
| 0433+27 | 8.868 | 33.158 | 5.933 | 28.9 | 7.3  |
| 0552-04 | 8.936 | 33.057 | 5.627 | 19.6 | 4.9  |
| 0553+05 | 8.903 | 33.107 | 5.775 | 23.7 | 5.96 |
| 0727+48 | 9.016 | 32.869 | 5.200 | 10.6 | 2.7  |
| 0912+53 | 8.847 | 33.188 | 6.025 | 32.5 | 8.2  |
| 1039+14 | 8.888 | 33.134 | 5.848 | 26.1 | 6.6  |
| 1257+03 | 8.825 | 33.215 | 6.118 | 36.4 | 9.15 |
| 1334+03 | 9.105 | 32.643 | 4.706 | 5.1  | 1.3  |
| 1625+09 | 8.767 | 33.274 | 6.351 | 47.7 | 12.0 |
| 1633+57 | 8.911 | 33.093 | 5.739 | 22.6 | 5.7  |
| 1705+03 | 8.860 | 33.170 | 5.969 | 30.3 | 7.6  |
| 1748+70 | 8.843 | 33.193 | 6.043 | 33.2 | 8.4  |
| 1818+12 | 9.163 | 32.477 | 4.367 | 3.06 | 0.77 |
| 1917+38 | 8.820 | 33.220 | 6.137 | 37.2 | 9.4  |
| 2011+06 | 8.838 | 33.193 | 6.056 | 33.6 | 8.4  |
| 2054-05 | 9.098 | 32.643 | 4.728 | 5.2  | 1.3  |
| 2207+14 | 8.797 | 33.241 | 6.228 | 41.2 | 10.4 |
| 2312-02 | 8.892 | 33.127 | 5.830 | 25.5 | 6.4  |
| 0007+30 | 8.888 | 33.134 | 5.848 | 26.1 | 6.57 |

|         |       |        |       |       |      |
|---------|-------|--------|-------|-------|------|
| 0038+55 | 8.860 | 33.170 | 5.969 | 30.3  | 7.6  |
| 0046+05 | 8.982 | 32.964 | 5.394 | 14.2  | 3.6  |
| 0115+15 | 8.811 | 33.225 | 6.170 | 38.5  | 9.7  |
| 0426+58 | 8.903 | 33.107 | 5.775 | 23.7  | 6.0  |
| 0437+13 | 8.860 | 33.170 | 5.969 | 30.3  | 7.6  |
| 0551+12 | 8.838 | 33.199 | 6.062 | 34.0  | 8.55 |
| 0615-59 | 8.767 | 33.274 | 6.351 | 47.7  | 12.0 |
| 0625+10 | 8.816 | 33.225 | 6.156 | 38.1  | 9.6  |
| 0706+37 | 8.802 | 33.236 | 6.208 | 40.3  | 10.1 |
| 0738-17 | 8.825 | 33.215 | 6.118 | 36.4  | 9.16 |
| 0751+57 | 8.960 | 33.009 | 5.507 | 16.6  | 4.2  |
| 0802+38 | 8.851 | 33.182 | 6.006 | 31.75 | 8.0  |
| 0856+33 | 8.700 | 33.326 | 6.604 | 62.7  | 15.8 |
| 0912+53 | 8.950 | 33.033 | 5.562 | 18.0  | 4.5  |
| 1039+14 | 9.027 | 32.845 | 5.141 | 9.7   | 2.45 |
| 1115-02 | 8.872 | 33.158 | 5.920 | 28.7  | 7.2  |
| 1142-64 | 8.864 | 33.164 | 5.951 | 29.6  | 7.45 |
| 1425+54 | 8.936 | 33.057 | 5.627 | 19.6  | 4.9  |
| 1626+36 | 8.966 | 33.000 | 5.479 | 16.0  | 4.0  |
| 1705+03 | 8.933 | 33.057 | 5.637 | 19.7  | 5.0  |
| 1900+70 | 8.746 | 33.292 | 6.433 | 52.2  | 13.1 |
| 1917-07 | 8.946 | 33.033 | 5.572 | 18.1  | 4.56 |
| 2059+31 | 8.970 | 32.991 | 5.460 | 15.6  | 3.9  |
| 2107+42 | 8.914 | 33.093 | 5.728 | 22.4  | 5.6  |
| 2129+00 | 8.922 | 33.079 | 5.692 | 21.3  | 5.4  |
| 2140+20 | 8.989 | 32.944 | 5.356 | 13.4  | 3.4  |
| 2153-51 | 8.694 | 33.326 | 6.623 | 63.6  | 16.0 |

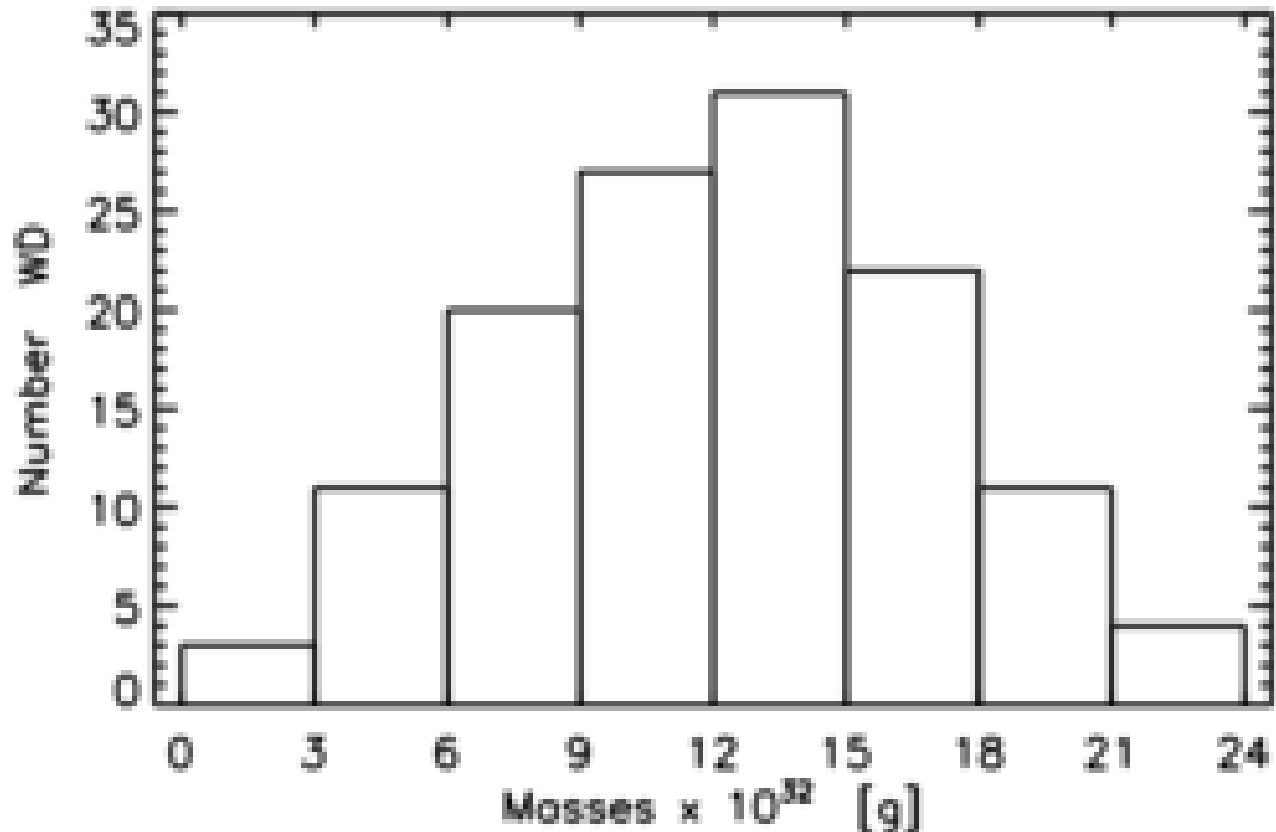


**Fig (23). Distribution over masses of the 129 white dwarfs of Table 9 from Shipman [97].**

From Fig (23) it is apparent that the mass-distribution of WDs is non-symmetric, with the high-mass branch being “cut”. There could be different interpretations of this asymmetry. In the orthodox theory the asymmetry could be explained by the well known Chandrasekhar rule for a WD mass limit. Accordingly, WDs’ masses could not be larger than  $\sim 1.4$  solar masses. It is also important to note that in the orthodox theory the evolution to the white dwarfs proceeds with a substantial mass loss.

In the disintegration scenario of evolution the asymmetry of the mass-distribution on Fig (23) should be explained by a different reason, possibly by the dependence of evolution on mass. It could be that all of the high mass WDs have already evolved, as mentioned above, possibly to the next stage of evolution - the assumed transition to the MS stars. It should be noted that the original mass distribution of WDs in the disintegration scenario remains unknown. It seems also that the process of stellar build-up was a continuous one and not a single act. We observe on the MS stars with smaller masses than the masses of some WDs and these MS stars should have been built before the WDs with larger masses. It seems quite plausible that the mass-dependence of evolution remains throughout the whole process of stellar evolution. If the transition from WDs to MS stars is assumed, how does the mass distribution of the MS stars compare with the mass distribution of WD stars? The dependence of evolution on stellar mass should exist also for MS stars, therefore, we should expect that asymmetry of the mass-distribution on the MS also

exists. Indeed, stellar-mass distribution on the MS shows similar asymmetry with the high mass branch being “cut” due to faster evolution of more massive MS stars away from the MS. For the MS stars some 86% of all stars are G-K-M stars and the O-B-A stars together are only ~1%. Obviously, the mass distribution of MS stars is strongly asymmetric and the presence of massive stars on the MS could be due to the evolution of these stars from the stage of WDs, where they are missing.

Thus the same reason could explain the mass-distribution asymmetry of both the MS and the WD stars. There are additional problems that have to be considered. The sample of the MS stars is much larger than the sample of WD stars, due to MS stars higher luminosity. As mentioned above on the main sequence there are many low mass M stars. Obviously, they should have arrived on the MS before the more massive WDs were born (disintegration scenario). The time of evolution elapsed since “the origin” to the WDs stage remains unknown, as well as the time spent on the WDs stage, and also the time for the assumed transition from the WDs to the MS stars. The effect of all these factors on mass distribution of WDs and of MS stars is difficult to assess. Having considered all the above precautions, the mass-asymmetry on the main sequence seems not to contradict to the assumed evolutionary transition from the WD stars to the MS. This picture seems at least to be consistent. Consistency is not a proof, but could be a good lead. If the evolutionary transition on the HR-diagram proceeds from the WDs to the MS stars and further from the MS stars to the red giants, then this evolution could be attributed to the expansion of the stars and to the increase of stellar luminosity all the way from the WDs to the red giants. In this (disintegration) scenario of stellar evolution the stages of the WDs and the MS on the HR- diagram should be regarded as stages of “slow down” of evolution – relative and temporary stability, due to yet unknown reasons. On the linear density diagram the evolution follows from higher to lower densities and therefore also to lower reduced densities, all the way from the WDs to the red giants. If the disintegration scenario of evolution is assumed, the fate of the stars after the red giant stage remains unknown.

Among the first discovered WDs were the WDs found in the systems of Sirius A / B (B is the white dwarf), Procyon A / B, (B is the WD), IK Pegasi A / B (B is the WD), and 40 Eridani A / BC (BC is a binary in orbit around 40 Eridani A), B being the WD. According to published data other binaries with WD components are: Epsilon Ret / WD 0415-594 (K2 IV +DA3.8), WD 1620-391 (G2 V + DA2), WD 0208-510 (K1 V + DA10). In all these binaries the primary is a main sequence (more massive) star and some of these systems are wide binaries. Such binaries are not easily understood in the orthodox concept of evolution. In all these systems, it should be safe to assume that the components in each respective system have a common origin and, therefore, the same age. For all these systems the evolutionary status of the components could only be explained in the orthodox scenario if a mass-transfer occurred from the initially more massive component B (WD) to the respective A - component. In this way the obvious contradiction could be explained that the less massive (now) WD is further evolved than the more massive (now) A - component. Therefore, the orthodox scenario needs to introduce a mass-transfer in all of the above binaries with WD component. There are questions, however. Mass-transfer in a wide binary system is unlikely (e.g. the system 40

Eridani, A/BC). In 40 Eridani the component C is much closer to component B, B/C being a pair in orbit around component A. If we assume that there was mass-transfer from B to A, it should be expected that mass would be transferred also from B to the much closer component C. However, apparently that did not happen as 40 Eridani C is a very low mass star (according to published data).

In the disintegration scenario of evolution with WDs stage preceding the MS stage no mass transfer is necessary to explain the evolutionary status of the components in binary systems with WD component. The more massive A -components, now on the MS are further evolved because the main sequence should follow to the stage of white dwarfs. In this scenario pre-main sequence stars should occupy in the HR-diagram the region between the WDs and the MS.

This scenario could put other evolutionary problems, e.g. the famous problem of the Pleiades cluster [98-100] in new prospective and stellar positions below the MS would be the natural places for young, pre-main sequence stars.

Since the publication of the degeneracy equation by Chandrasekhar in 1933, it was possible to establish a theoretical “mass-radius” relation for white dwarfs. Many attempts were made to verify the theoretical “mass-radius” relation with the best known observational WDs data and some embarrassing discrepancies were reported [101]. In several well known WDs Provencal and Shipman [101] found evidence of existence of iron cores, in contradiction with the orthodox theory. On the other hand, iron cores, possibly containing also other heavy elements, could be expected by the disintegration concept.

Obviously, the orthodox stellar evolutionary scenario encounters difficulties that may or may not be resolved in future. This should be a good reason to consider the alternative scenario – the evolution due to disintegration.

There is yet another important relation that should exist if the disintegration scenario holds. It is the “radius – density” relation. In the disintegration scenario with increasing radii of structures by preserving their respective mass the densities of structures should decrease. Mass loss during evolution with expansion will further contribute to decreasing density. This relation has already been presented for quasars (Fig 8), but does it exist for stars? On Fig (24) the “radius – density” relation is presented for the evolved giant stars of Table 8. On Fig (25) the “radius – density” diagram is presented for the 129 WDs (Table 9) of the Shipman’s sample [97]. The “radius – density” diagram for the MS stars of Table 7 is presented below on Fig (34). Clearly, the “radius - density” relation exists for main sequence stars, for the WDs, and for the evolved giant stars. This remarkable result is consistent with the evolutionary scenario based on the disintegration concept. There are also unsolved problems in the disintegration scenario, e.g. with the WDs “mass – radius” relation, shown on Fig (26) with data from [97]. Apparently, the masses of WDs increase with decreasing radii. For the MS stars this relation runs in the opposite sense: with increasing MS stars masses radii also increase, see Fig (6).

On Fig (27) the “density - mass” relation is shown for the 129 WDs of the Shipman’s sample [97].

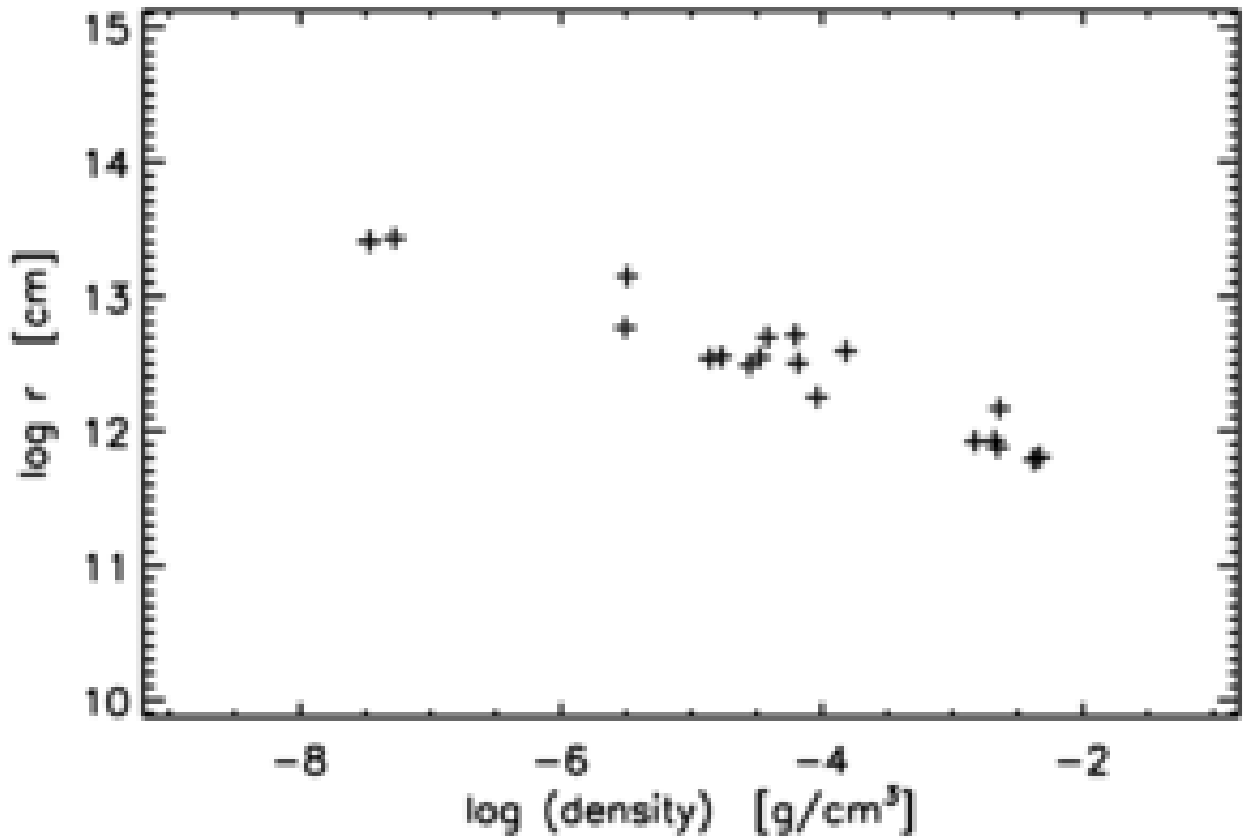


Fig (24). “Radius – density” relation for evolved giant stars of Table 8.

It is apparent that larger masses correspond to larger densities. For MS stars this relation also runs in the opposite sense (Fig 7). The orthodox theory of WDs explains the “mass – radius” relation on Fig (26) with the electron degeneracy pressure. However, some discrepancies seem to exist as mentioned above [101]. On the other hand, the same relation remains presently unexplained by the concept of disintegration.

On Fig (28) the “mass versus radius” plot is presented for the evolved giants. No obvious relation could be seen.

On Fig (29) the “density versus mass” plot is shown for the evolved giants. No obvious relation could be seen.

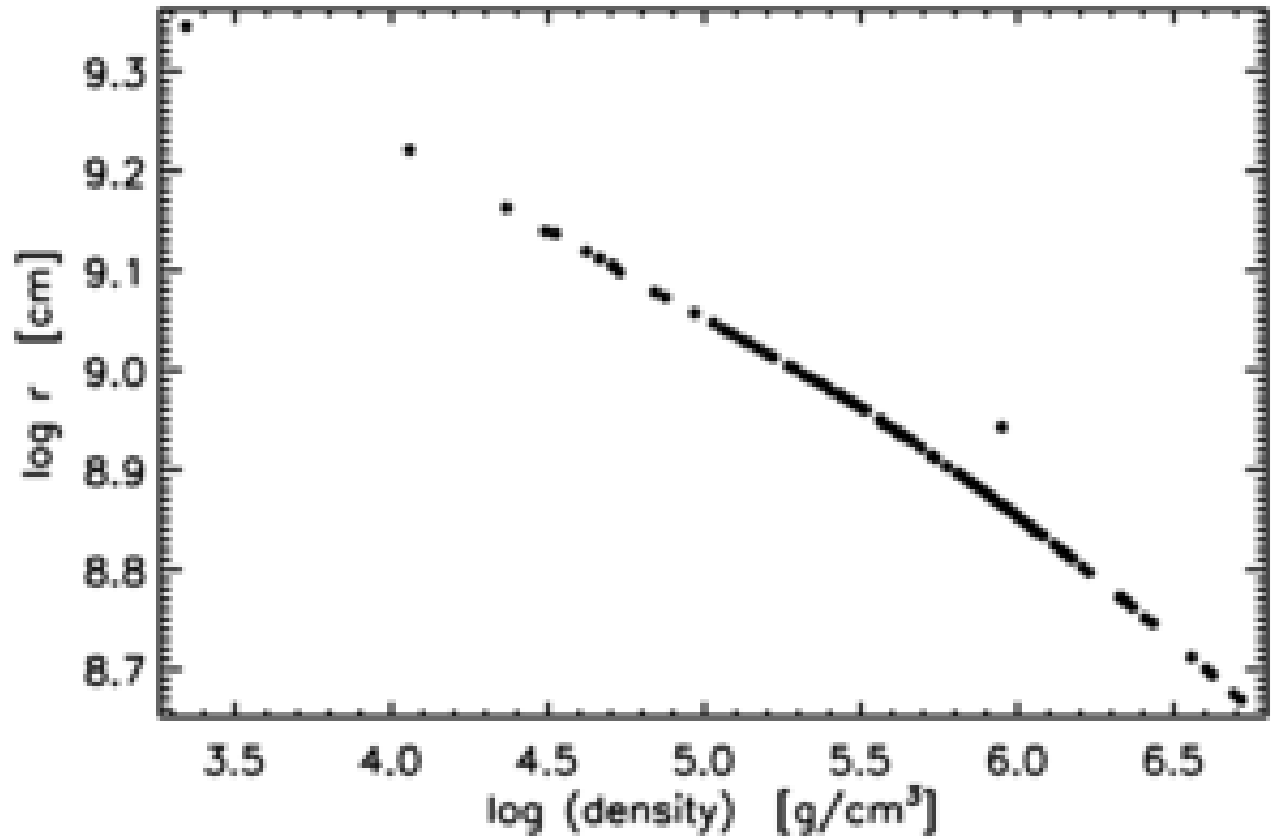


Fig (25). The “radius – density” relation for 129 white dwarfs from Shipman [97], Table 9.

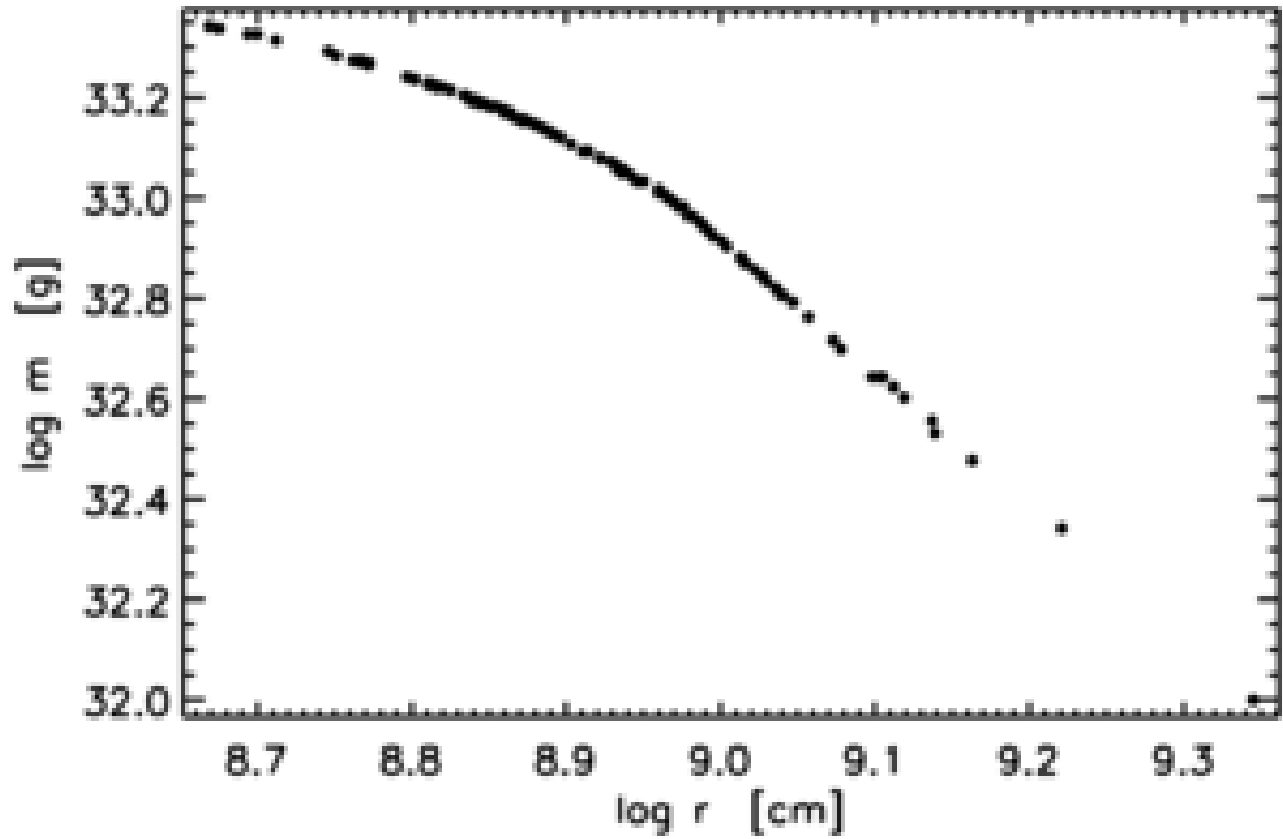


Fig (26). The “mass – radius” relation for the 129 white dwarfs of the Shipman’s sample [97], Table 9.

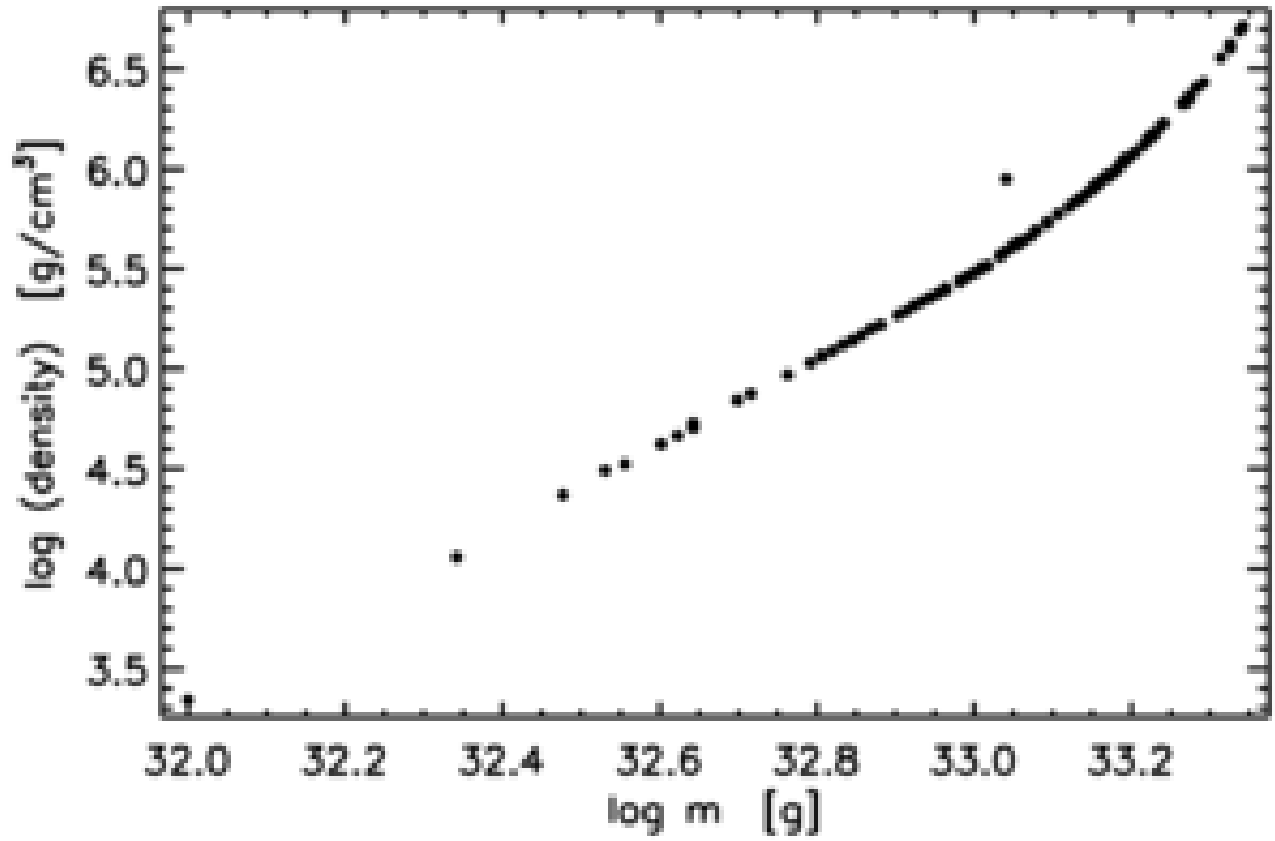


Fig (27). The relation “density – mass” for 129 white dwarfs of the Shipman’s sample [97], Table 9.

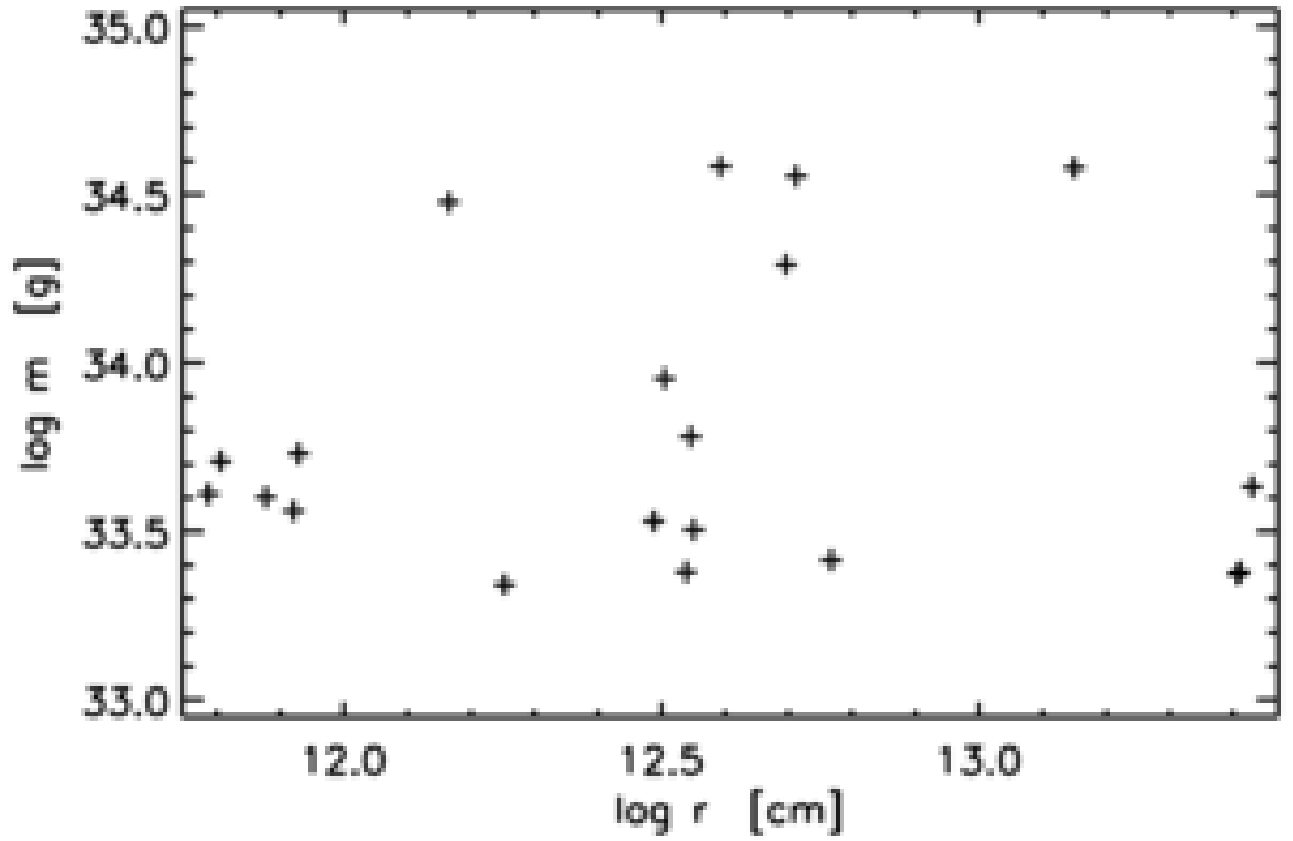
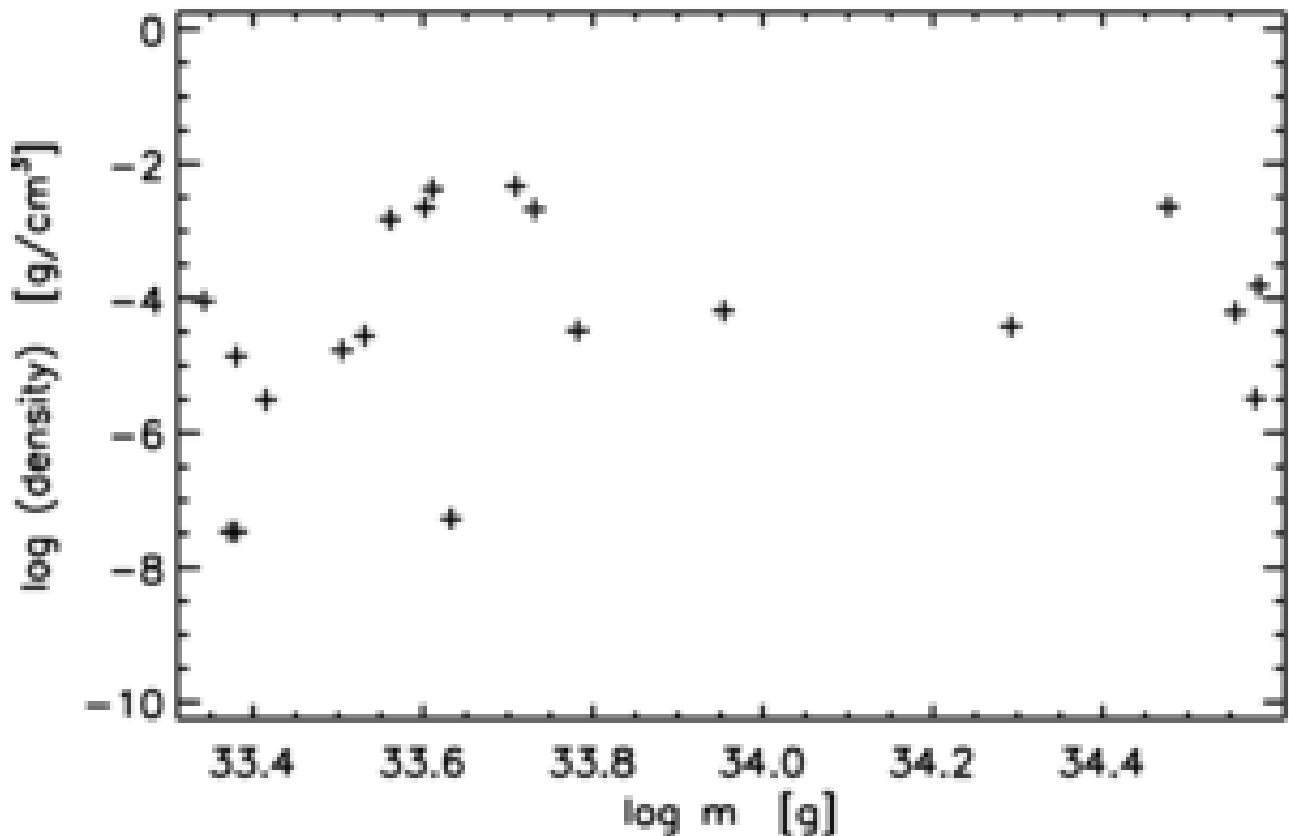


Fig (28). Masses versus radii plot for the evolved giants of Table 8.



**Fig (29). Densities versus masses plot for evolved giants of Table 8.**

Summarizing the evidence, there are substantial arguments in favor of the presented evolutionary scenario from the WDs to the main sequence stars, and from the main sequence stars to the evolved giants. The support comes from the linear density diagram with the reduced densities decreasing all the way from the WDs to MS stars and further from the MS stars to the evolved giants. Decreasing densities (and reduced densities) are consistent with the disintegration scenario. Additional support comes from the “radius – density” diagram of all three categories of stars. The trends in all “radius – density” diagrams - for WDs, for MS stars, and for evolved giants are consistent with the disintegration scenario. However, there are also a number of problems unsolved. It is interesting to note that the two diagrams - the “density – mass” relation and the “mass – radius” relation, show two-fold behavior for the considered groups of stars. The MS stars on the one hand, and the WDs on the other hand are the representatives of this two-fold behavior. The trends for MS stars show increasing radii for increasing masses, and decreasing densities for increasing masses. For the WDs these trends are opposite: decreasing radii for increasing masses, and increasing densities for increasing masses. The behavior of QSOs as shown above on the respective “mass-radius” and “density-mass” relations is similar to the behavior of MS stars. The same behavior will be shown to exist also for the planets of the solar system. From all considered here structures only

the WDs show opposite behavior with respect to these two relations, the “mass – radius” and the “density – mass” relations. What is the cause of this riddle remains uncertain. Despite of this two-fold behavior, all structures (including the WDs!) show the same “radius-density” relation. This is a remarkable result.

In the disintegration scenario there is no “Zero Age Main Sequence” (ZAMS). No time-characteristics of evolution could be determined at present in the disintegration scenario. It is interesting to note, however, that the age of the Earth (~4.5 billion years) was determined by processes of radioactive decay which are processes of disintegration. Having in mind the estimate of Earth’s age, the age of Sun should be larger in the disintegration scenario. The important consequence for the Sun if disintegration scenario is accepted is that Sun should have arrived on the MS more recently than estimated by the orthodox theory. From the age of the Sun ( $\sim 5 \cdot 10^9$  y ?) we would have to subtract the time spent from “origin” to the WD - stage (unknown), duration as WD (unknown) as well as the time spent for transition to the MS (also unknown). Therefore, the time Sun spent on the MS so far could be much less than  $5 \cdot 10^9$  y. How this could have influenced the Earth’s climate and the development of life? It is also important to note that with the disintegration scenario no predictions could be made about how much longer our Sun will stay on the MS. It depends on the rest of fissile matter still remaining in the solar core. This could make a big difference from the estimated duration of the Sun’s life on the MS by the orthodox theory.

In this presentation, I have completely neglected the neutron stars. Data for neutron stars are still scarce and do not allow for a detailed study. Let me only mention that if we accept that a “typical” neutron star has a mass of ~1 solar mass and a radius of ~ 15 km, this neutron star would be on the same LDD in the region of higher reduced density than the WDs region.

Here is a brief summary of the evidence from this chapter with possible conclusions:

- The linear density relation (eq 27) holds for white dwarfs, for main sequence stars, and for evolved giant stars (as expected) and each group of stars has its particular place on this diagram;
- The reduced densities (always with respect to a radius of  $8 \cdot 10^{13}$  cm) decrease from white dwarfs to main sequence stars, and decrease further from the main sequence stars to the evolved giant stars;
- The linear density diagram shows clearly the evolution from MS stars to the red giant stars and could possibly be used for studies of evolution in general.
- Stellar evolution in all cases seems to proceed along the linear density diagram by sliding down to lower reduced densities and in agreement with the disintegration scenario;
- There are stages in the stellar evolution (we considered here three of them), presented by white dwarfs, main sequence stars, and evolved giant stars. These stages seem to be stages where stellar evolution slows down for yet unknown reasons. Because of the “slow-down” of evolution these groups of stars show up on the HR - diagram as the well known patterns. The evolutionary sequence assuming

evolution with decreasing densities could be: WDs to MS stars and MS stars to red giant stars.

- Disintegration concept is supported also by the relation “radius – density” found for white dwarfs, for main sequence stars, and for evolved giant stars. In all these stars larger radii correspond to lower densities, as it should be in the disintegration scenario;
- On the linear density diagram of all considered groups of stars the upper part is occupied by the large mass objects. This holds also for quasars and for planets (see below);
- The speed of evolution depends on mass and the stars with larger masses on the linear density diagram have to be younger. It is the same situation on the HR - diagram where the massive O-and B- stars occupy the upper part of the main sequence and have not evolved away from the MS only because these stars are young;
- The transition of young stars to the main sequence from the region below the main sequence on the HR - diagram opens the possibility to explain in a natural way the existence of stars on the HR - diagram below the main sequence. This could solve a long standing problem in the Pleiades (and other young clusters), where some K and M stars seem to occupy a region below the MS. In the disintegration scenario pre-main sequence stars could be found in the whole region between the WD stars and the main sequence;
- In the disintegration scenario there is no “zero age main sequence”;
- The disintegration scenario offers the possibility to present the stellar evolution from WDs to red giants in one and the same direction, due to one and the same reason: disintegration and expansion. On the HR - diagram evolutionary transition is from low to higher luminosities. On the linear density diagram transition is from high to lower densities;

## Chapter 7.

### *Quasar – stellar – planetary connection? A lead to the atomic structure.*

In the previous chapters linear density diagrams with reduced densities were considered for quasars and also for stars (MS stars, WDs, and evolved giants), and which closely correspond to eq (27) as it should be. The linear density diagram should be the same for quasars and for stars by definition of the LDD and reduced densities if all reduced densities are reckoned to the same radius ( $r = 8 \cdot 10^{13}$  cm). The important finding is the fact that every group of the structures here considered (QSOs, MS stars, WDs, evolved giants) has its specific place, a distinct part on the linear density diagram. In this scenario it seems possible to include also the planets and satellites. On Fig (30) the 9 big planets and 19 satellites of the solar system (SS) are plotted on a logarithmic scale and the linear density diagram clearly corresponds to eq (27) as expected. Note that the solar system planets occupy a region on the LDD with lower reduced densities than the evolved giants. Does this mean that planets and satellites are further evolved than stars? In the disintegration concept it should be the logical interpretation of the planetary LDD.

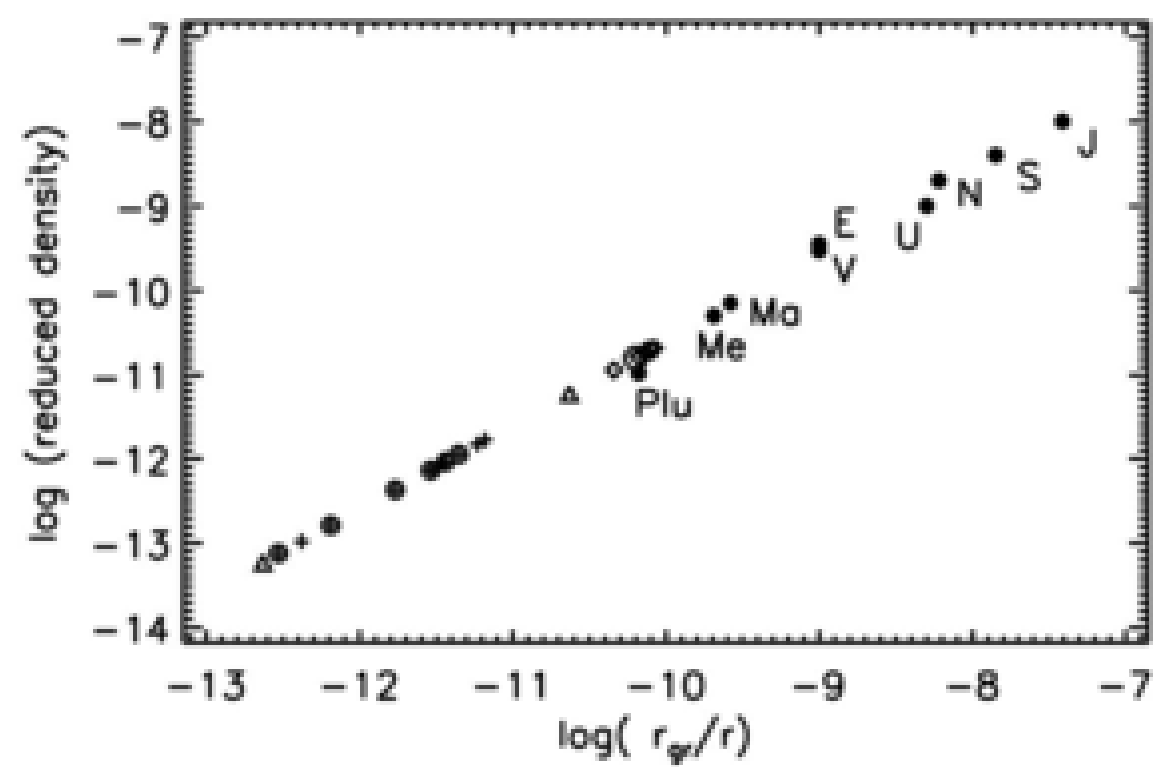


**Fig (30).** Reduced density [ $\text{g/cm}^3$ ] to  $r = 8 \cdot 10^{13}$  cm versus  $r_{gr}/r$  for planets and satellites of the solar system. Dots – planets, empty circle – the Moon, rhombs – satellites of Jupiter (Io, Europa, Ganymed, Callisto), crossed circles – satellites of Saturn (Mimas, Enceladus, Tethys, Dione, Rhea, Titan, Iapetus), crosses – satellites of Uranus (Ariel, Umbriel, Titania, Oberon, Miranda), and triangles – satellites of

**Neptune (Triton and Nereid). At the left lower end is Nereid. Courtesy of Bentham Open OAJ [95].**

In Table 10 solutions of eq (27) are listed for quasars, stars, planets and satellites.

**Table 10. Summary of coefficients for eq (27), applied to quasars (Table 2), 129 white dwarfs of Table 9 from Shipman [97], main sequence stars as mean values B0 – M5 (Table 7), evolved giant stars (Table 8), the 9 big planets of the solar system, and the 19 satellites, list in caption of Fig (30).**

|               | Coeff “a”            | Coeff “b” | Correlation coeff | Range of the reduced density [g/cm <sup>3</sup> ] to 8.10 <sup>13</sup> cm |
|---------------|----------------------|-----------|-------------------|--|
| 341 quasars   | 0.0002               | 0.251     | 0.998             | 0.02 – 0.25  |
| 129 WD        | 8. 10 <sup>-8</sup>  | 0.25145   | 0.9999            | 2. 10 <sup>-6</sup> - 2. 10 <sup>-4</sup>                                  |
| Stars B0-M5   | -2.10 <sup>-9</sup>  | 0.2505    | 0.998             | 0.8 .10 <sup>-6</sup> - 2.3 .10 <sup>-6</sup>                              |
| 20 giants     | 7.10 <sup>-11</sup>  | 0.2525    | 0.9999            | 3. 10 <sup>-9</sup> - 8. 10 <sup>-7</sup>                                  |
| 9 Planets     | 7.10 <sup>-11</sup>  | 0.258     | 0.998             | 1.1 .10 <sup>-11</sup> - 1. 10 <sup>-8</sup>                               |
| 19 Satellites | -2.10 <sup>-16</sup> | 0.25155   | 0.9999            | 5.9 .10 <sup>-14</sup> – 2.1 .10 <sup>-11</sup>                            |

From the linear density diagram (Table 10) it is apparent that the reduced densities decrease by transition from quasars to stars, stars to planets, and planets to satellites. Simultaneously decreasing are also the  $r_{gr}/r$  ratios. The same trend is observed also on stellar level by transition: WDs – MS stars – evolved giants. Assuming that evolution of quasars and stars goes along the linear density diagram to lower reduced densities this could mean that there could be some “link” between all these structures that could also provide the reason for evolution in terms of physics. This “link” should be fundamental in order to link such different structures. On Fig (31) atoms of the elements of the periodic table are presented on the same linear density diagram.

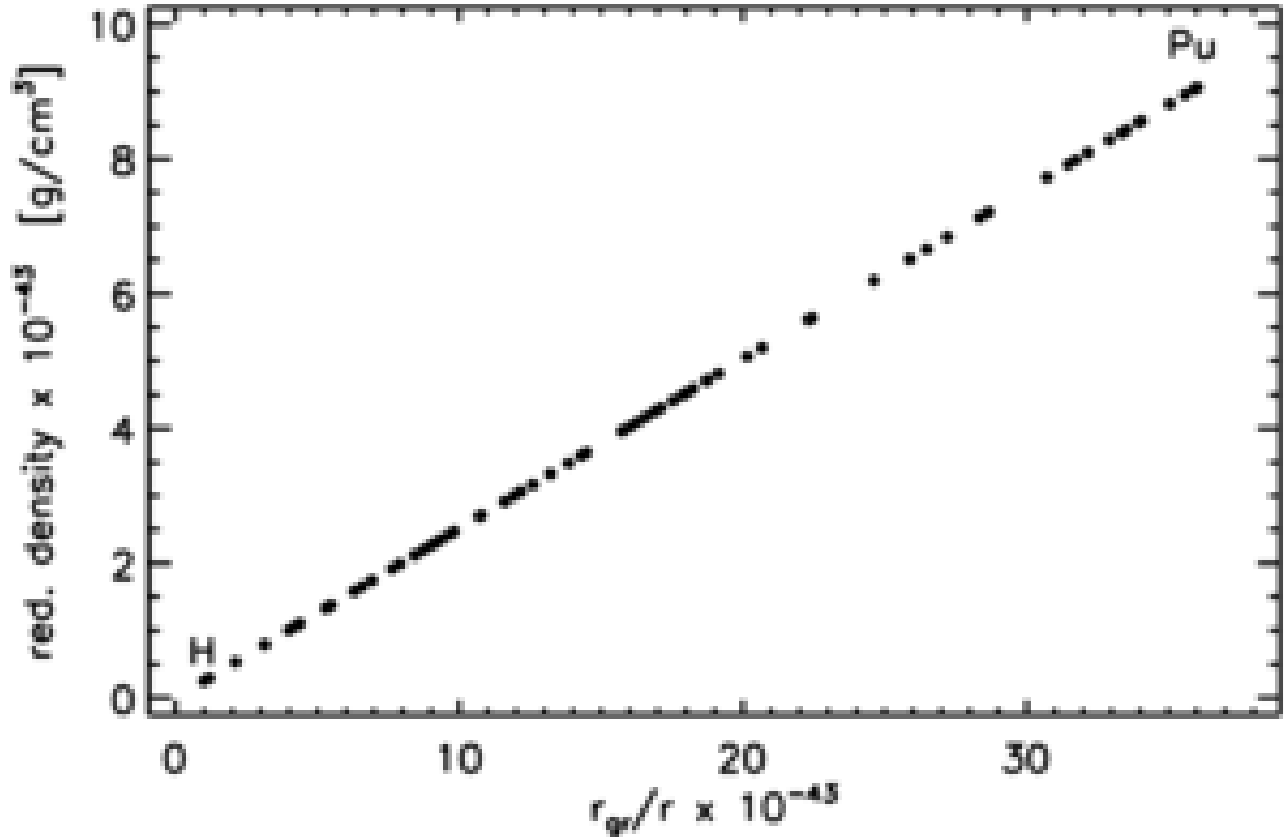


**Fig (31). The linear density diagram with reduced densities [g/cm<sup>3</sup>] to  $r = 8 \cdot 10^{13}$  cm for the atoms from Hydrogen to Plutonium. In the upper part are the most massive elements as Au, Os, Ir, Pt, Pu. The linear relation is:  $\rho \sim = 0.2515491 \cdot r_{gr}/r$**

The linear density relation is shown for the atoms of the whole periodic table of elements, from Hydrogen to Plutonium. As always reduced densities are calculated to the same radius of reference,  $r = 8 \cdot 10^{13}$  cm, in order to place the atoms on the same linear density diagram. The numbers involved are rather small. Yet, the conclusion is obvious: it is the same linear density relation as it should be by definition of the LDD. The coefficients of this relation are exactly equal (with 6 decimal digits!) to the theoretical ones (eq. 27):

$$\rho \sim = -1 \cdot 10^{-51} + 0.251549 \cdot r_{gr}/r \quad (28)$$

Atomic radii are taken from [102]. The coefficient “a” in eq (28) is practically zero. In direction from H to Pu on the LDD the general trend is to higher atomic masses and higher densities although there are some variations. This trend is more clearly seen in the second part of the periodic table. It should be noted that in the upper part of this diagram there are a number of heavy radioactive elements: Th, U, Np, Pu etc, but also stable heavy atoms as Au, Os, Ir, Pt, etc. Generally, it is the upper part of the LDD on Fig (31) that contains most of the unstable (radioactive) elements, while the lower part of the diagram is “stable”. If some radioactive atom in the upper part suffers disintegration by alpha-decay, or spontaneous fission the end-products of each decay chain, i.e. the stable

atoms at the end of each respective chain of disintegration processes will “slide down” on the same diagram. It provides an illustration of “*evolution down the linear density diagram,*” discussed in the previous chapters for quasars and for stars. But it could be more than an illustration. Tantalizing possibility arises that relation (28) could provide for a “link” between the macro- world of QSOs, stars, and planets and the world of atoms. This relation may well be the mysterious link between quasars, stars, and planets, being the physical reason for evolution in all these structures. All structures are made of atoms. From Fig (31) it is apparent that this relation will remain the same no matter what combination of elements (chemical composition) is taken. In this way, the obviously different chemical composition of the different quasars, stars or planets would have no impact on the relation (28) – it will remain the same for any chemical composition. The crucial problem to be solved is to show that a great number of atomic transitions on the LDD of elements would produce the observed transitions on the LDD by stellar evolution, e.g. from MS stars to evolved giants. Eq (28) seems to be an important lead in understanding all previously discussed linear density diagrams.

With the evidence of Fig (31) we could try to understand the evolution of structures down the linear density diagram. Radioactive elements disintegrate and all the end- products of decay and fission will slide down on the same LDD. Possibly, this could be the reason for the evolution of structures - QSOs, stars, and planets could slide down on the same linear density diagram because of processes of decay of radioactive atoms. Such scenario implies that quasars, stars, and planets should have substantial quantities of heavy elements (radioactive elements included) probably in their cores. Planets and satellites could actually not slide much further down on the linear density diagram because there seems to be not much left of fissile material in their respective cores. Most of the planetary matter seems to consist of atoms that are already on the “stable” (lower) part of the LDD on Fig (31), i.e. non-fissile atoms. Let me point out that the outlined here scenario of evolution of structures could only be understood with the disintegration hypothesis. This scenario implies very different stellar structure and stellar cores of heavy (including radioactive) elements.

In the outlined here concept there could be a simple explanation for the origin of hydrogen, the seemingly most abundant element in the Universe. Fission of the heavy radioactive atoms always releases a number of free neutrons, which then in a short time decay to protons and electrons. We only need to combine the protons with electrons to get hydrogen. On the other hand, part of the helium observed could be due to alpha-decay processes. Therefore, disintegration processes on a large scale could possibly provide for the observed abundances of H and He as well as of all the other elements. In the concept of disintegration all structures considered here should have core of heavy elements. Thus the processes of disintegration could be responsible for the production of all elements observed, including the elements heavier than helium (designated in astrophysics as Z – elements). But is there any observational evidence of existence of heavy elements in stellar cores?

During the last decades O. Manuel ([www.omatumr.com](http://www.omatumr.com)) in a series of papers maintains his findings of an “iron rich core” in the Sun. Without discussing the details of the

Manuel's model of the solar interior and his evolutionary scenario (there are important differences from the presented here, anyway), the important result of O. Manuel that may change astrophysics is his finding of an iron rich solar core. The possibility of existence of an iron-rich core in the Sun changes everything in solar (and stellar!) astrophysics: origin, internal structure, energy production, and evolution. Needless to say, the finding of O. Manuel is of utmost importance for astrophysics and confirmation by observational evidence of the existence of an "iron-rich" solar core should be given priority.

As mentioned in the previous section in the concept of disintegration the Sun could have arrived on the MS more recently than predicted by the standard theory. It is also not possible to predict the time when Sun will depart from the MS for its transit to the red giant stars.

## ***Chapter 8.***

### ***From quasars to planets: a cascade of “jumps” in evolution?***

In the previous chapters the linear density relation (eq 27) was shown to hold for different structures as quasars, stars, planets, and satellites of the Solar system (see Table 10) as it should be by definition of the LDD. It should be noted that on the LDD structures follow in reduced density as: QSOs, WDs, MS stars, evolved giants, planets, and satellites. Is there a connection between all these structures? I have already discussed the possibility of evolution by sliding down on the linear density diagram from the main sequence stars to the evolved giant stars, but also the tantalizing possibility of transition of the white dwarfs to the main sequence stars on the same LDD. However, this is evolution on the same (stellar) level. Is it possible that there is also evolution from “higher” to a “lower” level, e.g. from quasars to stars? In Chapter 5 evidence was shown in support of the Arp’s scenario [52, 94] of evolution of QSOs to small mass galaxies. If confirmed, this scenario predicts building of galaxies around quasars in the course of evolution. If the concept of disintegration is joined to the Arp’s scenario quasars should lose a large part of their mass to build stellar population around the quasar, actually building a small mass companion galaxy. In other words, this could be an indication of evolution from a higher level (quasar) to the lower level of structures (stars). Is it conceivable to extend this scenario down to planets and satellites? Could it be that stars ejected matter that built their planets, and the planets ejected further their satellites? The only other theory for the origin of stars and planetary systems is the theory of gravitational collapse. It seems conceivable that a disintegration scenario as alternative could be applied also to the stars, planets and satellites, i.e. to the levels below the quasars. At this point that is only hypothesis, but the gravitational collapse scenario is a hypothesis too. If the disintegration scenario is applied to all these structures it would be like a “ladder (or a cascade) of disintegration processes” with each “stair” corresponding to a different level of structures: quasars, stars, planets, and satellites. There are important questions that arise from a “down-ladder” disintegration scenario. What are the “first stairs”, the highest levels where the evolution starts? And what is the “last stair”, the lowest level of structures at the end of the disintegration scenario? Both questions are difficult and only some general remarks could be considered here. We could safely assume that stars, planets and satellites are subsequent levels (“stairs”) and the satellites of planets are probably the last level of disintegration. Satellites do not have their own satellites. In the “up-ladder” direction, to the previous than local quasars level there is observational evidence that local quasars have been ejected by large active galaxies (Chapter 2). If so, the large (parent) galaxies could be the “one level up” on the “ladder of disintegration”. How did the large galaxies originate is by now only a matter of speculation since no positive observational evidence exists. However, it seems that it would be highly inconsistent with the rest of the picture, considered in a disintegration scenario to assume that the large galaxies originated by gravitational collapse events. Even though the highest and lowest levels of the “ladder” are not undoubtedly identified, we could still do research on the “part of the ladder” which seems to be within the “grasp” of our studies, i.e. galaxies, quasars, stars, planets, and satellites.

There are other aspects of this “down-ladder” disintegration scenario. Dimensions and masses of structures are decreasing all the way down the “ladder”, possibly due to the “exhaustion” of the process. This is quite obvious. In order to have evolution by sliding down on the LDD, the masses of structures “down the ladder” should decrease faster than the dimensions. Second, the densities of structures should be decreasing all the way “down the ladder” if the disintegration scenario holds. This is not so obvious with the “normal” densities. The behavior of the densities of QSOs, stars, planets, and satellites is shown on Fig (32). Clearly, mean densities increase from QSOs to MS stars, and they increase further from MS stars to the inner planets of the solar system. There is an apparent maximum of mean densities by the inner planets of the solar system. On first sight this contradicts to the disintegration scenario as we should expect densities to decrease all the way “down the ladder” of disintegration. Solution of this apparent contradiction could be found if all considered structures consist of fissile, high density core and a non-fissile, low density envelope. Such a possibility was discussed in the previous chapter. Decreasing density by disintegration processes applies only to fissile matter. If structures consist of fissile core and non-fissile envelope the mean density of these structures will depend on both the core density and the density of the envelope as well. In this way the trend of the densities on Fig (32) could be explained as shown below.

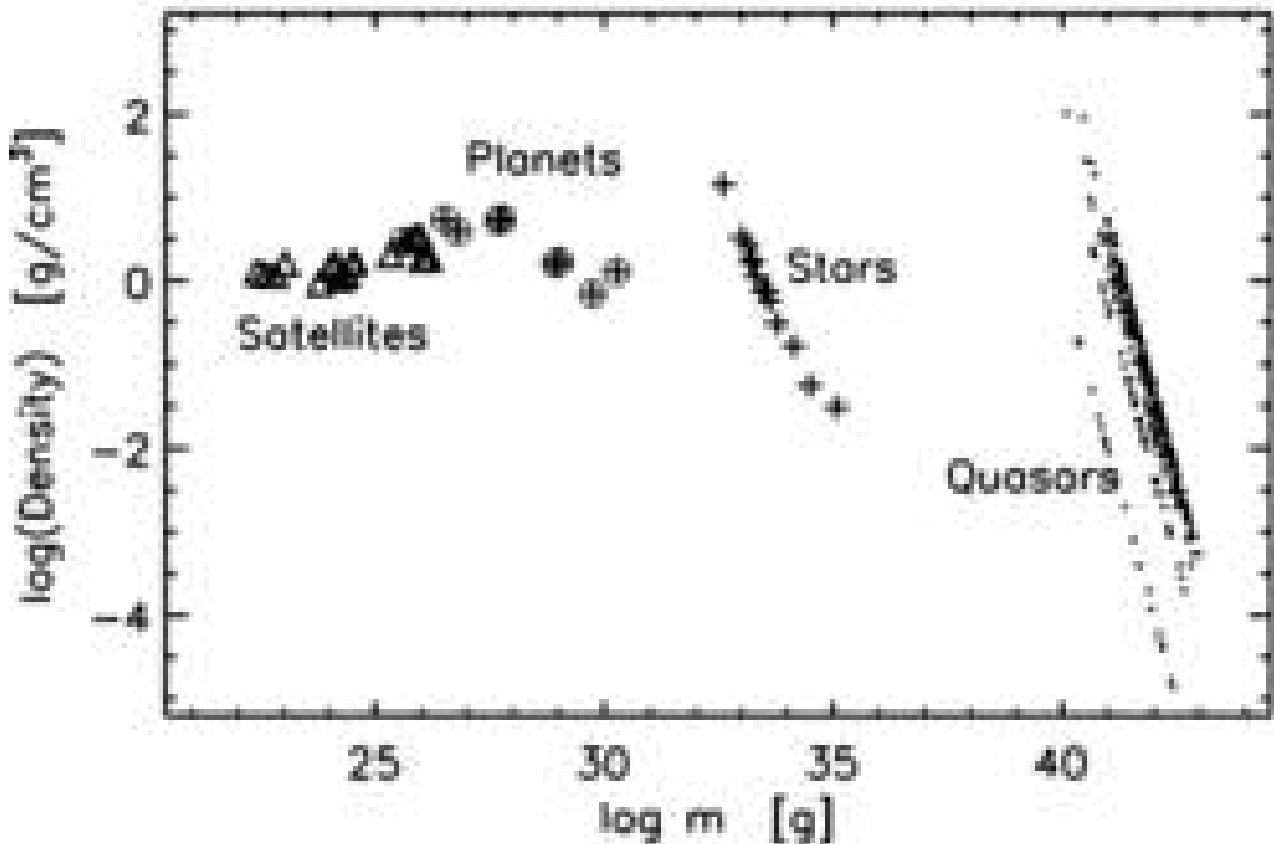


**Fig (32).** Cumulative diagram of the “density-mass” relation for quasars (dots), main sequence stars (crosses) as mean values for O5, B0, B5,..., M5, for the 9 big

**planets of the solar system (encircled crosses), and for 19 satellites (triangles, the list is as in caption of Fig 30). Courtesy of Bentham Open OAJ [95].**

Large envelopes of hydrogen will clearly contribute to the mean density by decreasing its value. In this scenario QSOs should have large envelopes of non-fissile matter, probably hydrogen in the first place. That would decrease their mean densities as seen on Fig (32) with respect to the other structures. Indeed, as decay processes supposedly proceed it is to be expected that a lot of non-fissile material will be produced, in the first place hydrogen. The mean densities, therefore, reflect the combined effect of elements – fissile core with higher density and non-fissile envelope with lower density, and their respective contribution to mean density. Possibly, it is the contribution of non-fissile hydrogen envelopes that determines the lower densities of quasars on Fig (32). However, the spread of densities of quasars is large as apparent from Fig (32).

With the stars the hydrogen envelopes are probably less massive compared to QSOs and therefore their contribution to stellar mean densities should be less. This is implied by the smaller stellar masses with respect to quasar masses. In other words, by transition from quasars to stars the contribution to mean density of stellar cores gets stronger as compared with contribution of quasar cores to their respective mean density, although stellar cores densities should be decreasing with respect to quasar cores densities. In this way mean stellar densities could be higher than mean densities of quasars (Fig 32), although stellar cores could be less dense than cores of QSOs. The same consideration could also hold by the transition from stars to the planets of the solar system and so the mean densities of planets could be higher than stellar mean densities. Thus mean densities could reach maximum values with the inner planets of the solar system. By the inner planets of the solar system the contribution of envelopes (atmospheres) to mean planetary density is less compared with stars and also compared with the giant planets. One could say that by the inner planets of the SS mean densities closely reflect the densities of their respective cores. Considering core densities only, the planetary cores should be less dense than the stellar cores and stellar cores should be less dense than quasar cores, according to the concept of disintegration. The guiding evidence of evolution in the disintegration scenario is indeed decreasing densities of structures in the course of evolution, but this conclusion is true only for the fissile matter (cores). Real structures – QSOs, stars, and planets should probably consist of fissile and non-fissile matter (cores and envelopes), and the density trend of structures is more complicated as seen on Fig (32). In this consideration the planetary envelopes are their atmospheres, i.e. planetary cores could contain also non-fissile matter.

In this scenario it could be expected that with decreasing masses of structures “down the ladder” of disintegration the contribution of envelopes of gases will decrease, due to decreasing efficiency of the decay processes. At some point mean density of structures will reflect predominantly the core densities. That seems to be the case with the transition from planets to satellites. There is a conspicuous fact and an old problem: why is the density of the Moon ( $\sim 3.3 \text{ g/cm}^3$ ) less than the density of the Earth ( $\sim 5.5 \text{ g/cm}^3$ )? The same problem concerns densities of many satellites, not just the Moon (see Fig 40

below). Densities of satellites are generally less than the densities of the inner planets. This is an obvious problem for the theory of gravitational collapse. Indeed, since the Moon is supposed to have originated by a collapse nearby the Earth their densities should be expected to be about the same. Disintegration scenario provides a simple answer to the observed discrepancy which is, however, not a detailed explanation. Densities of the satellites are expected to be less compared with densities of the inner planets because satellites are one step “down the ladder” of disintegration. In these arguments I have repeatedly used the “inner planets” as comparison because the inner planets have smaller masses and less massive atmospheres. The giant planets have very extensive atmospheres (large masses also!) and as a consequence lower mean densities. Some researchers believe that the giant planets are entirely made of gases. If disintegration scenario holds the giant planets should have inner cores of heavy elements as all the other structures considered here, but the contribution of their mighty atmospheres to their respective mean density should be substantial and the mean densities of the giant planets are much less than densities of the inner planets. Coming back to the lower densities of the satellites in the SS it seems that disintegration scenario could handle this problem. Looking on Fig (32) it could be noticed that the density trend for QSOs has the steepest slope, then this slope gets less steep for stars, and even less steep for planets. With the satellites this slope is actually reversed with respect to the trend of quasars, stars, and planets (all planets plotted together). For QSOs, stars, and planets densities decrease with increasing masses. For the satellites apparently this trend is reversed: densities decrease with decreasing masses. This two-fold behavior was considered in the previous Chapter 6 when discussing stellar evolution. It looks as the satellites behave on a “density – mass” diagram in a similar way (but with a different slope) as the WDs. It should also be noted that similar trend is observed also with the heavy elements of the periodic table. Is this a coincidence? Or, may be, heavy elements determine the shape of the “density-mass” diagram in WDs and in the satellites? Such conclusion would be consistent with the disintegration scenario, but it needs a detailed study in order to be confirmed. According to the same scenario stellar cores also should consist of heavy elements, but stellar mighty envelopes effectively mask the cores.

The slopes on Fig (32) could be described by the following equations. For QSOs holds the family of equations (23) with slope of -2 in each equation.

The relation “density – mass” for stars (mean values for O5, B0, B5, A0,.....,M5) is:

$$\log \rho = 36.415 - 1.088 \log m \quad (29)$$

Note that larger masses correspond to less density (as for QSOs!) but the slope in eq (29) is significantly less than the respective slope for QSOs.

The “density – mass” relation for the 9 big solar system planets is:

$$\log \rho = 4.794 - 0.156 \log m \quad (30)$$

Again, larger masses correspond to less density, but the slope of trend for the planets is significantly less than the slope for stars. This is also obvious on Fig (32). The reason for

that difference of slopes could be the decreasing contribution of hydrogen envelopes to mean density of stars with respect to envelopes in QSOs, or decreasing contribution of atmospheres to mean density of planets with respect to envelopes in stars. The decreasing trend of density (Fig 32) by transition: QSOs – stars – planets, therefore, reflects the decreasing masses of structures and the decreasing efficiency (activity) of disintegration processes.

The “density – mass” relation for the 19 satellites (see list in caption of Fig 30) to which also the planets Pluto, Mercury, and Mars are added is:

$$\log \rho = -2.625 + 0.117 \log m \quad (31)$$

Note the reversed slope of the last relation: larger masses of satellites correspond to larger densities. Possibly, the reversed slope is due to the predominant contribution to mean density of satellites of their Z – cores. The same is true also for the included planets Mercury, Mars, and Pluto. As stated above, this change of sign of slope in the eq (31) is probably to be explained with the insignificant contribution of the atmospheres of satellites to their respective mean densities. In this way eq (31) could “reflect” closely the genuine relation “density – mass” for the Z – cores of the satellites. “Reflecting closely” means that there is a small contribution of atmospheres in eq (31) which is not accounted for.

Is it possible that similar relation with a positive trend as in eq (31) exists also for the Z – cores of the giant planets of the SS and may be even for the Z – cores of the stars? Such a possibility is not excluded by the disintegration scenario, but there is no way at present to present any evidence.

Several comments are due to relation (31). All the inner planets of the solar system seem to be in the range (if extended) of the “density-mass” relation, determined from the satellites (see also Fig 32). This could be interpreted as a possibility to apply the “density – mass” relation (31) also to the Z-cores of all the inner planets and for Pluto. On the other hand it was considered above the possibility of different stages (cascades) in the processes of disintegration. This means that planets and satellites should belong to subsequent, but different stages in this scenario and which should concern also their Z-core densities. As planets and satellites belong to different stages it would be appropriate to expect different relations for the cores of planets and satellites. May be such a difference could be detected in future with a larger sample of planets and satellites (extra-solar systems?). Due to the limited number of planets and satellites used here this is impossible.

It is interesting to note that also the planets Mercury, Mars, and Pluto correspond closely to the extension of the density diagram for satellites. It could be because their atmospheres are “negligible” with respect to their respective total mass and do not contribute substantially to their respective mean densities, the same way as satellites. On the other hand, Mercury, Mars, and Pluto could also be included into the respective diagram of all planets i.e. they build some sort of “intersection” of the two diagrams - for

satellites and for planets. The trend of the Z- core densities is only seen with the satellites and with the inner planets of the solar system, but it is not entirely free from contribution of atmospheres.

The evidence from Fig (32) and the eqs (29-31) could be summarized as follows. There may be a cascade of “jumps” in the evolution of structures, from QSOs to planets and satellites.

The amplitude of “jumps” decreases by transitions: QSOs – stars – planets - satellites. No apparent “jump” could be noticed from planets to the satellites, apart from the reversed sign of the “density – mass” relation.

The guiding evidence in a disintegration scenario is decreasing density in the process of evolution. However, this is true only for fissile matter. If real structures – quasars, stars, and planets consist of both fissile and non-fissile matter, the trend of density in the course of evolution reflects all components in respective structures and their contribution to their mean density. The apparently increasing trend of mean density by transition: QSOs – stars – planets could be due to the increasing contribution to mean density of the heavy elements Z – cores and decreasing contribution of envelopes. The physical reason behind this trend should be the gradually exhausted processes of disintegration in the course of evolution. These processes should be most vigorous in QSOs, producing mighty hydrogen envelopes, due to their larger masses. In stars disintegration processes are less vigorous, producing less massive envelopes. Respectively, mean stellar densities are higher because of the stronger contribution of the stellar Z – cores. In planets and satellites the contribution of the envelopes (atmospheres) is even less and the trend of density reaches maximum with the inner planets of the SS. This scenario is consistent with the decreasing slopes in eqs (23, 29-30). The reversed trend of density by satellites, eq (31) could reflect the density trend of their Z – cores.

The disintegration concept of evolution of structures requires Z – cores of heavy (including radioactive!) elements in all structures considered here: QSOs, stars, and planets. The absence of Z-cores in planets, stars, or in quasars would mean failure of the disintegration concept.

Indeed, it seems inevitable in the framework of the disintegration concept to assume that there should be also a different way to produce heavy elements in Nature, as a result of the processes of disintegration. That is a radically different view, in contradiction to the popular theory of producing heavy elements by nuclear fusion in the late stages of stellar evolution. It may actually be the other way around: fission, not fusion produced all the elements. Since we do not have direct evidence – fission or fusion, we should keep both options free and test both hypotheses by their implications.

In the context of the disintegration concept steeper slope of “density – mass” relation would mean that the processes are more vigorous and the evolution is faster. It means that the speed of evolution depends on the mass, and larger masses should be disintegrating (evolving) faster. The orthodox scenario of stellar evolution also is based on the same

principle: evolution depends on mass. However, the physical reason behind that principal is different for both concepts. A possible physics behind this principal in the concept of disintegration could be the law of radioactive decay. The dependence of evolution on mass of structures could be generalized for all structures we observe – quasars, stars, and planets. Apparently, the efficiency of processes of disintegration (whatever they are) decreases from quasars to stars, and decreases further from stars to planets and satellites. It would seem that by the satellites this process has been already “exhausted”.

The range of density spread is largest with quasars and gets smaller by transition to stars and further to planets and satellites.

The decreasing reduced densities of structures by transition: QSOs – stars – planets - satellites (Table 10) show clearly the direction of evolution. By this transition proportionally decreasing are also the ratios  $r_{gr}/r$ . In the previous Chapter 6 decreasing reduced densities were discussed in the context of stellar evolution (evolution on the same “level”). In this case the expansion of stars was considered as possible physical reason. In the presumed evolution of structures QSOs – stars – planets – satellites both the masses and the radii of structures are decreasing (see Table 12 below). But the masses of structures have to decrease stronger in order to produce decreasing  $r_{gr}/r$  ratios and also decreasing reduced densities on the LDD. It clearly shows that the LDD could be useful and meaningful if used with real structures.

On Fig (33) cumulative diagram is shown for the relation “mass – radius”, including quasars, main sequence stars, planets and satellites.

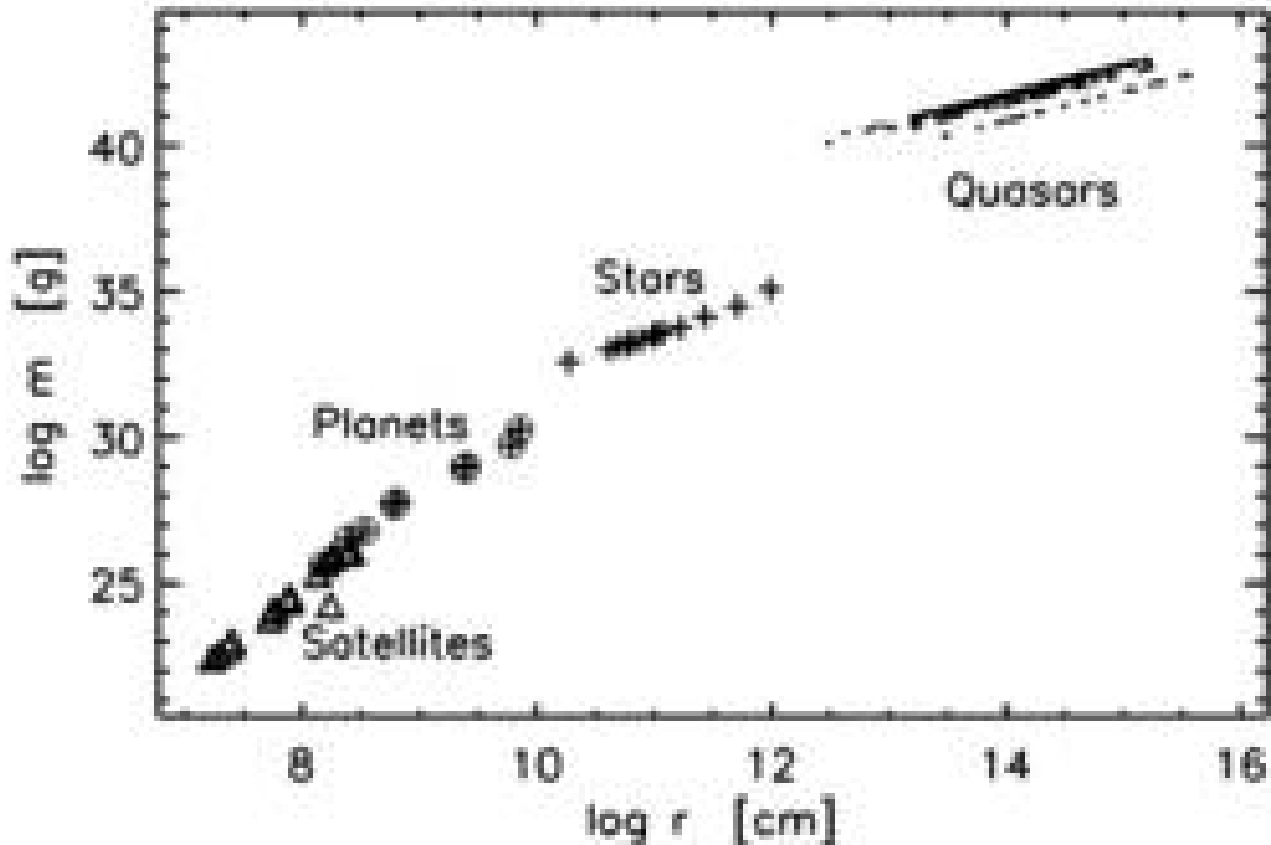


**Fig (33). Cumulative diagram of the “mass-radius” relation for quasars (dots), stars O5, B0, B5,...M5 (crosses), for 9 big planets of the solar system (encircled crosses), and for 19 satellites (triangles, the list is as in caption of Fig 30). Courtesy of Bentham Open OAJ [95].**

The “jump” from quasars to stars is clearly seen and the next “jump” from stars to planets is obviously smaller. A “jump” from planets to satellites is not obvious.

Note the steadily increasing slopes of the diagrams of different structures, proceeding from quasars to stars, and further from stars to planets and satellites.

On Fig (34), cumulative diagram is shown for the relation “radius – density”, including quasars, main sequence stars as mean values for O5, B0, B5, ...,M5, planets and satellites. Again, the “jumps” between different structures are apparent and clearly seen are decreasing dimensions of structures “down the “ladder” of disintegration. On Fig (34) it could be seen again that the range of density spread is largest with quasars and gets smaller following the transition to stars, planets, and satellites.

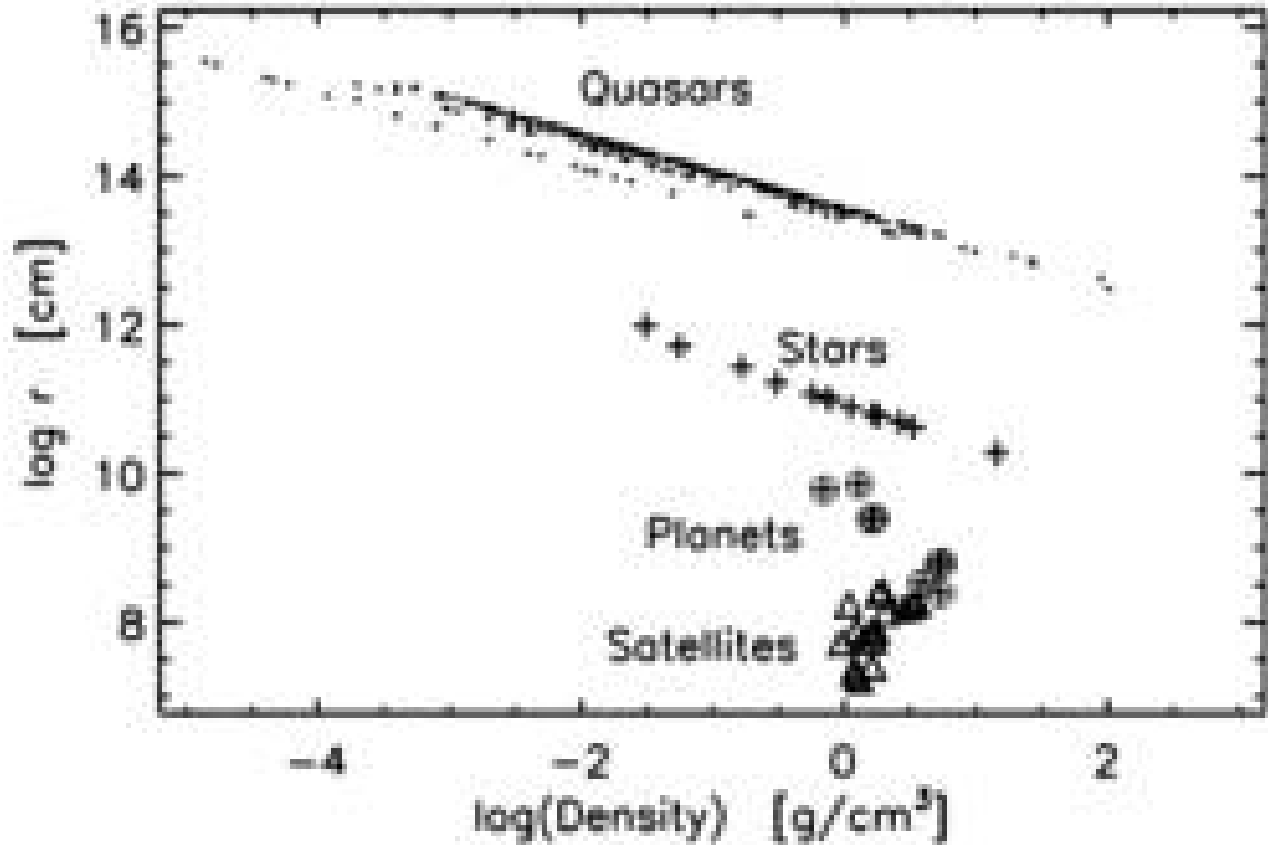


**Fig (34). Cumulative diagram of the “radius-density” relation for quasars (dots), main sequence stars (crosses), the 9 big planets of the solar system (encircled crosses), and for 19 satellites (triangles, the list is as in caption of Fig 30). Courtesy of Bentham Open OAJ [95].**

In Chapter 4, equations (18, 22, 24) were introduced for quasars, respectively for the “mass – radius”, “density – mass”, and the “radius – density” relations. Here again they are written without the subscript “q” (for quasars):

$$\log m = 27.83 + \log r + \log (r_{gr}/r) \quad (32)$$

$$\log \rho = 82.86 - 2.\log m + 3.\log (r_{gr}/r) \quad (33)$$

$$\log r = 13.60 - \frac{1}{2} \log \rho + \frac{1}{2} \log (r_{gr}/r) \quad (34)$$

It can be shown that these equations could be used also for stars, planets and satellites. In the right side of each equation, the observed values are put to calculate the respective value of mass, or density, or radius. Then the calculated value could be compared with the observed one. A sample of objects is listed in Table 11.

**Table 11. Comparison of calculated with eqs (32-34) values and the observed values for stars O5-M5, for planets and satellites of the solar system. (Courtesy of Bentham Open OAJ [95]).**

| Object   | $\log(r_{gr}/r)$ | $\log m$<br>[g]<br>observed | $\log m$<br>[g]<br>eq (29) | $\log \rho$<br>[g/cm <sup>3</sup> ]<br>observed | $\log \rho$<br>[g/cm <sup>3</sup> ]<br>eq (30) | $\log r$<br>[cm]<br>observed | $\log r$<br>[cm]<br>eq (31) |
|----------|------------------|-----------------------------|----------------------------|---|--|------------------------------|-----------------------------|
| Stars O5 | -4.921           | 35.079                      | 34.898                     | -1.509  | -2.061   | 11.989                       | 11.894                      |
| Stars B0 | -5.036           | 34.505                      | 34.506                     | -1.252  | -1.258   | 11.712                       | 11.708                      |
| Stars B5 | -5.119           | 34.146                      | 34.145                     | -0.777  | -0.789   | 11.434                       | 11.429                      |
| Stars A0 | -5.276           | 33.778                      | 33.777                     | -0.513  | -0.524   | 11.223                       | 11.219                      |
| Stars A5 | -5.301           | 33.602                      | 33.602                     | -0.240  | -0.247   | 11.073                       | 11.070                      |
| Stars F0 | -5.292           | 33.556                      | 33.557                     | -0.122  | -0.128   | 11.019                       | 11.015                      |
| Stars F5 | -5.337           | 33.477                      | 33.482                     | -0.111  | -0.105   | 10.989                       | 10.987                      |
| Stars G0 | -5.387           | 33.322                      | 33.327                     | 0.048   | 0.055  | 10.884                       | 10.883                      |
| Stars G5 | -5.367           | 33.265                      | 33.269                     | 0.223   | 0.229  | 10.806                       | 10.805                      |
| Stars K0 | -5.409           | 33.193                      | 33.193                     | 0.255   | 0.247  | 10.772                       | 10.768                      |
| Stars K5 | -5.387           | 33.140                      | 33.143                     | 0.418   | 0.419  | 10.700                       | 10.698                      |
| Stars M0 | -5.444           | 33.009                      | 33.007                     | 0.524   | 0.510  | 10.621                       | 10.616                      |
| Stars M5 | -5.495           | 32.602                      | 32.609                     | 1.158   | 1.171  | 10.274                       | 10.274                      |
|          |                  |                             |                            |   |  |                              |                             |
| Mercury  | -9.6975          | 26.519                      | 26.520                     | 0.735   | 0.730  | 8.387                        | 8.384                       |
| Venus    | -8.9235          | 27.687                      | 27.688                     | 0.719   | 0.7155   | 8.782                        | 8.779                       |
| Earth    | -8.857           | 27.776                      | 27.777                     | 0.742   | 0.737  | 8.804                        | 8.801                       |
| Mars     | -9.551           | 26.807                      | 26.809                     | 0.594   | 0.593  | 8.530                        | 8.527                       |
| Jupiter  | -7.395           | 30.278                      | 30.2795                    | 0.124   | 0.119  | 9.8445                       | 9.841                       |
| Saturn   | -7.854           | 29.755                      | 29.756                     | -0.161  | -0.212   | 9.780                        | 9.753                       |
| Uranus   | -8.293           | 28.939                      | 28.9395                    | 0.104   | 0.104  | 9.4025                       | 9.402                       |
| Neptune  | -8.209           | 29.010                      | 29.0115                    | 0.215   | 0.213  | 9.390                        | 9.388                       |
| Pluto    | -11.076          | 25.116                      | 25.117                     | 0.301   | -0.600   | 8.363                        | 7.912                       |
|          |                  |                             |                            |   |  |                              |                             |
| Moon     | -10.2025         | 25.866                      | 25.867                     | 0.525   | 0.520  | 8.240                        | 8.236                       |
| Io       | -10.138          | 25.951                      | 25.952                     | 0.550   | 0.545  | 8.260                        | 8.256                       |
| Europa   | -10.341          | 25.681                      | 25.682                     | 0.479   | 0.475  | 8.193                        | 8.190                       |
| Ganymed  | -10.079          | 26.171                      | 26.172                     | 0.287   | 0.282  | 8.421                        | 8.417                       |
| Callisto | -10.179          | 26.032                      | 26.033                     | 0.2645  | 0.260  | 8.382                        | 8.378                       |
| Tethys   | -11.766          | 23.792                      | 23.7935                    | -0.018  | -0.0225  | 7.729                        | 7.726                       |
| Dione    | -11.538          | 24.041                      | 24.0425                    | 0.169   | 0.164  | 7.750                        | 7.747                       |
| Rhea     | -11.3505         | 24.362                      | 24.363                     | 0.0895  | 0.085  | 7.883                        | 7.880                       |
| Titan    | -10.109          | 26.130                      | 26.1315                    | 0.276   | 0.271  | 8.411                        | 8.4075                      |
| Iapetus  | -11.440          | 24.255                      | 24.256                     | 0.034   | 0.030  | 7.866                        | 7.863                       |
| Ariel    | -11.460          | 24.131                      | 24.132                     | 0.221   | 0.217  | 7.763                        | 7.759                       |
| Umbriel  | -11.527          | 24.069                      | 24.070                     | 0.146   | 0.1415   | 7.767                        | 7.764                       |
| Titania  | -11.1785         | 24.547                      | 24.5485                    | 0.234   | 0.230  | 7.897                        | 7.894                       |
| Oberon   | -11.231          | 24.479                      | 24.480                     | 0.212   | 0.208  | 7.882                        | 7.878                       |
| Triton   | -10.629          | 25.331                      | 25.332                     | 0.315   | 0.311  | 8.131                        | 8.128                       |

The agreement between the calculated and the observed values are generally satisfactory with a few percent discrepancies. The only big discrepancies are for stars of spectral class O5 and for the planet Pluto. It can, therefore, be concluded that eqs (32-34) hold also for stars, planets and satellites of the solar system.

Here is a brief summary of possible conclusions from this chapter:

- Cumulative diagrams for “density – mass”, “mass – radius”, and “radius – density” including quasars, main sequence stars, planets and satellites show jumps (“cascades”) which gradually decrease in amplitude by transition QSOs – stars – planets. The biggest jump in all diagrams is from quasars to stars. The jump from planets to satellites is not obvious. These diagrams possibly imply evolution of structures from larger masses and dimensions to smaller masses and dimensions in a sequence of “cascades”.
- Cumulative diagrams together with the LDDs of structures imply two possible ways of evolution due to processes of disintegration: evolution from larger to smaller structures with jumps (quasars to stars, stars to planets, planets to satellites), and evolution on the same “level” (quasar level, stellar level, planetary level). In this picture there has to be a theoretical “jump” from planets to satellites, which is, however, not noticeable (too small?) on the respective diagrams. In both ways of evolution reduced densities are decreasing, i.e. evolution proceeds “down the LDD”.
- The three levels (“cascades”) of disintegration – stars, planets and satellites seem to be successive “cascades”. It is not clear whether or not there is an additional level between quasars and stars. It is also not clear what are the higher levels above the local quasars. Parent galaxies that ejected quasars could represent “one level up”.
- The slope of trends on the “density – mass” diagram is steepest for quasars, indicating most vigorous processes of disintegration (whatever they might be). It also indicates that large masses evolve faster.
- The slopes of trends on the “density- mass” diagram gradually decrease from quasars to stars, and further from stars to planets, indicating gradually decreasing efficiency of the processes of disintegration from quasars to planets and satellites.
- There is a large spread of quasars’ densities and a gradual decrease of density spread by transition to stars and further to planets.
- The density trends on Fig (32) could be explained if all structures considered consist of high density fissile core and low density, non-fissile envelope.
- There seems to be the tendency: larger masses produce larger (hydrogen?) envelopes and large envelopes contribute to less mean densities of structures. This seems to explain the transition: QSOs – stars – planets on the “density-mass diagram. The envelopes for planets are their respective atmospheres.
- The trend in the “density – mass” relation is reversed for the satellites (and possibly also for the inner planets of solar system) because the contribution of their atmospheres to their respective mean density is not essential. The reversed sense of this relation with satellites means that larger masses correspond to higher densities.
- All structures discussed – giant planets, stars, and quasars, should have in their interior Z - cores if the disintegration scenario holds. The absence of Z-cores would mean failure of the disintegration concept.
- All planets and satellites show spherical form which is an obvious proof that all planets and satellites were molten in their early phases of evolution. The cause of

melting could only be due to the internal processes of disintegration in their respective cores. The spherical form of planets and satellites represents serious difficulty for the gravitational collapse theory,

- The last stages of disintegration could be the well known radioactive decay and fission processes with radioactive elements.

- Generally, it is the decreasing density of structures that is the guiding evidence for the evolution of structures if disintegration scenario holds. Densities should be decreasing “down the ladder” of disintegration. Evolution on the “same level”, e.g. stellar evolution proceeds with increasing stellar radii which is consistent with disintegration concept.

- Reduced densities (to the same radius of reference!) are always decreasing in the direction of evolution. Assuming that structures evolve in cascade disintegration from quasars to planets and satellites the masses of structures should decrease stronger than dimensions of structures, in order that reduced densities are decreasing as observed.

- The evolution from quasars to stars and further from stars to planets means gradually decreasing activity and efficiency of disintegration processes.

Radii, masses, and densities are summarized in Table 12 for possible stages in evolution.

**Table 12. Radii, masses, and densities of possible stages of evolution.**

| Structure     | log r<br>[cm] | log m<br>[g] | log(density)<br>[g/cm <sup>3</sup> ] | Range of the reduced<br>density [g/cm <sup>3</sup> ] to<br>8.10 <sup>13</sup> cm |
|---------------|---------------|--------------|--------------------------------------|--|
| 341 quasars   | 12.5 – 15.5   | 40 - 43      | -4.8 - (+2)                          | 0.02 – 0.25  |
| 129 WD        | 8.67 - 9.35   | 32 - 33.35   | 3.4 - 6.7                            | 2. 10 <sup>-6</sup> - 2. 10 <sup>-4</sup>  |
| Stars B0-M5   | 10.3 - 12     | 32.6 – 35.1  | -1.5 –(+1.2)                         | 0.8 .10 <sup>-6</sup> - 2.3 .10 <sup>-6</sup>                                    |
| 20 giants     | 11.8 - 13.4   | 33.4 – 34.6  | -7.5 – (-2.4)                        | 3. 10 <sup>-9</sup> - 8. 10 <sup>-7</sup>  |
| 9 Planets     | 8.4 - 9.8     | 25.1 – 30.3  | 0.30 – 0.74                          | 1.1 .10 <sup>-11</sup> - 1. 10 <sup>-8</sup>                                     |
| 19 Satellites | 7.2 - 8.4     | 22.4 - 26.2  | 0.12 – 0.55                          | 5.9 .10 <sup>-14</sup> – 2.1 .10 <sup>-11</sup>                                  |

## Chapter 9.

### *Looking for a planetary orbital distances law.*

In the Introduction I have briefly reviewed the story of the orbital distances law in planetary systems. The existence of such a distances law contradicts to the gravitational collapse theory in two conspicuous ways. First, it is not likely for a random process of collapses that presumably built planetary systems to create regular distances of these planets from their respective central star. The second difficulty arises for exoplanetary systems. In a number of extra-solar systems exoplanets have been found very close to the respective central star, so close actually that a gravitational collapse at that distance from the star should have been impossible. To save the collapse hypothesis spiraling down scenario was invoked by assuming that exoplanets were built far away from the star and later were brought closer to the star by friction (or drag) with the environment. If so, the existence of an orbital distances law (whatever the formula may be) is also crucial. The friction with the environment is also a random process and if a planetary distances law exists in exoplanetary systems the spiraling down scenario would be severely compromised. Indeed, it would be highly unlikely to assume that a random friction could bring some exoplanet at exactly the right distance from the respective star, in order to fulfill the respective distances law in this exoplanetary system. The alternative is that these close-by exoplanets were built “*in situ*”. But the origin then should be different – not a collapse. Generally, this “friction-scenario” should affect many planets in an exoplanetary system, may be all. Within such a scenario then a law of planetary distances, no matter what this law is, appears to be impossible.

In this section an attempt is presented to fit an exponential distances formula to the data available, including the solar system planets and some exoplanets. For exoplanets data were taken from The Extrasolar Planets Encyclopaedia and the NASA Exoplanet Archive. The exponential distances formula has been applied in [5, 103, 104]. Here I will take the formula from [5]:

$$a_n = C \cdot e^{2n/k} \quad (35)$$

with “n” being the orbital number and C and k being parameters. The form of this formula seems preferable for the following reason. It could be shown that a similar formula exists for the orbital velocities of the planets of the Solar system:

$$V_n = 63.9 \cdot e^{-n/k} \quad [\text{km} \cdot \text{s}^{-1}] \quad (36)$$

Substituting eq (36) into the 3<sup>rd</sup> law of Kepler we get the eq (35). Note that the parameter k is the same in both eqs (35) and (36), while C is different. In Table 13, solutions for eq (35) are listed for the solar system (planets and satellites) and for a number of exoplanetary systems with at least 5 known planets.

**Table 13. Solutions of eq (35) for the solar system planets and satellites and for extrasolar planetary systems. Data for exoplanets are from the Extrasolar Planets Encyclopaedia and the NASA Exoplanet Archive.**

| Planetary system      | Orbital number | Orbital parameter k | Orbital parameter C [km] | Error $\Delta a_n/a_n$ |
|-----------------------|----------------|---------------------|--------------------------|------------------------|
| Solar system          |                | 3.722               | 31 933 974               |                        |
| Mercury               | n = 1          |                     |                          | -0.06                  |
| Venus                 | n = 2          |                     |                          | -0.14                  |
| Erth                  | n = 3          |                     |                          | 0.07                   |
| Mars                  | n = 4          |                     |                          | 0.20                   |
| Ceres                 | n = 5          |                     |                          | 0.14                   |
| Jupiter               | n = 6          |                     |                          | 0.03                   |
| Saturn                | n = 7          |                     |                          | -0.04                  |
| Uranus                | n = 8          |                     |                          | -0.18                  |
| Neptune               | n = 9          |                     |                          | -0.11                  |
| Pluto                 | n = 10         |                     |                          | 0.16                   |
| Satellites of Jupiter |                |                     |                          |                        |
| Metis                 | n = 1          | 10.05 (n=1-4)       | 97 632                   | -0.07                  |
| Adrastea              | n = 2          |                     |                          | 0.13                   |
| Amaltea               | n = 3          |                     |                          | -0.02                  |
| Thebe                 | n = 4          |                     |                          | -0.02                  |
| Io                    | n = 5          | 4.04 (n=5-8)        | 34 704                   | -0.02                  |
| Europa                | n = 6          |                     |                          | 0.01                   |
| Ganymed               | n = 7          |                     |                          | 0.04                   |
| Callisto              | n = 8          |                     |                          | 0.03                   |
| Satellites of Saturn  |                |                     |                          |                        |
| Pan                   | n = 1          | 91.42 (n=1-7)       | 129 679                  | -0.01                  |
| S/2005 S1             | n = 2          |                     |                          | -0.01                  |
| Atlas                 | n = 3          |                     |                          | 0.01                   |
| Prometheus            | n = 4          |                     |                          | 0.02                   |
| Pandora               | n = 5          |                     |                          | 0.02                   |
| Epimetheus            | n = 6          |                     |                          | -0.02                  |
| Janus                 | n = 7          |                     |                          | 0.00                   |
| Mimas                 | n = 8          | 11.68 (n=8-14)      | 41 103                   | -0.13                  |
| S/2004 S1             | n = 9          |                     |                          | -0.01                  |
| S/2004 S2             | n = 10         |                     |                          | 0.08                   |
| Enceladus             | n = 11         |                     |                          | 0.13                   |
| Tethys                | n = 12         |                     |                          | 0.09                   |
| Dione                 | n = 13         |                     |                          | 0.01                   |
| Rhea                  | n = 14         |                     |                          | -0.14                  |
| Titan                 | n = 15         | 3.74 (n=15-17)      | 356                      | -0.11                  |

|                       |        |                  |           |       |
|-----------------------|--------|------------------|-----------|-------|
| Hyperion              | n = 16 |                  |           | 0.26  |
| Iapetus               | n = 17 |                  |           | -0.11 |
| Kiviuq                | n = 18 | 21.65 (n=18-22)  | 2 080 415 | -0.03 |
| Ljirak                | n = 19 |                  |           | 0.05  |
| Phoebe                | n = 20 |                  |           | 0.02  |
| Paaliak               | n = 21 |                  |           | -0.05 |
| Skathi                | n = 22 |                  |           | 0.01  |
| Satellites of Uranus  |        |                  |           |       |
| Cordelia              | n = 1  | 39.16 (n=1-6)    | 48 821    | 0.03  |
| Ophelia               | n = 2  |                  |           | 0.01  |
| Bianca                | n = 3  |                  |           | -0.04 |
| Cressida              | n = 4  |                  |           | -0.03 |
| Desdemona             | n = 5  |                  |           | 0.01  |
| Juliet                | n = 6  |                  |           | 0.03  |
| Portia                | n = 7  | 34.8 (n=7-13)    | 43 593    | -0.01 |
| Rosalind              | n = 8  |                  |           | -0.01 |
| S/2003/ U2            | n = 9  |                  |           | -0.02 |
| Belinda               | n = 10 |                  |           | 0.03  |
| S/1986 U10            | n = 11 |                  |           | 0.07  |
| Puck                  | n = 12 |                  |           | 0.01  |
| S/2003 U1             | n = 13 |                  |           | -0.06 |
| Miranda               | n = 14 | 5.22 (n=14-18)   | 607       | 0.00  |
| Ariel                 | n = 15 |                  |           | 0.00  |
| Umbriel               | n = 16 |                  |           | 0.05  |
| Titania               | n = 17 |                  |           | -0.06 |
| Oberon                | n = 18 |                  |           | 0.03  |
| S/2001 U3             | n = 19 | 10.985 (n=19-27) | 165 511   | 0.23  |
| Caliban               | n = 20 |                  |           | -0.13 |
| Stephano              | n = 21 |                  |           | -0.05 |
| Trinkulo              | n = 22 |                  |           | 0.07  |
| Sycorax               | n = 23 |                  |           | -0.10 |
| S/2003 U3             | n = 24 |                  |           | -0.09 |
| Prospero              | n = 25 |                  |           | -0.03 |
| Setebos               | n = 26 |                  |           | 0.08  |
| S/2001 U2             | n = 27 |                  |           | 0.08  |
| Satellites of Neptune |        |                  |           |       |
| Naiad                 | n = 1  | 24.93 (n=1-4)    | 43 328    | -0.03 |
| Thalassa              | n = 2  |                  |           | 0.02  |
| Despina               | n = 3  |                  |           | 0.05  |
| Galatea               | n = 4  |                  |           | -0.04 |
| Larisa                | n = 5  | 2.54 (n=5-7)     | 1 292     | -0.10 |
| Proteus               | n = 6  |                  |           | 0.24  |
| Triton                | n = 7  |                  |           | -0.10 |

|                      |       |               |                |       |
|----------------------|-------|---------------|----------------|-------|
| Gliese 667 C planets |       | 5.6292        | 5 825 115      |       |
| b                    | n = 1 |               |                | 0.10  |
| h                    | n = 2 |               |                | -0.11 |
| c                    | n = 3 |               |                | -0.10 |
| f                    | n = 4 |               |                | 0.03  |
| e                    | n = 5 |               |                | 0.08  |
| d                    | n = 6 |               |                | 0.19  |
| g                    | n = 7 |               |                | -0.15 |
| Tau Cet planets      |       | 3.253         | 8 416 791      |       |
| b                    | n = 1 |               |                | -0.01 |
| c                    | n = 2 |               |                | -0.01 |
| d                    | n = 3 |               |                | -0.05 |
| e                    | n = 4 |               |                | 0.19  |
| f                    | n = 5 |               |                | -0.10 |
| 55 Cnc planets       |       | 1.771         | 1 160 242      |       |
| e                    | n = 1 |               |                | 0.52  |
| b                    | n = 2 |               |                | -0.35 |
| c                    | n = 3 |               |                | -0.04 |
| f                    | n = 4 |               |                | -0.09 |
| missing ?            | n = 5 | Distance from | Star = 2.20 AU |       |
| d                    | n = 6 |               |                | 0.18  |
| HD 10180 planets     |       | 3.5446        | 2 211 694      |       |
| b                    | n = 1 |               |                | 0.17  |
| c                    | n = 2 |               |                | -0.29 |
| i                    | n = 3 |               |                | -0.11 |
| d                    | n = 4 |               |                | 0.10  |
| e                    | n = 5 |               |                | -0.08 |
| j                    | n = 6 |               |                | 0.32  |
| f                    | n = 7 |               |                | 0.55  |
| g                    | n = 8 |               |                | -0.05 |
| h                    | n = 9 |               |                | -0.32 |
| HD 40307 planets     |       | 4.243         | 4 451 284      |       |
| b                    | n = 1 |               |                | 0.02  |
| c                    | n = 2 |               |                | -0.04 |
| d                    | n = 3 |               |                | -0.07 |
| e                    | n = 4 |               |                | 0.04  |
| f                    | n = 5 |               |                | 0.27  |
| g                    | n = 6 |               |                | -0.16 |
| Kepler – 11 planets  |       | 6.424         | 9 072 413      |       |

|                   |       |               |                |       |
|-------------------|-------|---------------|----------------|-------|
| b                 | n = 1 |               |                | 0.09  |
| c                 | n = 2 |               |                | -0.07 |
| d                 | n = 3 |               |                | 0.03  |
| e                 | n = 4 |               |                | -0.09 |
| f                 | n = 5 |               |                | -0.15 |
| g                 | n = 6 |               |                | 0.15  |
| Kepler 20 planets |       | 4.1354        | 3 678 848      |       |
| b                 | n = 1 |               |                | -0.12 |
| e                 | n = 2 |               |                | 0.02  |
| c                 | n = 3 |               |                | 0.13  |
| f                 | n = 4 |               |                | 0.23  |
| d                 | n = 5 |               |                | -0.20 |
| Kepler 32 planets |       | 3.5759        | 1 334 986      |       |
| f                 | n = 1 |               |                | 0.20  |
| e                 | n = 2 |               |                | -0.17 |
| b                 | n = 3 |               |                | -0.04 |
| c                 | n = 4 |               |                | -0.07 |
| d                 | n = 5 |               |                | 0.13  |
| Kepler 33 planets |       | 6.197         | 8 443 591      |       |
| b                 | n = 1 |               |                | 0.15  |
| c                 | n = 2 |               |                | -0.09 |
| d                 | n = 3 |               |                | -0.11 |
| e                 | n = 4 |               |                | -0.04 |
| f                 | n = 5 |               |                | 0.12  |
| Kepler 62 planets |       | 3.8652        | 4 636 373      |       |
| b                 | n = 1 |               |                | -0.06 |
| c                 | n = 2 |               |                | -0.06 |
| d                 | n = 3 |               |                | 0.22  |
| missing ?         | n = 4 | Distance from | Star = 0.25 AU |       |
| e                 | n = 5 |               |                | -0.04 |
| f                 | n = 6 |               |                | -0.04 |
| Kepler 90 planets |       | 4.5163        | 8 004 304      |       |
| b                 | n = 1 |               |                | 0.13  |
| c                 | n = 2 |               |                | 0.46  |
| d                 | n = 3 |               |                | -0.37 |
| e                 | n = 4 |               |                | -0.25 |
| f                 | n = 5 |               |                | 0.02  |
| g                 | n = 6 |               |                | 0.07  |
| h                 | n = 7 |               |                | 0.18  |
| Kepler 102        |       | 7.2830        | 5 939 078      |       |

|                    |       |               |                |        |
|--------------------|-------|---------------|----------------|--------|
| planets            |       |               |                |        |
| b                  | n = 1 |               |                | -0.05  |
| c                  | n = 2 |               |                | 0.03   |
| d                  | n = 3 |               |                | 0.05   |
| e                  | n = 4 |               |                | 0.03   |
| f                  | n = 5 |               |                | -0.05  |
| Kepler 186 planets |       | 4.3388        | 3 344 862      |        |
| b                  | n = 1 |               |                | -0.06  |
| c                  | n = 2 |               |                | -0.02  |
| d                  | n = 3 |               |                | 0.035  |
| e                  | n = 4 |               |                | 0.16   |
| missing ?          | n = 5 | Distance from | Star = 0.22 AU |        |
| f                  | n = 6 |               |                | -0.095 |

From Table 13, following conclusions seem appropriate:

- The orbital distances formula eq (35) seems to hold for the solar system (for the big planets and for large groups of satellites), as well as for a number of extra-solar planetary systems. The parameters  $k$  and  $C$  are, however, different for the different planetary systems and for the different groups of satellites;
- In some extra-solar systems (e.g. Kepler 62, Kepler 186, and 55 Cnc), it is necessary to introduce a missing planet to get a reasonable solution;
- The errors in some extra-solar planetary systems are larger than in the solar system (which is understandable), but in other systems errors are quite comparable to the errors for the solar system;
- It is interesting to note that the orbital parameter  $k$  for the solar system ( $k = 3.722$ ) is comparable with the  $k$  - values for a number of extra-solar planetary systems. On Fig (35) a plot is shown of the orbital parameter  $k$  versus the mass of the parent star. The purpose of this diagram is to look for a possible relation between the  $k$  - parameter and the mass of the respective parent star. Apparently, this plot is inconclusive and there is no clear evidence with the present data. But the efforts in this respect should be continued;
- The parameters  $C$  for all extra-solar planetary systems are comparable but there is a big discrepancy when compared with the  $C$  parameter of the solar system. For the solar system  $C$  is about 6 times larger than the values of  $C$  for any of the here presented exoplanetary systems. This discrepancy shows that in extra-solar planetary systems the orbits of planets are closer to each other and are also closer (the innermost planet) to the respective central star. What could be the reason for this difference? It seems possible to explain partly the above discrepancy with the observational bias. Detecting methods of exoplanets rely on repetition of some effect (photometric dimming or spectral effect) which is observed at some orbital phase (e.g. transition of exoplanet on the stellar disk). Clearly, these effects could be observed more oft if exoplanets are closer to their respective star. Detection of exoplanets is therefore easier for short orbital (closer to star) exoplanets;

- This argument could explain the seemingly missing long-period exoplanets which may have simply escaped as yet detection. However, it does not explain why there are no planets closer to the Sun than Mercury in the solar system. Did such intra-Mercury planets exist in the past? If so, what happened to them? ;
- There could be a relation between the two orbital parameters  $k$  and  $C$  (see Fig 36), but the evidence is slim. The solar system is not shown on this plot because of the large discrepancy in  $C$  as mentioned above;
- The parameter  $k$  shows some trends if the satellites are considered, Fig (37). For the innermost satellites of all giant planets the parameter  $k$  has a large value then  $k$  decreases with increasing distance from the respective planet. For the outermost satellites of the giant planets it seems that  $k$  increases again. However, the evidence about the outermost satellites should be taken with caution because of possible dynamical perturbations of the outermost satellites (see Fig 37);
- The evidence in this chapter seems to confirm the possibility to describe orbital distances of planets and satellites by a simple exponential formula. It seems that eq (35) could either be the looked for orbital distances formula, or else a good approximation to yet unknown formula of the orbital distances law. In both cases there could be important consequences for the theory of origin of planets. The most popular theory of gravitational collapse should be able to explain the two problems, mentioned above that arise from an orbital distances law. How a random process of collapses could create the observed regularity in the distances of planetary orbits? Second, how in a number of extra-solar planetary systems it was possible to build planets so close to the respective central star? Clearly, the gravitational force of the nearby star should have prevented the build-up of a planet at that close distance from the central star. The “spiraling down” scenario would be compromised by the existence of any kind of planetary distances law because the friction (or drag) with the environment is also a random process. If the gravitational collapse theory fails in explaining the origin of planetary systems the alternative could be the disintegration scenario, but a specific model is as yet not possible;

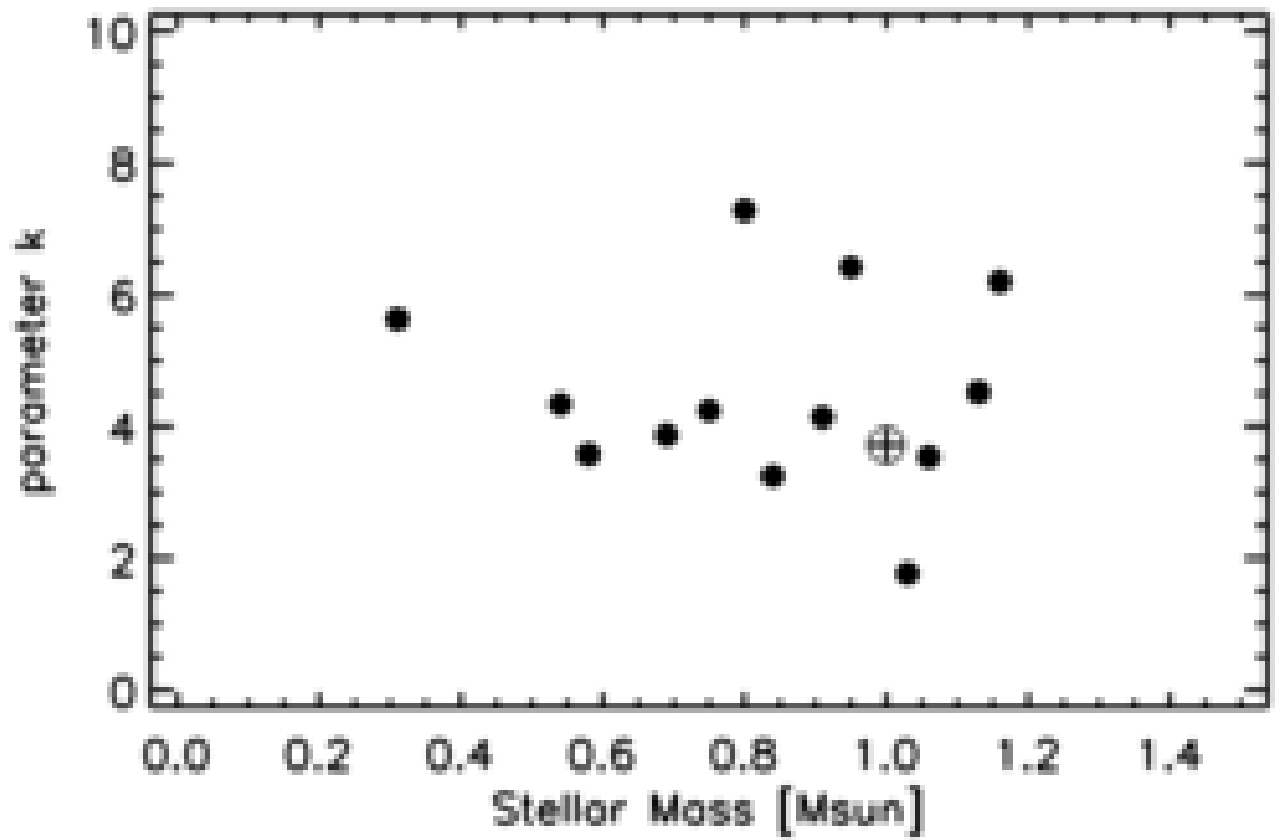


**Fig (35).** Parameter  $k$  of exoplanetary systems versus mass of respective parent star (in units of solar mass). The crossed circle is the solar system (see Table 13).

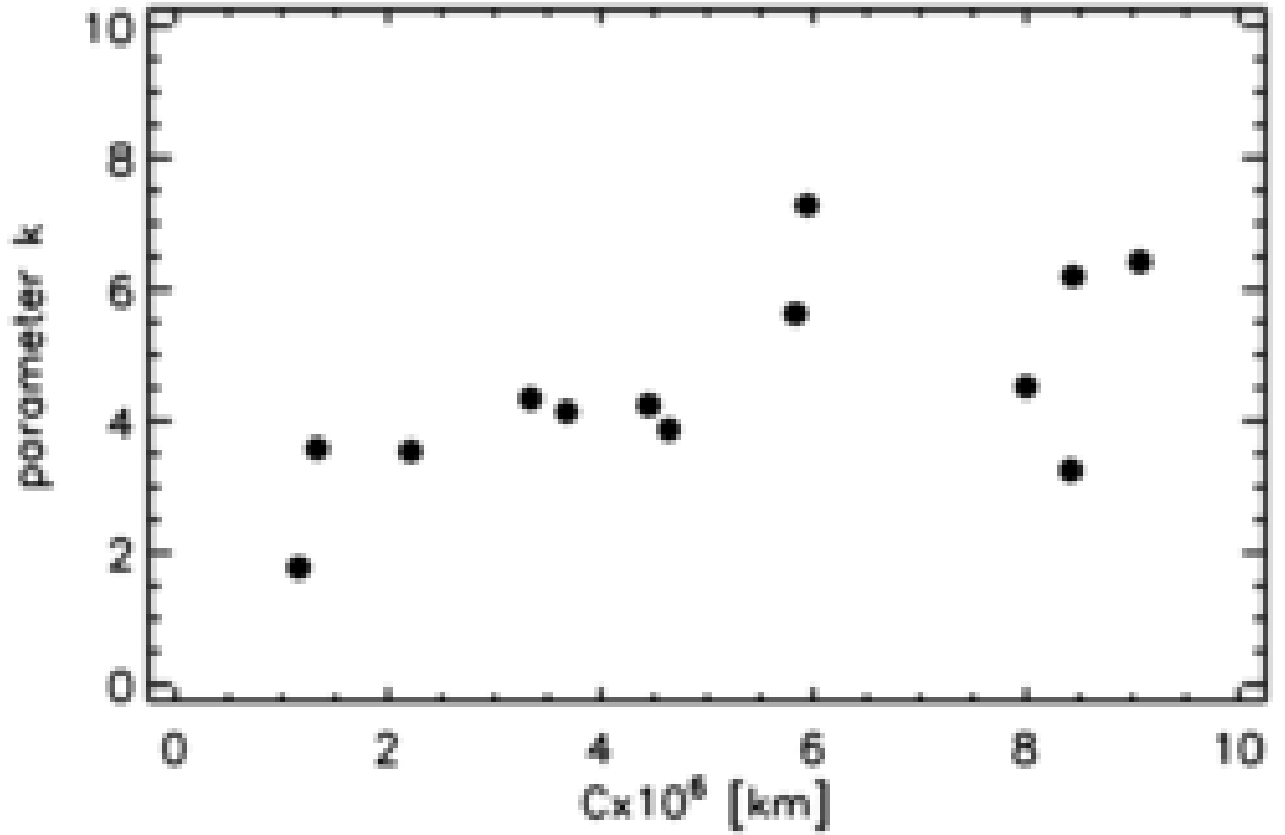


**Fig (36).** Parameter  $k$  versus parameter  $C$  for the exoplanetary systems of Table 13. Note that the solar system is not shown on this diagram (see text).

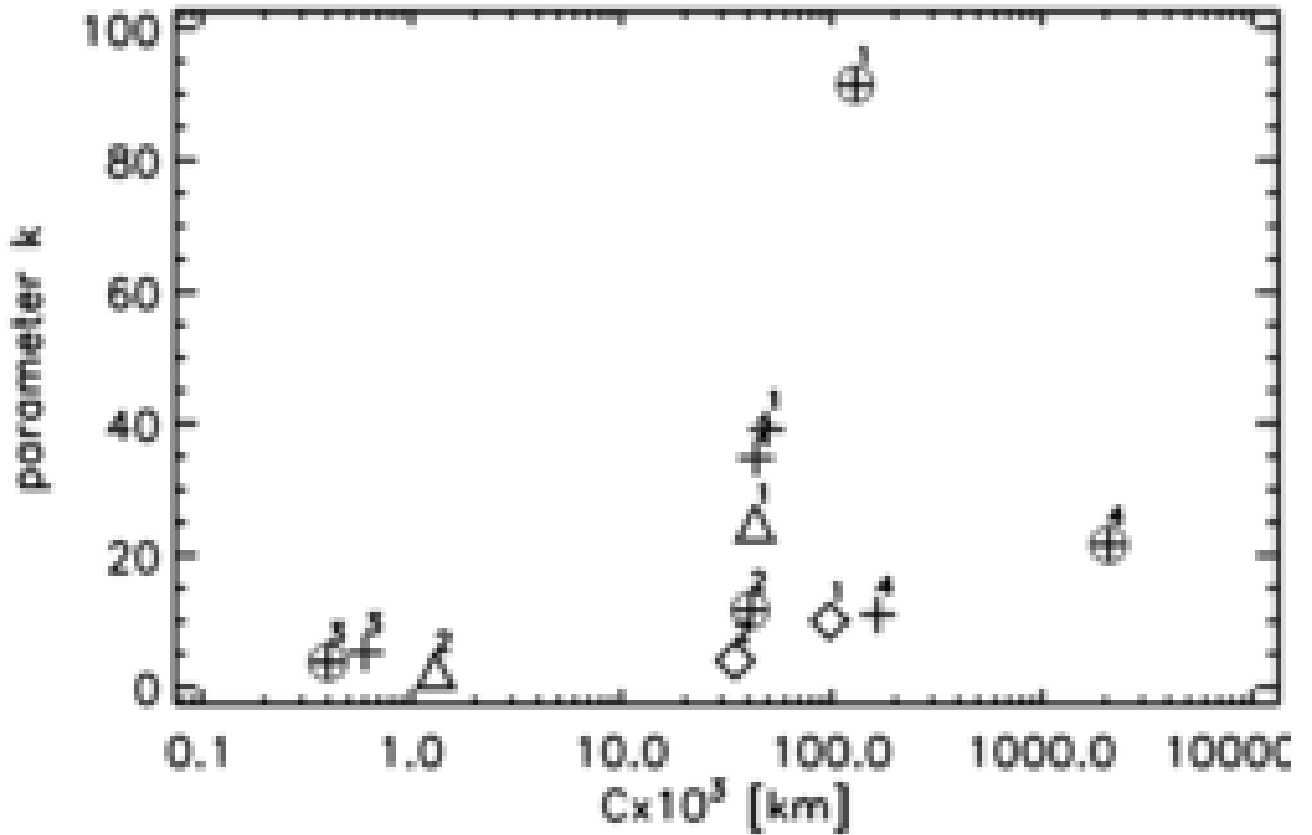


**Fig (37). Parameter  $k$  versus parameter  $C$  for satellites of Jupiter (rhombs), Saturn (crossed circles), Uranus (crosses), and Neptune (triangles). Satellites are divided in groups and the number above the sign of each group increases with the increasing distance from the respective planet (number 1 is innermost group). Groups of satellites are the same as in Table 13 (see text).**

## *Chapter 10.*

### *The inevitable rotation.*

Rotation is very fundamental feature of structures in the Universe. Planets, stars, and galaxies rotate. Rotation seems inevitable but also quite enigmatic. Rotation seems to be inherent to structures. There are difficulties in understanding stellar rotation in terms of the gravitational collapse theory. Strictly speaking, a collapse has a direction to some gravitational center and a rotational angular momentum should be prevented to occur if there is symmetry of the in-falling matter. If we are to comprehend rotation as accidental deviations from the symmetry of the collapse (i.e. an asymmetric collapse) then the occurrence of rotation in stars should be more or less accidental. We could expect then that some stars have been formed in an “ideal” gravitational collapse scenario without asymmetries in the collapse direction and such stars should not rotate at all. If the asymmetry is changing during the collapse (which would be quite possible), the end result could still be some angular momentum as an average of all changes of the asymmetry during the collapse. In this way the fact of stellar rotation could possibly be explained, but not relations involving angular momentum. The rotational velocity of a star would be more or less a random value due to the randomness of the gravitational collapse. Relations involving rotational angular momentum are not supposed to be observed if stars originate in a gravitational collapse scenario. For instance, why should the stellar angular momentum depend on stellar mass, or on stellar density? It would be very unlikely to suppose that the asymmetry of the collapse was preserved throughout the whole process of the collapse. Therefore, looking for relations involving rotation is very important in order to understand its origin. Planetary data alone are not suitable for such kind of studies because we know well only one planetary system – the solar system. Maybe, a couple of exoplanetary systems with several detected planets could also be taken into consideration, but there are constraints at present because, as discussed in the previous chapter long period exoplanets (distant from star) have as yet escaped detection. Statistical studies involving rotation are possible only with stars as there are reliable data for a large number of different types of stars. There are catalogues of data for stellar rotation (Uesugi and Fukuda, 1982 [105], Bernacca and Perinotto, 1973 [106], Gleboki and Stawikowski, 2000 [107]) that make conclusions possible. But let me start at the beginning.

Pioneering work on stellar rotation has been carried out by O. Struve, C.T. Elvey, and Miss C. Westgate in the early 1930s. During the 1940s – 1970s, extensive research gradually revealed important characteristics of stellar rotation: the dependence of rotation on spectral type, dependence on luminosity class, and dependence on age (evolution). In this way, the observational basis was created for later theoretical considerations. For the basics of stellar rotation, presentations can be found in [108-110]. Further reviews of the problem are presented in [111-115]. The complicated dependence of rotation on both spectral type and luminosity class is discussed by G.H. Herbig and J.F.Jr. Spalding [116], by A. Slettebak [117], and by A. Slettebak and R.F. Howard [118], with the confirmation of already previously noticed sudden break of rotation in stars of spectral type near F5. Studies of rotation in giant stars [119-121] revealed that rotation in evolved giants is

consistent with evolution off the main sequence with conservation of angular momentum. Additional evidence was gained by the studies of stellar rotation in galactic clusters [122-125] - the dependence of rotation on luminosity class, on age, and on stellar evolution. Turning back to the rotation in the main sequence stars the general picture revealed by the published research and also presented in Table 14 (according to published sources) could be summarized as follows:

- In the spectral range B7 – F0, rotational velocity and also the angular momentum depend on spectral type, gradually decreasing from late B – stars to late A – stars;
- There is a maximum of rotational velocity around type B6, about 230 km/s.
- Rotational velocity decreases somewhat in the O – stars, which are, however, also very fast rotators. Note, however, that rotational angular momentum in O- stars increases compared to the B- stars;
- There is a sharp deceleration of rotational velocity in the early F stars and an apparent break of angular momentum near type F5;
- Rotation is very slow for stars of types later than G0 and the velocities in Table 14 for these stars could be only an upper limit. However, rapidly rotating K and M dwarfs were detected in young stellar clusters, originally in the Pleiades [126-127]. As these stars are probably very young, they would need separate discussion.

These are the observed features of rotational velocity and rotational momentum on the main sequence which are also presented on Fig (38) and Fig (39) below. The observed features raise important and difficult questions:

- The trend of decreasing rotational velocity in stars of B6 – F0 coincides with decreasing masses and decreasing radii of these stars, therefore, there is a net decrease of angular momentum in this spectral range. We should not forget, however, that stellar ages in the same direction are increasing.
- The dependence of angular momentum, mentioned above seems to be related to the stellar masses. How is this to be understood in terms of a gravitational collapse?
- The drop of rotational velocity from B– stars to O– stars is a very peculiar feature. It could be due to some kind of evolution since the rotational angular momentum seems not to be diminished (on the contrary – it is increased!) in O- stars (Fig 38), but what evolution?
- Even more peculiar is the sharp rotational deceleration at F5 – F6 [116-118]. In this case, however, there is a clear and substantial loss of angular momentum.

No doubt, the more massive is the star, the faster is its rotation. This is direct observational evidence and needs explanation by every theory of stellar origin. However, there is a second factor that has to be considered. All along the main sequence the stellar ages increase from the massive stars (O- and B- stars) to the least massive stars (M5-stars). I would refrain from citation of specific stellar ages because the estimates available are model- dependent. Even though these ages may be corrected in the framework of the disintegration scenario the fact of increase of stellar ages will remain along the main sequence. The questions to be addressed below are: how could be determined the rotational angular momentum in stars and which was presented in Table 14 and Figs (38-39)? What is the dependence of stellar angular momentum on mass, or on density, or on age? The first question seems simple but in reality it is not. The formula for the angular

momentum is  $\mathbf{L}^{\text{am}} = \mathbf{J} \cdot \boldsymbol{\omega}$ , where the moment of inertia for a sphere is  $\mathbf{J} = 2/5 \cdot \mathbf{m} \cdot \mathbf{r}^2$  and  $\boldsymbol{\omega}$  is the angular velocity. This expression for  $\mathbf{J}$  holds only for a homogeneous sphere and this is certainly not true, neither for stars, nor for planets. Besides, shapes of rapidly rotating stars should be deviating from a spherical form. Clearly, the densities increase in stars and in planets towards their respective center. Therefore, in order to determine moments of inertia  $\mathbf{J}$ , we should be able to integrate different shells of the rotating body considering the density profile over the radius of the star (or the planet), i.e. considering sequence of layers in stars (or planets) with different density in each layer. But these density profiles are unknown. So, the above formula could be applied only as a first approximation and it presents an upper limit for  $\mathbf{J}$ . There are attempts to introduce specific expressions for  $\mathbf{J}$ , but these are model-dependent and may or may not be correct. Let me stress one important feature, however. The above simple formula for the moment of inertia of a sphere gives an upper limit when applied for stars and planets. Because the density always increases towards the center of a star or a planet the true moment of inertia has to be less than the adopted simple formula above presents. The second question, is there time evolution of stellar rotational characteristics? A.P. Skumanich [128] concluded that the equatorial angular velocity in stars decreases according to  $\boldsymbol{\omega} \sim t^{-1/2}$  in a time interval from  $\sim 0.03 \cdot 10^9$  y to  $4.5 \cdot 10^9$  y. Schatzman [129] and later Wilson [130] suggested the hypothesis of “magnetic braking”. It relies on the fact that in the early F-stars and in all stars of later spectral types a deep sub-photospheric convective zone should develop. This is the basic reason which is supposed to generate magnetic fields in stars with all their manifestations: photospheric spots, active chromospheres, emissions in the CaII K-line, and stellar winds. Indeed, stellar winds coupled with the magnetic lines could carry away from the star angular momentum, but would it be enough to explain the break of rotation at F5? In the discussion of the dependence of stellar rotation in main sequence stars along the spectral sequence it is essential to discriminate between a loss of angular momentum  $\mathbf{L}^{\text{am}}$  and the rotational break due to increase of the moment of inertia  $\mathbf{J}$ . In the second case rotational velocity will drop, but the angular momentum remains constant. Preservation of momentum would be the cause of decreasing rotational velocity if the stellar radius is increased. It seems possible to discriminate between the two possibilities considering Fig (38) where a plot of the angular momentum versus stellar densities is presented. For the later than F5- type stars it is indeed a clear loss of angular momentum that is apparent from Fig (38). How is this loss of momentum to be explained, does it concern only the stellar envelope, or the star as a whole? A loss of angular momentum could be possible due to magnetic braking as mentioned above. A different possibility will be considered below. The second case – an increase of stellar moment of inertia could be invoked for the O – type stars where the angular moment is smoothly increasing but the rotational velocity is less compared with B – stars. A decrease of angular velocity could be due to the preservation of angular momentum if the stellar radius and the moment of inertia increase. If the moment of inertia increases it should theoretically be possible to use the “breaking” of angular velocity to determine the radius increase. However, this does not seem possible at present because of the same obstacle: the unknown density profile over the stellar radius. In addition, if the stars are expanding as expected from the disintegration scenario there will be re-distribution of the stellar mass over stellar radius leading to a variable density profile in the course of expansion. The unknown (and variable!) density profile in

expanding stars should be a daunting task to solve! In summary, it seems possible that decreasing rotational velocities in O – stars compared with B – stars could be due to rapid evolution (expansion). Rapid evolution is consistent with the very large masses of O-stars.

Let us consider now some relations involving rotation. In Table 14, the rotational angular momentum is calculated with a spherical moment of inertia,  $J = 2/5 \cdot m \cdot r^2$ . As mentioned above this is only true for homogeneous distribution of mass in the rotating sphere and the real moments of inertia have to be less. Data for the rotational momentum in Table 14 are only to be considered as first approximation. Yet, it seems that some conclusions could be obtained from the data in Table 14 as discussed above and also illustrated on Figs (38-39).

**Table 14. Masses, radii, and rotational characteristics of main sequence stars (mean values) and planets of the solar system, from published sources. The rotational angular momentum is  $L^{am} = 2/5 \cdot m \cdot V_e \cdot r$ . Columns are: 1 – ID of object; 2 – mass [g]; 3 – equatorial rotational velocity [cm/s]; 4 - radius [cm]; 5 – angular momentum,  $\log L^{am}$  [ $g \cdot cm^2 \cdot s^{-1}$ ]; 6 – angular momentum per unit mass,  $\log (L^{am}/m)$  [ $cm^2 \cdot s^{-1}$ ]; 7 –  $\log$  (density) [ $g/cm^3$ ].**

| ID –object | m<br>[g]             | Ve<br>[cm/s]        | r<br>[cm]             | $\log L^{am}$<br>[ $g \cdot cm^2 \cdot s^{-1}$ ] | $\log(L^{am}/m)$<br>[ $cm^2 \cdot s^{-1}$ ] | $\log \rho$<br>[ $g/cm^3$ ] |
|------------|----------------------|---------------------|-----------------------|--|---|-----------------------------|
| Stars O5   | $1.2 \cdot 10^{35}$  | $180 \cdot 10^5$    | $9.744 \cdot 10^{11}$ | 53.93  | 18.85                                       | -1.51                       |
| Stars B0   | $3.2 \cdot 10^{34}$  | $200 \cdot 10^5$    | $5.150 \cdot 10^{11}$ | 53.12  | 18.61                                       | -1.25                       |
| Stars B5   | $1.4 \cdot 10^{34}$  | $230 \cdot 10^5$    | $2.714 \cdot 10^{11}$ | 52.54  | 18.40                                       | -0.78                       |
| Stars A0   | $6 \cdot 10^{33}$    | $190 \cdot 10^5$    | $1.670 \cdot 10^{11}$ | 51.88  | 18.10                                       | -0.51                       |
| Stars A5   | $4 \cdot 10^{33}$    | $150 \cdot 10^5$    | $1.183 \cdot 10^{11}$ | 51.45  | 17.85                                       | -0.24                       |
| Stars F0   | $3.6 \cdot 10^{33}$  | $100 \cdot 10^5$    | $1.044 \cdot 10^{11}$ | 51.18  | 17.62                                       | -0.12                       |
| Stars F5   | $3 \cdot 10^{33}$    | $30 \cdot 10^5$     | $9.744 \cdot 10^{10}$ | 50.55  | 17.07                                       | -0.11                       |
| Stars G0   | $2.1 \cdot 10^{33}$  | $4 \cdot 10^5$      | $7.656 \cdot 10^{10}$ | 49.41  | 16.09                                       | 0.05                        |
| Stars G5   | $1.84 \cdot 10^{33}$ | $2 \cdot 10^5$      | $6.403 \cdot 10^{10}$ | 48.97  | 15.71                                       | 0.22                        |
| Stars K0   | $1.56 \cdot 10^{33}$ | $\sim 1 \cdot 10^5$ | $5.916 \cdot 10^{10}$ | 48.57  | 15.37                                       | 0.26                        |
| Stars K5   | $1.38 \cdot 10^{33}$ | $\sim 1 \cdot 10^5$ | $5.011 \cdot 10^{10}$ | 48.44  | 15.30                                       | 0.42                        |
| Stars M0   | $1.02 \cdot 10^{33}$ | $\sim 1 \cdot 10^5$ | $4.176 \cdot 10^{10}$ | 48.23  | 15.22                                       | 0.52                        |
| Stars M5   | $4 \cdot 10^{32}$    | $\sim 1 \cdot 10^5$ | $1.879 \cdot 10^{10}$ | 47.48  | 14.88                                       | 1.16                        |
| Earth      | $5.98 \cdot 10^{27}$ | 46509               | $6378 \cdot 10^5$     | 40.85  | 13.07                                       | 0.74                        |
| Mars       | $6.40 \cdot 10^{26}$ | 24050               | $3393 \cdot 10^5$     | 39.32  | 12.51                                       | 0.59                        |
| Jupiter    | $1.90 \cdot 10^{30}$ | 1 266 213           | $71400 \cdot 10^5$    | 45.84  | 15.56                                       | 0.12                        |
| Saturn     | $5.68 \cdot 10^{29}$ | 1 030 142           | $60400 \cdot 10^5$    | 45.15  | 15.40                                       | -0.15                       |
| Uranus     | $8.70 \cdot 10^{28}$ | 392 094             | $24300 \cdot 10^5$    | 43.52  | 14.58                                       | 0.16                        |
| Neptune    | $1.03 \cdot 10^{29}$ | 279 067             | $25050 \cdot 10^5$    | 43.46  | 14.45                                       | 0.20                        |

Let me first consider Fig (38). There is a clear trend of decreasing rotational angular momentum along the main sequence from O5 to M5, i.e. with the increasing density but decreasing mass. This relation is quite smooth from stars of O5 to F0 and corresponds to:

$$\log L^{\text{am}} = 50.97 - 1.88 \cdot \log \rho \quad (\text{for stars O5- F0}) \quad (37)$$

For stars later than F0 this relation is “broken” and the angular momentum strongly decreases from F0 to G0, but then continues smoothly to drop from G0 to M5, according to:

$$\log L^{\text{am}} = 49.23 - 1.62 \cdot \log \rho \quad (\text{for stars G0-M5}) \quad (38)$$

Relation (38) should be taken with caution as rotational velocities in late type stars are very small and uncertain.

As expected the stellar rotational angular momentum depends also on stellar mass:

$$\log L^{\text{am}} = -49.49 + 2.975 \cdot \log m \quad (\text{for stars O5- M5}) \quad (39)$$

Note that relation (39) includes the whole spectral range and implies that angular momentum depends on stellar mass as  $L^{\text{am}} \sim m^{2.98}$  !

The respective relation for the rotational angular momentum of planets (Earth to Neptune) with planetary density is:

$$\log L^{\text{am}} = 44.88 - 6.69 \cdot \log \rho \quad (40)$$

The planets Mercury and Venus are not included in eq (40) because of the strong tidal interaction of these planets with the Sun.

Let me turn again to the problem seen in Table 14 and apparent from Fig (38). Why is this large drop of angular momentum in the short spectral interval from F0 to G0 that shifts the momentum to much lower values? Is it magnetic braking alone sufficient to break stellar angular momentum so strongly? Considerable part of the stellar rotational angular momentum has disappeared and this loss is generally present in all of the late type stars. Where has the lost momentum gone? Could there be another cause except for magnetic braking? Looking for answers the position of the Sun is also plotted on Fig (38) and it fits quite well to the lower sequence. The planetary orbital angular momentum  $L^{\text{am}} = \mathbf{m} \cdot \mathbf{V}_{\text{orb}} \cdot \mathbf{a}$ , added to the solar rotational angular momentum is also plotted above the plot for the Sun, i.e. this is the total of the solar- plus planetary angular momentum for the 9 large planets of the solar system. Interestingly, the total angular momentum (Sun plus planets) seems to be near the upper relation on Fig (38) or, to be precise, near to the extension of the upper relation to spectral class G2. This raises a tantalizing question: could it be possible that part of the solar rotational angular momentum has been transferred to the orbital angular momentum of the planets? This is a very unconventional question, to say the least. Even asking that question would be impossible in the framework of the theory of gravitational collapse. We could ask it in the concept of

disintegration, but the answer is not obvious. If it should be so we are still far away from understanding the origin of the solar system and the origin of planets in general. How is it to comprehend the process of transfer of ~ 98% of the supposed solar angular momentum to the planets?

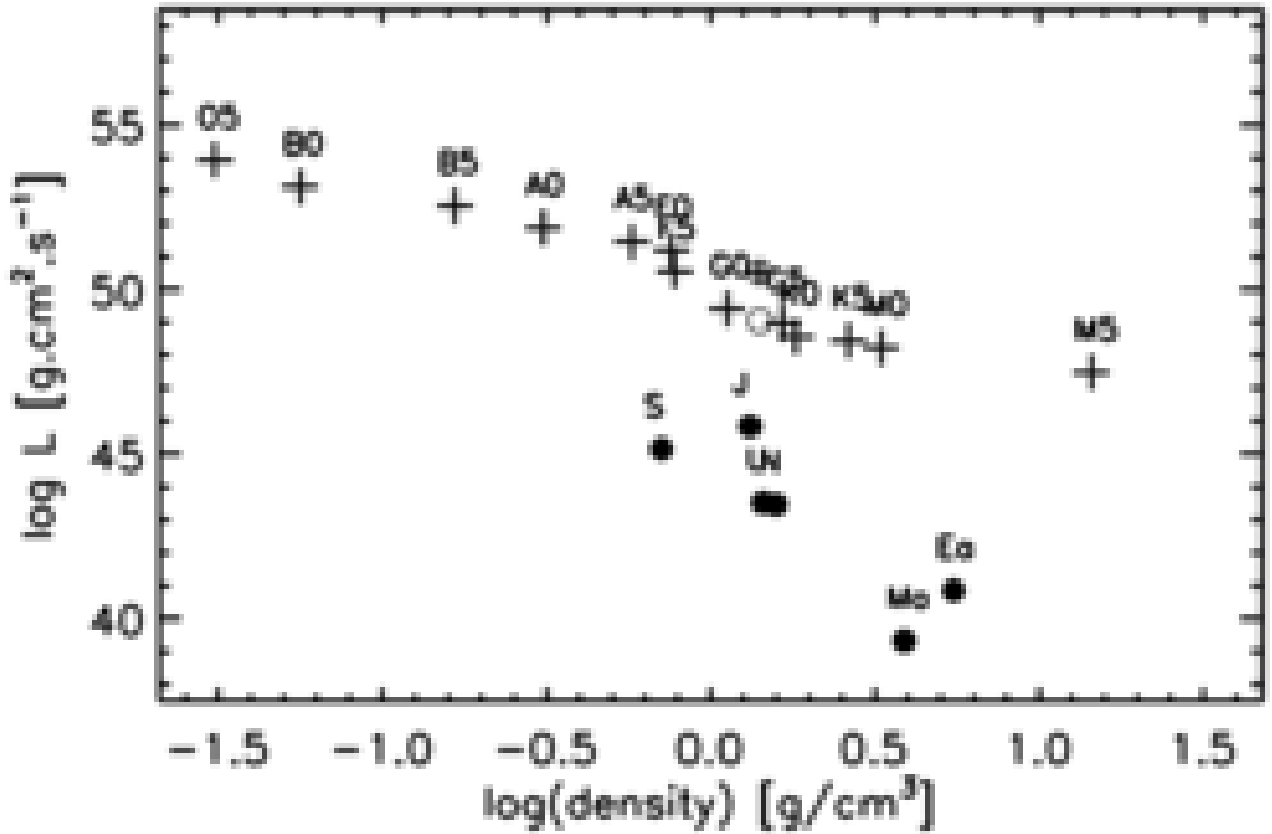


**Fig (38). Rotational angular momentum (see text) for stars and planets of the solar system plotted versus density. For stars (crosses) mean values are shown for O5, B0, B5,....,M5. The planets are: Jupiter, Saturn, Uranus, Neptune, Mars and Earth (dots). The circle shows the Sun and the crossed circle shows the total of solar plus planetary angular momentum. Data from Table 14.**

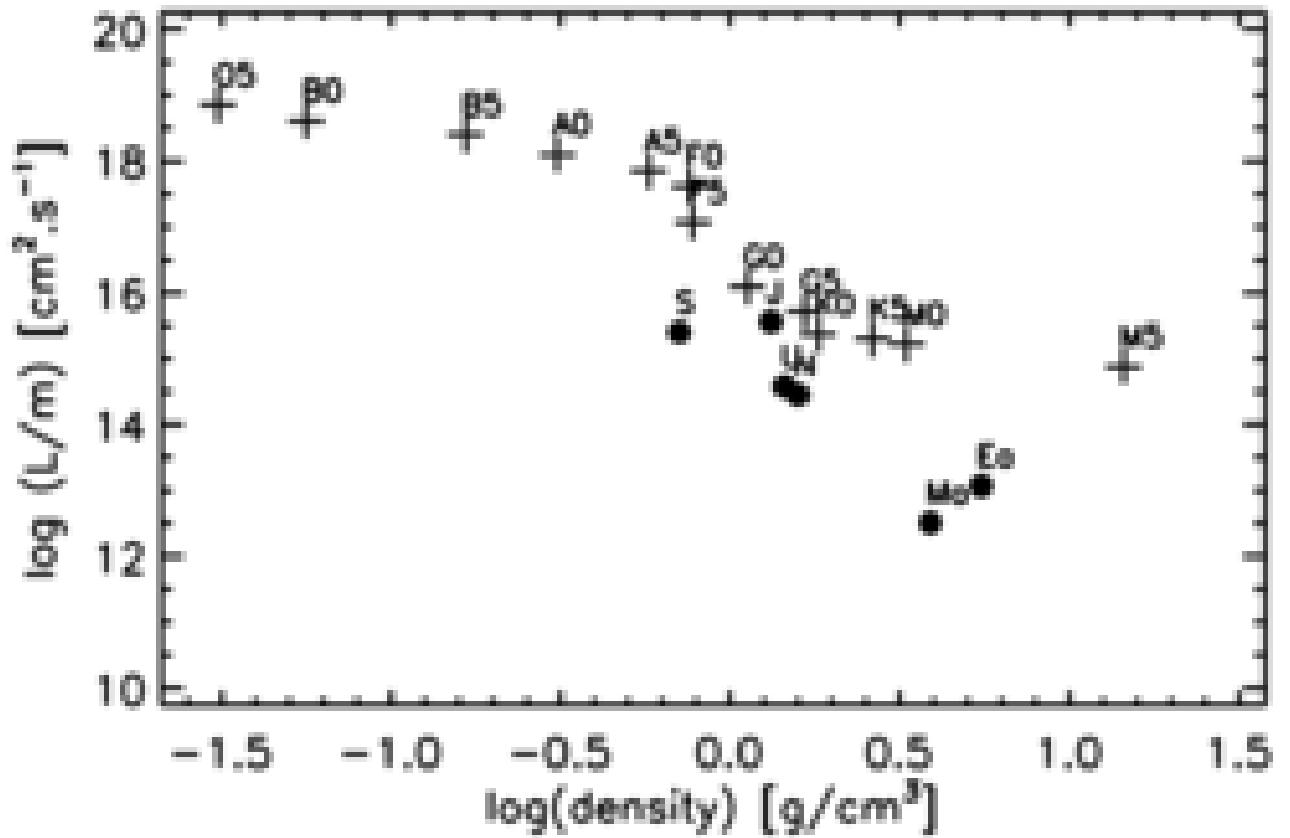


**Fig (39). Rotational angular momentum per unit mass (see text) versus density for stars (crosses) as mean values for O5, B0, B5,....., M5, and for planets (dots) for Jupiter, Saturn, Uranus, Neptune, Mars, and Earth. Data from Table 14.**

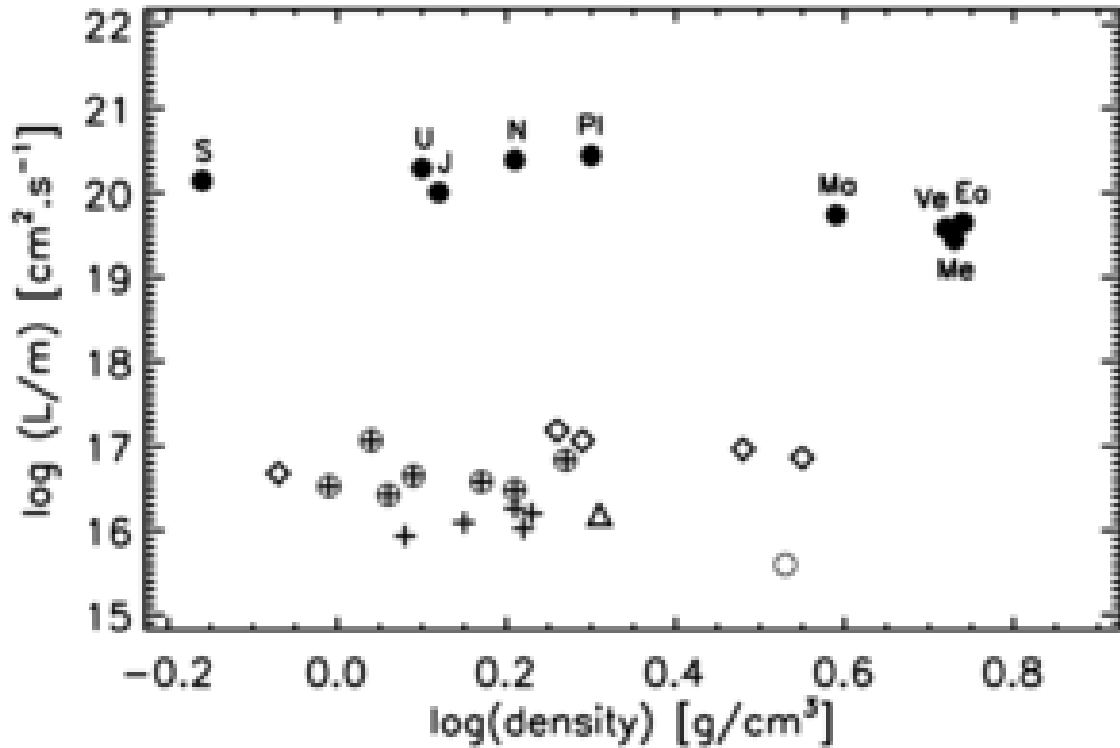
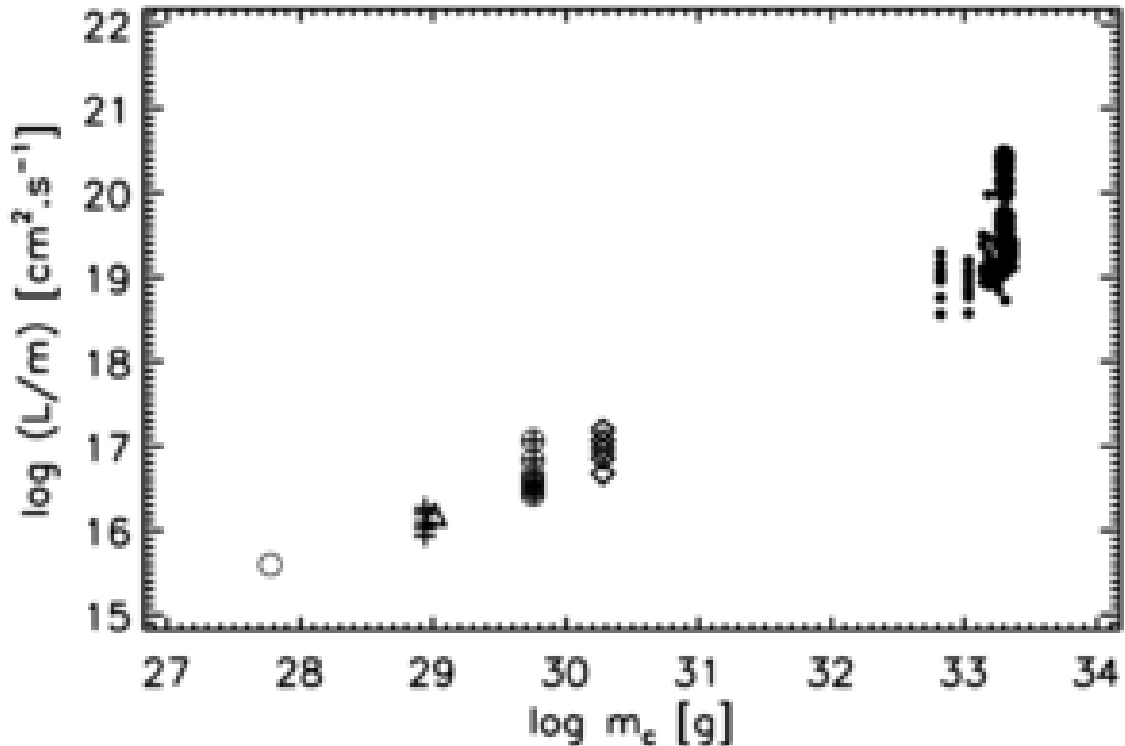


Fig (40). Solar system planetary orbital momentum per unit mass,  $L^{am} = \text{Vorb} \cdot a$  versus density. Planets are: Jupiter, Saturn, Uranus, Neptune, Pluto, Mars, Earth, Venus, and Mercury. Orbital momentum per unit mass is shown also for the satellites of Jupiter: Io, Europa, Ganymed, Calisto, Amalthea (rhombs), Saturn: Mimas, Enceladus, Tethys, Dione, Rhea, Titan, Iapetus (crossed circles), Uranus: Miranda, Ariel, Umbriel, Titania, Oberon (crosses), Neptune - Triton (triangle), and Moon (circle).



**Fig (41). Orbital angular momentum per unit mass of the big planets of SS (big dots) and main satellites of Jupiter (rhombs), Saturn (crossed circles), Uranus (crosses), Neptune (triangle), the Moon (circle), and a number of exoplanets (small dots, see Table 15), versus mass of the respective gravitational center (progenitor?). Note that the spread of data in the vertical is primarily due to the increasing distances of planets or satellites in each system, the closest to the gravitational center being always the lower ones on the diagram. The list of satellites is as in Fig (40).**

It looks, nevertheless, more likely to succeed in search for a solution in the framework of the disintegration concept. We could try to look for a support of that idea – the transfer of momentum from parent star to the planets, with extra-solar planetary systems.

Unfortunately, there is at present an obstacle that was already mentioned in the previous chapter. Despite of the large number of exoplanets already known only a few systems are known with several planets (6-7 planets) and, unfortunately, all of these planets are short orbital period planets compared with the solar system. No doubt, in exoplanetary systems should also be present distant planets from the respective parent star, but it is much more difficult to detect them as already explained in the previous chapter. If an exoplanet would have, e.g. 11- y orbital period (about the Jupiter's period) we will have to wait for almost a century to observe several repetitions of the expected effect (e.g. the photometric dimming), in order to be sure that detection is real. One could generally say that the exoplanets discovered so far are predominantly short orbital period planets and we still miss the long period ones. However, the longer period (distant from star!) exoplanets are contributing most (per unit mass!) to the planetary orbital angular

momentum! In short, we are presently left with the only planetary system we know well - the solar system. Let's move to the next question. If the build-up of planetary systems takes the orbital angular momentum from the respective parent star, then we could expect from the lower part of the diagram on Fig (38) that a large number of stars later than G0, may be most of late type stars should have planetary systems. This follows from the smooth trend of the lower sequence on Fig (38) which remains below the extension of the upper part. It is, of course, not possible to detect planets in all late type stars and in many cases the geometry of the exoplanetary system with respect to the observer might not be favorable to allow detection. But we could turn the argument: If it were true that the majority of late type stars do have planets then this should show up in the spectral type of stars for which we already know detected planets. Indeed, almost all of the detected exoplanets belong to stars later than G0 with only a few stars being of spectral class F. This seems to be consistent with the above conclusion. However, we should also estimate the observational bias. The early stars are much more luminous and detection of a planet around a luminous star by photometric dimming should be more difficult. If it is confirmed that stars earlier than F0 have no planets and we find them around stars of later than G0, why should the process of planetary building depend on the spectral class of the parent star? The reason may be found in the ages of the main sequence stars. The main sequence of spectral classes as mentioned above is also a sequence of ages, and the ages of the stars are increasing all the way from O-stars to M-stars. With this consideration it would appear that planets originate at certain age of the star and therefore they would have to be the product of stellar evolution. If this is true it would be in sharp contradiction with the theory of gravitational collapse. Let me remind you that I have used a number of "ifs" above.

There are at least two reasons for caution in this unorthodox scenario. As already mentioned the lower part of the diagram on Fig (38) in the spectral region G0 – M5 is uncertain, because of the difficulties in obtaining rotational velocities in late type stars. The second reason for concern is the possible observational bias to lower stellar luminosities - a lower chance to detect a planet in an early type bright star.

On Fig (39), the rotational angular momentum per unit mass  $L^{am}/m$  is plotted against the density and the trend is still there as well as the break at F5.  $L^{am}/m$  is increasing toward earlier spectral class and this can be seen also in the relation of  $L^{am}/m$  with mass:

$$\log (L^{am}/m) = -49.49 + 1.975 \cdot \log m \quad (\text{for stars O5- M5}) \quad (41)$$

This relation is less steep than relation (39) and the slope coefficient corresponds exactly to the division with  $m$ , if compared with eq (39). This behavior of angular momentum in stars and its dependence on mass could only be understood if the larger stellar masses correspond to larger angular velocities  $\omega$ . Are larger masses "inducing" larger rotational angular momentum? This is not an easy problem to solve and it is seemingly incompatible with the gravitational collapse theory as discussed in the Introduction. The break of the diagram on Fig (39) around F5-stars is clearly seen again. It is also interesting to notice that the giant planets Jupiter and Saturn have comparable rotational angular momentum per unit mass as compared with the late type stars. On both Figs

(38,39), the trend of angular momentum for planets seems steeper than for stars, but the number of planets used is too small to reach reliable conclusions.

On Fig (40) the orbital angular momentum per unit mass  $L^{am}/m$  is shown for the 9 big planets of the solar system and for the most massive satellites of the giant planets as plotted versus density. The first and obvious conclusion is that densities of the satellites are less than the densities of the inner planets. This is in accord with the disintegration scenario, but it is not understood with the theory of gravitational collapse. The systematic decrease of momentum per unit mass from the planets to the satellites of Jupiter, and further decrease from the satellites of Jupiter to the satellites of Uranus and Neptune could be due to the decrease of semi- major axes following from the big planets of the SS to the most massive satellites in Uranus and Neptune. At face value this could be a reasonable argument. But why are the distances of the most massive satellites depending on mass of respective planet and the same is true also for the planetary distances from the Sun – they are still larger? In the theory of the collapse the large central mass could have “cleared” by its gravitational force a larger space around it and so the planets could be formed only further away from Sun than the satellites from respective planet. In the concept of disintegration a larger central mass – the progenitor could have ejected the orbiting bodies at larger distances. But the specific physics remains obscure.

On Fig (41) the relation is shown of the orbital angular momentum per unit mass for SS planets and for the most massive satellites as depending on the mass of the Sun for the SS planets, and on mass of respective planet for the satellites. In this plot also a number of exoplanets are included with their respective central star. The exoplanets shown on Fig (41) are listed in Table 15.

**Table 15. List of exoplanets plotted on Fig (41). The orbital angular momentum per unit mass is:  $L^{am}/m = V_{orb} \cdot a$  [ $cm^2 \cdot s^{-1}$ ]. Data from The Extrasolar Planets Encyclopaedia and from NASA Exoplanet Archive.**

| Star        | Stellar mass<br>log $m_c$<br>[g] | Planet b<br>log $L^{am}/m$ | Planet c<br>log $L^{am}/m$ | Planet d<br>log $L^{am}/m$ | Planet e<br>log $L^{am}/m$ | Planet f<br>log $L^{am}/m$ | Planet g<br>log $L^{am}/m$ | Planet h<br>log $L^{am}/m$ |
|-------------|----------------------------------|----------------------------|----------------------------|----------------------------|----------------------------|----------------------------|----------------------------|----------------------------|
| Gleise 667C | 32.82                            | 18.76                      | 18.96                      | -                          | 19.07                      | 19.01                      | 19.28                      | -                          |
| Gliese876   | 32.82                            | 19.06                      | 18.96                      | 18.56                      | 19.16                      | -                          | -                          | -                          |
| 55 Cnc      | 33.31                            | 19.15                      | 19.33                      | 20.01                      | 18.73                      | 19.58                      | -                          | -                          |
| HD10180     | 33.32                            | -                          | 19.06                      | 19.22                      | 19.38                      | 19.51                      | 19.74                      | 19.93                      |
| HD40307     | 33.18                            | 18.92                      | 19.03                      | 19.14                      | 19.22                      | 19.28                      | 19.47                      | -                          |
| Kepler 11   | 33.28                            | 19.12                      | 19.15                      | 19.26                      | 19.28                      | 19.34                      | 19.47                      | -                          |
| Kepler 20   | 33.26                            | 18.96                      | 19.11                      | 19.40                      | 18.84                      | -                          | -                          | -                          |
| Kepler 32   | 33.03                            | 18.84                      | 19.18                      | 19.07                      | 18.77                      | 18.57                      | -                          | -                          |
| Kepler 33   | 33.37                            | 19.12                      | 19.24                      | 19.31                      | 19.37                      | 19.41                      | -                          | -                          |
| Kepler 62   | 33.14                            | 18.94                      | 19.05                      | 19.11                      | 19.38                      | 19.50                      | -                          | -                          |

|           |       |       |       |       |       |       |       |       |
|-----------|-------|-------|-------|-------|-------|-------|-------|-------|
| Kepler 84 | 33.30 | 19.11 | 19.17 | 19.02 | 19.29 | 19.36 | -     | -     |
| Kepler 90 | 33.35 | 19.10 | 19.17 | 19.45 | 19.49 | 19.48 | 19.59 | 19.70 |
| Kepler122 | 33.30 | 19.06 | 19.18 | 19.26 | 19.34 | -     | -     | -     |
| Kepler169 | 33.24 | 18.90 | 19.00 | 19.04 | 19.12 | 19.38 | -     | -     |
| Kepler186 | 33.03 | 18.83 | 18.92 | 19.00 | 19.08 | 19.20 | -     | -     |
| Kepler292 | 33.25 | 18.89 | 18.95 | 19.03 | 19.11 | 19.19 | -     | -     |
| Kepler444 | 33.18 | 18.90 | 18.93 | 18.98 | 19.01 | 19.04 | -     | -     |

Clearly, the larger is the mass of the “progenitor” (the gravitational center), the larger also the orbital angular momentum per unit mass of the main orbiting bodies. This relation implies the obvious fact that the planets were built at greater distances from the Sun, than the massive satellites from their respective planet. And for the planets the massive satellites are closer to the planet with the smaller mass. In the disintegration concept, it could be related to the energies of ejection released assuming that larger masses release larger energies of ejection. The physics of this process as already mentioned remains obscure. If we look further into Fig (41) it seems amazing that a close relation should exist between the orbital angular momentum per unit mass and the mass of the respective gravitational center. Why should the mass of the central body (progenitor?) determine an orbital characteristic of orbiting bodies? At present, the answer to that with the gravitational collapse theory seems impossible, while with disintegration scenario this answer is not obvious. Interestingly, the relation on Fig (41) seems to be the same for a system “star – planets” as for a system “planet – satellites”. Another tantalizing question could be asked, is the relation on Fig (41) showing support to the above suggested scenario for a “transfer of angular momentum” from the central star to its orbiting planets? It may be a tantalizing possibility, since some kind of connection is implied by Fig (41).

The aim of this chapter was to look for relations involving angular momentum. The relations of rotational angular momentum with the mass of the rotating body - eqs (39, 41) and with density - eqs (37, 38, 40), shown on Figs (38, 39), seem to contradict to the gravitational collapse theory. The orbital angular momentum per unit mass of the main orbiting bodies was shown to depend on the mass of the respective gravitational center (Fig 41). This should be a clear link between the gravitational center and the orbital characteristics of the main satellites (of planets), or of planets (of stars).

If rotation is the result of an asymmetric collapse (thus more or less accidental) rotation should not be supposed to be involved in relations of this kind. Changes in the asymmetry during the collapse are to be expected and by these random changes the angular momentum should be induced with respect to different directions. Since a collapse should have a random behavior the same random behavior should be expected also for the induced average angular momentum. Furthermore, there is a tantalizing hint that the planets of the solar system occur at some stage of the evolution of the Sun.

I am, therefore, tempted to conclude that stellar rotation is not accidental, but inevitable, i.e. inherent to, and depending on the masses of stars and planets.

## *Chapter 11.*

### *Earth's expansion and the extinction of dinosaurs.*

Why did the dinosaurs disappear? That is a question most popular not only with the scientific community, but also with the general public. Dinosaurs appeared during the Triassic period, some 230 million years ago. They dominated terrestrial life for more than 130 million years, especially during the Jurassic period. Then, by the end of the Cretaceous period (about 65 million years ago) dinosaurs suddenly disappeared. Suddenly means very fast with respect to geological timing. Nobody knows how fast - it could be several years, or may be, several decades. What happened on Earth? Obviously, some terrible global catastrophic event occurred. Could it be a major impact of an asteroid? During the history of Earth catastrophic impacts by asteroids or comets could have happened repeatedly although big asteroid encounters are quite rare. In 1980 Walter Alvarez and collaborators [131] came up with the hypothesis about major impact event by the end of the Cretaceous era, some 65 million years ago. This hypothesis is supported by the detection of global-wide enhanced layer of iridium dated at about the same time. This element is rare in the Earth's crust, but is often found in meteorites. In addition, traces of giant crater (the Chicxulub crater) with diameter of ~180 km were found on the Yucatan peninsula (Mexico) that could be dated at about the same time – 65 million years ago. Such a major impact could indeed cause a mass-extinction of life on a global scale. It is not so much the direct hit that killed terrestrial species (~ 70% of all species on Earth!), but the global cooling caused by the enormous amount of dust and ashes ejected by the impact in the atmosphere. This layer of dust in the atmosphere shielded solar irradiance during many years. The effect of cooling for the animals was that the chain of food was broken and most affected by the insufficient food were the largest animals – the dinosaurs. It was not possible for them to adapt to the suddenly cooled global environment and so they had to disappear. On top of the food disaster dinosaurs probably had also reproductive problem. They used to lay their eggs in the ground that was obviously warm enough before the impact. In the cool aftermath conditions the ground may have been insufficiently warm to hatch their eggs. With both the food and the reproductive difficulties dinosaurs were doomed. Smaller animals that needed less food and birds that learned to brood their eggs themselves could partly survive the impact starting a new era of life on Earth. The birds of today and a few species of reptiles are the only animal descendants from the Jurassic life.

So, it seems that the big dino's turned to be the most vulnerable in time of catastrophic event. But why should Nature create such large animals in the Jurassic era, since an excess of muscles needs an excess of food and that makes them vulnerable? This is a very interesting question. Animals find their food by moving. The capability to move (on the solid ground or in the air) is of primary importance for the animals' survival. What would happen if we would live in an environment of stronger gravity? Then the animals would have to "struggle" against a stronger gravitational force in order to move around. Since Nature always tends to adapt to the ambience we could expect that in a stronger gravity environment animals will gradually develop by evolution large strong muscles and large strong bones to support these muscles. Does this remind you of the Jurassic era? But why

should the gravitational force be stronger in the “dino’s-era”, and why should the gravitational force decrease afterwards? At this point we may be touching a most fundamental problem, a problem that concerns the origin and evolution of quasars, galaxies, stars, and planets. It is the problem of the disintegration scenario already discussed in the previous chapters for quasars, stars, and planets. The orthodox theory as already pointed out believes that structures in the Universe originated in events of gravitational collapse on different scales – to build structures as galaxies, stars, and planets. In the framework of this theory it would be impossible to comprehend how the gravity could have been stronger on Earth in the Jurassic era, and how the gravitational force could have decreased afterwards to reach its present day value. The disintegration scenario leads to very different picture of evolution of structures in the Universe. There is a common trend in the evolution of quasars, stars, and planets – a trend of decreasing densities by increasing dimensions of structures. If this concept is applied to the Earth it should be that the Earth in the past was smaller but with the same mass which means, mean density of Earth was higher. Higher density means stronger gravitational force at the Earth’s surface and this is how we could explain why dinosaurs had to be big and strong. The evolution of Earth since the Jurassic time increased the Earth’s dimensions by preserving the Earth’s mass. Therefore, mean density of the planet decreased. This is how we came to the present day lower gravity value at the Earth’s surface. Presently there are no such giant animals on the solid surface, neither in the air, as in the Jurassic era (except for the oceans, but this is a different story). Animals are generally smaller now because they can now move reasonably well with smaller muscles. This also means less food needed, i.e. better chance for survival. This line of argument leads to the interesting question: what would have happened if there were no catastrophic impact 65 million years ago? My answer to that is: dinosaurs would have had to disappear anyway. They became obsolete in the later low-gravity environment. They did not fit to this environment because they needed too much food which was no longer necessary – moving could be sustained by less food. The “*natural selection*” principal and the “*survival of the fittest*” would give advantage to smaller animals as it actually happened.

Dinosaurs would have disappeared anyway.

The scenario of an expanding Earth has already been considered by S. W. Hurrell in his book “Dinosaurs and the Expanding Earth – Solving the Mystery of the Dinosaurs Gigantic Size” (2004). More recent account could be found in [132]. In the Hurrell’s scenario the Earth should have expanded because of accumulation of additional mass. The evolution of Earth in his view proceeded with increasing mass and increasing density. He attributes the large sizes of dinosaurs to the lower gravity in the past, quite the opposite to the scenario presented here. From the astronomical point of view even in the concept of gravitational collapse there could be not that much mass to be accreted during the past 300 million years. This is very unlikely. Besides, if the mass of the Earth increased that much as S. W. Hurrell believes the orbit of the Earth would have changed with severe consequences for life. But the Idea of the expanding Earth is correct in my view. Only, it should be for a different reason which was described above.

In the disintegration scenario the Earth was smaller (and denser!) in the distant past and gradually expanded to the present day dimensions and density. In the beginning all planets and satellites were molten, due to the heat released by processes of disintegration (including radioactive decay). The spherical form of planets and satellites is conspicuous proof that all planets and satellites were molten in the distant past. An outside source of heat, e.g. the Sun could really be ruled out as cause of that melting. Only the internal heat of each planet or satellite could be responsible for their respective melting, therefore, for the spherical form observed. With the gradual cooling of the early Earth a solid crust could have been built at some stage on the Earth's surface. Continuing disintegration in Earth's core would have pushed to continue the expansion of Earth and which produced a mounting pressure on the crust from the inside. At some point the pressure from the inside could have broken the crust and the "*ancient continents*", the parts of the ancient crust had to move apart with new magma material flowing in-between from the inside. Volcanic activity and earthquakes on a large scale were the natural consequences of these events and the natural ambience of early life. Such catastrophic events may have been repeated producing mass-extirmination of life on Earth. It is well established that in the history of Earth there were several global disasters that exterminated life on a large scale. We should not always look for some asteroid or comet striking the Earth as causes of disasters on a large, global scale. The main and ever present danger for early life was in the Earth's interior, not in space. Major asteroid impacts as the one of 65 million years ago were rare events. It seems to be a real miracle that living creatures had to face in the past such enormous natural disasters and life could still survive. Survived, I mean, at least till now.

It seems that the scenario with Earth's expansion with decreasing density and gravity fits to the story of dinosaurs, but it is essential if this scenario fits also to the geological history. A brief comment should be given below.

In 1912 Alfred Wegener suggested a new theory of the "*drift of continents*". Although this theory seems to account for the obvious shapes of some continents (e.g. the shapes of Africa and South America) his theory was much debated and criticized because Wegener could not suggest the driving ("propelling") force for the drift of continents. Without a "driving force" his theory remained unfounded. Clearly, the driving force that moves continents has to be huge. Recently, precise GPS measurements confirmed that displacements of continents really exist, but the propelling force is still obscure. The only possible driving force on this extent, in my view, could be the expansion of the Earth. That takes us back to the disintegration scenario. The steady expansion of the Earth could provide for a powerful and inevitable force driving the plate tectonics. It could be that plates move because of the internal pressure that still exists. Is the process of expansion of Earth not yet finished? This is a question to be seriously considered.

In this scenario there is another important consequence. The early planet Earth should have rotated faster. Increasing dimensions by preserving the mass of the planet results in increasing Earth's moment of inertia. The slow down of angular rotation follows due to the preservation of angular momentum. The rate of rotation slow-down depends on the rate of expansion. Indeed, studies of the Earth's rotation revealed that our planet's

rotation is slowing down, some 1.7 seconds in 100 000 y [133]. It is, however, widely believed to be due to tidal interactions with the Moon. Yet, it would be worth to look further into this effect.

In fact, if some “residual effect” in the deceleration of Earth’s rotation should exist (after considering tidal effects) this could only be due to the expansion of the planet. A brief remark should be given to the thermal history of the Earth. Within the disintegration scenario the thermal history of Earth looks as determined by two sources of heat affecting the temperature on the Earth’s surface: the internal heat and the solar irradiation. Both these sources very probably were variable during the Earth’s history. The activity in the Earth’s interior in the early stages was very high, sufficiently high to melt the planet. Then this activity gradually decreased and is now manifested by occasional volcanic eruptions and earthquakes. On the contrary, the luminosity of the Sun probably gradually increased in the past and should increase also in future. The Sun is presently undergoing a phase of relative stability and this state will continue as long as the Sun remains on the “main sequence”. After this stage is finished expansion of the Sun will continue faster as Sun will evolve towards the “red giant” stage. Thus the solar luminosity and irradiance on Earth will continue to rise. During the past several hundred million years some “balance” of temperature on the Earth’s surface could have been achieved with the increasing solar luminosity having compensated for the decreasing Earth’s own heat. This balance of heat from both sources keeping the temperature on Earth’s surface stable and favorable was essential for life on Earth to develop. For how long more will this balance continue to exist? The solar luminosity will continue to increase as the Sun continues its way to the next stage - the stage of red giant star. So, no doubt, the evolution of Sun will make the Earth gradually but inevitably hotter and life will have to “move” to another planet. This is also the prediction of the orthodox theory of stellar evolution. The difference between the orthodox theory and the disintegration scenario could be in their respective time - scales. The orthodox theory predicts a comfortably long time to come – a few billion years more with about the same solar luminosity before the next critical phase in the solar evolution occurs. It may not be so long time with the disintegration scenario. There is no way at present to predict the time-scale of solar evolution and so there is no way to tell for how long more the temperature conditions on Earth will keep stable and favorable. This could be a big difference from the orthodox theory since a much faster scenario for the evolution of the solar luminosity could not be ruled out. That is, disintegration scenario prediction may not be so favorable for the future life conditions on Earth. Summarizing briefly the thermal history on the Earth’s surface, during the first billion of years it was the internal heat that melted the Earth and was the main source of heat. During the last billion of years it seems that a balance of decreasing Earth’s heat and increasing solar irradiance determined temperature conditions and has kept temperature on the Earth’s surface stable and favorable. This is how we find our planet today. And in future it will be only the increasing solar luminosity which determines conditions on Earth, and it will be a “hot future”. There is no doubt about that.

As far as major impacts by asteroids are concerned they are hazardous and therefore unpredictable. The decreasing Earth’s activity in future should present no danger on a

global scale- not on the extent as it was in the past. But the Sun is a different matter. Both the orthodox and the disintegration scenario predict an increase of solar luminosity and the beautiful planet Earth will be “burned” sometime in future. There is no escape. It is a “disaster postponed”. Life will have to “move” or perish. May be, at that time mankind could have moved to another planet (or satellite) further away from the Sun.

## Chapter 12.

### ***Black holes and the limits of science.***

Black hole is a body compressed to dimension smaller than its gravitational radius. The concept of “black holes” is widely used in astrophysics although this concept is quite controversial. Here is a brief review of some of the black hole controversies. It is often stated that nothing, not even light could escape from a black hole. The introduction of the “*event horizon*” at  $r = r_{gr}$  is justified by this assumption: nothing could escape from a black hole through the event horizon, not even light. Is that so?

Let me show again the well known formula for the gravitational radius, also called radius of Schwarzschild:

$$r_{gr} = (2Gm)/c^2$$

with  $c$  being the velocity of light and  $m$  being the mass.

The gravitational radius is proportional to the mass of the body, e.g. for the Sun  $r_{gr}$  is about 3 km while for the Earth it is only about 1 cm.

Solving the above expression for the light velocity we get:

$$c = (2Gm/r_{gr})^{1/2}$$

This relation for the light velocity is exactly the expression for the escape velocity from a gravitational center at distance  $r_{gr}$  from that center, i.e. the escape velocity at the *event horizon*. Therefore, the velocity of light  $c$  should be enough to escape from a black hole and light is obviously traveling at light velocity. So, what is actually the true situation, could light escape from the “event horizon”, or could it not? This contradiction was nicely reviewed by S.J. Crothers [134]

Let me take the assumption that light could escape from the event horizon. Going back to eq (12) we have:

$$r_{gr}/r_q = 1 - 1/(1 + z_{gr})^2$$

It shows that at  $r_{gr}/r_q = 1$  (the *event horizon*) gravitational reddening is  $z_{gr} = \infty$ . But with an infinitely large gravitational redshift no light frequencies could be seen, anyway. Therefore, light that “escapes” from a black hole can not be seen? Clearly, this deepens the controversy. By the way, implying formula (12) for the region inside the *event horizon*, i.e. for  $r < r_{gr}$  the gravitational redshift becomes an imaginary number - an impossible situation.

Science could not tolerate ambiguous situations like this one. The problem of emerging light from a black hole shows how deep the controversy is. But there are other

inconsistencies. What will happen with some in-falling matter crossing the event horizon of a black hole? Will it fall down “forever”? If so, the central region dimension of a black hole, no matter how massive it is, will tend to zero, and the density will reach infinity. This is not realistic and absolutely incomprehensible. Speculations about black holes being “gates” to other Universes are even more inappropriate and pure imagination. So, what should be the approach to such an unusual problem? It may be that laws of physics break down at the *event horizon* and we would need different physics to deal with black holes. Different physics could provide for a different state of stability beyond the *event horizon*. In this way, black holes could have an enormous, but not infinite density. The closest structures to a black hole, according to the results presented here seem to be the quasars. In Chapter 4 relations for quasars were used and which are referred here again (eqs 19, 23, 25) for the boundary of the *event horizon*:

$$\begin{aligned} \text{for } r_{gr}/r_q = 1, \quad \log m_q &= 27.83 + \log r_q \\ \log \rho_q &= 82.86 - 2.\log m_q \\ \log r_q &= 13.60 - \frac{1}{2} \log \rho_q \end{aligned} \quad (42)$$

In Table 16 data calculated with eqs (42) are listed for the boundary of the “*event horizon*”.

**Table 16. Masses, densities, and radii for quasars with  $r_{gr}/r_q = 1$ , from eqs (42)**

| Mass [g]            | Density [g/cm <sup>3</sup> ] | Radius [cm]            |
|---------------------|------------------------------|------------------------|
| 5x 10 <sup>40</sup> | 28.97                        | 7.40x 10 <sup>12</sup> |
| 1x 10 <sup>41</sup> | 7.24                         | 1.48x 10 <sup>13</sup> |
| 5x 10 <sup>41</sup> | 0.29                         | 7.40x 10 <sup>13</sup> |
| 1x 10 <sup>42</sup> | 0.072                        | 1.48x 10 <sup>14</sup> |
| 5x 10 <sup>42</sup> | 0.003                        | 7.40x 10 <sup>14</sup> |
| 1x 10 <sup>43</sup> | 0.0007                       | 1.48x 10 <sup>15</sup> |

Data in Table 16 are inferred by eq (42), but it should be noted that in Table 2 for local quasars there are no quasars with  $r_{gr}/r_q = 1$ .

If, however, the hypotheses that physical laws break down at the *event horizon* is accepted it is not clear whether or not the above relations (42) could hold at the *event horizon*. They could hold at least for the “close vicinity”, but “outside” of the *event horizon*.

Even though the black hole concept is controversial it is now widely believed that black holes reside in the central region of most (may be all?) galaxies. Black hole is supposed to be in the center of our galaxy, too. The masses of black holes in some large galaxies, reckoned by their gravitational action on orbiting stars are found to be quite large - billions of solar masses, called also “*Super massive black holes*”. Black holes in galaxies could be detected by their gravitational forces and their influence on the

orbiting stars in the black hole vicinity. This is how the black hole was discovered in the Sagittarius A region of our galaxy, about 4 billion solar masses. In the orthodox scenario accreting black holes are supposed to be the model of quasars. However, there is a different possibility for a quasar model described in the first chapters above. Black holes on a stellar level, according to the orthodox theory, are supposed to be the end phase of stellar evolution of very massive stars. The Big Bang should also be regarded as a *Super Massive Black Hole* since the mass of the whole observable Universe was “contained” in a very small volume before the Big Bang (the so called “*singularity*”, another word for a black hole). But then, it is the same Big Bang event that manifests the unknown physical processes that caused the Universe to expand and to explode through its *event horizon*, and to build the presently observed Universe!

Since the Universe could explode out of its *event horizon*, may be this could be the case also with the quasars which by disintegration processes expanded and exploded out of their respective *event horizon*, building whole galaxies around them? Such a picture would be at least consistent with the Big Bang scenario. If this is so the building of galaxies could be designated as “local”, “Galactic Bangs”, which should be the same process as the Big Bang, but on a smaller scale. In Chapter 8 the hypothesis was outlined about possible cascade of disintegration processes that built different structures on different scales and could be designated as “bangs” on the respective level. The build-up of galaxies, stars, and even planets in this picture looks like a series of decreasing “bangs”, down the “ladder of disintegration”. The energies released and the masses and dimensions of structures decrease “down the ladder”. This picture shows a different approach to the properties of black holes. They could possibly evolve (for some unknown reasons) and could possibly expand and explode out of their respective *event horizon*. This picture seems quite compatible with the concept of disintegration, but not easily comprehended in the concept of gravitational collapse.

You may say that all these comments are speculations and you are right.

The whole matter about black holes is still in the “*domain of pride and prejudice*”. But this “domain” is going to be the subject of my next (and last) chapter.

## ***Chapter 13.***

### ***Pride and prejudice in astrophysics.***

There are problems in astrophysics that will remain unresolved for a long time to come. Discussion of such intricate problems presupposes considerable amount of pride and suggested solutions require a due amount of prejudice. On the other hand, problems could only be solved if they are first properly formulated. In our present day textbooks astrophysical problems are formulated on the ground of three basic premises:

- The first premise is the *Big Bang* theory;
- *Gravitational collapse* theory is the second premise. Structures in the Universe – galaxies, stars, and planets, are supposed to be built by processes of gravitational collapse on different scales, of some primordial clouds of matter that emerged from the Big Bang;
- Energy is produced and released in stellar cores by the process of *hydrogen fusion* (third premise). With the on-going stellar evolution fusion continues in stellar cores with heavier than hydrogen elements and production of even heavier elements continues which are then thrown away by a SN explosion in the late stages of stellar evolution.

Following from the third premise the evolution of chemical elements starts with hydrogen and proceeds to heavier elements. The enrichment of the interstellar matter with heavy elements is due to the SN explosions and the next generation of stars could acquire some heavy elements from this “enriched” environment. This is the orthodox theory.

Obviously, the basic premises of orthodox astrophysics are tightly interrelated and if one premise fails there is danger that a large part of the whole system of ideas breaks down. It would all be all right if observations corroborate this system of basic ideas. However, in the previous chapters strong evidence was presented of relations concerning quasars, stars, and planets, and which contradict (or are at least not compatible) with the theory of gravitational collapse. The alternative in all cases is the disintegration scenario which could possibly provide for solutions, but no specific models are as yet possible. Should we turn to the “*benefit of the doubt*” in this new concept of disintegration? This could at least be a temporary outcome in a difficult situation. The introduction of the disintegration concept inevitably requires very profound changes in the whole of astrophysics. Here I will try to review the basic problems again within the framework of the disintegration scenario which already were discussed in the previous chapters and to confront possible solutions with the respective orthodox solutions. It could give the reader some preliminary taste of what may come to astrophysics as a result of future developments. Is this the right way to go or not – only future will tell. The evidence presented so far for the disintegration scenario is indirect, but so is also the evidence for the orthodox theory of the gravitational collapse. There is as yet a great deal of consistency in the results following from the concept of disintegration. Since the orthodox scenario (theory of gravitational collapse and hydrogen burning in stars) relies also on indirect evidence, in my view, the alternative scenario should be at least as

credible as the orthodox scenario is. And as long as neither scenario is proven beyond doubt the whole matter remains in the domain of “*pride and prejudice*”.

In a summary of basic ideas let me start again with the old problem of stability of solar irradiance. The stability of the hydrogen fusion (orthodox scenario) is a problem that has as yet not been solved. As already discussed in the previous chapters, solar luminosity probably evolved in the past and was gradually increasing due to the expansion of Sun. Possible solution could be found in decay (fission) processes of heavy radioactive elements. I am thereby admitting that all known radioactive elements could be the last parts of many chains of disintegration of the *primordial dense matter*.

The possibility of existence of an iron rich core in Sun was pointed out by O. Manuel (Chapter 7). If Sun does indeed harbor an iron rich core it would be possible that also other heavy (included radioactive) elements exist in its core. It is a general premise of the disintegration concept - heavy element cores should exist in all structures we observe: QSOs, stars, and planets. The absence of such cores would mean failure of the disintegration concept. In the Sun and in all stars some substantial part of the energy should be produced by decay processes of radioactive elements in the core. Obviously, hydrogen fusion in a core of heavy elements is not possible. The radioactive decay is a very stable process. However, in order to sustain the solar (and stellar) luminosity for billions of years it is necessary that radioactive elements are “replenished” by disintegration of the assumed *original dense matter and they have to be in radioactive equilibrium with this original matter*. It is known that traces of uranium are present in the solar spectrum. The question is are these traces of U only an admixture with no significance for the energy production of the Sun, or is there a more significant amount of U in the solar core? The existence of an iron core in the Sun (and therefore this problem refers to all main sequence stars!) changes everything in astrophysics. It changes the whole theory of stellar structure and stellar energy production and puts the hydrogen fusion theory in serious doubt.

Proponents of the orthodox astrophysics point out that the solar neutrino problem was solved and neutrino experiments support the scenario of neutrino oscillations. Indeed, neutrino oscillations are presently widely accepted as a possible solution, but a different solution for a neutrino source in the Sun based on decay processes could not be ruled out. Besides, our neutrino environment on Earth may look different from what is now believed and, if so, the neutrino experiments may well turn to be inconclusive. If decay processes exist also in the Earth’s core can we be sure that neutrino experiments have not registered partly also Earth’s own neutrinos?

In the disintegration concept core of heavy elements existed from the “beginning” as a result of disintegration of the *primordial dense matter*. Clearly, the concept of evolution of elements could also be reversed: from heavy to light elements - decay instead of fusion. All the elements found now in the Sun, in Earth, and in the planets could therefore be the products of long chains of disintegration processes still going on in the solar core and on a lower extent possibly also in the cores of the planets and satellites. Volcanic

activity on planets and satellites could be the last manifestations of these disintegration processes.

The origin of all chains of radioactive elements could only be in the *primordial dense matter*, supposed to be still present in the solar core. Some fragments of it were possibly later ejected to build the planets. In a similar way planets could have possibly ejected their satellites. The energy output could consist of a great number of different decay processes which could be in a *radioactive equilibrium* for billions of years with this primordial dense matter. The *radioactive equilibrium* could be maintained as long as the primordial dense kernel is not being exhausted. The radius of the presumed core of Z-elements inside the Sun and its structure and chemical composition remain presently unknown. But there is some support from solar seismology. The solar interior (below  $0.6 R_{\text{sun}}$ ) seems to be in rigid (solid body) rotation. This could possibly be an indication of a Z - composed core. The good news from this scenario is that the solar energy production could be maintained for long periods of time and possibly could cover the solar life-time. This is not implying that the solar luminosity remained constant for billions of years. Indeed, if the interpretation of the linear density diagrams is correct and the evolution follows from the white dwarfs to the main sequence stars the solar luminosity should have increased substantially. This implies transition of the young Sun (and, therefore, all other pre-main sequence stars) on the HR- diagram from the region of the white dwarfs to the main sequence. In this scenario the arrival of Sun on the MS happened more recently than believed by the orthodox theory. More importantly, the increase of solar dimensions and luminosity will further continue as the Sun will continue its way to the red giant stage. In the disintegration scenario there is no way to predict the time of departure of Sun off the main sequence.

On the main sequence for some yet unknown reasons the process of stellar evolution apparently slows down, providing for a relative stability of solar (and stellar) physical parameters as long as stars remain on the main sequence. The time spent on the main sequence depends on the stellar mass and it is very short for the massive O- stars. The slow down of evolution on the main sequence should explain the “pattern” called “main sequence” on the HR- diagram. It seems that decay processes in radioactive equilibrium could sustain the solar luminosity for billions of years. That was the good news. The bad news is, it is not possible to tell how much of this original nuclear “fuel” (*primordial matter*) is left in the solar core and a prediction for the time-scale of solar evolution is impossible. The orthodox theory believes that the Sun would have a few billion years more to stay on the main sequence. With the disintegration scenario such a prediction is impossible. This time could be much shorter. The transition of Sun to the red giant stage will proceed due to continuous disintegration and expansion of the solar interior and which leads to the expansion of Sun as a whole. However, the fate of the Sun after the red giant stage would be uncertain. As soon as the *dense progenitor* is depleted in the solar core the radioactive equilibrium will cease and all of the radioactive chains of processes will gradually die out. The Sun will then slowly cool down. The “white dwarf” stage looks in the disintegration scenario as being past already long ago. In this scenario there are important differences from the orthodox theory, e.g. the evolution from the white dwarfs to main sequence stars.

It may be that the steady increase of solar luminosity compensated for the decreasing Earth's own activity, providing for the favorable temperature conditions on the Earth's surface during the past hundreds of millions of years.

Already at this point several different concepts are outlined that contradict to the orthodox theory. These concern stellar origin, stellar structure, stellar energy production, the interpretation of solar neutrino experiments, and the evolution of chemical elements. More differences between the disintegration concept and the orthodox theory will be summarized below.

In the planetary science it should be stressed the possible existence of an orbital distances law holding for the solar system and possibly also for extra-solar planetary systems. The exponential formula eq (35) could be an approximation to such a law or even the proper law itself. The existence of an orbital distances law is a serious obstacle for the theory of gravitational collapse, no matter what the exact formula is. The additional problem is the existence of exoplanets close to their respective central star. An orbital distances law for exoplanetary systems compromises the "spiraling down" scenario. Therefore, the "close-by" exoplanets probably originated "in situ" - not far away from the star. But in this case the gravitational collapse scenario should be abandoned.

There is another important implication of the disintegration concept. All the planets and satellites should have expanded during their respective evolution, due to processes of disintegration. This process was probably very violent in the past - violent enough to melt all planets and satellites in their respective early phase of evolution. Even now the last signs of this already decayed activity are manifested by volcanic activity and earthquakes. As far as the Earth is concerned the internal activity due to processes of disintegration seems to have decayed to the extent that no major tectonic activity could present danger for life and civilization on a global scale.

There is another dividing line between the two concepts of origin of planets. According to the gravitational collapse concept the giant planets of the solar system could be entirely made of gases. Not so in the disintegration concept. The giant planets (Jupiter, Saturn, Uranus, and Neptune) should harbor in their interiors cores of Z- elements, including heavy radioactive elements. The absence of Z-cores would mean failure of the disintegration concept.

All planets and satellites were molten in the distant past and that is how they all took spherical shape. The source of energy for that melting could only be in their respective interiors and an "*outside source*" of heat that could have melted the planets could really be ruled out. This simple fact should present difficulties for the gravitational collapse scenario.

Important evidence comes from the distribution of spectral classes of "parent" stars in exoplanetary systems: why are "parent" stars mostly of late spectral classes? Is this an observational selection effect alone, or is there some real deficit of early type "parent" stars? Since late type stars on the main sequence are older the presence of planets around

late type stars could possibly be a “*product of evolution*”. As already pointed out above, planets could have been formed in the process of stellar evolution (disintegration scenario). And besides, stars after the type F5 have obviously lost significant amount of their rotational angular momentum. Is it possible that lost angular momentum has been transferred from the “parent” star to the planets as orbital momentum?

Many of the arguments made for the Sun in the disintegration scenario have to be introduced also for stars, at least for the main sequence stars. Here is a brief summary:

- Stars should have cores of Z – elements, including heavy (radioactive) elements;
- Hydrogen fusion into helium as energy source in stars will probably have to be abandoned as this reaction should have to operate in a shell around a Z- core and that would be unlikely;
- The source of energy could probably be found in a great number of decay processes, in radioactive equilibrium with the primordial dense matter in core;
- The energy output could continue as long as the primordial dense kernel is not depleted;
- With the disintegration scenario the trend of decreasing reduced densities indicates possible evolution from white dwarfs to main sequence stars, and from main sequence stars to the red giants;
- If the above statement is confirmed on the Hertzsprung-Russell diagram the evolutionary treks should proceed from white dwarfs to the main sequence, and evolution should proceed further to the red giant stars. During the whole process of evolution luminosities and radii are increasing, and stellar densities are decreasing.
- The fate of stars after the red giant stage seems uncertain. After the primordial dense kernel is depleted all chains of decay processes will die gradually out and the star should gradually cool down.

In Chapter 10 evidence was presented of possible connection between stars and the planetary systems. It could be that (see Figs 38 and 39) planetary systems develop from stars at some stage of the stellar evolution. There is a hint that large amount of the solar rotational angular momentum may have been transferred to the planets as orbital angular momentum. Such a scenario would be in contradiction to the gravitational collapse theory. It is also interesting to note that rotational angular momentum depends on the stellar mass and on stellar density which is not easily explained by an asymmetric, random gravitational collapse. Furthermore, there is a clear relation between the orbital angular momentum per unit mass of orbiting bodies (planets or satellites) and the mass of the central body - the gravitational center. Such relation exists for the main (most massive) satellites with respect to their planet as well as for the planets with respect to their central star (Fig 41). How is this relation to be explained with the theory of the gravitational collapse? The alternative may be looked for in the disintegration scenario, but the solution is not obvious.

Studies of stellar evolution should also include the evolution of stellar rotation. In Chapter 10 two interesting features were discussed and which are related to the distribution of stellar angular momentum. The first is the well known break of angular momentum near type F5 which is a real loss of angular momentum. The second feature

is the drop of angular velocity in the O- stars with respect to the B – stars, despite of the increase of angular momentum in O - stars. The second effect could be understood if the radii of the O- stars rapidly increased and the angular momentum was preserved. This would mean that even in the short time O- stars remain on the main sequence there is rapid evolution due to their large masses with the result that their rotational velocities decrease with respect to the B- stars. Published studies show that the evolution away from the main sequence proceeds with decreasing rotational velocity and preservation of angular momentum. It is actually the same idea that could be applied to the O - stars which evolution should be very fast - even during their life on the MS. But what happens with the stellar rotation before stars reach the main sequence? And what is the real place of pre-main sequence stars on the H-R diagram? Here is a short comment on a very interesting story - the story that moved minds during the past ~50 years and the problem still seems unresolved. It is the story of the Pleiades cluster. Herbig [98] in 1962 pointed out that there is a problem with stellar ages in the Pleiades. The bright massive stars suggest an age much less than the age derived from the K- and M- dwarfs in this cluster. Jones [99] confirmed the result of Herbig and found that the position of some Pleiades K-dwarfs in the Color- Magnitude Diagram (CMD) contradicts to the theoretical models because they were found to be below the theoretical Zero Age Main Sequence. This should not be possible in the theory of gravitational collapse. It prompted an extensive research on both the observational and on the theoretical sides. Additional evidence of this problem was presented in [100]. According to the theoretical models based on the gravitational collapse theory young stars in the Pleiades should occupy positions above the ZAMS and not below it. At the ZAMS the hydrogen burning is supposed to set in. These studies revealed two problems in the Pleiades: the bright massive stars and the faint K-M stars probably have different ages, as it is on the main sequence of the “field stars”. The second problem is the position of some K-M stars, apparently below the ZAMS. The second problem is serious. It touches the very credibility of the gravitational collapse scenario. But the young Pleiades cluster persisted to puzzle the researchers. The ground based photometry [100] confirmed the early results – some faint K and M dwarfs seemed to lie below the ZAMS. Models also were re-examined in a bid to meet observations. The decisive parameter for solving the Pleiades problem with the orthodox theory seemed to be the distance to this cluster. For a distance of 130-135 parsecs (pc) as implied by later photometry it seems possible for the theory to meet observations [135]. Surprise came from the Hipparcos data. Direct parallaxes obtained by Hipparcos implied much closer distance of the Pleiades, ~ 118 pc [136, 137]. Even after careful re-examination of possible errors in the parallaxes the distance of the Pleiades from Hipparcos remained substantially closer, ~ 120 pc [138]. This distance seems to be incompatible with the theoretical models based on gravitational collapse. In a new twist of the story determination of the Pleiades distance was carried out by the VLBI (Very Long Base-line Interferometer) [139] and the distance obtained was 136.2 pc. Is the theory saved? This story is quite remarkable and may also be decisive to reject the theory of gravitational collapse, if the cluster distance would indeed be incompatible with theoretical models. My feeling is that the “fronts” in this controversy are not yet appeased and the new results from the GAIA space mission (since 2014 in operation) in this respect are very much anticipated.

In the story of the Pleiades a second line of evidence has unexpectedly developed and which could have a bearing on stellar evolution. Reports have revealed very fast rotation in some K-type dwarfs in the Pleiades, indicating rotational periods of stars less than one day [126,127,140]. The rotational modulation of light for these K-dwarfs is very probably due to the well known BY Dra syndrome which has been detected earlier in many late type active stars. The periodic variability of the light of the star due to rotational modulation of light by photospheric spots allows rotational periods to be determined. The presence of photospheric spots also implies that these stars exhibit active stellar photospheres. All researchers seem to agree upon one thing: the rapidly rotating K-dwarfs in the Pleiades have to be very young stars and the question arises about their position on the Pleiades CMD- diagram. Not less important is also the question, how is it possible that these K-dwarfs have such rapid rotation?

Let me make some general remarks about the Pleiades problem from a point of view of the disintegration concept. To begin with, in the disintegration concept there is no ZAMS as defined by the theory of gravitational collapse. The ZAMS does not exist in a disintegration scenario as the main sequence is supposed to be a location on the HR – diagram where the stellar evolution slows down. If the position of some K- or M-dwarfs in the HR diagram is found below the main sequence as pointed out by many researchers, this should not present a problem. This should be the place where young stars in transition to the main sequence should be found. A long standing problem could be solved in a simple and natural way. The main sequence would be just the locus on the HR diagram of the field stars where stellar evolution slows down. In this picture based on the disintegration scenario pre-main sequence stars should be expected to occupy positions below the main sequence – not above the main sequence. That is important difference between the theory of gravitational collapse and the concept of disintegration. As to the evolution after the main sequence the general direction in both concepts is the same – from the main sequence to the red giant stars. There is one more common feature in both concepts – stars with larger masses evolve faster. Therefore, the relative ages of clusters determined by their “turn- off points” on the HR-diagram (departure from the MS) will follow in the same way also in the disintegration concept. However, the absolute age calibration may need some adjustment.

In the Pleiades the striking evidence of very fast rotating K-dwarfs may be suggesting that very young stars have recently been built and the signs for young age are the rapid rotation and enhanced activity on the photospheric and on the chromospheric levels. In the disintegration scenario these young stars would be expected to be somewhat sub-luminous and their radii should be smaller than for respective K – stars on the main sequence. With increasing dimensions as they evolve to the main sequence we could expect their luminosities to increase but also their rapid rotation should slow down due to preservation of angular momentum. It would be interesting to calculate the position and the rotational angular momentum of some rapidly rotating Pleiades star. From [127] there is the rapidly rotating H II 2927, a K7 - star with rotational period  $P = 6.29$  hours,  $B-V = 1.27$ , and  $\langle V \rangle = 14.0$ . The magnitude  $\langle V \rangle$  denotes the “mean light” by the rotational light variation. In Table 17 data for H II 2927 is presented with the two possible distances to the Pleiades - 120.2 pc and 136.2 pc, respectively. As in the

previous Chapter 10 the rotational angular momentum is:  $L^{am} = 2/5 \cdot m \cdot V_{eq} \cdot r$ , where the parameters have already been explained. Note that the different cluster distances result in different values also for the absolute magnitude  $M_v$ , for the luminosity  $L$ , and for the stellar radius  $r$ . Luminosity is obtained from the absolute magnitude and the radius is obtained from the relation:  $L = 4\pi r^2 \sigma T^4$ . Here  $\sigma$  is the Stefan-Boltzmann constant. The mass for this star is taken as  $1.2 \cdot 10^{33}$  g. Note that from Table 17 both the luminosity  $L$  and the radius  $r$  of this star are less than respective values for a MS K7 star.

**Table 17. Data for the Pleiades rapidly rotating star H II 2927 with rotational period of 6.29 hours, for two possible distances of this cluster**

| Distance<br>[pc] | Mass<br>[g]         | $M_v$<br>[absmag] | $T_{eff}$ | $L$<br>[erg/s]       | $r$<br>[cm]          | $V_e$<br>[cm/s] | $\log L^{am}$<br>[g.cm <sup>2</sup> /s] |
|------------------|---------------------|-------------------|-----------|----------------------|----------------------|-----------------|---|
| 120.2            | $1.2 \cdot 10^{33}$ | 8.60              | 3700      | $1.13 \cdot 10^{32}$ | $2.91 \cdot 10^{10}$ | 8074576         | 50.05                                   |
| 136.2            | $1.2 \cdot 10^{33}$ | 8.33              | 3700      | $1.45 \cdot 10^{32}$ | $3.30 \cdot 10^{10}$ | 9156735         | 50.16                                   |

The first comment is due on the position of this star with respect to the MS. H II 2927 is obviously sub-luminous for its spectral type and its radius is smaller. This conclusion holds for both distances of the Pleiades discussed above. This could mean that even the distance of 136.2 pc could not remove the problem. On the other hand, H II 2927 fits quite well to the disintegration scenario: it is a young, rapidly rotating star, located below the main sequence, possibly a “pre-main sequence” star. The presumed evolution to the main sequence by expansion should increase its luminosity by preservation of its rotational angular momentum. We could then compare the data in the last column of Table 17 with the prediction of eq. (37). From eq (37), extended to a K7 star we get  $\log L^{am} = 50.08$ . This value is close to the respective value corresponding to a distance of 120.2 pc. This is, of course, not a decisive point about the cluster distance, but only an “interesting observation”. It could mean that if this rapidly rotating star HII 2927 evolves with expanding radius towards the main sequence and the angular momentum is preserved, the star would be near the extension of the upper sequence in Fig (38). On this extension, as previously discussed, we find also the solar system (Sun plus planets). Is it possible that this young star has not yet built a planetary system? Presently it is only an “interesting observation”.

It has been said repeatedly that evolution depends on mass of the structure and that is a basic fact of the theory of stellar evolution. In the disintegration concept it was assumed that in stellar cores energy should be produced by a great number of different decay processes. Is this assumption consistent with the fact that evolution depends on mass? The well known law of radioactive decay is:

$$N = N_0 \cdot e^{-\lambda \cdot t} \quad (43)$$

Here  $N_0$  is the number of the original radioactive atoms ( $t = 0$ ) and  $N$  will be the number of the remaining (not yet decayed) atoms at time  $t$ . The number of the decayed atoms  $N^*$  is therefore:

$$N^* = N_0 - N = N_0 (1 - e^{-\lambda t}) \quad (44)$$

Clearly, the number of decayed (“evolved”) atoms depends on the original number of atoms (the mass!), but the “evolution” of atoms as a process is exponentially decaying. Eqs (43) and (44) imply that the disintegration is most vigorous “in the beginning” and it is exponentially decaying with time. We should not forget that a countless different processes of decay should be involved with different constants of decay  $\lambda$ , but they all follow the same law of decay, eq (43). It is to be expected that the evolution based on all decay processes should also depend on the initial mass of the fissile matter and the process of evolution of activity should be decaying with time. Comparing with the Earth’s decaying activity over its long history there seems to be consistency.

There are other problems with the stellar evolution that remain here unanswered. The linear density diagram for the atoms (Fig 31) seems to be a link in evolution of the different structures as quasars, stars and planets. The question remains, can the total sum of all “shifts” of all decayed radioactive atoms produce the slide-down on the LDD of main sequence stars to bring them to the position of the red giant stars on the same diagram?

The other problem mentioned above is the “mass – radius” diagram for WDs shown on Fig (26). The orthodox theory explains it with the electron degeneracy. Obviously, disintegration scenario needs a different explanation.

On Fig (42) the “mass – radius” diagram is shown for the atoms of the periodic table. Some elements are not included because of missing data for radii of their atoms. The shape of this diagram is very interesting and shows two trends. Clearly seen are the different periods of the table (Li - F, Na – Ar, etc) with trends pointing to larger masses corresponding to smaller radii. Going back to Fig (26) showing the same diagram for white dwarfs there is a similarity - larger masses correspond to smaller radii. If, however, the Hydrogen is taken into account and the whole diagram is considered - from Hydrogen to the heavy elements, the “average” slope could be in the opposite sense: larger masses correspond to larger radii. Going back to Fig (6) this is similar to “mass-radius” relation for main sequence stars and for quasars. This suggestion is by no means conclusive – it is, again, only an “interesting observation”. But the question remains, is it possible that the “mass – radius” diagram of structures could depend strongly on the respective chemical composition of a structure and especially on the amount of hydrogen? Thus it is worth asking the question, is it possible to explain the two-fold “mass-radius” relations by implementation of the atomic diagram on Fig (42)?

In previous chapters problems were outlined concerning local quasars and which concern also galaxies. The main findings seem to be consistent with the following suggestions:

- Local quasars are structures close to their “event horizon”, i.e. to the ratio  $r_{gr}/r_q = 1$ ;
- The cause for quasar evolution as well as the cause for several relations, found for quasars could be the disintegration of some primordial dense matter as first suggested by Ambartsumian [9];
- The evolution of quasars apparently consists of more stable periods where the values of their  $r_{gr}/r_q$ , corresponding to the  $z_{gr}$  of the Karlsson sequence, and more rapid transition between these values. The quasar expansion leads to decreasing gravitational redshift due to the decreasing gravitational potential at the surface;
- Local quasars could evolve into small mass companion galaxies as suggested by Arp [52, 94];

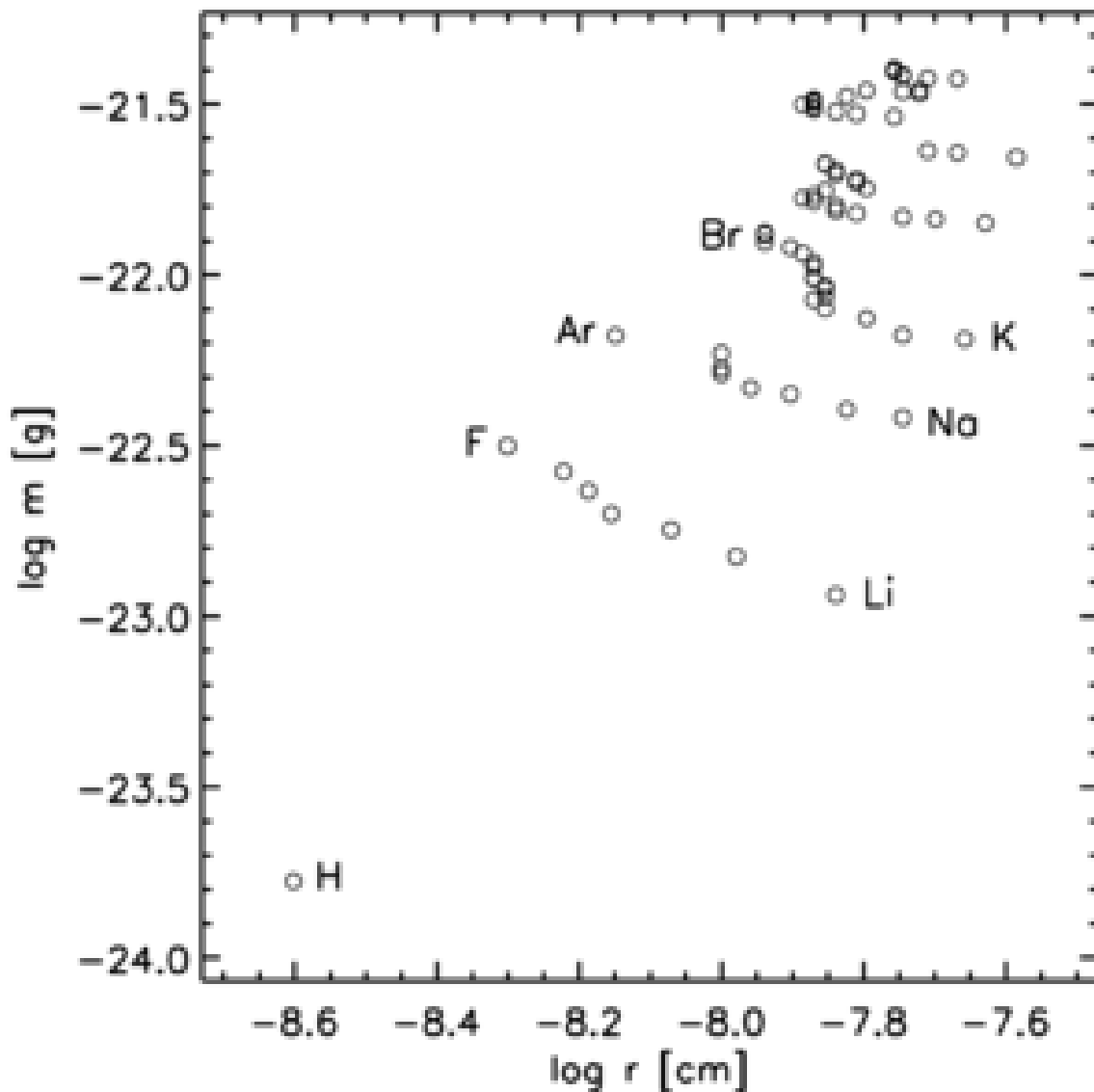


**Fig (42). The “mass – radius” diagram for the atoms of elements of the periodic table. Some elements are not included because of missing atomic data for radii. At the top of the diagram are the elements U, Np, and Pu.**

The dependence of quasar luminosity on the quasar density (Fig 12) is in the sense that lower density quasars are more luminous and vice versa. The same dependence of luminosity on density is observed also in main sequence stars.

If increasing density corresponds to lower luminosity, how far could that go? Could it have a bearing on the important and much discussed problem of the “dark matter”? The “dark matter” could be dark because of very high density, is this possible? If so, the cosmological implication for the stability of clusters of galaxies could well be possible. In clusters of galaxies there could be an additional dark (dense) mass in the cores of the individual galaxies and that could possibly keep the clusters stable. On the other hand, the problem of *flat rotational curves* in galaxies could not be solved with this concept alone. The problem of the *flat rotational curves* probably needs additional new ideas. Possible approach to solve this problem could be the study the dynamical stability of spiral arms. Are we sure that spiral arms are dynamically stable?

Since local quasars are assumed to be ejected by local low redshift galaxies there is the immediate question, how did these parent (large) galaxies originate? We have no direct observational evidence to solve this problem and it should be left to the future studies. However, if the concept of disintegration holds for local quasars, stars, and planets, it would be highly inconsistent to assume that large (parent) galaxies originate in a different way. The natural approach should be again in the framework of the concept of disintegration.

The concept of black holes is very actively debated in astrophysics. It is a most controversial concept as discussed in Chapter 12. All studies of QSOs in this presentation - equations, diagrams, and discussions always started with  $r_{gr}/r = 1$ , i.e. at the “*event horizon*”. What is the physics inside the boundary of the event horizon is a mystery. It is widely believed that nothing could escape from a black hole, but it was shown that this statement is dubious with respect to light. The physics of these strange objects is unknown. We could assume that black holes are “extremely”, but not “infinitely” dense structures. Could it be that black holes have something to do with quasars? Could it be that at some stage of evolution black holes could eject matter and energy in large quantities through the event horizon, despite our present views? Are black holes rotating? Since we do not know their physics, this could not be ruled out. If so, a black hole could evolve and become a “*white hole*”, ejecting matter and energy. Could it be that a quasar is the next step of evolution of “*white hole*” and could build a galaxy around it as a result of evolution? And, finally, could it be that the *Big Bang* itself was a kind of “*Big White Hole*”? Many problems about activity of galactic nuclei, the origin of spiral arms, etc. could be put into an entirely different perspective. All these questions remind us of the disintegration concept.

In the disintegration scenario the possibility was discussed for two kinds of evolution: jumps from a “higher level” to the next lower level (quasars to stars, stars to planets, planets to satellites), and evolution on the same level (white dwarfs – main sequence stars – evolved red giants). The first line of evolution resembles to a “*ladder*” or a “*cascade of disintegration*” where steps (cascades) follow down as QSOs – stars – planets – satellites. In both lines of evolution - down the “ladder” and on the same level of the “ladder”, evolution seems to proceed always in the same direction - with decreasing reduced densities on the linear density diagram. This is the primary, *the guiding evidence for the disintegration scenario*. The evolution of structures to lower levels (“cascades”) proceeds with decreasing masses and radii on each next step down the “ladder” and masses are decreasing stronger than radii. Decreasing densities, masses and radii of structures down the “*cascade of disintegration*” are probably signs of “*exhaustion*” of the activity of the primordial fissile dense matter. Another possible mark of depletion of the original dense matter could be the decreasing slopes of the “density - mass” diagrams for the different structures, Fig (32).

The question most interesting but also most difficult is, could the *Big Bang* be regarded as the first act of disintegration? If so, that could bring important changes in cosmological theories and we would have to consider that the *Big Bang* released not only an “ocean” of elementary particles, but also a great number of “*chunks*” of the *primordial dense fissile matter*. Such a possibility would be almost inevitable in the disintegration scenario. Since it all started with the *Big Bang*, this should be the only possible source of matter in the Universe, the original dense matter included. These “*chunks*” of dense matter continued to further disintegrate after the *Big Bang*, as mentioned above, down the “ladder”. It should be noted again that in this scenario the first stages are not yet well identified.

Another important “ingredient” of the *Big Bang* aftermath should be a great number of free neutrons, decaying further to protons and electrons according to the well known reaction:



Fission of radioactive elements on a large scale could produce neutrons on a large scale. This reaction could produce the hydrogen content in the Universe, but also background of neutrinos. Neutrons (and neutrinos) could have been released not only in the *Big Bang*, but also at all stages down the “ladder of disintegration” with decreasing efficiency at each lower step of the cascade. The main contribution is, however, to be expected from the *Big Bang* itself and also possibly from the build-up of the galaxies (“*Local Galactic Bangs*”).

Relation (45) could have produced the hydrogen content of all structures we observe. Neutrinos are the other ingredient resulting from eq (45), but also from countless other processes involving elementary particles. What happened to the enormous amount of neutrinos released? Could it be that a neutrino background exists much like the background of micro- waves? Such considerations have already been done and it is

believed that there are relict neutrinos expanding independently of matter. This scenario would be quite possible in the disintegration concept. The implication of the supposed *Local Galactic Bangs* could provide for additional supply of neutrinos, but also for micro-waves.

It would be conceivable that on the background of neutrinos and micro-waves leftover by the Big Bang some local “galactic peaks” are superposed, leftover by the build-up of the galaxies. The energy of relict neutrinos is believed at present to be very low and relict neutrinos should be technically undetectable. How the possible local peaks of neutrinos and micro-waves, if confirmed, could affect the cosmological models remains to be seen.

Clearly, Nature could provide many surprises and each option should be carefully considered before fundamental conclusions are reached. What seems to be unavoidable conclusion is that disintegration scenario is an almost natural consequence of the *Big Bang* theory. And vice versa, the *Big Bang* could be the “*First Act*” in the disintegration scenario.

## *Closing words.*

The evidence in this book goes in line with the Big Bang, but contradicts to the theory of gravitational collapse and to the hydrogen nuclear burning as energy source in stars. It was my intention to show that a very different astrophysics – based on the concept of disintegration could well be possible. The concept of disintegration of some primordial dense matter is still in its early stage and many questions linger. It is a simple concept - from high to lower density, disintegration and expansion. You may say that I tried to rearrange the puzzle of Nature, but this task is much too complex for me. Building models for quasars, stars, etc. remains impossible as long as the whole physics remains unknown. There is a good (so far) overall consistency of the results, but consistency is not a proof. Many ideas presented here are bold departure from the conventional theories and a lot of research is needed if they are to be confirmed. Not least, the “devil is in the details”. Given the difficulties with the conventional theories the options provided by the disintegration scenario should be kept free. Most important is that the young generation of astronomers has the right to know all possible options when starting their research work.

*The truth is out there for the unbiased minds.*

A word of caution for those who are trying to build a thermo-nuclear reactor based on controlled hydrogen fusion. It was the theory of hydrogen fusion in the solar core that prompted the development of hydrogen fusion reactor. Yet, the problem remains unsolved even after several decades of research. The evidence presented in this book suggests that possibly no nuclear fusion works in the Sun and one may be researching for a reactor that may not have a “prototype” in the Sun, neither in other stars, nor anywhere else in the Universe. Such a unique project is bound to be difficult.

This is the end of the book, but not the end of the story. Because, “*c’est par la fin que tout commence*”. (*The end of everything is a new beginning*).

## *Acknowledgments*

For this work, I used data from the SIMBAD and the VizieR data-bases, operated by CDS, Strasbourg, France, as well as from The Extrasolar Planets Encyclopaedia and the NASA Exoplanet Archive. My thanks are due to Dr D. Dimitrov for his valuable help in preparation of the figures, and to the administration of the Institute of Astronomy and National Astronomical Observatory, Bulgarian Academy of Sciences for using the facilities of the institute. I would like to thank BENTHAM OPEN for the kind permission to use in the book data (tables, figures, equations), already published in The Open Astronomy Journal. I also acknowledge the permission to use published data in the THALES edition in honor of Prof Emeritus M.E. Contadakis, by ZITI Publishing, Greece. Chapter 11 has been published in a shorter version by The Bibliotheque: World Wide- Society and the Institute for Positive Global Solutions.

Thank you, all my READERS, for your patience with my book.

## ***Bibliography***

- [1] Pontecorvo B. Mesonium and anti-mesonium. *Zh Eksp Teor Fiz* 1957; 33: 549-551.
- [2] Pontecorvo B. Neutrino Experiments and the Problem of Conservation of Leptonic Charge. *Zh Eksp Teor Fiz* 1967; 53: 1717.
- [3] Ahmad QR, et al. Measurement of the rate of interactions produced by 8B solar neutrinos at the Sudbury Neutrino Observatory. *Phys Rev Letters* 2001; 87: 071301.
- [4] Nieto MM. The Titius – Bode Law of Planetary Distances: Its History and Theory, 1972, Oxford, Pergamon Press.
- [5] Panov K. The Orbital Distances Law in Planetary Systems. *OAJ* 2009; 2: 90-94.
- [6] Rubin VC, Ford WKJr. Rotation of the Andromeda Nebula from a Spectroscopic Survey of Emission Regions. *Astrophys J* 1970; 159: 379-403.
- [7] Ghez AM, Salim S, et al. Measuring Distance and Properties of the Milky Way's Central Suppermassive Black Hole with Stellar Orbits. *Astrophys J* 2008; 689: 1044-1062.
- [8] Gillessen S, Eisenhauer F, et al. Monitoring Stellar Orbits Around the Massive Black Hole in the Galactic Center. *Astrophys J* 2009; 692: 1075- 1109.
- [9] Ambartsumian VA. La structure et l'évolution de l'univers. 11<sup>th</sup> Conseil de Physic Solvay, 1958, Bruxelles.
- [10] Antonucci, R. Unified models for active galactic nuclei and quasars. *AR Astron Astrophys* 1993; 31: 473-521.
- [11] Djorgowski SG, Volonteri M, Springel V, Bromm V, Meylan G. The origins and the early evolution of quasars and supermassive black holes. *Proceed. of XI Marcel Grossmann meeting on General Relativity* 2008.
- [12] Kembhavi AK, Narlikar JV. *Quasars and Active Galactic Nuclei: an introduction.* Cambridge University Press, Cambridge 1999.
- [13] Greenstein JL, Schmidt M. The Quasi-Stellar Radio Sources 3C48 and 3C273. *Astrophys J* 1964; 140: 1-37.
- [14] Hoyle F, Fowler WA. Gravitational Red-shifts in Quasi-Stellar Objects. *Nature* 1967; 213: 373-374.
- [15] Das PK. Physical properties of collapsed objects with large central gravitational redshifts. *Mon Not RAS* 1976; 177: 391-408.
- [16] Narlikar JV. Two Astrophysical Applications of Conformal Gravity. *Ann Phys* 1977; 107: 325-336.
- [17] Narlikar JV, Arp HC. Flat Spacetime Cosmology - a Unified Framework for Extragalactic Redshifts. *Astrophys J* 1993; 405: 51-56.
- [18] Canalizo G, Stockton A. 3C48: Stellar Populations and the Kinematics of Stars and Gas in the Host Galaxy. *Astrophys J* 2000; 528: 201-218.
- [19] Courbin F, Letawe G, Magain P et al. On-axis spatially resolved spectroscopy of low redshift quasar host galaxies: HE1503+0228, at  $z=0.135$ . *Astron Astrophys* 2002; 394:863-872.
- [20] Galianni P, Burbidge EM, Arp H, ey al. The discovery of a high redshift X – ray emitting QSO very close to the nucleus of NGC7319. *arXiv/astro-ph/0409215* 2004.
- [21] Karlsson KG. Possible Discretization of Quasar Redshifts. *Astron Astrophys* 1971; 13: 333-335.

- [22] Karlsson KG. On the existence of significant peaks in the quasar redshift distribution. *Astron Astrophys* 1977; 58: 237-240.
- [23] Burbidge G, Napier WM. The Distribution of Redshifts in New Samples of Quasi-Stellar Objects. *Astron J* 2001; 121: 21-30.
- [24] Arp H, Bi H, Chu Y, Zhu X. Periodicity of quasar redshifts. *Astron Astrophys* 1990; 239: 33-49.
- [25] Panov KP. Study of Possible Local Quasars I. The First Sample. *OAJ* 2011; 4: 14-26.
- [26] Arp HC. Catalogue of discordant redshift associations. APEIRON, Montreal, Canada, 2003.
- [27] Arp HC. Quasars, Redshifts, and Controversies. Interstellar Medium, Berkely, USA, 1987.
- [28] Burbidge G. The reality of anomalous redshifts in the spectra of some QSOs and its implications. *Astron Astrophys* 1996; 309: 9-22.
- [29] Burbidge GR. Noncosmological Redshifts. *Publ Astron Soc Pacific* 2001; 113: 899-902.
- [30] Hoyle F, Burbidge G. Anomalous redshifts in the spectra of extragalactic objects. *Astron Astrophys* 1996; 309: 335-344.
- [31] Burbidge G, Hewitt A, Narlikar JV, Gupta PD. Associations between quasi-stellar objects and galaxies. *Astrophys J Suppl Ser* 1990; 74: 675-730.
- [32] Williams LLR, Irwin M. Angular correlations between LBQS and APM: weak lensing by the large-scale structure. *Mon Not RAS* 1998; 298: 378-388.
- [33] Bell MB. Further Evidence for Large Intrinsic Redshifts. *Astrophys J* 2002; 566: 705-711.
- [34] Jain B, Scranton R, Sheth RK. Quasar-galaxy and galaxy-galaxy cross-correlations: model predictions with realistic galaxies. *Mon Not RAS* 2003; 345: 62-70.
- [35] Lopez-Corredoira M, Gutierrez CM. Research on candidates for non-cosmological redshifts. *AIP Conf Proceed of First Crisis in Cosmology Conf.* NY, USA. 2006; 822: 75-92.
- [36] Burbidge G, Napier WM. Associations of High-Redshift Quasi-Stellar Objects with Active, Low-Redshift Spiral Galaxies. *Astrophys J* 2009; 706: 657-664.
- [37] Burbidge EM, Burbidge GR, Solomon PM, and Strittmatter PA. Apparent associations between bright galaxies and quasi-stellar objects. *Astrophys J* 1971; 170: 233-240.
- [38] Sulentic JW, Arp HC. The galaxy-quasar connection: NGC4319 and Markarian 205. I Direct imagery. *Astrophys J* 1987; 319: 687-692.
- [39] Carilli CL, van Gorkom JH, Stocke J. 3C232 and NGC 3067: Quasars, Galaxies, and Absorption Lines. *Bull AAS* 1988; 20, 1027.
- [40] Carilli CL, van Gorkom JH, Stocke JT. Disturbed neutral hydrogen in the galaxy NGC3067 pointing to the quasar 3C232. *Nature* 1989; 338:134-136.
- [41] Arp H. A QSO 2.4 arcsec from a dwarf galaxy – the rest of the story. *Astron Astrophys* 1999; 341: L5-L8.
- [42] Lopez-Corredoira M, Gutierrez CM. The field surrounding NGC7603: Cosmological or non-cosmological redshifts? *Astron Astrophys* 2004; 421: 407-422.

- [43] Lopez-Corredoira M, Gutierrez CM. First tentative detection of anisotropy in the QSO distribution around nearby edge-on spiral galaxies. *Astron Astrophys* 2007; 461: 59-69.
- [44] Gosset E, Moreau O, Surdej J, et al. Surveys of ultraviolet-excess quasar candidates in large fields. *Astron Astrophys Suppl Ser* 1997; 123: 529-568.
- [45] Arp H. X-ray Observations of NGC1097 and Nearby Quasars. *Astrophys Sp Sci* 1998; 262: 337-361.
- [46] Arp H, Burbidge EM, Chu Y, et al. NGC3628: Ejection activity associated with quasars. *Astron Astrophys* 2002; 391: 833-840.
- [47] Arp H, Burbidge EM, Carosati D. Quasars and Galaxy Clusters Paired Across NGC4410. arXiv astro-ph/ 0605453 2006.
- [48] Burbidge EM, Burbidge G. QSOs in the Field of the Seyfert Galaxy NGC5548. *Publ Astron Soc Pacific* 2002; 114: 253-256.
- [49] Burbidge EM. Spectra of two quasars possibly ejected from NGC 4258. *Astron Astrophys* 1995; 298: L1-L4.
- [50] Burbidge EM. Spectra of two X-Ray emitting Quasi-Stellar Objects apparently ejected from the Seyfert Galaxy NGC 2639. *Astrophys J* 1997; 484: L99-L101.
- [51] Burbidge EM, Burbidge G. Ejection of Matter and Energy from NGC 4258. *Astrophys J* 1997; 477: L13-L15.
- [52] Arp, H. Quasar Creation and Evolution into Galaxies. *J Astrophys Astron* 1997; 18: 393-406.
- [53] Arp H, Burbidge EM, Chu Y et al. NGC 3628: Ejection activity associated with quasars. *Astron Astrophys* 2002; 391: 833-840.
- [54] Panov KP, Dimitrov DP. Study of possible local quasars II. A sample of 225 QSOs. Volume of contributions dedicated to Prof M. Contadakis, Thessaloniki, pp 78-105.
- [55] Panov KP. Study of possible local quasars and search for a quasar-stellar connection. III. A sample of 341 QSOs. *OAJ* 2013; 6: 20-47.
- [56] Fan X, Narayanan VK, Lupton RH, et al. A Survey of  $z > 5.8$  Quasars in the Sloan Digital Sky Survey I. Discovery of three new quasars and the spatial density of luminous quasars at  $z \sim 6$ . *Astron J* 2001; 122: 2833-2849.
- [57] Simon LE, Hamann FW, Pettini M. Physical Properties of Absorbers in High Redshift Quasars. *Rev Mex Astron Astrophys* 2007; 29: 177.
- [58] Maiolino R. Gas and Dust in the Most Distant Quasars. 2004; IAUS 222: 229-234.
- [59] Vermeulen RC, Cohen MH. Superluminal motion statistics and cosmology. *Astrophys J* 1994; 430: 467-494.
- [60] Zensus JA, Cohen MH, Unwin SC. The parsec-scale jet in quasar 3C345. *Astrophys J* 1995; 443: 35-53.
- [61] Burbidge G. NGC 6212, 3C345, and other quasi-stellar objects associated with them. *Astrophys J* 2003; 586: L119-L122.
- [62] Bahcall JN, Kirhakos S, Saxe DH. HUBBLE SPACE TELESCOPE images of a sample of 20 nearby luminous quasars. *Astrophys J* 1997; 479: 642-658.
- [63] McLure RJ, Kukula MJ, Dunlop JS et al. A comparative HST imaging study of the host galaxies of radio-quiet quasars, radio-loud-quasars, and radio galaxies-I. *Mon Not RAS* 1999; 308: 377-404.
- [64] Di Matteo T, Springel V, Hernquist L. Energy input from quasars regulates the growth and activity of black holes and their host galaxies. *Nature* 2004; 433: 604-607.

- [65] Dunlop JS, McLure RJ, Kukuła MJ, et al. Quasars, their host galaxies, and their central black holes. *Mon Not RAS* 2003; 340: 1095-1135.
- [66] Grogin NA, Conselice CJ, Chatzichristou E, et al. AGN host galaxies at  $z \sim 0.4 - 1.3$ : Bulge – dominated and lacking merger – AGN connection. *Astrophys J* 2005; 627: L97 –L100.
- [67] Cattaneo A, Faber SM, Binney J, et al. The role of black holes in galaxy formation and evolution. *Nature* 2009; 460: 213-219.
- [68] Burbidge G. Two universes. *Astrophys Sp Sci* 1996; 244: 169-176.
- [69] Veron-Cetty MP, Veron P. A catalogue of quasars and active nuclei: 13<sup>th</sup> edition. *Astron Astrophys* 2010; 518A: A10.
- [70] Croom SM, Smith RJ, Boyle BJ, et al. The 2dF QSO Redshift Survey –V. The 10k catalogue. *Mon Not RAS* 2001; 322: L29-L36.
- [71] Arp H, Surdej J, Swings J-P. Two quasars seen near the spiral galaxy NGC 470. *Astron Astrophys* 1984; 138:179-182.
- [72] Arp H, Duhalde O. Quasars near NGC 520. *Publ Astron Soc Pacific* 1985; 97: 1149-1157.
- [73] Arp H. Quasars associated with NGC 613, NGC 936 and NGC 941. *Astrophys Sp Sci* 2006; 301:117-126.
- [74] Abazajian K, Adelman-McCarthy JK, et al. The second data release of the Sloan Digital Sky Survey. *Astron J* 2004; 128:502-512.
- [75] Burbidge EM. A group of quasi-stellar objects closely associated with NGC 1068. *Astrophys J* 1999; 511: L9-L11.
- [76] Arp H, Sulentic JW. Three quasars near the spiral arms of NGC 1073. *Astrophys J* 1979; 229: 496-502.
- [77] Kaaret P. Optical Sources near the bright X-Ray Source in NGC 1073. *Astrophys J* 2005; 629: 233-238.
- [78] Arp H. Pairs of X-ray sources across Seyferts: the NGC 4235 field. *Astron Astrophys* 1997; 328: L17-L20.
- [79] Arp H. Further Observations and Analysis of Quasars near Companion Galaxies. *Astrophys J* 1983; 271: 479-506.
- [80] Arp H. Quasars near companion galaxies. *Astrophys J* 1981; 250: 31-42.
- [81] Arp H. High – redshift objects near the companion galaxies to NGC 2859. *Astrophys J* 1980; 240: 415-420.
- [82] Burbidge EM, Burbidge G, Arp HC, Zibetti S. QSOs associated with M82. *Astrophys J* 2003; 591: 690-694.
- [83] Burbidge EM, Burbidge G, Arp HC, Napier WM. An anomalous concentration of QSOs around NGC 3079. *arXiv astro-ph/10815* 2005.
- [84] Arp H, Sulentic JW, di Tullio G. Quasars aligned across NGC 3384. *Astrophys J* 1979; 229: 489-495.
- [85] Chu Y, Wei J, Hu J, et al. Quasars around the Seyfert Galaxy NGC 3516. *Astrophys J* 1998; 500: 596-598.
- [86] Arp H. Two newly discovered quasars closely spaced across a galaxy. *Astrophys J* 1984; 283: 59-63.
- [87] Arp H, Gavazzi G. A third quasar close to NGC 3842. *Astron Astrophys* 1984; 139: 240-242.

- [88] Zhu X, Chu Y, Wei J et al. A quasar possibly ejected from NGC 4579. *Chinese Sci Bull* 2000; 45: 886-888.
- [89] Arp H, Russell D. A Possible Relationship between Quasars and Clusters of Galaxies. *Astrophys J* 2001; 549: 802-819.
- [90] Arp HC, Burbidge EM, Chu Y, Zhu X. X-Ray emitting QSOs Ejected from Arp 220. *Astrophys J* 2001; 553: L11-L13.
- [91] Arp H, The surroundings of disturbed, active galaxies. *Astrophys J* 2001; 549: 780-801.
- [92] Weedman DW. A Photometric Study of Markarian Galaxies. *Astrophys J* 1973; 183: 29-39.
- [93] Arp H, Fulton C. A Cluster of High Redshift Quasars with Apparent Diameter 2.3 Degrees. 2<sup>nd</sup> Crisis in Cosmology Conference, Ed. Frank Potter, ASP Conf Ser 2009, vol 413, p 66.
- [94] Arp H. Evolution of Quasars into Galaxies and its implications for the birth and evolution of matter. *APEIRON* 1998; 5: 135-142.
- [95] Panov KP. Study of Possible Local Quasars IV. Effects of Discretization in Relations for QSOs and Search for Quasar-Stellar-Planetary Connections. *OAJ* 2014; 7: 12-21.
- [96] Heger A, Fryer CL, Woosley SE et al. How Massive Single Stars End Their Life. *Astrophys J* 2003; 591: 288-300.
- [97] Shipman HL. Masses and Radii of White – Dwarf Stars. III. Results for 110 H- rich and 28 He- rich Stars. *Astrophys J* 1979; 228: 240- 256.
- [98] Herbig GH. Spectral Classification of Faint Members of the Hyades and Pleiades and the Dating Problem in Galactic Clusters. *Astrophys J* 1962; 135: 736-747.
- [99] Jones BF. The Pleiades Lower Main Sequence. *Astrophys J* 1972; 171: L57-L60.
- [100] Stauffer JR, Jones BF, et al. Why are the K Dwarfs in the Pleiades so blue? *Astron J* 2003; 126: 833-847.
- [101] Provencal JL, Shipman HL et al. Testing the White Dwarf Mass-Radius Relation with HIPPARCOS. *Astrophys J* 1998; 494: 759-767
- [102] Slater, JC. Atomic Radii in Crystals. *J Chem Phys* 1964; 41: 3199-3205.
- [103] Poveda A, Lara P. The exo-planetary system of 55 Cancri and the Titius-Bode Law. *Revista Mexicana de Astronomia y Astrofisica* 2008; 44: 243-246.
- [104] Panov KP. The Law of Orbital Distances in the Solar System. *Comptes Rendus Bulgarian Acad Sci* 2009; 62(2): 143-152.
- [105] Uesugi A, Fukuda I. Catalogue of Stellar Rotational Velocities (revised). 1982, Kyoto: University of Kyoto, Dept of Astronomy.
- [106] Bernacca PL, Perinotto M. A Catalogue of Stellar Rotational Velocities. Vol 1: Main Sequence Single Stars. Vol 2: Main Sequence spectroscopic Binaries. Vol 4: Evolved Stars. 1973, Contributi dell'Osservatorio Astrofisico dell'Universita di Padova in Asiago, Padova: Cleup 1970-1973.
- [107] Glebocki R, Stawikowski A. Catalogue of Projected Rotational Velocities. *Acta Astron* 2000; 50: 509-515.
- [108] Struve O. The cosmogonical Significance of Stellar Rotation. *Popular Astron* 1945; 53: 201-217, and 259-275.
- [109] Huang Su-Shu. A Statistical Study of the Rotation of the Stars. *Astrophys J* 1953; 118: 285-303.

- [110] Boiarchuk AA, Kopylov IM. On the Distribution of Stellar Rotational Velocities. *Soviet AJ* 1958; 2: 752.
- [111] Abt HA. Line Broadening in High-Luminosity Stars. II. Less Luminous Supergiants. *Astrophys J* 1958; 127: 659-666.
- [112] Treanor PJ. Stellar Rotation in Galactic Open Clusters. *Mon Not RAS* 1960; 121: 503-518.
- [113] Deutsch, AJ. The Statistics of Stellar Rotation. *Astron J* 1965; 70: 673.
- [114] Kraft RP. Studies of Stellar Rotation. V. The Dependence of Rotation on Age among Solar-Type Stars. *Astrophys J* 1967; 150: 551-557.
- [115] Kraft RP. *Stellar Rotation*. 1970; University of California Press, Berkeley, CA.
- [116] Herbig GH, Spalding JF Jr. Axial Rotation and Line Broadening in Stars of Spectral Types F0-K5. *Astrophys J* 1955; 121:118-143.
- [117] Slettebak A. The Spectra and Rotational Velocities of the Bright Stars of Draper Types A3-G0. *Astrophys J* 1955; 121: 653-669.
- [118] Slettebak A, Howard RF. Axial Rotation in the Brighter Stars of Draper Types B2-B5. *Astrophys J* 1955; 121:102-117.
- [119] Oke JB, Greenstein JL. The Rotational Velocities of A-, F-, and G-Type Giant Stars. *Astrophys J* 1954; 120: 384-390.
- [120] Sandage AR. Axial Rotation and Stellar Evolution. *Astrophys J* 1955; 122: 263-269.
- [121] Kraft RP. Stellar Rotation and Stellar Evolution among Cepheids and other Luminous Stars in the Hertzsprung Gap. *Astrophys J* 1966; 144: 1008-1015.
- [122] Abt HA, Hunter JH Jr. Stellar Rotation in Galactic Clusters. *Astrophys J* 1962; 136:381-392.
- [123] Kraft RP. Studies of Stellar Rotation. I. Comparison of Rotational Velocities in the Hyades and Coma Clusters. *Astrophys J* 1965; 142: 681-702.
- [124] Kraft RP, Wrubel MH. Studies of Stellar Rotation. II. The Effect of Rotation on the Colors and Magnitudes of A- and F- Type Stars in the Hyades. *Astrophys J* 1965; 142: 703-711.
- [125] Kraft RP. Studies of Stellar Rotation. IV. A Comparison of Rotational Velocities in the Alpha Persei Cluster and the Pleiades. *Astrophys J* 1967; 148: 129-139.
- [126] van Leeuwen F, Alphenaar P. Variable K-type stars in the Pleiades cluster. *ESO Messenger* 1982; June vol : 15-18.
- [127] Stauffer JR, Schild RA, et al. Photometric light curves for seven rapidly-rotating K dwarfs in the Pleiades and Alpha Persei clusters. *Publ Astron Soc Pacific* 1987; 99: 471-481.
- [128] Skumanich A. Time Scales for Ca II Emission Decay, Rotational Braking, and Lithium Depletion. *Astrophys J* 1972; 171:565-567.
- [129] Schatzman E. A Theory of the Role of Magnetic Activity during Star Formation. *An Astrophys* 1962; 25: 18-29.
- [130] Wilson OC. Stellar Convection Zones, Chromospheres, and Rotation. *Astrophys J* 1966; 144: 695-708.
- [131] Alvarez LW, Alvarez W, et al. Extraterrestrial cause for the Cretaceous-Tertiary extinction. *Science* 1980; 208 (4448): 1095-1108.
- [132] Hurrell S. Ancient Life's Gravity and its Implications for the Expanding Earth. 2012, (eds) Scalera G, Boschi E, and Cwojdzinski S. *Proceedings of the 37<sup>th</sup>*

- International School of Geophysics, The Earth Expansion Evidence – a Challenge for Geology, Geophysics, and Astronomy, EMFCSC, p 307.
- [133] McCarthy DD, Seidelmann PK. TIME: From Earth Rotation to Atomic Physics. Weinheim, Wiley-VCH 2009; pp 88-89.
- [134] Crothers SJ. Black Hole Escape Velocity – a Case Study in the Decay of Physics and Astronomy. <http://vixra.org/pdf/1508.0066v1.pdf>
- [135] Pinsonneault MH, Terndrup DM, et al. The distances to open clusters as derived from main-sequence fitting. II. Construction of empirically calibrated Isocrones. *Astrophys J* 2004; 600: 946-959.
- [136] van Leeuwen F. HIPPARCOS Distance Calibrations for 9 open Clusters. *Astron Astrophys* 1999; 341: L71-L74.
- [137] Robichon N, Arenou F, et al. Open Clusters with Hipparcos. I. Mean astrometric parameters. *Astron Astrophys* 1999; 345: 471-484.
- [138] van Leeuwen F. Parallaxes and proper motions for 20 open clusters as based on the new Hipparcos catalogue. *Astron Astrophys* 2009; 497: 209-242.
- [139] Melis C, Reid MJ, et al. A VLBI resolution of the Pleiades distance controversy. *Science* 2014; 345: 1029-1032.
- [140] van Leeuwen F, Alphenaar P, Meys JJM. VBLUW observations of Pleiades G and K dwarfs. *Astron Astrophys Suppl Ser* 1987; 67: 483-506.